

THE SYNTHESIS AND CHEMICAL PROFILING OF 3,4-METHYLENE- DIOXYMETHAMPHETAMINE (MDMA) AND ANALOGUES

by Erin Heather

Thesis submitted in fulfilment of the requirements for
the degree of

Doctor of Philosophy

under the supervision of Assoc. Prof. Andrew McDonagh
and Dr Adrian De Grazia

University of Technology Sydney
Faculty of Science

October 2020

Certificate of Original Authorship

I, Erin Heather, declare that this thesis is submitted in fulfilment of the requirements for the award of Doctor of Philosophy, in the Faculty of Science at the University of Technology Sydney.

This thesis is wholly my own work unless otherwise reference or acknowledged. In addition, I certify that all information sources and literature used are indicated in the thesis.

This document has not been submitted for qualifications at any other academic institution.

This research is supported by an Australian Government Research Training Program.

Signature of Student: Erin Heather

Production Note:
Signature removed prior to publication.

Date: 1 October 2020

Acknowledgements

First and foremost, I would like to sincerely thank my supervisor Assoc. Prof. Andrew McDonagh for your guidance at each stage of this project. I could not have imagined a better supervisor for my doctoral research. In the end, your continuous support, advice, and timely reviews made completing this thesis and the associated journal articles as pain-free as possible. I would also like to thank my co-supervisor Dr Adrian De Grazia for your support over the years and insights into the world of forensic drug intelligence.

I acknowledge all academic and professional staff at the University of Technology Sydney who have provided support and assistance throughout the course of my doctoral research. In particular, I would like to thank Dr Ronald Shimmon, Alexander Angeloski, Dr Verena Taudte, and Dr David Bishop for your assistance in the organic synthesis laboratory and with the use of the analytical instruments.

I thank my fellow doctoral and honours students for your discussions in the laboratory and for keeping life interesting throughout the years. I will always be grateful to Dr Rachel Morison for her friendship and our lunch time television and cat discussions, which helped keep me sane throughout the years.

Last but not the least, I would like to thank my family and friends. To my husband John, I could not have completed this thesis without your encouragement, humour and IT support, and I wish you were here to see and celebrate this day.

Table of Contents

Certificate of Original Authorship	i
Acknowledgements	ii
Table of Contents	iii
List of Figures	vi
List of Schemes	x
List of Tables	xiv
List of Equations	xvi
List of Abbreviations	xvii
List of Publications	xviii
Abstract	xix
Chapter 1: Introduction	2
1.1 MDMA and Analogues	2
1.1.1 Legislation	3
1.1.2 Synthesis of MDMA	4
1.1.3 Synthesis of Methylone	7
1.2 Synthesis of MDMA and Methylone from Uncontrolled Precursors	9
1.2.1 Vanillin	10
1.2.2 Piperine	10
1.2.3 Eugenol	11
1.2.4 Catechol	12
1.3 Chemical Profiling	13
1.3.1 Organic Impurity Profiling	15
1.3.2 Inorganic Impurity Profiling	21
1.3.3 Isotope Ratio Analysis	23
1.4 Research Aims	26
Chapter 2: Materials and Methods	29

2.1 General Experimental	29
2.2 Chemicals	29
2.3 Synthesis	30
2.3.1 Methylone	30
2.3.2 Safrole	31
2.3.3 MDMA	33
2.3.4 Synthesis of specific organic impurities	35
Chapter 3: Methylone	37
3.1 Introduction	37
3.2 Synthesis	37
3.2.1 1,3-Benzodioxole from Catechol	37
3.2.2 3,4-Methylenedioxypropiofenone from 1,3-benzodioxole.....	38
3.2.3 5-Bromo-3,4-methylenedioxypropiofenone from 3,4- methylenedioxypropiofenone.....	39
3.2.4 Methylone from 5-bromo-3,4-methylenedioxypropiofenone	40
3.3 Organic Impurity Profiling.....	41
3.3.1 Catechol	41
3.3.2 1,3-Benzodioxole from Catechol	41
3.3.3 3,4-Methylenedioxypropiofenone from 1,3-benzodioxole.....	47
3.3.4 5-Bromo-3,4-methylenedioxypropiofenone from 3,4- methylenedioxypropiofenone.....	59
3.3.5 Methylone from 5-bromo-3,4-methylenedioxypropiofenone	62
3.4 Route Specific Organic Impurities	66
3.5 Conclusions	67
Chapter 4: Safrole	70
4.1 Introduction	70
4.2 Synthesis of Safrole	70
4.2.1 Route 1: Safrole from Catechol	70

4.2.2 Route 2: Safrole from Catechol	72
4.2.3 Route 3: Safrole from Eugenol	74
4.3 Organic Impurity Profiling.....	75
4.3.1 Route 1: Safrole from Catechol	75
4.3.2 Route 2: Safrole from Catechol	81
4.3.3 Route 3: Safrole from Eugenol	89
4.4 Route Specific Organic Impurities	94
4.5 Conclusions	97
Chapter 5: MDMA	99
5.1 Introduction	99
5.2 Synthesis	99
5.2.1 Route A: MDMA from Safrole	99
5.2.2 Route B: MDMA from safrole	101
5.3 Organic Impurity Profiling.....	102
5.3.1 Routes 1A, 2A and 3A	103
5.3.2 Routes 1B, 2B and 3B.....	116
5.4 Route Specific Organic Impurities	131
5.5 Conclusions	137
Chapter 6: Conclusions and Future Research Recommendations.....	139
Appendix 1: Mass Spectra	145
Appendix 2: Gas Chromatograms	166
Appendix 3: NMR Spectra	175
Appendix 4: Organic Impurities	185
Appendix 5: Synthesis and organic impurity profiling of 4-methoxymethamphetamine hydrochloride and its precursors.....	192
References	204

List of Figures

Figure 1-1: Chemical structure of MDMA	2
Figure 1-2: Chemical structure of the MDMA analogues methylene	2
Figure 1-3: Chemical structures of MDP2P, safrole, isosafrole and piperonal	3
Figure 1-4: Chemical structure of vanillin	10
Figure 1-5: Chemical structure of piperine.....	11
Figure 1-6: Chemical structure of eugenol	11
Figure 1-7: Chemical structure of catechol	12
Figure 3-1: ¹ H NMR spectrum of catechol	41
Figure 3-2: GC-MS total ion chromatogram of 1,3-benzodioxole.....	42
Figure 3-3: Mass spectrum and proposed fragmentation scheme of 1,3-benzodioxole	42
Figure 3-4: ¹ H NMR spectrum of 1,3-benzodioxole	43
Figure 3-5: Mass spectrum and proposed fragmentation scheme of organic impurity 39.....	44
Figure 3-6: Mass spectrum and proposed fragmentation scheme of organic impurities 40 (a-c)	44
Figure 3-7: Mass spectrum and proposed fragmentation scheme of organic impurity 46.....	44
Figure 3-8: Mass spectrum and proposed fragmentation scheme of organic impurity 47.....	45
Figure 3-9: GC-MS total ion chromatogram of 3,4-methylenedioxypropylphenone	47
Figure 3-10: Mass spectrum and proposed fragmentation scheme of 3,4- methylenedioxypropylphenone	48
Figure 3-11: ¹ H NMR spectrum of 3,4-methylenedioxypropylphenone	48
Figure 3-12: Potential chemical structures of organic impurity 48 (top) and organic impurity 50 (bottom)	50
Figure 3-13: Mass spectrum and potential fragmentation pathways of organic impurity 48	50
Figure 3-14: Mass spectrum and potential fragmentation pathways of organic impurity 50	51
Figure 3-15: Gas chromatogram and mass spectra of synthesised (2-hydroxyphenyl) propanoate and (2-propanoyloxyphenyl) propanoate	52

Figure 3-16: ^1H NMR spectrum of (2-hydroxyphenyl) propanoate and (2-propanoyloxyphenyl) propanoate	53
Figure 3-17: Mass spectrum and proposed fragmentation scheme of organic impurity 49.....	54
Figure 3-18: Gas chromatogram of (5E) and (5Z)-7-(1,3-benzodioxol-5-yl)-5-ethylidene-6-methyl-cyclopenta[f][1,3]benzodioxole	55
Figure 3-19: Mass spectrum and proposed fragmentation scheme of organic impurity 52.....	57
Figure 3-20: ^1H NMR spectrum of (5E) and (5Z)-7-(1,3-benzodioxol-5-yl)-5-ethylidene-6-methyl-cyclopenta[f][1,3]benzodioxole	57
Figure 3-21: Mass spectrum and molecular ion of impurity 51.....	58
Figure 3-22: GC-MS total ion chromatogram of 5-bromo-3,4-methylenedioxypropiofenone.....	59
Figure 3-23: Mass spectrum and proposed fragmentation scheme of 5-bromo-3,4-methylenedioxypropiofenone	60
Figure 3-24: ^1H NMR spectrum of 5-bromo-3,4-methylenedioxypropiofenone and identified organic impurities	60
Figure 3-25: Mass spectrum and proposed fragmentation scheme of organic impurity 53.....	61
Figure 3-26: GC-MS total ion chromatogram of methylone.....	62
Figure 3-27: Mass spectrum and proposed fragmentation scheme of methylone	63
Figure 3-28: ^1H NNMR spectrum of methylone	63
Figure 3-29: Mass spectrum and proposed fragmentation scheme of organic impurity 43.....	64
Figure 3-30: Mass spectrum and proposed fragmentation scheme of organic impurity 54.....	65
Figure 3-31: Mass spectrum and proposed fragmentation scheme of organic impurity 55.....	65
Figure 3-32: Mass spectrum of organic impurity 56 (98% quality for butylated hydroxytoluene)	65
Figure 4-1: GC-MS total ion chromatogram of 1,3-benzodioxole synthesised via Route 1	76
Figure 4-2: ^1H NMR spectrum of 1,3-benzodioxole synthesised via Route 1	76
Figure 4-3: GC-MS total ion chromatogram of 5-bromo-1,3-benzodioxole synthesised via Route 1	77
Figure 4-4: ^1H NMR spectrum of 5-bromo-1,3-benzodioxole synthesised via Route 1	77

Figure 4-5: GC-MS total ion chromatogram of safrole synthesised via Route 1	79
Figure 4-6: ^1H NMR spectrum of safrole synthesised via Route 1	79
Figure 4-7: GC-MS total ion chromatogram of 2-allyloxyphenol synthesised via Route 2	82
Figure 4-8: ^1H NMR spectrum of 2-allyloxyphenol synthesised via Route 2	83
Figure 4-9: GC-MS total ion chromatogram of 4-allylcatechol synthesised via Route 2	84
Figure 4-10: ^1H NMR spectrum of 4-allylcatechol synthesised via Route 2	84
Figure 4-11: GC-MS total ion chromatogram of safrole synthesised via Route 2	86
Figure 4-12: ^1H NMR spectrum of safrole synthesised via Route 2	87
Figure 4-13: ^1H NMR spectrum of eugenol	89
Figure 4-14: GC-MS total ion chromatogram of 4-allylcatechol synthesised via Route 3	90
Figure 4-15: ^1H NMR spectrum of 4-allylcatechol synthesised via Route 3	90
Figure 4-16: GC-MS total ion chromatogram of safrole synthesised via Route 3	92
Figure 4-17: ^1H NMR spectrum of safrole synthesised via Route 3	92
Figure 5-1: GC-MS total ion chromatogram of MDP2P synthesised via Route 1A	104
Figure 5-2: GC-MS total ion chromatogram of MDP2P synthesised via Route 2A	105
Figure 5-3: GC-MS total ion chromatogram of MDP2P synthesised via Route 3A	105
Figure 5-4: GC-MS total ion chromatogram of MDMA synthesised via Route 1A	110
Figure 5-5: GC-MS total ion chromatogram of MDMA synthesised via Route 2A	111
Figure 5-6: GC-MS total ion chromatogram of MDMA synthesised via Route 3A	111
Figure 5-7: GC-MS total ion chromatogram of isosafrole synthesised via Route 1B	117
Figure 5-8: GC-MS total ion chromatogram of isosafrole synthesised via Route 2B	117
Figure 5-9: GC-MS total ion chromatogram of isosafrole synthesised via Route 3B	118
Figure 5-10: GC-MS total ion chromatogram of MDP2P synthesised via Route 1B	122
Figure 5-11: GC-MS total ion chromatogram of MDP2P synthesised via Route 2B	123
Figure 5-12: GC-MS total ion chromatogram of MDP2P synthesised via Route 3B	123
Figure 5-13: GC-MS total ion chromatogram of MDMA synthesised via Route 1B	127
Figure 5-14: GC-MS total ion chromatogram of MDMA synthesised via Route 2B	128

Figure 5-15: GC-MS total ion chromatogram of MDMA synthesised via Route 3B	128
--	-----

List of Schemes

Scheme 1-1: Synthesis of isosafrole and piperonal from safrole	4
Scheme 1-2: Synthesis of piperonal from catechol	5
Scheme 1-3: Synthesis of MDP2P from safrole via Wacker oxidation	5
Scheme 1-4: Synthesis of MDP2P from isosafrole via peracid oxidation and acidic dehydration	6
Scheme 1-5: Synthesis of MDP2P from piperonal via condensation and oxidation	6
Scheme 1-6: Synthesis of MDP2P from piperonal via glycidic oxidation, hydrolysis and decarboxylation	6
Scheme 1-7: Synthesis of MDMA via reductive amination	7
Scheme 1-8: Synthesis of MDMA via the Leuckart reaction	7
Scheme 1-9: Synthesis MDMA·HCl from MDMA	7
Scheme 1-10: Synthesis of methylonone from 3,4-methylenedioxypropiofenone	8
Scheme 1-11: Synthesis of 3,4-methylenedioxypropiofenone from 1,3-benzodioxole and piperonal	8
Scheme 1-12: Synthesis of piperonal from vanillin	10
Scheme 1-13: Synthesis of piperonal from piperine	11
Scheme 1-14: Synthesis of safrole from eugenol	12
Scheme 1-15: Synthesis of safrole from catechol via methylenation, bromination and a Grignard reaction	12
Scheme 1-16: Synthesis of safrole from catechol via etherification, claisen rearrangement and methylenation	13
Scheme 1-17: Synthesis of methylonone from catechol	13
Scheme 1-18: Synthesis of MDMA from catechol and eugenol via a safrole intermediate	26
Scheme 3-1: Synthesis of methylonone from catechol	37
Scheme 3-2: Reaction mechanism for the synthesis of 1,3-benzodioxole from catechol	38
Scheme 3-3: Reaction mechanism for the synthesis of 3,4-methylenedioxypropiofenone from 1,3-benzodioxole	38

Scheme 3-4: Reaction mechanism for the synthesis of 5-bromo-3,4-methylenedioxypropiofenone from 3,4-methylenedioxypropiofenone	40
Scheme 3-5: Reaction mechanism for the synthesis of methylone from 5-bromo-3,4-methylenedioxypropiofenone	40
Scheme 3-6: Formation of 2-[(2-hydroxyphenoxy)methoxy]phenol and organic impurities 39 and 47.....	46
Scheme 3-7: Formation of organic impurity 46	46
Scheme 3-8: Formation of organic impurities 40 (a-c).....	47
Scheme 3-9: The synthesis of (2-hydroxyphenyl) propanoate and (2-propanoyloxyphenyl) propanoate	52
Scheme 3-10: Reaction mechanism for the formation of organic impurities 48, 49 and 50	54
Scheme 3-11: The synthesis of (5E)- and (5Z)-7-(1,3-benzodioxol-5-yl)-5-ethylidene-6-methyl-cyclopenta[f][1,3]benzodioxole	55
Scheme 3-12: Reaction mechanism for the formation of organic impurity 51	58
Scheme 3-13: Reaction mechanism for the formation of organic impurity 52 (a-b).....	58
Scheme 3-14: Formation of organic impurity 53	62
Scheme 3-15: Formation of organic impurity 54	66
Scheme 4-1: Synthesis of safrole from catechol via Route 1	70
Scheme 4-2: Reaction mechanism for the formation of the 5-bromo-1,3-benzodioxole.....	71
Scheme 4-3: The in situ formation of hypobromous acid	71
Scheme 4-4: Reaction mechanism for the synthesis of the Grignard reagent.....	71
Scheme 4-5: Reaction mechanism for the synthesis of safrole from the Grignard reagent and allyl bromide	72
Scheme 4-6: The synthesis of safrole from catechol via Route 2.	72
Scheme 4-7: Reaction mechanism for the synthesis of 2-allyloxyphenol from catechol.....	72
Scheme 4-8: Reaction mechanism for the synthesis of 4-allylcatechol from 2-allyloxyphenol ..	73
Scheme 4-9: Reaction mechanism for the synthesis of safrole from 4-allylcatechol	74
Scheme 4-10: The synthesis of safrole from eugenol via Route 3	74

Scheme 4-11: Reaction mechanism for the synthesis of 4-allylcatechol from eugenol	74
Scheme 4-12: Formation of organic impurity 57	78
Scheme 4-13: Formation of organic impurities 5 and 42	81
Scheme 4-14: Formation of organic impurities 58 and 59	81
Scheme 4-15: Origin of organic impurities 60 and 61	83
Scheme 4-16: Reaction mechanism for the formation of organic impurity 63	86
Scheme 4-17: Formation of organic impurities 64 and 65 (a-b)	88
Scheme 4-18: Formation of organic impurity 66	89
Scheme 4-19: Formation of organic impurities 67 (a-c)	91
Scheme 5-1: Synthesis of MDMA from safrole via Route A	99
Scheme 5-2: Reaction mechanism for the synthesis of MDP2P from safrole	100
Scheme 5-3: Reaction mechanism for the synthesis of MDMA from MDP2P	101
Scheme 5-4: Synthesis of MDMA from safrole via Route B	101
Scheme 5-5: Reaction mechanism for the synthesis of cis- and trans- isosafrole from safrole	101
Scheme 5-6: Reaction mechanism for the peracid oxidation of isosafrole	102
Scheme 5-7: Reaction mechanism for the acidic dehydration of isosafrole glycol to form MDP2P	102
Scheme 5-8: Synthesis of MDMA from catechol and eugenol via safrole by Routes 1A, 2A and 3A	103
Scheme 5-9: Formation of organic impurities 70 and 71 in Route 1A	109
Scheme 5-10: Formation of organic impurities 72 and 73 in Route 2A	110
Scheme 5-11: Formation of organic impurity 74 in Route 1A	115
Scheme 5-12: Formation of organic impurities 75 and 76 in Route 2A	115
Scheme 5-13: Synthesis of MDMA from catechol and eugenol via safrole by Routes 1B, 2B and 3B	116
Scheme 5-14: Formation of organic impurities 78 and 79 in Route 1B	121
Scheme 5-15: Formation of organic impurities 65 and 80 in Route 2B	121

Scheme 5-16: Formation of organic impurities 81 (a-b) in Route 2B and 3B	122
Scheme 5-17: Formation of organic impurity 84	126
Scheme 5-18: Formation of organic impurities 72 and 82 (a-b) in Route 1B	126
Scheme 5-19: Formation of organic impurity 83 in Route 2B and 3B.....	126
Scheme 5-20: Formation of organic impurity 75 in Route 2B	131

List of Tables

Table 1-1: Organic impurities in MDMA synthesised from MDP2P, safrole, isosafrole and piperonal [17, 19-21, 23, 24, 54, 61, 62].	16
Table 1-2: Organic impurities in MDMA resulting from uncontrolled precursors [31, 35, 41]	19
Table 1-3: Organic impurities from the synthesis of methylone [8, 29]	21
Table 3-1: Reaction conditions trialled for the synthesis of 5-bromo-3,4-methylenedioxypropiofenone and reaction completion (%) determined through the starting material : product O-CH ₂ -O ¹ H integration ratio.	39
Table 3-2: Organic impurities identified in 1,3-benzodioxole	43
Table 3-3: Organic impurities identified in 3,4-methylenedioxypropiofenone	49
Table 3-4: Summarised NMR data for the structural elucidation of 7-(1,3-benzodioxol-5-yl)-5-ethylidene-6-methyl-cyclopenta[f][1,3]benzodioxole	56
Table 3-5: Organic impurities identified in 5-bromo 3,4-methylenedioxypropiofenone.	61
Table 3-6: Organic impurities identified in methylone	64
Table 4-1: Reaction progress of the Claisen rearrangement of 2-allyloxyphenol	73
Table 4-2: Organic impurities identified in 5-bromo-1,3-benzodioxole synthesised via Route 1	78
Table 4-3: Organic impurities identified in safrole synthesised via Route 1	80
Table 4-4: Organic impurities identified in 2-allyloxyphenol via Route 2	82
Table 4-5: Organic impurities identified in 4-allylcatechol synthesised via Route 2	85
Table 4-6: Organic impurities identified in safrole synthesised via Route 2	87
Table 4-7: Organic impurities identified in 4-allylcatechol synthesised via Route 3	91
Table 4-8: Organic impurities identified in safrole synthesised via Route 3	93
Table 4-9: Comparison of organic Impurities identified in safrole synthesised via Route 1, 2 and 3.	94
Table 5-1: Organic impurities identified in MDP2P synthesised via Route 1A, 2A and 3A	106
Table 5-2: Organic impurities identified in MDMA synthesised via Route 1A, 2A and 3A.	112
Table 5-3: Organic impurities identified in isosafrole synthesised via Route 1B, 2B and 3B	119

Table 5-4: Organic impurities identified in MDP2P synthesised via Route 1B, 2B and 3B	124
Table 5-5: Organic impurities identified in MDMA synthesised via Route 1B, 2B and 3B	129
Table 5-6: Organic impurities identified in MDMA that result from use of the 'pre-precursors' catechol and eugenol	132
Table 5-7: Organic Impurities identified in MDMA that result from synthesis from safrole	136

List of Equations

Equation 1-1: The calculation of isotope ratios	24
---	----

List of Abbreviations

APAAN	<i>alpha</i> -Phenylacetoacetonitrile
ATS	Amphetamine type stimulant
DIBAH	Diisobutylaluminium hydride
GC-MS	Gas chromatography - mass spectrometry
HPLC	High performance - liquid chromatography
LC-MS/MS	Liquid chromatography tandem mass spectrometry
MDA	3,4-Methylenedioxyamphetamine
MDMA	3,4-Methylenedioxymethamphetamine
MDMA·HCl	3,4-Methylenedioxymethamphetamine hydrochloride
MDP2NP	3,4-Methylenedioxyphenyl-2-nitropropene
MDP2P	3,4-Methylenedioxyphenyl-2-propanone
MMDMG	Methyl 3-[3',4'-(methylenedioxy)phenyl]-2-methyl glycidate
MW	Molecular weight
NMR	Nuclear magnetic resonance
NPS	New psychoactive substances
P2P	1-Phenyl-2-propanone
PMA	<i>p</i> -Methoxymethamphetamine

List of Publications

Journal Articles

Erin Heather, Ronald Shimmon and Andrew McDonagh. Organic impurity profiling of 3,4-methylenedioxymethamphetamine (MDMA) synthesised from catechol and eugenol via 4-allylcatechol. *Forensic Science International* 309 (2020) 110176.

Erin Heather, Adam Bortz, Ronald Shimmon and Andrew McDonagh. Synthesis and organic impurity profiling of methylone and its precursors. *Drug Testing and Analysis* 9 (2017) 436 – 445.

Erin Heather, Ronald Shimmon and Andrew McDonagh. Organic impurity profiling of 3,4-methylenedioxymethamphetamine (MDMA) synthesised from catechol. *Forensic Science International* 248 (2015) 140 – 147.

Rebecca Tam, **Erin Heather**, Ronald Shimmon, Brandon Lam, Andrew McDonagh. Synthesis and organic impurity profiling of 4-methoxymethamphetamine hydrochloride and its precursors. *Forensic Science International* 272 (2017) 184 – 189.

Conference Presentations

Organic Impurity Profiling of 3,4-Methylenedioxymethamphetamine (MDMA) Synthesised from Catechol, 2014, 22nd International Symposium on the Forensic Sciences of the Australian and New Zealand Forensic Science Society

Organic Impurity Profiling of Methylone Synthesized from Catechol, 2015, 7th European Academy of Forensic Science Conference

Organic Impurity Profiling of the MDMA Precursor Safrole and Methylone Synthesised from Catechol, 2016, 23rd International Symposium on the Forensic Sciences of the Australian and New Zealand Forensic Science Society

Abstract

This work examines the organic impurity profiles of 3,4-methylenedioxymethamphetamine (MDMA) and its analogue methylone that were synthesised from uncontrolled ‘pre-precursors’. Methylone was synthesised from catechol by one synthetic route. Safrole was synthesised from catechol by two synthetic routes (Routes 1 and 2) and from eugenol by one synthetic route (Route 3). MDMA was synthesised from catechol- and eugenol-derived safrole via two routes (Routes A and B), which resulted in the synthesis of MDMA from catechol via four routes (Routes 1A, 1B, 2A and 2B) and from eugenol via two routes (Routes 3A and 3B).

Five organic impurities were identified in methylone, and fourteen organic impurities were identified in the three intermediate compounds. Neither the catechol precursor nor the 1,3-benzodioxole intermediate could be identified based on the impurities detected in methylone using standard techniques, which demonstrated limitations in the determination of the precursor chemical and synthetic pathways used.

Eight organic impurities were identified in safrole synthesised from catechol via Routes 1 and 2, and seven organic impurities in safrole synthesised from eugenol via Route 3. Importantly, nine impurities had not previously been reported in literature. Seven, four and seven route specific impurities were identified in safrole from Routes 1, 2 and 3, respectively. The route specific impurities indicated both the use of the ‘pre-precursors’ catechol and eugenol, and the route used to synthesise safrole from the respective ‘pre-precursor’.

Thirteen organic impurities were identified in MDMA synthesised by Route 1A, ten organic impurities in MDMA from Route 1B, twelve organic impurities in MDMA from Routes 2A and 2B, and eleven organic impurities in MDMA from Routes 3A and 3B. Importantly, thirteen impurities had not previously been reported in literature. Six impurities in MDMA from Route 1A, four impurities in MDMA from Routes 1B, 2A, and 2B, and three impurities in MDMA from Routes 3A and 3B were considered specific to the use of catechol- or eugenol-derived safrole.

The route specific impurities identified in MDMA indicated that the ‘pre-precursors’ catechol and eugenol were used in the respective synthetic pathways. The route specific impurities identified in MDMA also indicated the route used to synthesise safrole from the respective ‘pre-precursor’, and the route used to synthesise MDMA from the safrole intermediate. Thus, the use of the ‘pre-precursors’ catechol and eugenol, and the synthetic routes that were used in its preparation, could be ascertained by the organic impurity profiling of MDMA under the conditions used here.

Chapter 1: Introduction

Chapter 1: Introduction

1.1 MDMA and Analogues

The amphetamine type stimulant (ATS) MDMA, shown in Figure 1-1, is the traditional active ingredient in the drug colloquially referred to as 'ecstasy'. The supply of MDMA has increased in recent years, with high purity MDMA tablets and powder/crystals becoming available on the illicit drug market [1, 2]. MDMA is a psychotropic substance that may invoke feelings of euphoria, increased energy and increased self-esteem in the user [3, 4]. As such, 'ecstasy' is typically used by young people in high-income countries as a 'club drug' [2]. There are three main forms of 'ecstasy' currently available: tablets or pills that have a very high MDMA content, powder or crystals of highly pure MDMA, and tablets that contain little to no MDMA [1, 5].

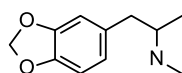


Figure 1-1: Chemical structure of MDMA

There was a shortage of MDMA in the late 2000s, and the illicit drug market was unable to meet the unchanged demand for 'ecstasy' [2]. This MDMA shortage has been attributed to increased international control of the precursor chemicals traditionally used to synthesise MDMA [1, 6]. As a result, 'ecstasy' tablets that contained little to no MDMA began to be sold on the illicit drug market [1, 2]. These tablets typically contained substitute non-controlled chemicals, including new psychoactive substances (NPS) [1, 5]. Analogues of MDMA, such as methylone shown in Figure 1-2, comprised a portion of the substitute NPS used in 'ecstasy' tablets.

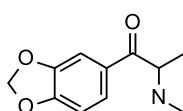


Figure 1-2: Chemical structure of the MDMA analogue methylone

Methylone is a β -ketone analogue of MDMA and one of the most commonly used synthetic cathinones [7]. Methylone was patented in 1996 by Jacob and Shulgin as an anti-depressant and treatment for symptoms of Parkinson's disease [8, 9]. The psychoactive effects of methylone are similar to those of MDMA and include stimulant and hallucinogenic properties; the β -ketone group does not appear to remove amphetamine-like activity and potency [10].

The global 'ecstasy' market has seemingly recovered in recent years, with 14 tonnes of 'ecstasy' seized internationally in 2016, almost triple the quantity seized in 2012 [2]. The increased prevalence of MDMA in the illicit drug market is particularly evident in Europe, where industrial-scale MDMA manufacturing laboratories and tablets with a very high MDMA content have been

seized [1]. This resurgence of MDMA indicates that clandestine laboratory operators have circumvented the international controls placed on the main MDMA precursor chemicals. Clandestine laboratory operators may be obtaining these precursor chemicals through more sophisticated means, or may be using uncontrolled precursors, including alternative precursors and 'pre-precursors' [6].

1.1.1 Legislation

The United Nations placed MDMA under international control by listing it in Schedule I of the *Convention of Psychotropic substances 1971* in 1986. This limits the application of MDMA to scientific or medical purposes that are controlled or approved of by the Government of countries that have ratified this convention, and requires licensing, restricted quantities and suitable records for the manufacture, trade and use. The United Nations also recently placed methylone under international control by including it in Schedule II of the *Convention of Psychotropic substances 1971* in 2015 [11].

The *Convention against Illicit Traffic in Narcotic and Psychotropic Substances 1988* was implemented by the United Nations to control the precursors used in the synthesis of illicit substances and equipment that is used in the manufacturing process. The four main precursors of MDMA (MDP2P, safrole, isosafrole and piperonal; shown in Figure 1-3) are controlled substances under this convention and their use is therefore monitored.

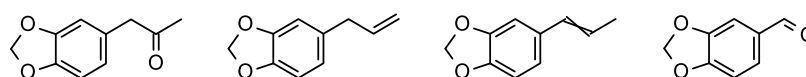


Figure 1-3: Chemical structures of MDP2P, safrole, isosafrole and piperonal

Australia ratified the United Nations *Convention of Psychotropic Substances 1971* in 1982 and the *Convention Against Illicit Traffic in Narcotic and Psychotropic Substances 1988* in 1992. The Australian Federal Legislation lists MDMA as a controlled substance in Schedule 3, and as a border-controlled substance in Schedule 4 of the *Criminal Code Regulations 2002*. MDP2P, safrole, isosafrole and piperonal are listed as controlled and border-controlled precursors in Section 5C and Section 5F, respectively, of the *Criminal Code Regulations 2002*.

Under Australian federal legislation, a drug analogue of a listed controlled or border-controlled drug is also considered a controlled or border-controlled drug. Section 301.9 of the *Criminal Code Act 1995* lists the structural modifications that define the meaning of a drug analogue. However, as a result of the increase in NPS, the lists of controlled and border-controlled drugs were updated and moved from the *Criminal Code Act 1995* to Schedule 3 and 4, respectively, of

the *Criminal Code Regulations 2002* in 2013. Methylone was listed in Schedule 3 of the *Criminal Code Regulations 2002* at this time.

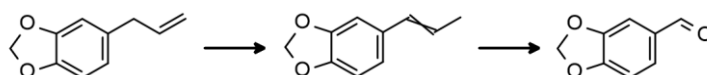
MDMA, MDP2P, safrole, isosafrole and piperonal are controlled substances in the legislation of all states and territories of Australia. For example, in New South Wales, MDMA and MDP2P are listed as controlled substances in Schedule I of the *Drugs Misuse and Trafficking Act 1985 (NSW)*, and MDP2P, safrole, isosafrole and piperonal are listed as controlled precursors under the *Drug Misuse and Trafficking Regulation 2011*. Methylone is also listed as a controlled substance in the legislation of New South Wales, Australian Capital Territory, Victoria, Queensland, South Australia, Tasmania, and the Northern Territory, however, is not listed as a controlled substance in the legislation of Western Australia.

1.1.2 Synthesis of MDMA

The synthesis of MDMA for the production of ‘ecstasy’ is known to occur in clandestine laboratories in Asia, North America, Oceania, South America, and notably in Europe, where industrial scale laboratories have been seized [1]. In 2014 – 2016, 35 clandestine laboratories were detected in Australia that were manufacturing MDMA [2]. The techniques and procedures for the synthesis of MDMA from traditional precursors MDP2P, safrole, isosafrole and piperonal are available in numerous freely accessible documents on the internet [12].

1.1.2.1 Precursors

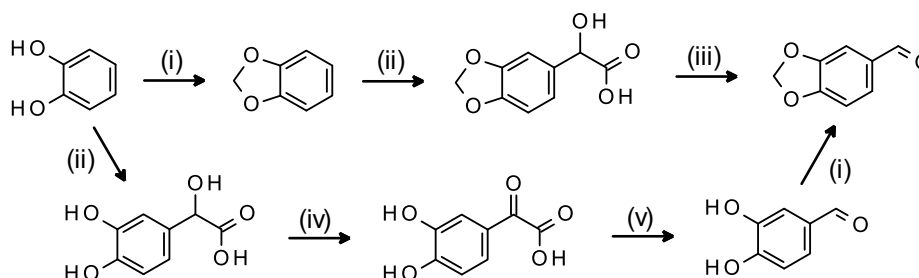
The most common precursor in the synthesis of MDMA is MDP2P, however, the diversion of MDP2P for illicit purposes can be problematic for clandestine laboratories due to its limited legitimate applications [1, 4, 6, 13]. Therefore, MDP2P is often synthesised in clandestine laboratories from the precursors safrole, isosafrole and piperonal. Safrole, isosafrole and piperonal have legitimate applications in the chemical and pharmaceutical industries for the production of fragrances, flavours and some insecticides and, therefore, could be obtained by clandestine laboratories through the diversion of legitimate supplies [1, 6, 14].



Scheme 1-1: Synthesis of isosafrole and piperonal from safrole

Safrole is produced through extraction from sassafras oil, with extraction yields of approximately 90% [14, 15]. Sassafras oil was first extracted through steam distillation of the *Sassafras albidum* bark, however, production has since moved towards utilising *Ocotea pretiosa* in Brazil and *Cinnamomum camphora* in China that have a higher concentration of oil in their bark [14].

Industrial isosafrole can be synthesised from safrole via an isomerisation reaction, and industrial piperonal from isosafrole via an oxidation reaction, as shown in the synthetic pathway in Scheme 1-1 [1, 15, 16]. Piperonal is also industrially synthesised from catechol via the synthetic pathways shown in Scheme 1-2 [16].

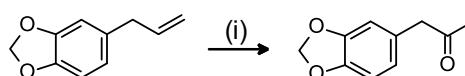


Scheme 1-2: Synthesis of piperonal from catechol
(i) CH_2Cl_2 (ii) OHCCOOH (iii) HNO_3 (iv) CuO (v) H^+

The current worldwide industrial dependence on *Ocotea pretiosa* and *Cinnamomum camphora* for safrole production is unsustainable [14]. The production of safrole is destructive, requiring the felling of these trees to process the bark for the extraction of sassafrass oil. There has been significant reduction in the numbers of *Ocotea pretiosa* and *Cinnamomum camphora* plants [14]. In Brazil, there has been no significant replanting of the *Ocotea pretiosa* since the production of safrole began and, as a result of this depletion, regulations were put in place that limit harvesting. The quantities of safrole exported from China are also expected to reduce due to the depletion of the *Cinnamomum camphora* plants and increasing internal requirements. The use synthetic safrole will therefore become attractive to industries and clandestine laboratories alike as the supply of natural safrole decreases and price increases.

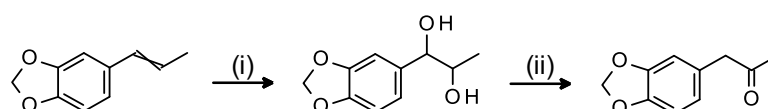
1.1.2.1 Synthetic Pathways

There are numerous synthetic pathways utilised by clandestine laboratories in order to synthesise MDP2P from safrole, isosafrole and piperonal [1, 17, 18]. The Wacker oxidation reaction is used to synthesise MDP2P from safrole in one step, as shown in Scheme 1-3 [19]. This synthetic pathway was discovered in a seized clandestine laboratory in South Australia, where water, p-benzoquinone and palladium chloride were utilised as reagents and methanol was utilised as a solvent [19].



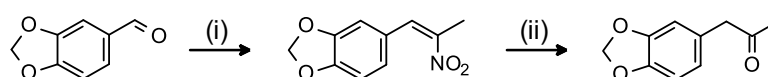
Scheme 1-3: Synthesis of MDP2P from safrole via Wacker oxidation
(i) H_2O , PdCl_2 , *p*-benzoquinone

The synthesis of MDP2P from isosafrole is a two-step reaction process, as shown in Scheme 1-4 [4, 20]. The first stage of this reaction is the peracid oxidation of isosafrole to form the glycol intermediate. This glycol intermediate then undergoes acidic dehydration to form MDP2P. Safrole can also be utilised as a precursor for this reaction pathway, as isosafrole can be synthesised in one step via an isomerisation reaction (Scheme 1-1).



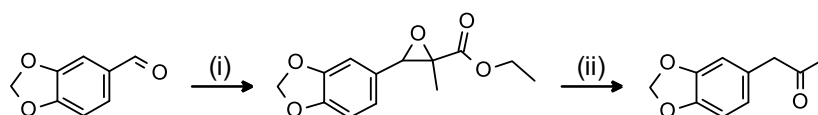
*Scheme 1-4: Synthesis of MDP2P from isosafrole via peracid oxidation and acidic dehydration
(i) H_2O_2 , HCOOH (ii) H_2SO_4*

The synthetic pathway shown in Scheme 1-5 is the most common method used to synthesise MDP2P from piperonal [4, 17]. In this route, piperonal is reacted with nitroethane in a condensation reaction to form 3,4-methylenedioxyphenyl-2-nitropropene (MDP2NP). MDP2P is then synthesised via the oxidation of MDP2NP.



*Scheme 1-5: Synthesis of MDP2P from piperonal via condensation and oxidation
(i) $\text{CH}_3\text{CH}_2\text{NO}_2$, cyclohexylamine (ii) Fe , CH_3COOH*

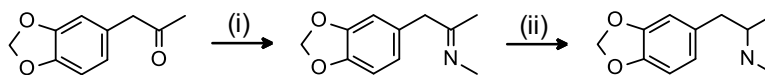
MDP2P can also be synthesised from piperonal via a second synthetic pathway, which is shown in Scheme 1-6 [1, 18]. The first stage of this reaction is the glycidic oxidation of piperonal to form the intermediate for 3,4-MDP2P methyl glycidate, which subsequently undergoes hydrolysis and decarboxylation to form MDP2P. This synthetic route was developed by clandestine laboratory operators presumably as 3,4-MDP2P methyl glycidate is not under international control. This is an example of how clandestine laboratory operators will adapt their methodologies in order to prevent detection and circumvent international controls.



*Scheme 1-6: Synthesis of MDP2P from piperonal via glycidic oxidation, hydrolysis and decarboxylation
(i) NaOC_2H_5 , $\text{CH}_3\text{CHBrCOOC}_2\text{H}_5$ (ii) 1. MeOH , H_2O , NaOH 2. Cu , Δ*

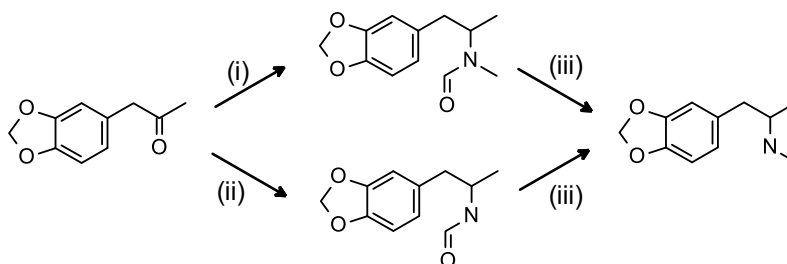
The reductive amination of MDP2P, shown in Scheme 1-7, is the most common method used to synthesise MDMA in clandestine laboratories [17, 21]. The reducing agents most commonly utilised are sodium borohydride, an aluminium / mercury amalgam or hydrogen gas with a platinum catalyst [22]. Reductive amination using sodium borohydride is typically conducted below room temperature to prevent the formation of unwanted by-products. An

aluminium/mercury amalgam can be simply prepared through the dissolution of aluminium foil in mercuric chloride. Hydrogen gas must be at an elevated pressure of 3 - 4 bar when used for the synthesis of MDMA.



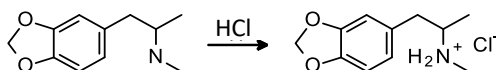
*Scheme 1-7: Synthesis of MDMA via reductive amination
(i) CH_3NH_2 (ii) NaBH_4 or Al(Hg) or H_2/Pt*

MDMA can also be synthesised from MDP2P via a Leuckart reaction, shown in Scheme 1-8 [17, 23]. This method, however, is less common than the reductive amination of MDP2P in clandestine laboratories [21]. The first stage of the synthetic route is the reaction of MDP2P with formic acid and either N-methylformamide or formamide. The intermediate of the reaction is then hydrolysed with either a reducing agent, such as lithium aluminium hydride, or a strong acid, such as concentrated hydrochloric acid.



*Scheme 1-8: Synthesis of MDMA via the Leuckart reaction
(i) HCONHCH_3 , HCOOH (ii) HCONH , HCOOH (iii) HCl or LiAlH_4*

Clandestine laboratories will typically convert MDMA into a salt in the final step of the production of ecstasy. This is advantageous as it permits the distribution of ecstasy in tablet or powder form instead of an organic liquid state. The hydrochloride salt of MDMA ($\text{MDMA} \cdot \text{HCl}$) is the most common form detected, though phosphate salts have also been identified [22]. The most common method of synthesis involves the dissolution of concentrated hydrochloric acid and MDMA into a solvent system, as shown in Scheme 1-9 [4]. $\text{MDMA} \cdot \text{HCl}$ can also be formed by bubbling hydrogen chloride gas through a solution of MDMA [24].



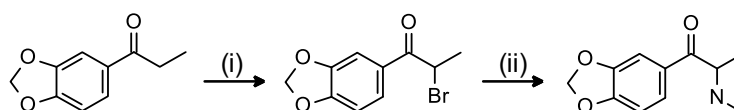
Scheme 1-9: Synthesis $\text{MDMA} \cdot \text{HCl}$ from MDMA

1.1.3 Synthesis of Mephylone

The methods used to synthesise racemic synthetic cathinones are appropriate for the synthesis of mephylone. The main precursor used for racemic synthetic cathinones is an appropriately

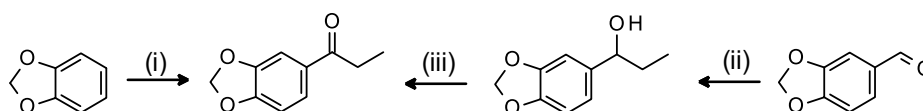
ring-substituted propiophenone [25], which in the case of methylone is 3,4-methylenedioxypropiphenone [8, 26, 27]. 3,4-Methylenedioxypropiphenone can in turn be synthesised from the controlled precursor piperonal or 1,3-benzodioxole [8], which is monitored under Category II of the *Code of Practice for the Supply Diversion into Illicit Drug Manufacture* [28]. Therefore, chemical suppliers require non-account customers are sign an end user declaration when purchasing 1,3-benzodioxole [28].

The first reported synthesis of methylone was by Jacob and Shulgin in 1996, which utilised both piperonal and 1,3-benzodioxole as precursors and a 3,4-methylenedioxypropiphenone intermediate [8]. Methylone was synthesised from 3,4-methylenedioxypropiphenone via a two-step process involving the bromination of 3,4-methylenedioxypropiphenone and the amination of 5-bromo-3,4-methylenedioxypropiphenone, as shown in Scheme 1-10. The reaction conditions in this synthetic pathway have been modified in subsequent reported syntheses to improve efficiencies, such as the use of potassium bromide in addition to copper (II) bromide in the bromination reaction [26, 27].



Scheme 1-10: Synthesis of methylone from 3,4-methylenedioxypropiphenone
(i) CuBr_2 or CuBr_2 , KBr (ii) CH_3NH_2

The intermediate 3,4-methylenedioxypropiphenone was synthesised from the precursors piperonal and 1,3-benzodioxole through the synthetic pathways shown in Scheme 1-11 [8]. The synthesis of 3,4-methylenedioxypropiphenone from piperonal is a two-step process that involves a Grignard reaction between piperonal and ethyl magnesium chloride, and the subsequent oxidation of 1-(1,3-benzodioxol-5-yl)propan-1-ol. The synthesis of 3,4-methylenedioxypropiphenone from 1,3-benzodioxole is a one-step process that involves the acylation of 1,3-benzodioxole [8, 29], and is stated to be the preferential route by Jacob and Shulgin [8].



Scheme 1-11: Synthesis of 3,4-methylenedioxypropiphenone from 1,3-benzodioxole and piperonal
(i) $(\text{CH}_3\text{CH}_2\text{CO})_2\text{O}$, I or $\text{CH}_3\text{CH}_2\text{COCl}$, ZnCl_2 (ii) CH_3MgCl (iii) $\text{K}_2\text{Cr}_2\text{O}_7$, H_2SO_4

1.2 Synthesis of MDMA and Methyldone from Uncontrolled Precursors

The use of uncontrolled precursors has gained popularity with clandestine laboratory operators for the synthesis of ATS [6]. Pseudoephedrine and ephedrine, in bulk form or extracted from pharmaceutical preparations, were the main precursors originally used for the synthesis of methamphetamine [1]. However, clandestine laboratory operators adapted when stricter controls were placed on these pharmaceutical chemicals. The synthesis of methamphetamine from uncontrolled precursors, including *alpha*-phenylacetoacetonitrile (APAAN), esters of phenylacetate, phenylacetamide, benzylchloride, styrene, benzaldehyde and benzyl cyanide, via 1-phenyl-2-propanone (P2P) became evident and is now the primary methodology detected in the United States of America [1, 6, 30]. The use of uncontrolled precursors is also a potentially feasible alternative for other synthetic drugs, including amphetamine, MDA, MDMA and NPS.

The main precursors to MDMA are under international control under the United Nations Convention against Illicit Traffic in Narcotic Drugs and Psychotropic Substances of 1988. Safrole, isosafrole and piperonal can be diverted from legitimate sources, however, MDP2P does not have licit sources of use. The shortage of MDMA that occurred in the late 2000's has been attributed to improved international control of the aforementioned precursor chemicals [6]. As such, the use of uncontrolled precursors, including alternative precursors and 'pre-precursors', is an attractive option for clandestine laboratory operators [1, 6].

An alternative precursor that has gained popularity for the synthesis of MDMA is 3,4-MDP2P methyl glycidate, which can easily be converted into the traditional precursor MDP2P [1, 6, 18]. The first reported seizure of 3,4-MDP2P methyl glycidate was in Port Botany, Sydney, Australia in 2004, and it has since been seized in the Netherlands, Slovakia, Belgium, Poland, Estonia and Denmark [6, 18]. The primary rationale for 3,4-MDP2P methyl glycidate is to circumvent the national and international controls in place around the illicit trafficking of precursor chemicals [1, 6]. However, the synthesis of 3,4-MDP2P methyl glycidate requires access to the controlled precursor piperonal [1, 6, 18].

The use of 'pre-precursors' eliminates the requirement for clandestine laboratory operators to obtain internationally controlled precursor chemicals. This is an attractive option for clandestine laboratory operators as, in addition to reducing the risks of trafficking controlled precursor chemicals, it overcomes the restrictions associated with obtaining traditional precursors and reduces the detection risks related to the production of illicit drugs.

1.2.1 Vanillin

Vanillin (Figure 1-4) is a common, uncontrolled chemical that is synthesised on an industrial scale of ~15,000 tonnes per year [31]. Natural vanillin is extracted from vanilla beans although synthetic vanillin is more practical for industrial use due to the expense and limited availability of vanilla beans. Vanillin is industrially synthesised from waste sulfite liquors or guaiacol [16]. There are numerous applications of vanillin in the cosmetic, food, pharmaceutical and chemical industries [16, 32]. Vanillin is commercially available in tonnage quantities and, therefore, can be obtained through diversion of supplies.

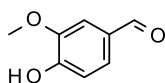
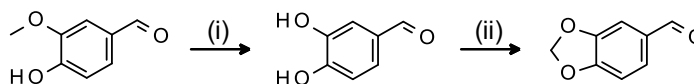


Figure 1-4: Chemical structure of vanillin

Piperonal can be synthesised from vanillin in a two-step synthetic route, making it a viable 'pre-precursor' for the synthesis of MDMA. This synthetic pathway, shown in Scheme 1-12, involves the demethylation of vanillin and a subsequent methylenation reaction of the resulting product. The associated experimental procedures for this route are readily accessible on websites dedicated to the synthesis of illicit drugs [33, 34]. This synthetic pathway was also used in the preparation of MDMA during the organic impurity profiling studies by Gallagher *et al.* [31] and Heather *et al.* [35].



Scheme 1-12: Synthesis of piperonal from vanillin
(i) pyridine, $AlCl_3$ or nitrobenzene, $AlBr_3$ (ii) CH_2X_2 , base

1.2.2 Piperine

Piperine (Figure 1-5) is the alkaloid responsible for taste and aroma in the common spice pepper, and comprises roughly 3 - 9% of the pepper mass [36, 37]. Piperine can be extracted from pepper by heat-reflux extraction, Soxhlet extraction, supercritical fluid extraction, microwave-assisted extraction, or ultrasound-assisted extraction [31, 35, 36, 38]. The concentration of piperine extracted from pepper using these techniques is variable, ranging from 2 - 5% of the pepper mass [31, 35, 36, 38]. Piperine can also be purchased in small quantities from chemical suppliers and within dietary supplements.

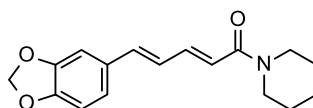
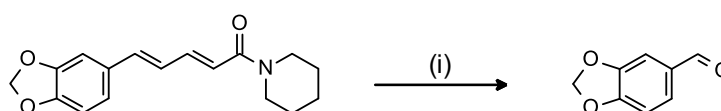


Figure 1-5: Chemical structure of piperine

Piperine is a viable 'pre-precursor' for MDMA, as piperonal can be synthesised from piperine in one-step through oxidative cleavage. The associated experimental procedures for the extraction and oxidative cleavage of piperine are readily accessible on websites dedicated to the synthesis of illicit drugs [39, 40]. This synthetic pathway was also used in the preparation of MDMA during the organic impurity profiling studies by Gallagher *et al.* [31], Heather *et al.* [35] and Plummer *et al.* [41]. In these studies, oxidative cleavage was performed using potassium permanganate [31], ozone [31, 35], and ruthenium chloride with a co-oxidant [41].



Scheme 1-13: Synthesis of piperonal from piperine.
(i) KMnO_4 or O_3 or RuCl_3 , HKO_5S

1.2.3 Eugenol

Eugenol (Figure 1-6) is the principal essential oil in clove oil, and is responsible for its aroma and antiseptic properties [15]. Clove oil can be extracted from clove buds in yields of 15-20% (75-85% eugenol), from clove stems in yields of approximately 5% (83-92% eugenol), and from clove leaves in yields of 2-3% (80-92% eugenol) [15]. Eugenol is also present in cinnamon leaf oil (70-83%), pimento oil (75-90%), bay oil (42-56%) and basil oil (2-15%) [15]. Industrially, eugenol is extracted and purified from clove leaf oil through acid/base extraction and steam distillation [16]. Eugenol can also be purchased from chemical suppliers, however, sales of eugenol are monitored due to its listing in Category II of the *Code of Practice for the Supply Diversion into Illicit Drug Manufacture* [28].

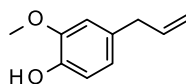
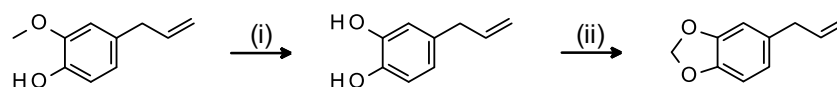


Figure 1-6: Chemical structure of eugenol

Safrole can be synthesised from eugenol in a two-step synthetic route, making it a viable 'pre-precursor' for the synthesis of MDMA. This synthetic pathway, shown in Scheme 1-14, involves the demethylation of eugenol and the subsequent methylenation of the resulting product. The associated experimental procedures for this route are readily accessible on websites dedicated to the synthesis of illicit drugs [33, 34, 42]. The experimental procedures for the synthesis of

piperalon from vanillin are also applicable to the synthesis of safrole from eugenol, as both synthetic routes involve a demethylation and subsequent methylenation reaction.



Scheme 1-14: Synthesis of safrole from eugenol
(i) AlI_3 or pyridine HCl or LiPPh_2 or LiCl (ii) CH_2Cl_2 , NaOH

1.2.4 Catechol

Catechol (Figure 1-7) is an uncontrolled, common chemical reagent that is synthesised on an industrial scale of ~20,000 tonnes per year [43]. Industrial synthesis most commonly involves the hydroxylation of phenol [43]. Catechol has significant industrial applications in the synthesis of fragrances, pesticides, pharmaceuticals and dyes [43]. It is commercially available in tonnage quantities and, therefore, can be obtained through diversion of supplies for use in illicit operations.

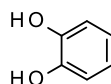
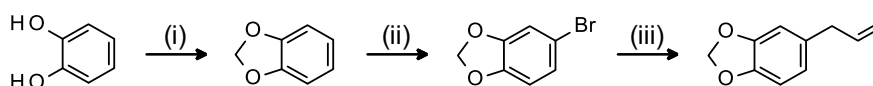


Figure 1-7: Chemical structure of catechol

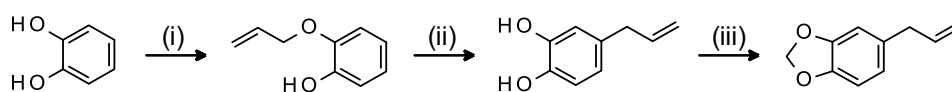
Catechol is a viable 'pre-precursor' for MDMA, which has been investigated as the starting material for the synthesis of safrole in academic publications [44] and on websites dedicated to the synthesis of illicit drugs [12]. In research by Lin *et al.* [44], safrole was synthesised from catechol in a three-step reaction pathway involving a methylenation reaction, a bromination reaction and a Grignard reaction (Scheme 1-15). This route was also used by Heather *et al.* [35] in an organic impurity profiling study. This synthetic pathway and associated experimental procedures are readily accessible on the rhodium archives [45]. While these sources utilise the same synthetic pathway, there is some variation in the reaction conditions.



Scheme 1-15: Synthesis of safrole from catechol via methylenation, bromination and a Grignard reaction
(i) CH_2Br_2 or CH_2Cl_2 , NaOH (ii) NBS or Br_2 or HBr , H_2O_2 (iii) 1. Mg 2. $\text{CH}_2\text{CHCH}_2\text{Br}$, CuI or DIBAL [35, 44, 45]

The synthetic pathway shown in Scheme 1-16 can also be used to synthesise safrole from catechol. In this route, the required methylenation reaction is performed in the final step of the reaction pathway, unlike in the previous route (Scheme 1-15) where it was performed in the first step. Catechol is first reacted with allyl bromide in an etherification reaction and the resulting

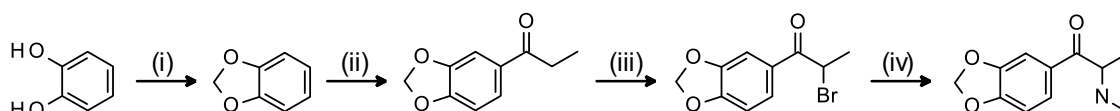
product undergoes a base-catalysed Claisen rearrangement. The experimental procedures for this synthetic pathway are readily accessible on the website *Rhodium Archives* [33, 46, 47].



Scheme 1-16: Synthesis of safrole from catechol via etherification, claisen rearrangement and methylenation
(i) K_2CO_3 , CH_2CHCH_2Br (ii) Δ , $NaOCH_2CH_3$ (iii) CH_2Cl_2 , $NaOH$

Catechol is also a viable 'pre-precursor' for the synthesis of MDMA via a piperonal intermediate. Piperonal is industrially synthesised from catechol via the synthetic pathways shown in Scheme 1-2 [16], and these production processes could be adapted and utilised in a clandestine laboratory setting. The synthesis of piperonal from catechol through a piperonyl chloride or protocatechualdehyde intermediate has also been investigated on websites dedicated to the synthesis of illicit drugs, with associated experimental procedures readily accessible [33].

The synthesis of methylone from catechol is also a viable synthetic pathway. The methylone precursor, 1,3-benzodioxole, can be synthesised from the uncontrolled precursor catechol in one step, which is advantageous for clandestine laboratory operators. There are numerous readily available sources from which methods for the synthesis of 1,3-benzodioxole from catechol can be obtained [12]. The synthetic pathway, shown in Scheme 1-17, was used in an organic impurity profiling study by Bortz *et al.* [29].



Scheme 1-17: Synthesis of methylone from catechol
(i) CH_2Cl_2 , K_2CO_3 (ii) CH_3CH_2COCl , $ZnCl_2$ and $(CH_3CH_2CO)_2O$, I (iii) $CuBr_2$, KBr (iv) CH_3NH_2

1.3 Chemical Profiling

When law enforcement agencies seize illicit drugs, their physical and chemical characteristics are often analysed. Thus, illicit drug profiling generates intelligence information for law enforcement agencies, which complements intelligence gathered through other traditional policing approaches [48, 49]. Physical profiling examines the physical forensic aspects of illicit drugs, such as appearance and packaging. Valuable intelligence can be gained from this physical examination; for example, connections between seizures may be evident due to a mark on 'ecstasy' tablets or heroin blocks which resulted from an imperfection in the press used [48].

Chemical profiling examines the chemical forensic aspects of illicit drugs. The chemical profiles of cultivated or semi-cultivated illicit drugs, such as cannabis, heroin and cocaine, is dependent

on the environmental conditions where the plant was grown [48]. The soil, climate, altitude, and distance from the coast affect the plant's internal chemistry, and thus the chemical profile of the illicit drug [48]. The chemical profiles of synthetic drugs, such as ATS and NPS, is dependent on the method of manufacture, including the identity and source of the precursor chemical and the synthetic methods that are used [17]. Therefore, the analysis of chemical profiles can reveal details pertaining to the origin and/or manufacture of illicit drugs, which in turn can provide information regarding connections between seizures, the supply sources of relevant chemicals, and drug trafficking routes [17, 30, 48].

The chemical profiling of illicit drugs provides law enforcement agencies with strategic and tactical intelligence, with the aim of identifying and disrupting drug trafficking organisations [48, 50]. Tactical intelligence is investigation specific and involves identifying links between different seizures and/or criminal organisations [48, 49]. Strategic intelligence relates to the behavioural patterns and environmental influences of criminal organisations in a broader context [49]. For the chemical profiling of illicit drugs, this involves identifying the geographical origin of cultivated or semi-cultivated drugs and identifying the manufacturing processes of synthetic drugs [48, 50]. Strategic intelligence can also influence policy decisions, such as the regulation of industrial chemicals and harm minimisation strategies [48, 49].

The chemical profiles of synthetic drugs can incorporate organic impurities, inorganic impurities and isotope ratios. The enantiomeric composition can also comprise a portion of the chemical profile of chiral synthetic drugs, such as methamphetamine [30]. Recent research indicates that the analysis of organic impurities alone can provide adequate information for intelligence purposes [51]. The use of a single analytical technique is advantageous for law enforcement agencies, who are required to generate valuable but timely intelligence [51]. The examination of additional chemical profile components, however, is of significant value when a high-purity synthetic drug is seized that contains few to no organic impurities [30, 52, 53].

There has been significant chemical profiling performed on seized MDMA tablets, and on MDMA synthesised from MDP2P, safrole, isosafrole and piperonal in a research laboratory. This analysis has included organic impurity profiling, inorganic impurity profiling and isotope ratio analysis. There has, however, only been limited organic impurity profiling of methylone, presumably as it is a relatively new illicit drug, and of MDMA that has been synthesised from uncontrolled 'pre-precursors'. Ongoing relevant research is required to adapt to the changing manufacturing techniques in the illicit drug market [50], and therefore further research into the chemical profiles of these substances is of significant interest to law enforcement agencies.

1.3.1 Organic Impurity Profiling

Organic impurities can be introduced during the synthesis of synthetic drugs through precursors, intermediates or reaction by-products [54]. Synthetic drugs prepared using a particular synthetic route are expected to have similar organic impurity profiles [55] and, therefore, the detection and identification of these impurities can provide valuable information. The precursors and synthetic route used to synthesise a particular synthetic drug may be determined through the identification of route specific organic impurities [17].

Organic impurities can also be introduced to a synthetic drug post synthesis in the form of diluents, adulterants and contaminants [17, 51]. Diluents and adulterants, such as lactose, caffeine and paracetamol, are readily available and are added to reduce the mass of the synthetic drug required for a tablet. Contaminants often include additional illicit synthetic drugs, due to multiple substances synthesised in one clandestine laboratory [56, 57], or lubricants, added for tableting purposes [55]. The identification of these organic impurities can link different seizures together or link a seizure to a specific clandestine laboratory. They do not, however, provide any significant information about the synthetic process and, thus, are not investigated in the scope of this project.

Organic impurity profiling is typically performed using gas chromatography - mass spectrometry (GC-MS), with comparable analytical methods used by law enforcement agencies in Australia, some European countries and the United States of America [48, 58, 59]. This is advantageous as it can facilitate the international exchange of data and intelligence, which is necessary to interpret the global illicit drug market [30, 48]. Additional analytical techniques including high performance - liquid chromatography (HPLC), nuclear magnetic resonance (NMR) spectroscopy, ultraviolet spectroscopy, and infrared spectroscopy can also be used for the analysis of organic impurities in synthetic drugs [30, 48, 60].

1.3.1.1 MDMA

The organic impurity profiling of seized MDMA tablets first requires the extraction of the organic components, typically performed via liquid - liquid extraction in basic or neutral conditions [24]. In a study by Świst et al. [24], it was determined that significantly more organic impurities are extracted using basic conditions compared to using neutral conditions. This is due to the fact that many of the organic impurities formed during the synthesis of MDMA are basic amines.

There has been significant research determining the organic impurities formed in the synthesis of MDMA from MDP2P, safrole, isosafrole and piperonal [17]. This is achieved through the analysis of seized 'ecstasy' samples, and through the analysis of MDMA synthesised in research

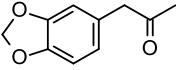
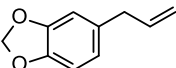
laboratories. Common organic impurities identified in MDMA that result from precursors, intermediates and reaction by-products are listed in Table 1 [17, 19-21, 23, 24, 54, 61, 62].

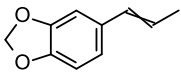
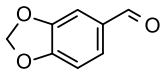
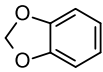
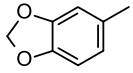
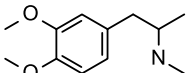
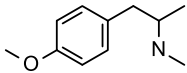
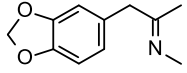
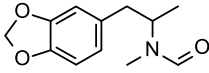
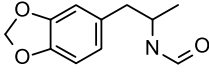
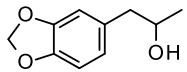
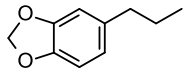
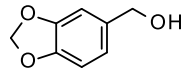
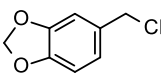
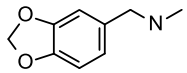
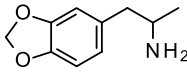
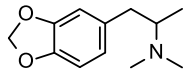
The organic impurities MDP2P (1), safrole (2), isosafrole (3) or piperonal (4) are the most common precursors used in the synthesis of MDMA and can be present due to incomplete reaction of the precursor. The detection of these impurities does not confirm that they were the precursor in the synthesis of MDMA, as they could be an intermediate or a reaction by-product [23, 62]. Organic impurities can also be introduced in the synthesis of MDMA as a result of impurities in the initial precursor, such as the organic impurities 5 – 8 [21, 62].

The organic impurities 9 – 11 are intermediates in the synthesis of MDMA from MDP2P. The intermediate in the reductive amination of MDP2P (9) is a route specific impurity as it is only detected in MDMA synthesised via this synthetic pathway [54]. The intermediates in the Leuckart reaction (10 – 11), however, are not route specific, as they have also been detected in MDMA synthesised via reductive amination [23, 54]. The organic impurities 13 – 21 are reaction by-products that can be formed in the synthesis of MDMA from MDP2P [17, 61, 62]. They are not route specific impurities as they result from reductive reaction conditions that are utilised in both the reductive amination reaction and the Leuckart reaction.

The organic impurities 22 – 31 are indicative of the route utilised in the synthesis of MDP2P from safrole, isosafrole or piperonal. The organic impurities 22 – 25 are reaction by-products of the peracid oxidation of isosafrole; however, impurity 25 is not route specific as it has also been identified in MDMA synthesised by the Wacker oxidation of safrole [19, 20]. The organic impurities 26 – 29 are route specific impurities for the Wacker oxidation of safrole using methanol as a solvent [19]. The organic impurities formed in this reaction differ according to the solvent used in the reaction, with methanol being the most common. The organic impurities 30 – 31 are route specific for the synthesis of MDP2P via the condensation of piperonal and oxidation of MDP2NP, as impurity 30 is a reaction by-product and impurity 31 is formed through the reduction of the reaction intermediate [21, 61].

Table 1-1: Organic impurities in MDMA synthesised from MDP2P, safrole, isosafrole and piperonal [17, 19-21, 23, 24, 54, 61, 62].

NO.	IMPURITY NAME	IMPURITY STRUCTURE	SOURCE
1	3,4-Methylenedioxyphenyl-2-propanone (MDP2P)		Precursor or impurity
2	Safrole		Precursor or impurity

NO.	IMPURITY NAME	IMPURITY STRUCTURE	SOURCE
3	Isosafrole		Precursor or impurity
4	Piperonal		Precursor or impurity
5	1,3-Benzodioxole		Impurity in safrole
6	3,4-Methylenedioxy toluene		Impurity in safrole, isosafrole and piperonal
7	N-Methyl-1-[1,2-dimethoxy-4-(2-aminopropyl)]benzene		Reaction of estragole impurity in safrole
8	p-Methoxymethamphetamine (PMA)		Reaction of methyl eugenol impurity in safrole
9	1,2-(Methylenedioxy)-4-(2-N-methyl-aminopropyl) benzene		Reductive amination intermediate
10	N-Formyl-3,4-methylene dioxymethamphetamine		Leuckart reaction intermediate
11	N-Formyl-3,4-methylene dioxymphetamine		Leuckart reaction intermediate
12	1-(3,4-Methylenedioxy) phenylpropan-2-ol		Reduction of MDP2P
13	3,4-Methylenedioxyphenylpropane		Reduction of safrole or isosafrole
14	3,4-Methylenedioxyphenylmethanol		Reduction of piperonal
15	Piperonyl chloride		Reaction of no. 14 with hydrochloric acid
16	3,4-Methylenedioxy-N-methylbenzylamine		Reductive amination of piperonal
17	3,4-Methylenedioxyamphetamine (MDA)		MDP2P reductive reaction by-product
18	N,N-Dimethyl-3,4-methylenedioxy amphetamine		MDP2P reductive reaction by-product

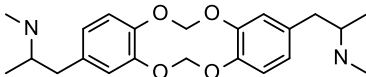
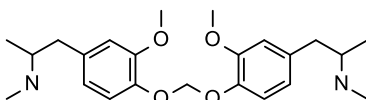
NO.	IMPURITY NAME	IMPURITY STRUCTURE	SOURCE
19	N-Ethyl-3,4-methylene dioxy amphetamine		MDP2P reductive reaction by-product
20	N-Ethyl-N-methyl-3,4-methylenedioxy amphetamine		MDP2P reductive reaction by-product
21	N,N-Di-(1-3,4-methylenedioxy)phenyl-2-propylmethanamine		Reaction of MDP2P with MDMA
22	2,4-Dimethyl-3,5-bis(3,4-methylenedioxyphenyl) tetrahydrofuran		Peracid oxidation by-product
23	3,4-Methylenedioxy propiophenone		Peracid oxidation by-product
24	1-(1,3-Benzodioxol-5-yl)-1-methoxy-propan-2-ol		Peracid oxidation by-product
25	1-(3,4-Methylenedioxy phenyl)-1-methoxypropan-2-one		Peracid oxidation and Wacker oxidation by-product
26	1-(3,4-Methylenedioxyphenyl)-1-methoxypropane		Wacker oxidation by-product with methanol solvent
27	Methyl 3-(1,3-benzodioxol-5-yl)propanoate		Wacker oxidation by-product with methanol solvent
28	1-(3,4-Methylenedioxyphenyl)-1,3-dimethoxypropane		Wacker oxidation by-product with methanol solvent
29	3-(3,4-Methylenedioxyphenyl)-1,1-dimethoxypropane		Wacker oxidation by-product with methanol solvent
30	Piperonylnitrile		Piperonal condensation by-product
31	1-(3,4-Methylenedioxyphenyl)-2-propanone oxime		Reduction of MDP2NP

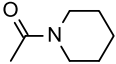
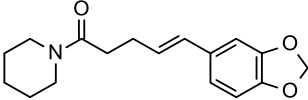
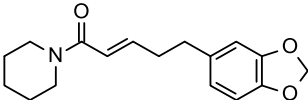
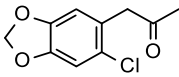
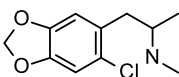
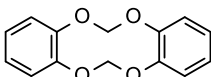
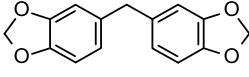
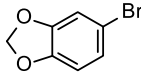
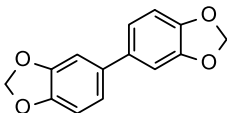
There has been relatively little research into the organic impurity profiling of MDMA that has been synthesised from uncontrolled precursors. The organic impurities identified in MDMA resulting from these uncontrolled precursors are shown in Table 1-2 [31, 35, 41]. In a study by Gallagher *et al.* [31], organic impurities 32 and 33 were formed through the dimerization, condensation and oxidation, and reductive amination of piperonal and vanillin, respectively, and identified in MDMA. It could, therefore, be determined through organic impurity analysis that vanillin was utilised as a precursor to first synthesise piperonal. These impurities, however, were not detected in a repetition of this study by Heather *et al.* [35].

In a study by Gallagher *et al.* [31], organic impurities 34 - 36 were detected in MDMA synthesised from piperine, irrespective of whether potassium permanganate or ozone was used in the oxidative cleavage of piperine. Impurity 34 formed due to the reaction of acetic acid with piperidine, a by-product of the hydrolysis of piperine, and was the only piperine dependant organic impurity identified in a repeat study by Heather *et al.* [35]. Impurities 35 and 36 were formed through the hydrogenation of one double bond in the piperine organic impurity during the reductive amination reaction. In a study by Plummer *et al.* [41], impurities 37 and 38 were identified in MDMA due to the formation of 6-chloropiperonal in piperonal that was synthesised the catalytic oxidative cleavage of piperine. These organic impurities were deemed route specific, as they arose due to an unknown mechanism involving the reagent ruthenium chloride.

In the study by Heather *et al.* [35], organic impurities 39 – 42 were identified in MDMA synthesised from catechol, which indicated the precursor and synthetic pathway used to prepare the synthetic safrole. Impurities 39 and 40 formed during the methylenation of catechol and are therefore indicative of the precursor, catechol, and the first step in the synthetic route. Impurities 41 and 42 are characteristic of the bromination and Grignard reaction, respectively, that were used to synthesise safrole.

Table 1-2: Organic impurities in MDMA resulting from uncontrolled precursors [31, 35, 41]

NO.	IMPURITY NAME	IMPURITY STRUCTURE	SOURCE
32	Piperonal dimer		Methylenation of vanillin reaction by-product
33	Vanillin dimer		Methylenation of vanillin reaction by-product

NO.	IMPURITY NAME	IMPURITY STRUCTURE	SOURCE
34	N-Acetylpiperidine		Oxidative cleavage of piperine reaction by-product
35	(5-(1,3-Benzodioxol-5-yl)-1-(1-piperidyl)pent-4-en-1-one		Oxidative cleavage of piperine reaction by-product
36	(5-(1,3-Benzodioxol-5-yl)-1-(1-piperidyl)pent-2-en-1-one		Oxidative cleavage of piperine reaction by-product
37	2-Chloro-4,5-methylenedioxyphenyl-2-propanone		Catalytic oxidation of piperine reaction by-product
38	2-Chloro-4,5-methylenedioxy methamphetamine		Catalytic oxidation of piperine reaction by-product
39	1,3-Benzodioxole dimer		Methylenation of catechol reaction by-product
40	5,5'-Methylene-bis-1,3-benzodioxole		Methylenation of catechol reaction by-product
41	5-Bromo-1,3-benzodioxole		Intermediate in synthesis of safrole from catechol
42	5,5'-Bi-1,3-benzodioxole		Grignard reaction by-product

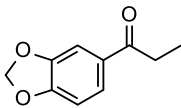
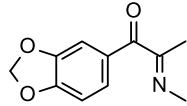
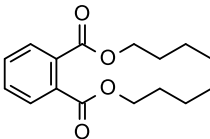
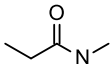
1.3.1.2 Methylone

There have been few reports of the organic impurity profiling of synthetic cathinones [29, 63-68], including the illicit drug methylone. This is presumably because these psychoactive substances are relatively new to the recreational drug market. The vast majority of chemical analysis research involving synthetic cathinones has focused on characterization and structural elucidation, including the analysis of methylone [69-73].

The organic impurities that have been identified in methylone are listed in Table 1-3 [8, 29]. Shulgin *et al.* [8] first identified compound 43 in methylone that was synthesised via the reactions in Scheme 1-10, which is a characteristic artifact that is consistent with compounds that contain a β -aminophenone structure. In a study by Bortz *et al.* [29], organic impurities 23,

43 – 45 were identified in methylone that was synthesised from catechol via the reactions shown in Scheme 1-17. There were also a significant number of organic impurities detected in methylone that were not identified. The identification of these organic impurities 23, 43 – 45 was consistent, irrespective of which reagent was utilised in the acylation of 1,3-benzodioxole. Impurity 23 is an intermediate in the reaction pathway that indicated the bromination reaction did not go to completion. Impurity 44 was determined to be a result of solvents, such as dichloromethane, coming into contact with plastic. Impurity 45 was formed through a reaction of propionyl chloride with methylamine.

Table 1-3: Organic impurities from the synthesis of methylone [8, 29]

NO.	IMPURITY NAME	IMPURITY STRUCTURE	SOURCE
23	3,4-Methylenedioxy propiophenone		Intermediate in the synthetic pathway
43	1-(1,3-Benzodioxol-5-yl)-2-methylimino-propan-1-one		Characteristic artifact
44	Dibutyl benzene-1,2-dicarboxylate		Impurity in dichloromethane due to contact with plastic
45	N-Methylpropanamide		Reaction of methylamine and propionyl chloride

1.3.2 Inorganic Impurity Profiling

Inorganic impurities can be introduced during the preparation of synthetic drugs through inorganic reagents, catalysts and reducing agents [55, 74]. The analysis of these inorganic impurities provides additional information to the organic impurity profile that can support identification and provide further evidence of the synthetic route utilised. Inorganic impurities can also be introduced post synthesis through dyes, additives and equipment contamination [55, 74]. These substances can have a significant effect on the inorganic impurity profiles of seized samples and complicate analysis. For example, in MDMA an iron inorganic impurity could be introduced post synthesis as a dye or during synthesis as a catalyst in the oxidation of MDP2NP (Scheme 1-5) [75].

The analysis of inorganic impurities in illicit drugs has been performed by numerous techniques such as inductively coupled plasma – mass spectrometry (ICP-MS), flame atomic absorption spectroscopy (FAAS) and inductively coupled plasma – atomic emission spectroscopy (ICP-AES) [55, 74]. The most effective technique, however, is ICP-MS as it permits a multi-element analysis of a single sample and is the most sensitive of the techniques [74]. The sample preparation for ICP-MS is a lengthy process involving the digestion of samples in concentrated acid [76]. Polyatomic isobaric interferences, multiply charged ions and oxides can also form in the argon plasma and interfere with the analysis of certain ions [76]. It is therefore necessary to ensure that the ion analysed has no interferences and that ICP-MS instrument parameters minimise potential interferences.

Laser ablation – inductively coupled plasma – mass spectrometry (LA-ICP-MS) is an analytical technique that analyses inorganic impurities in solid samples. This would improve the inorganic impurity analysis process of drug samples as it requires little or no sample preparation, reduces the mass of the sample required and reduces the risk of contamination [77]. In a study by Walting *et al.* [55, 77], cannabis crops were analysed using LA-ICP-MS and the geographical location of growth was determined based on the elemental composition. The use of LA-ICP-MS is a promising alternative for inorganic impurity analysis but issues such as a lack of quantitative information that is available and variations in the mass ablated between replicates of samples analysed have limited its application [55, 77].

1.3.2.1 MDMA

A study by Comment *et al.* [75] demonstrated that inorganic impurity profiling alone does not provide enough evidentiary information to establish links between MDMA samples. Two seized MDMA tablets analysed in this study had very similar inorganic impurity profiles but further organic impurity analysis demonstrated that they did not originate from the same batch of synthesised MDMA. A study by Wadell *et al.* [78] also demonstrated that MDMA tablets from different seizures could not be differentiated solely by inorganic impurity analysis. This was attributed to the significant variations in the concentration of inorganic impurities detected within a seizure. Inorganic impurity profiling of seized MDMA samples should therefore always be performed in conjunction with another profiling technique, such as organic impurity profiling.

There are three reported methods in which MDMA samples are prepared for ICP-MS analysis. These methods include:

- Direct digestion in HNO_3 [75]
- Microwave oven digestion in HNO_3 and H_2O_2 [22, 75]

- Heating block digestion in HNO_3 and H_2O_2 [22]

A study by Comment *et al.* [75] compared the direct digestion and microwave oven digestion sample preparation techniques on seized MDMA tablets. It was determined that a significantly higher concentration of inorganic impurities was detected through the microwave digestion technique. Sample preparation using microwave digestion, however, requires specialised equipment, is a significantly longer process and has a higher risk of introducing contaminants [22, 75]. As a result of these issues, Koper *et al.* [22] compared the microwave oven digestion to a heating block digestion technique. Heating block digestion was determined to be a much more practical sample preparation technique, with the concentration of the majority of elements not deviating by more than 20% in comparison to microwave oven digestion.

There have been limited reports on the use of inorganic impurity analysis to determine the pathway utilised in the synthesis of MDMA. In a study by Koper *et al.* [22], inorganic impurity analysis was used to determine whether sodium borohydride, an aluminium / mercury amalgam or hydrogen gas with a palladium catalyst was utilised as a reducing agent in the reductive amination of MDP2P. The elements boron, mercury and platinum were examined as sodium and aluminium are frequently detected in MDMA additives. The synthetic route was identified for 91% of the seized MDMA tablets, with platinum detected in 84 samples and boron detected in 4 samples. Platinum and boron were also detected in one seized MDMA tablet, indicating that MDMA synthesised separately were likely combined before tableting.

1.3.3 Isotope Ratio Analysis

The ratios of isotopes in synthetic drugs are dependent on the synthetic pathway and the starting materials utilised [79]. The stable isotopes of elements exist in a natural abundance ratio and the ratio of these isotopes can be changed through isotopic fractionation as a result of chemical, physical or biological processes [79]. The isotope ratios within a natural compound are dependent on the biochemical and environmental factors and will therefore vary depending on the compounds source [80]. Isotopic fractionation will also occur during the production of synthetic compounds, resulting in an isotope ratio dependant on the materials and processes used [79]. Therefore, synthetic drugs that are manufactured through different production processes can often be differentiated based on their isotope ratios, and synthetic drugs with a common source can be identified.

The kinetic and thermodynamic isotope effects are the two principal processes in which isotopic fractionation occurs [79]. The kinetic isotope effect occurs as different isotopes have differing

bond strengths, resulting in variation in the reaction rates of isotopes. The lighter isotope is more reactive as it has a weaker bond strength and, therefore, reaction products will contain a higher concentration of the lighter isotope while the reactants contain a higher concentration of heavier isotope. The thermodynamic isotope effect is related to energy states, as a compound that contains a heavier isotope has less free energy than one composed of the lighter isotope. This causes isotopic fractionation in processes that do not involve the breaking or formation of chemical bonds, such as a change of state due to temperature or pressure deviations.

The isotope ratios of substances are measured through isotope ratio mass spectrometry (IRMS) [79]. This analysis of these isotope ratios is performed through the determination of delta values (δ), in which the heavy to light Isotope ratio (R) of the analyte is calculated and compared to a standard through the formula in Equation 1 [79]. The isotope ratios that can be examined in the chemical profiling of amphetamine-type stimulants (ATS) are $^{13}\text{C}/^{12}\text{C}$, $^{15}\text{N}/^{14}\text{N}$, $^2\text{H}/^1\text{H}$ and $^{18}\text{O}/^{16}\text{O}$, however, $^{18}\text{O}/^{16}\text{O}$ is not typically examined. The adulterants and diluents that are added to synthetic drugs each contain an individual isotope ratio and, therefore, the active ingredient must be extracted from seized samples for isotope ratio analysis [81]. It is crucial that no isotopic fractionation occurs throughout the sample handling, preparation or analysis as this introduces inaccuracies into the data obtained.

Equation 1-1: The calculation of isotope ratios

$$\delta = \frac{1000 (R_{\text{sample}} - R_{\text{standard}})}{R_{\text{standard}}} \text{‰}$$

1.3.3.1 MDMA

Isotope ratio analysis is not typically performed on seized samples of MDMA as there has been limited research performed [51]. In a study by Mas et al. [80], the $^{13}\text{C}/^{12}\text{C}$ and $^{15}\text{N}/^{14}\text{N}$ isotope ratios of seized MDMA tablets were analysed. It was determined that analysis through the $^{13}\text{C}/^{12}\text{C}$ isotope ratio was not conclusive, as samples from different batches of MDMA may have comparable isotope ratios, and that further discrimination may be obtained through the measurement of the $^{15}\text{N}/^{14}\text{N}$ isotope ratio. Palhol *et al.* [82, 83] measured the $^{15}\text{N}/^{14}\text{N}$ isotope ratio of seized MDMA tablets in conjunction with additional profiling techniques, such as physical analysis and organic impurity analysis. It was determined that the $^{15}\text{N}/^{14}\text{N}$ isotope ratio differentiated MDMA samples that were likely synthesised via different methods. It was concluded, however, that individual reaction conditions also have a large effect on isotopic fractionation that requires examination.

There has also been limited research performed on the isotope ratio analysis of MDMA synthesised in research laboratories. Billault *et al.* [84] examined the $^{13}\text{C}/^{12}\text{C}$ and $^{15}\text{N}/^{14}\text{N}$ isotope ratios of MDMA synthesised from MDP2P via four synthetic routes and from piperonal via one synthetic route. This study also varied the reductive agents and nitrogen sources used within the reductive amination synthetic route in order to determine the effect that occurred on the isotope ratios. It was determined that multivariate analysis was able to provide good discrimination of the majority of the different reactions, however, not all MDMA samples synthesised via different routes could be differentiated.

In studies by Buchanan *et al.* [13, 85], the $^{13}\text{C}/^{12}\text{C}$, $^{15}\text{N}/^{14}\text{N}$ and $^2\text{H}/^1\text{H}$ isotope ratios of MDMA synthesised via the reductive amination of MDP2P were examined. When the reaction conditions were kept constant, the analysis of these isotope ratios differentiated the MDMA according to what reducing agent was used. It was also determined that the $^2\text{H}/^1\text{H}$ isotope ratio was crucial for this discrimination and that there were significant variations in the $^{15}\text{N}/^{14}\text{N}$ isotope ratio within a synthetic route. The modification of reaction conditions, however, had a significant effect on the isotope ratios of MDMA that complicated analysis. It was determined that the $^{13}\text{C}/^{12}\text{C}$ isotope ratio was affected by the efficiency of the reaction, the $^2\text{H}/^1\text{H}$ isotope ratio was affected by reaction time and the $^{15}\text{N}/^{14}\text{N}$ isotope ratio was affected by the quantity of methylamine that was used.

1.3.3.2 Methylone

In a study by Collins *et al.* [52], the $^{13}\text{C}/^{12}\text{C}$, $^{15}\text{N}/^{14}\text{N}$ and $^2\text{H}/^1\text{H}$ isotope ratios of 74 samples of methylone from 21 seizures between 2009 and 2014 were analysed. There was variation in the isotope ratios of one to three of the elements tested across the different seizures, which allowed discrimination of the 21 different seizures. The results also indicated that 4 seizures contained methylone from two different sources or reaction batches, due to two distinct isotope ratio values within the samples tested. It was concluded that careful measurement of the $^{13}\text{C}/^{12}\text{C}$, $^{15}\text{N}/^{14}\text{N}$ and $^2\text{H}/^1\text{H}$ isotope ratios of synthetic cathinones could link or differentiate samples.

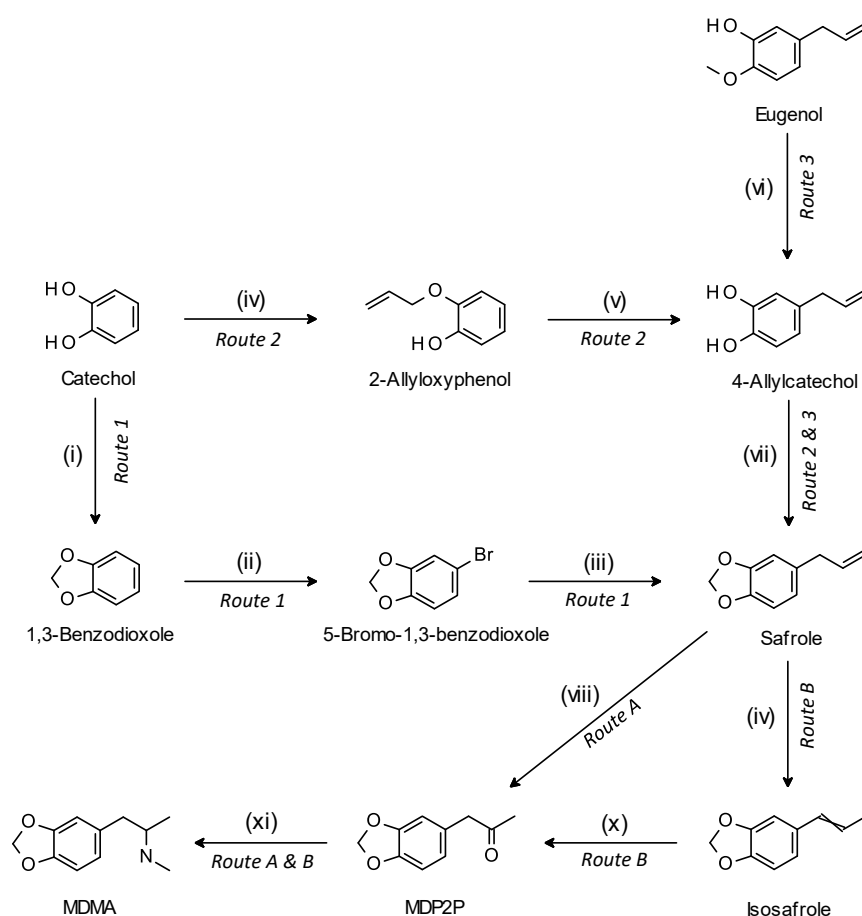
1.4 Research Aims

The use of uncontrolled 'pre-precursors' has gained popularity with clandestine laboratory operators for the synthesis of ATS [6], however, there has been limited research into the chemical profiles of MDMA and analogues that have been synthesised from uncontrolled 'pre-precursors'. This research aims to fill the gap in current knowledge relating to the organic impurity profiles of MDMA and analogues manufactured from uncontrolled 'pre-precursors'.

Therefore, the specific aims of this project are:

1. To synthesise safrole, MDMA and methyline from uncontrolled 'pre-precursors'

Catechol and eugenol are viable 'pre-precursors' for the synthesis of MDMA via a safrole intermediate. The synthesis of safrole and MDMA from catechol and eugenol via the synthetic routes illustrated in Scheme 1-18 are therefore investigated in this project. The synthetic route shown in Scheme 1-17 is also used to synthesise the MDMA analogue methyline from the viable 'pre-precursor' catechol.



Scheme 1-18: Synthesis of MDMA from catechol and eugenol via a safrole intermediate

(i) CH_2Cl_2 , NaOH (ii) HBr, HCOOH , CH_3COOH (iii) 1. Mg, DIBAL 2. $\text{CH}_2\text{CHCH}_2\text{Br}$ (iv) $\text{CH}_2\text{CHCH}_2\text{Br}$, K_2CO_3 (v) NaOC_2H_5 , Δ (vi) AlCl_3 , pyridine (vii) CH_2Cl_2 , NaOH (viii) H_2O , *p*-benzoquinone, PdCl_2 (ix) KOH, $\text{C}_4\text{H}_9\text{OH}$ (x) 1. HOOH , HCOOH 2. H_2SO_4 (xi) Al(Hg) , CH_3NO_2

2. To identify organic impurities in the products of each reaction

The chemical profiling of MDMA and analogues can include the analysis of organic impurities, inorganic impurities, and isotope ratios. However, research indicates that the analysis of organic impurities alone can provide sufficient information for intelligence purposes [51]. This project therefore focused on the organic impurity profiling of each reaction product in the synthesis of safrole, MDMA and methyllone from the 'pre-precursors' catechol and eugenol, to identify organic impurities that could be detected in seized substances manufactured by these routes.

3. To identify route specific organic impurities in safrole, MDMA and methyllone

The identification of route specific organic impurities in seized synthetic drugs can provide law enforcement agencies with strategic intelligence. Therefore, the organic impurity profiles of safrole and MDMA prepared by the routes shown in Scheme 1-18 are compared, and the organic impurity profiles of safrole, MDMA and methyllone are compared to literature organic impurity profiles. This is to ascertain the significance of the organic impurities detected in safrole, MDMA and methyllone, and to identify any route specific organic impurities.

Chapter 2: Materials and Methods

Chapter 2: Materials and Methods

2.1 General Experimental

Each reaction in the synthetic pathway for safrole and MDMA was performed at minimum in duplicate. For the synthesis of methylnone, each reaction was performed at minimum in triplicate. Gas chromatography-mass spectrometry (GC-MS) analysis was performed using an Agilent 6890 series gas chromatographic system coupled to an Agilent 5973 Network Mass Selective Detector. The column was a Zebron ZB-5ms with a length of 30 m, diameter of 250 μm and a film thickness of 0.25 μm . The front inlet was set at 250 $^{\circ}\text{C}$ and employed a split injection (50:1 split ratio) with a 1.0 μL injection volume. The transfer line was at a temperature of 280 $^{\circ}\text{C}$. Helium was used as a carrier gas at a rate of 1.2 mL/min. The temperature program started at 50 $^{\circ}\text{C}$ for 2 min, followed by a ramp of 10 $^{\circ}\text{C}/\text{min}$ until 290 $^{\circ}\text{C}$ where it was held for 4 min. The scan parameters enabled collection of a mass range of 40–450 amu with an abundance threshold of 100. The data were analysed using MSD ChemStation software. Nuclear magnetic resonance (NMR) spectroscopy used an Agilent Technologies 500 MHz NMR instrument. The frequency was 499.86 MHz for ^1H and 125.7 MHz for ^{13}C . Samples were dissolved in deuterated chloroform (CDCl_3) and the solvent residual chemical shift was used as an internal standard to calibrate the spectra. All NMR spectra were collected at 25 $^{\circ}\text{C}$.

2.2 Chemicals

The following chemicals were purchased from Sigma-Aldrich and used as received: catechol (1,2-dihydroxybenzene), eugenol, anhydrous ethanol, diisobutylaluminium hydride (DIBALH, 1.5 M solution in cyclohexane), allyl bromide, palladium (II) chloride, aluminium chloride, pyridine, sodium ethoxide, magnesium, anhydrous tetrahydrofuran, p-benzoquinone, formic acid, nitromethane, propionyl chloride, 1,2-dichloroethane, 40% wt aqueous methylamine and deuterated chloroform. The following chemicals were purchased from Ajax Chemicals (Finechem) and used as received: anhydrous sodium sulfate, copper (II) bromide, dimethylformamide, potassium bromide, hydrochloric acid (36%), mercuric chloride, and zinc (II) chloride. The following chemicals were purchased from Chem-Supply and used as received: dichloromethane, methanol, ethanol, 1-butanol, acetone, toluene, hydrogen peroxide (30%), ammonium chloride, potassium carbonate, sodium carbonate, sodium chloride, anhydrous sodium sulfate, diethyl ether, ethyl acetate, potassium hydroxide and sodium hydroxide. The following chemicals were purchased from UNILAB and used as received: dimethyl sulfoxide, mercuric chloride and hydrobromic acid (46 – 49%). The following chemicals were purchased from Labscan and used as received: glacial acetic acid, hydrochloric acid (36%) and sodium

bicarbonate. The following chemicals were purchased from various suppliers and used as received: sulfuric acid (BDH Chemicals), sodium bisulfite (Mallinckrodt Chemical Works), 1-butanol (Merck) and deuterated chloroform (Cambridge Isotope Laboratories, Inc).

2.3 Synthesis

2.3.1 Methylone

2.3.1.1 *1,3-Benzodioxole from catechol*

Catechol (16.5 g, 150 mmol), potassium carbonate (30 g, 217 mmol) and dimethylformamide (200 mL) were added to a 500 mL three-neck round bottom flask fitted with a condenser, a dropping funnel and a thermometer. The reaction was heated to 35 °C and dichloromethane (20 mL, 313 mmol) was added dropwise. The mixture was then heated at 110–120 °C for five hours and then left to cool. The solution was decanted, and 250 mL of water was added. The aqueous phase was extracted with diethyl ether (3 x 150 mL). The organic layers were then combined and washed with water (3 x 100 mL). The organic layer was dried over anhydrous sodium sulfate, decanted and the solvent was removed with a rotary evaporator to yield a light brown oil. Yield: 12.8 g. GC-MS: Figure 3-2. ¹H NMR (500MHz, CDCl₃): Figure 3-4.

2.3.1.2 *3,4-Methylenedioxypropiphenone from 1,3-benzodioxole*

1,3-Benzodioxole (3.0 g), zinc (II) chloride (5.1 g, 37 mmol) and 1,2-dichloroethane (15 mL) were added to a 50 mL two-neck round bottom flask under nitrogen and fitted with a dropping funnel. The resulting mixture was cooled in an ice bath. Propionyl chloride (3.3 mL, 38 mmol) was added to the mixture dropwise and the reaction was left to stir for 18 h. The reaction was quenched with water and 250 mL of diethyl ether was added. The aqueous layer was removed, and the organic layer was washed with a sodium carbonate solution (3 x 100 mL, 5% (w/v)) and brine (3 x 100 mL). The organic layer was then dried over anhydrous sodium sulfate, decanted and the solvent was removed using a rotary evaporator, producing a dark brown liquid. Yield 3.0 g. GC-MS: Figure 3-9. ¹H NMR (500MHz, CDCl₃): Figure 3-11.

2.3.1.3 *5-Bromo-3,4-methylenedioxypropiphenone from 3,4-methylenedioxypropiphenone*

3,4-Methylenedioxypropiphenone (1.5 g), copper(II) bromide (2.2 g, 9.8 mmol), potassium bromide (100 mg, 84 μmol) [27] and 40 mL of 1,2-dichloroethane were added to a 100 mL round bottom flask with a condenser under nitrogen. The solution was heated under reflux for 24 h and then quenched with dichloromethane. The resulting mixture was filtered, and the solids were washed with 20 mL of dichloromethane. The organic solution was dried over anhydrous

sodium sulfate, decanted and the solvent removed using a rotary evaporator, producing a dark brown liquid. Yield: 2.0 g. GC-MS: Figure 3-22. ^1H NMR (500MHz, CDCl_3): Figure 3-24.

2.3.1.4 Methylone from 5-bromo-3,4-methylenedioxypropiphenone

5-Bromo-3,4-methylenedioxypropiphenone (600 mg) and 20 mL of tetrahydrofuran were added to a 50 mL round bottom flask. Aqueous methylamine (5.0 mL, 40%, 64 mmol) was added dropwise to the solution over 30 min. The solution stirred for 18 h and then basified with aqueous sodium hydroxide (20 mL, 20% (w/v)). The product was extracted with ethyl acetate (3 x 25 mL) and washed with water (3 x 25 mL). The organic layer was dried over anhydrous sodium sulfate, decanted and the solvent removed using a rotary evaporator, producing a dark red liquid. Yield: 390 mg. GC-MS: Figure 3-26. ^1H NMR (500MHz, CDCl_3): Figure 3-28.

2.3.2 Safrole

2.3.2.1 1,3-Benzodioxole from catechol (Route 1)

Catechol (20.0 g, 182 mmol) and an aqueous solution of sodium hydroxide (30 mL, 19.4 M, 582 mmol) were dissolved in 200 mL of dimethyl sulfoxide. The resultant green solution was heated to 90 - 100 °C. Dichloromethane (40 mL, 630 mmol) was added drop wise to the solution, which was heated under reflux at 90 - 100 °C for four hours. The mixture was left to cool, and 200 mL of water was added. The mixture was decanted, and the product was extracted with diethyl ether (3 x 200 mL). The organic extracts were washed with water (3 x 200 mL), dried over anhydrous sodium sulfate and decanted. The solvent was removed with a rotary evaporator, producing a light brown oil. Yield: 14.8 g. GC-MS: Figure 4-1. ^1H NMR (500MHz, CDCl_3): Figure 4-2.

2.3.2.2 5-Bromo-1,3-benzodioxole from 1,3-benzodioxole (Route 1)

1,3-Benzodioxole (6.0 mL) was dissolved in a mixture of glacial acetic acid (2.6 mL, 45 mmol), 16 mL of methanol, and 2 mL of water. Hydrobromic acid (6.0 mL, 8.9 M, 53 mmol) was then added dropwise to the solution ensuring that the temperature remained below 25 °C. The solution was heated to approximately 35 °C, and hydrogen peroxide (6.0 mL, 30%, 59 mmol) was added drop wise, ensuring that the temperature did not exceed 50 °C. The resulting solution was stirred at 40 - 50 °C for three hours and allowed to cool. The red organic layer was extracted with diethyl ether (40 mL) and washed with an aqueous sodium bisulfite solution (10 mL, 10% (w/v)). The organic extracts were dried over anhydrous sodium sulfate and decanted. The solvent removed with a rotary evaporator, producing an orange oil. Yield: 8.9 g. GC-MS: Figure 4-3. ^1H NMR (500MHz, CDCl_3): Figure 4-4.

2.3.2.3 *Safrole from 5-bromo-1,3-benzodioxole (Route 1)*

The following Grignard reaction was conducted using dry glassware under nitrogen. Magnesium (0.60 g, 25 mmol), 5-bromo-1,3-benzodioxole (0.40 mL) and a solution of DIBALH in cyclohexane (0.10 mL, 1.5 M, 150 μ mol) were stirred in 20 mL of anhydrous tetrahydrofuran. Additional 5-bromo-1,3-benzodioxole (2.6 mL, 22 mmol) was added dropwise and the mixture was stirred for two hours. The solution was removed via syringe and added dropwise to allyl bromide (4.0 mL, 46 mmol) contained in an ice bath. The solution was stirred for 24 hours and reaction quenched by the addition of water (20 mL) and a saturated ammonium chloride solution (20 mL). The product was extracted into diethyl ether (3 x 80 mL) and washed with water (3 x 100 mL). The organic extracts were dried over anhydrous sodium sulfate, decanted, and the solvent removed with a rotary evaporator, producing a brown oil. Yield: 3.3 g. GC-MS: Figure 4-5. ^1H NMR (500MHz, CDCl_3): Figure 4-6.

2.3.2.4 *2-Allyloxyphenol from catechol (Route 2)*

Catechol (20.0 g, 182 mmol), potassium carbonate (25.2 g, 182 mmol) and 100 mL of acetone were cooled in an ice bath. Allyl bromide (22.0 g, 182 mmol) was added dropwise and the mixture was heated under reflux for 4 hrs. The resulting mixture was left to cool, and the solid material was removed through filtration. The volatile components of the mother liquor were removed on the rotary evaporator, leaving an orange residue. The residue was dissolved in diethyl ether (60 mL) and hydrochloric acid (40 mL, 1.6 M). The aqueous layer was removed, and the organic layer was washed with water (4 x 40 mL). The organic extracts were dried over anhydrous sodium sulfate and decanted. The solvent removed with a rotary evaporator, producing a yellow/orange liquid. Yield: 16.6 g. GC-MS: Figure 4-7. ^1H NMR (500MHz, CDCl_3): Figure 4-8.

2.3.2.5 *4-Allylcatechol from 2-allyloxyphenol (Route 2)*

The following Claisen rearrangement was conducted under nitrogen. 2-Allyloxyphenol (7.5 g) and sodium ethoxide (3.5 g, 51 mmol) were dissolved in 25 mL of anhydrous ethanol and heated under reflux. Additional sodium ethoxide (2.0 g, 29 mmol) was added to the reaction mixture every 24 hours. The resulting solution was heated under reflux for a total of 96 hrs and left to cool. The resulting mixture was dissolved in hydrochloric acid (20 mL, 3.2 M) and the product was extracted with dichloromethane (3 x 20 mL). The organic extracts were washed with 20 mL of water, dried over anhydrous sodium sulfate and decanted. The solvent removed with a rotary evaporator, producing a brown liquid. Yield: 6.6 g. GC-MS: Figure 4-9. ^1H NMR (500MHz, CDCl_3): Figure 4-10

2.3.2.6 4-Allylcatechol from eugenol (Route 3)

Eugenol (8.0 g), aluminium chloride (8.6 g, 64 mmol) and 250 mL of toluene were cooled in an ice bath. Pyridine (18.5 mL, 230 mmol) was added dropwise and the mixture heated under reflux for 5 hrs. The resulting mixture was left to cool, and the clear, yellow organic layer was decanted. The remaining solid was dissolved in hydrochloric acid (300 mL, 6.4 M) and extracted with diethyl ether (3 x 100 mL). The organic extracts were washed with water (3 x 100 mL), dried over anhydrous sodium sulfate, decanted and the solvent was removed with a rotary evaporator, to give a black liquid. Yield: 6.4 g. GC-MS: Figure 4-14. ¹H NMR (500MHz, CDCl₃): Figure 4-15.

2.3.2.7 Safrole from 4-allylcatechol (Route 2 and 3)

A solution containing dichloromethane (5.0 mL, 78 mmol) and 50 mL of dimethyl sulfoxide were heated at 120 – 130 °C. Sodium hydroxide (2.5 g, 63 mmol) was added to the solution. 4-Allylcatechol (4.0 g) was dissolved in 10 mL of dimethyl sulfoxide and added dropwise to the mixture, which was heated at 120 – 130 °C for 45 mins. The resulting mixture was decanted and water (50 mL) was added and left to cool. The resulting solution was extracted with diethyl ether (3 x 25 mL) and the organic layer was washed with water (3 x 25 mL). The organic extracts were dried over anhydrous sodium sulfate, decanted and the solvent was removed with a rotary evaporator, producing brown liquid.

Route 2 – Yield: 3.4 g. GC-MS: Figure 4-11; ¹H NMR (500MHz, CDCl₃): Figure 4-12.

Route 3 – Yield: 3.7 g. GC-MS: Figure 4-16. ¹H NMR (500MHz, CDCl₃): Figure 4-17.

2.3.3 MDMA

2.3.3.1 MDP2P from safrole (Route A)

Safrole (1.0 g) was dissolved in 1 mL of methanol and added dropwise to a mixture of palladium (II) chloride (12 mg, 68 µmol), p-benzoquinone (0.85 g, 7.9 mmol), 0.5 mL of water (30 mmol) and 5 mL of methanol. The resulting mixture was stirred for three hours and filtered. Hydrochloric acid (10 mL, 3.2 M) was added to the filtrate. The product was extracted with dichloromethane (3 x 20 mL) and washed with a saturated sodium bicarbonate solution (2 x 20 mL), aqueous sodium hydroxide (2 x 20 mL, 1.3 M) and brine (2 x 20 mL). The organic extracts were dried over anhydrous sodium sulfate, decanted and the solvent removed with a rotary evaporator, producing a brown oil.

Route 1A – Yield: 860 mg. GC-MS: Figure 5-1. ¹H NMR (500MHz, CDCl₃): Figure A3-6.

Route 2A – Yield: 940 mg. GC-MS: Figure 5-2. ¹H NMR (500MHz, CDCl₃): Figure A3-7.

Route 3A – Yield: 820 mg. GC-MS: Figure 5-3. ¹H NMR (500MHz, CDCl₃): Figure A3-8.

2.3.3.2 *Isosafrole from safrole (Route B)*

Safrole (1.4 g) was dissolved in a 3 M solution made from potassium hydroxide dissolved in 1-butanol (10 mL, 30 mmol). The resulting solution was heated under reflux for three hours and allowed to cool. To the solution, hydrochloric acid (10 mL, 1.6 M) solution was added. The product was extracted with diethyl ether (3 x 40 mL) and washed with water (3 x 40 mL). The organic extracts were dried over anhydrous sodium sulfate, decanted, and the solvent removed with a rotary evaporator, producing a brown oil.

Route 1B – Yield: 1.2 g. GC-MS: Figure 5-7. ^1H NMR (500MHz, CDCl_3): Figure A3-12.

Route 2B – Yield: 1.4 g. GC-MS: Figure 5-8. ^1H NMR (500MHz, CDCl_3): Figure A3-13.

Route 3B – Yield: 1.4 g. GC-MS: Figure 5-9. ^1H NMR (500MHz, CDCl_3): Figure A3-14.

2.3.3.3 *MDP2P from isosafrole (Route B)*

A solution of hydrogen peroxide (2.0 mL, 30%, 20 mmol) in formic acid (10 mL, 23.6 M, 240 mol) was stirred at room temperature for 30 minutes. A solution of isosafrole (800 mg) in acetone (6 mL) was added and stirred at room temperature for 16 hours. The volatile components of the resulting solution were removed in vacuo, leaving a red residue. The residue was dissolved in methanol (10 mL) and sulfuric acid (10 mL, 2.8 M) was added. The resulting solution was heated under reflux for three hours and allowed to cool. The product was extracted with diethyl ether (3 x 40 mL) and washed with of water (40 mL) and a saturated sodium bicarbonate solution (40 mL). The ether extracts were dried over anhydrous sodium sulfate, decanted and the solvent removed with a rotary evaporator, producing a brown oil.

Route 1B – Yield: 540 mg. GC-MS: Figure 5-10. ^1H NMR (500MHz, CDCl_3): Figure A3-15.

Route 2B – Yield: 570 mg. GC-MS: Figure 5-11. ^1H NMR (500MHz, CDCl_3): Figure A3-16.

Route 3B – Yield: 770 mg. GC-MS: Figure 5-12. ^1H NMR (500MHz, CDCl_3): Figure A3-17.

2.3.3.4 *MDMA from MDP2P (Route A and B)*

Aluminium foil (280 mg, 10.4 mmol) was cut in approximate 1 cm x 1cm squares and added to a solution of mercuric chloride (80.0 mg, 295 μmol) in 10 mL of methanol. The mixture was heated under reflux until the aluminium foil turned a dark grey and bubbles formed on the surface. Then, a solution of MDP2P (200 mg) and nitromethane (0.20 mL, 3.7 mmol) in 5 mL of methanol was added. The resulting mixture was heated under reflux for four hours and allowed to cool. An 8.8 M sodium hydroxide solution was added to the mixture until the majority of amalgam had dissolved. The mixture was filtered, and the product extracted from the filtrate with toluene (3 x 20 mL). The solvent was removed with a rotary evaporator, producing a light brown oil.

Route 1A – Yield: 180 mg. GC-MS: Figure 5-4. ^1H NMR (500MHz, CDCl_3): Figure A3-9.

Route 2A – Yield: 150 mg. GC-MS: Figure 5-5. ^1H NMR (500MHz, CDCl_3): Figure A3-10.

Route 3A – Yield: 170 mg. GC-MS: Figure 5-6. ^1H NMR (500MHz, CDCl_3): Figure A3-11.

Route 1B – Yield: 140 mg. GC-MS: Figure 5-13. ^1H NMR (500MHz, CDCl_3): Figure A3-18.

Route 2B – Yield: 120 mg. GC-MS: Figure 5-14. ^1H NMR (500MHz, CDCl_3): Figure A3-19.

Route 3B – Yield: 130 mg. GC-MS: Figure 5-15. ^1H NMR (500MHz, CDCl_3): Figure A3-20.

2.3.4 Synthesis of specific organic impurities

2.3.4.1 *(2-Hydroxyphenyl)propanoate and (2-propanoyloxyphenyl)propanoate*

Catechol (1.0 g, 9.1 mmol), zinc(II) chloride (2.0 g, 15 mmol) and 5 mL of dichloroethane were added to a 50 mL two-neck round bottom flask under nitrogen and fitted with a dropping funnel. The resulting mixture was cooled in an ice bath. Propionyl chloride (1.3 mL, 15 mmol) was added to the mixture dropwise and the reaction was stirred for 18 h. The reaction was quenched with water and 250 mL of diethyl ether was added. The aqueous layer was removed, and the organic layer was washed with brine (3 x 100 mL). The organic layer was then dried over anhydrous sodium sulfate, decanted and the solvent was removed using a rotary evaporator producing a brown liquid. GC-MS: Figure 3-15. ^1H NMR (500MHz, CDCl_3): Figure 3-16.

2.3.4.2 *(5E)- and (5Z)-7-(1,3-benzodioxol-5-yl)-5-ethylidene-6-methyl-cyclopenta[*f*][1,3]benzodioxole*

1,3-Benzodioxole (2.0 g, 16 mmol), zinc (II) chloride (10.2 g, 75 mmol), propionyl chloride (6.6 mL, 76 mmol) and 30 mL of dichloroethane were added to a 50 mL round bottom flask and the reaction was left to stir for 18 h. The reaction was quenched with water and 200 mL of diethyl ether was added. The aqueous layer was removed, and the organic layer was washed with water (3 x 100 mL). The organic layer was then dried over anhydrous sodium sulfate, decanted and the solvent was removed using a rotary evaporator and the high vacuum, producing a brown solid. This solid was purified by recrystallization from diethyl ether. GC-MS: Figure 3-18. ^1H NMR (500MHz, CDCl_3): Figure 3-20. ^{13}C NMR (500MHz, CDCl_3): Figure A3-2. ^{13}C DEPT NMR (500MHz, CDCl_3): Figure A3-3. COSY NMR (500MHz, CDCl_3): Figure A3-4. HMBC (500MHz, CDCl_3): Figure A3-5.

Chapter 3: Methylone

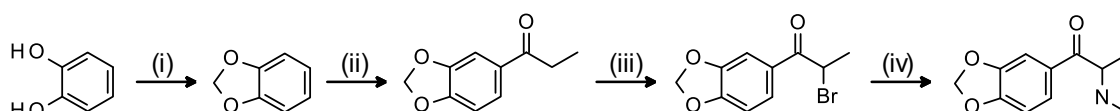
Chapter 3: Methylone

3.1 Introduction

This chapter discusses the synthesis and organic impurity profiling of methylone that was synthesised from the uncontrolled ‘pre-precursor’ catechol via one synthetic route. The reactions in this synthetic pathway are described in depth in Section 3.2. The reaction products of each step in the synthetic pathway were analysed using GC-MS and ^1H NMR spectroscopy. The chemical structures and origins of the detected organic impurities are detailed in Section 3.3. A number of exploratory syntheses were also conducted to unambiguously identify some of the organic impurities detected. The significance of the identified organic impurities was analysed, and route specific impurities are discussed in Section 3.4.

3.2 Synthesis

Methylone was synthesised from catechol via the reaction pathway shown in Scheme 3-1. This reaction pathway involved four steps: the methylenation of catechol, the Friedel-Crafts acylation of 1,3-benzodioxole, the bromination of 3,4-methylenedioxypropionophenone and the amination of 5-bromo-3,4-methylenedioxy-propionophenone. The synthesis of methylone from catechol was performed in triplicate using synthetic methods that are feasible in a reasonably equipped clandestine laboratory. All products were purified by unsophisticated purification techniques, such as liquid-liquid extraction and filtration, to mimic a clandestine laboratory setting.



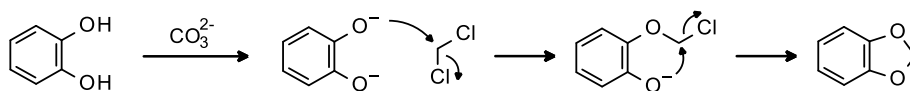
Scheme 3-1: Synthesis of methylone from catechol.
(i) CH_2Cl_2 , K_2CO_3 (ii) $\text{CH}_3\text{CH}_2\text{COCl}$, ZnCl_2 (iii) CuBr_2 , KBr (iv) CH_3NH_2

3.2.1 1,3-Benzodioxole from Catechol

The methylenation of catechol (Reaction i, Scheme 3-1) is a ring-forming reaction using a dihalomethane in a polar, aprotic solvent in alkaline conditions. There are numerous readily available information sources in which the methylenation of catechol and catechol derivatives are discussed [12, 33], together with advice about reactants, reagents and solvents. Dichloromethane is the most feasible dihalomethane used in this reaction due to its relatively low cost and accessibility. For example, a clandestine laboratory operator could obtain dichloromethane from retail suppliers in the form of paint stripper.

The reaction mechanism for the synthesis of 1,3-benzodioxole from catechol is shown in Scheme 3-2. Catechol reacts with the base, potassium carbonate, to form the catechoxide dianion, which

subsequently reacts with dichloromethane to form 1,3-benzodioxole. The reaction was performed using the polar, aprotic solvent, dimethylformamide, as it facilitates a relatively rapid rate of reaction [86].

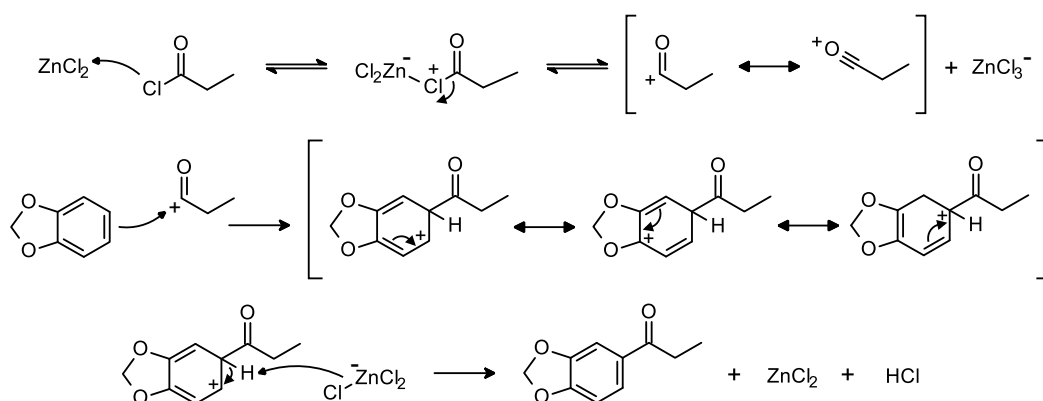


Scheme 3-2: Reaction mechanism for the synthesis of 1,3-benzodioxole from catechol

3.2.2 3,4-Methylenedioxypropionophenone from 1,3-benzodioxole

The Friedel-Crafts acylation of 1,3-benzodioxole (Reaction ii, Scheme 3-1) utilises an acyl chloride and a Lewis acid catalyst. The acyl chloride required for the synthesis of 3,4-methylenedioxypropionophenone is propionyl chloride. This acylation reaction could also be performed using propionic anhydride [8, 29], however this reagent is monitored under Category II of the *Code of Practice for the Supply Diversion into Illicit Drug Manufacture* [28]. There are numerous Lewis acid catalysts could be used for this reaction, but zinc chloride was chosen as it has been shown to lead to good yields [29].

The reaction mechanism for the synthesis of 3,4-methylenedioxypropionophenone from 1,3-benzodioxole is shown in Scheme 3-3. Propionyl chloride reacts with zinc chloride to form a resonance stabilised propionyl cation and a zinc chloride anion. The propionyl cation then reacts with 1,3-benzodioxole to form a resonance stabilised intermediate, which reacts with the zinc chloride anion to form 3,4-methylenedioxypropionophenone and hydrochloric acid, and regenerate zinc chloride.



Scheme 3-3: Reaction mechanism for the synthesis of 3,4-methylenedioxypropionophenone from 1,3-benzodioxole

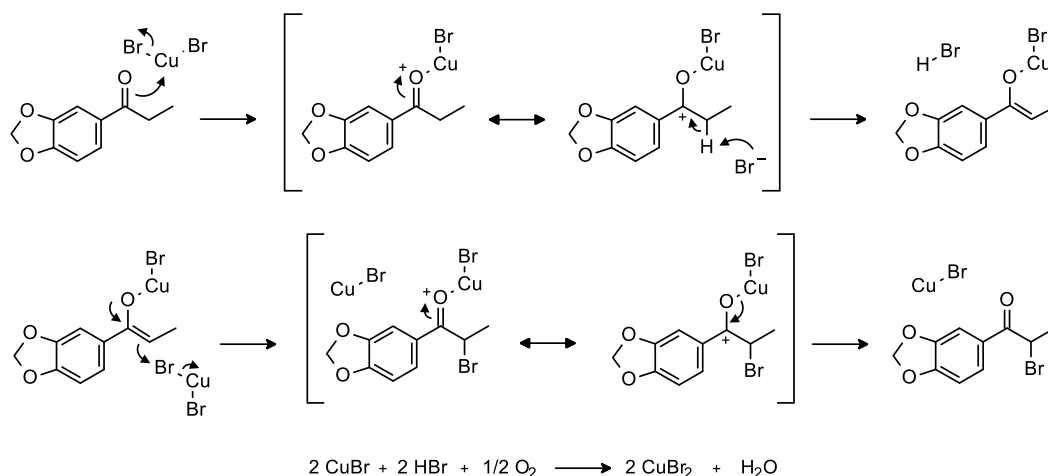
3.2.3 5-Bromo-3,4-methylenedioxypropiofenone from 3,4-methylenedioxypropiofenone

The bromination of 3,4-methylenedioxypropiofenone (Reaction iii, Scheme 3-1) is an α -halogenation reaction of the ketone functional group. The brominating agents used in this reaction are copper(II) bromide and potassium bromide. It has been shown that the combination of these two reagent improves reaction efficiency [26, 27]. The bromination reaction was trialled with dichloromethane as solvent and an 18- and 24-hour reaction time and with 1,2-dichloroethane as solvent and a 24-hour reaction time. The reaction progress (%) was determined by the ratio of the methylenedioxy proton signals of the starting material to those of the product in ^1H NMR spectra, as shown in Table 3-1. The most viable of the reaction conditions trialled used 1,2-dichloroethane as solvent with a 24-hour reaction time, and so these conditions were used for the synthesis of methylone. The published methodologies for the bromination of 3,4-methylenedioxypropiofenone utilise dichloromethane as a solvent [8, 26, 27], but this change in solvent was not deemed a significant variation to the synthetic route as 1,2-dichloroethane was also utilised as a solvent in the Friedel-Crafts acylation of 1,3-benzodioxole.

Table 3-1: Reaction conditions trialled for the synthesis of 5-bromo-3,4-methylenedioxypropiofenone and reaction completion (%) determined through the starting material : product O-CH₂-O ^1H integration ratio

Reaction Conditions (Time; Solvent)	O-CH ₂ -O ^1H Integration Ratio (Starting Material : Product)	Reaction Completion (%)
18 hours; dichloromethane	3.7 : 6.3	63%
24 hours; dichloromethane	2.2 : 7.8	78%
24 hours; 1,2-dichloroethane	1.2 : 8.8	88%

The reaction mechanism for the synthesis of 5-bromo-3,4-methylenedioxypropiofenone from 3,4-methylenedioxypropiofenone is shown in Scheme 3-4. Copper(II) bromide reacts with the ketone functional group in 3,4-methylenedioxypropiofenone to form a resonance stabilised cation and a bromide anion, which then forms an intermediate enol derivative and hydrogen bromide as a by-product [87, 88]. This enol derivative intermediate reacts with copper(II) bromide to form 5-bromo-3,4-methylenedioxypropiofenone and a copper(I) bromide by-product [87, 88]. It is feasible that potassium bromide could have also reacted with the enol derivative intermediate to facilitate the α -bromination reaction. Copper(II) bromide was regenerated *in-situ* under atmospheric conditions by the reaction of the copper(I) bromide and hydrogen bromide by-products with oxygen [89].

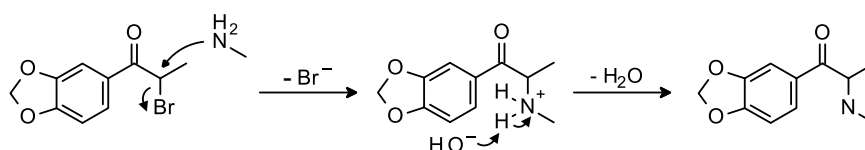


Scheme 3-4: Reaction mechanism for the synthesis of 5-bromo-3,4-methylenedioxypropiphenone from 3,4-methylenedioxypropiphenone

3.2.4 Methylone from 5-bromo-3,4-methylenedioxypropiphenone

The synthesis of methylone involves the nucleophilic substitution of bromine with methylamine (Reaction iv, Scheme 3-1). Methylamine is monitored under Category II of the *Code of Practice for the Supply Diversion into Illicit Drug Manufacture* [28] due to its practical use in the synthesis of numerous ATS [17]. However, it could be obtained through the diversion of legitimate industrial supplies or synthesised from methanol and ammonia or ammonium chloride [90]. Excess methylamine was required for the synthesis of methylone via the nucleophilic substitution of bromine. It was theorised that this was due to remaining copper(II) salts in the impure 5-bromo-3,4-methylenedioxypropiphenone used, which may react with methylamine.

The reaction mechanism for the synthesis of methylone from 5-bromo-3,4-methylenedioxypropiphenone is shown in Scheme 3-5. Bromine is substituted by nucleophile methylamine in an SN2 reaction, which forms a secondary ammonium salt intermediate. The reaction was performed using the polar, aprotic solvent, tetrahydrofuran, as it increases the rate of an SN2 reaction [88]. The addition of aqueous sodium hydroxide to the reaction mixture caused deprotonation of the secondary ammonium salt intermediate and the formation of methylone.



Scheme 3-5: Reaction mechanism for the synthesis of methylone from 5-bromo-3,4-methylenedioxypropiphenone

3.3 Organic Impurity Profiling

In the synthesis of methylone from catechol, the reaction products of each step in the synthetic pathway were analysed using GC-MS and ^1H NMR spectroscopy. Organic impurities were typically identified based on the fragmentation pattern of their mass spectrum. The identification of these organic impurities was also confirmed by ^1H NMR spectroscopy when impurities were of a sufficient concentration to produce distinct signals. Exploratory synthesis of potential organic impurity structures was also performed when additional evidence was required for identification purposes. The origin of the organic impurities and their formation during the respective reactions was also investigated.

3.3.1 Catechol

The catechol utilised as a starting material for the synthesis of methylone was analysed via ^1H NMR spectroscopy. The signals that correspond to proton environments of catechol are labelled A and B in the ^1H NMR spectrum shown in Figure 3-1. The multiplet at 6.81 ppm corresponds to the two aromatic protons (A) that are to the adjacent hydroxyl groups, while the multiplet at 6.87 ppm corresponds to the two aromatic protons (B) that are opposite the hydroxyl groups. There are no additional significant signals within the ^1H NMR spectrum of catechol, which demonstrated that there were no significant quantities of organic impurities contained within the catechol starting material. This catechol was also used to synthesise safrole via Routes 1 and 2 and MDMA via Routes 1A, 1B, 2A and 2B, as discussed in detail in Chapters 4 and 5 respectively.

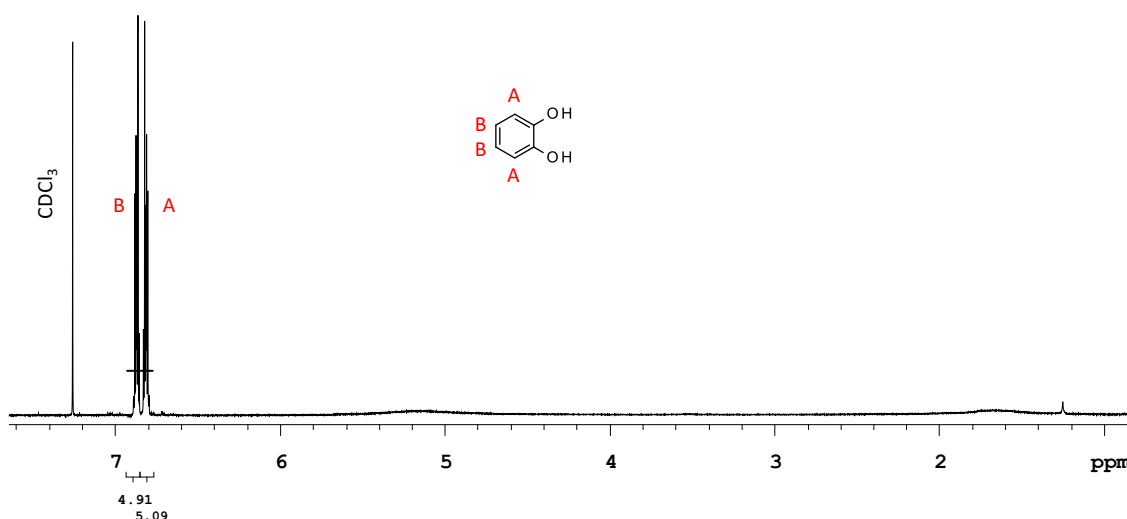


Figure 3-1: ^1H NMR spectrum of catechol

3.3.2 1,3-Benzodioxole from Catechol

The analysis of the product of the methylenation of catechol with GC-MS and ^1H NMR spectroscopy confirmed that 1,3-benzodioxole is the principal component. The mass spectrum

of the largest peak in the gas chromatogram in Figure 3-2 corresponds to the library reference of 1,3-benzodioxole with a 98% quality, as shown in Figure 3-3. The signals that correspond to proton environments of 1,3-benzodioxole are labelled A and B in the ^1H NMR spectrum of the reaction product, shown in Figure 3-4.

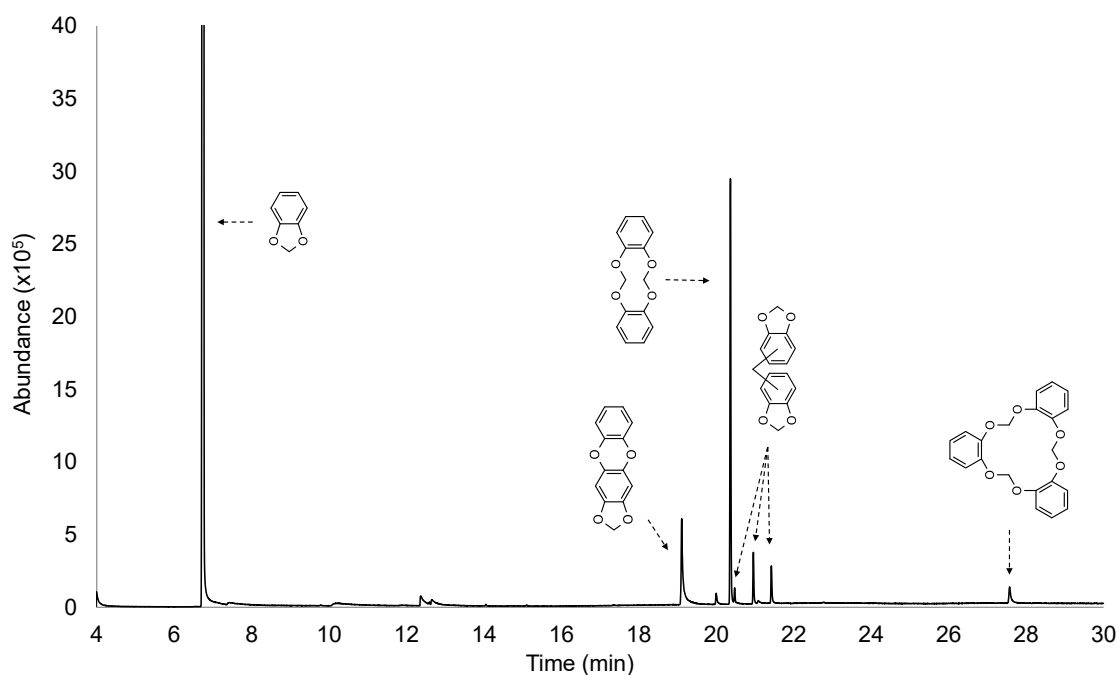


Figure 3-2: GC-MS total ion chromatogram of 1,3-benzodioxole

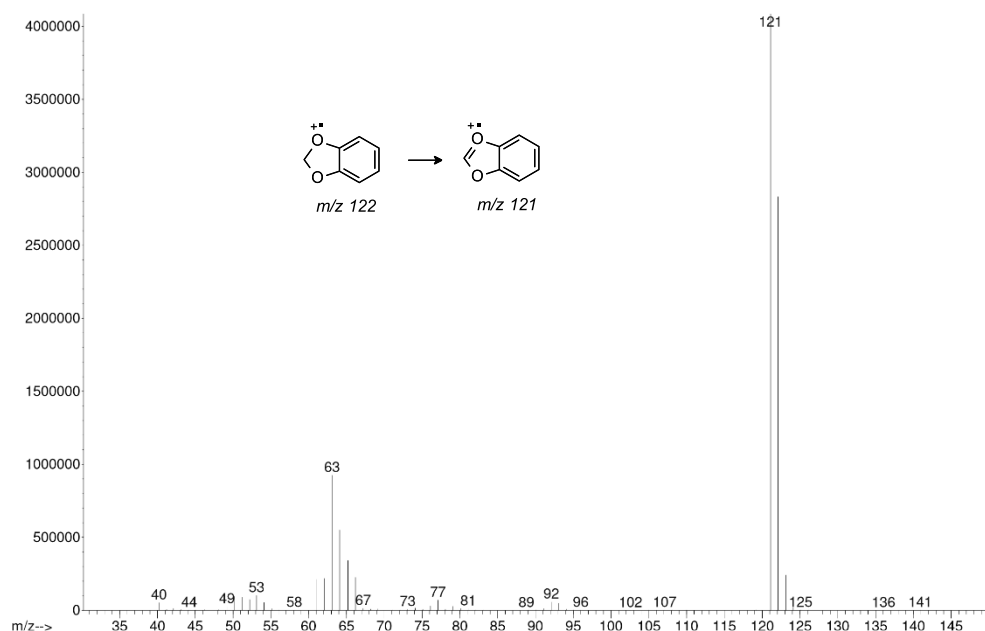
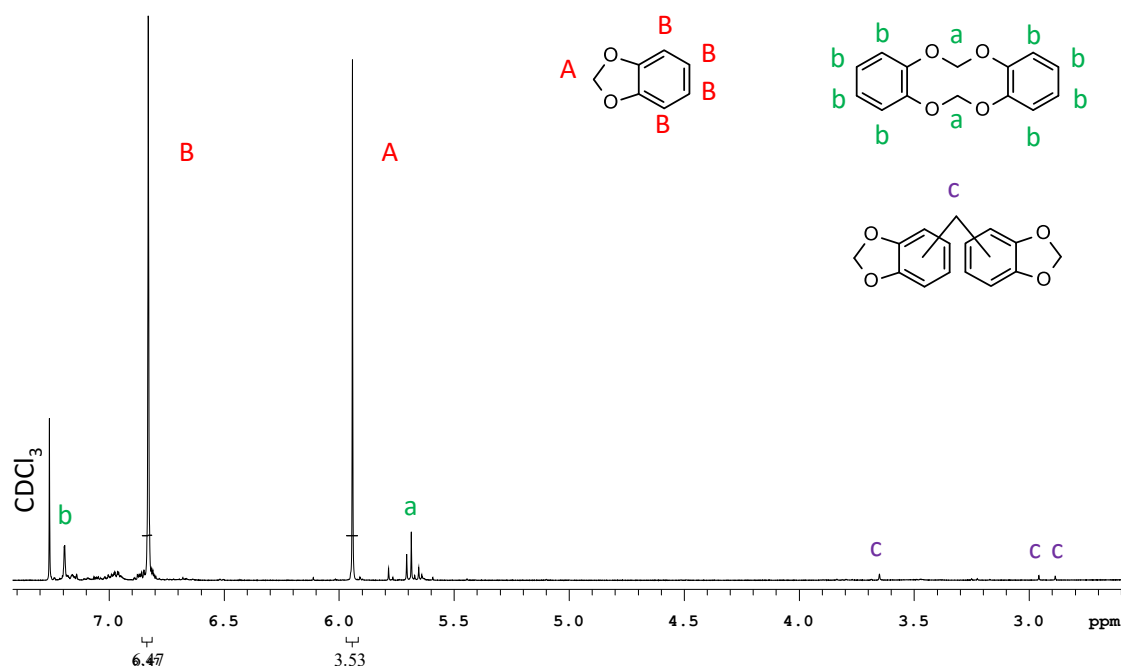


Figure 3-3: Mass spectrum and proposed fragmentation scheme of 1,3-benzodioxole

Figure 3-4: ^1H NMR spectrum of 1,3-benzodioxole

The gas chromatogram in Figure 3-2 shows the six organic impurities that were identified in the reaction product mixture. Organic impurities 39, 40 (a-c; three isomers), 46 and 47 were consistently identified in the three preparations of 1,3-benzodioxole. The assigned numbers, chemical structures, names, molecular weights, and m/z data of these organic impurities are shown in Table 3-2. Organic impurities 39, 40 (a-c), 46 and 47 were identified based on the fragmentation pattern of their mass spectra, as shown in Figure 3-5 to Figure 3-8.

Table 3-2: Organic impurities identified in 1,3-benzodioxole

No.	Impurity Structure	Impurity Name	MW (g/mol)	m/z
39		1,3-benzodioxole dimer	244.2	244, 135, 122/121, 63
40 (a-c)		4,4'-, 4,5'-, and 5,5'-methylenebis-1,3-benzodioxole	256.3	256, 225, 196, 168, 135, 77
46		[1,3]dioxolo[4,5-b]oxanthrene	228.2	228, 122/121, 110, 95, 77
47		1,3-benzodioxole trimer	366.4	366, 244, 135, 122/121

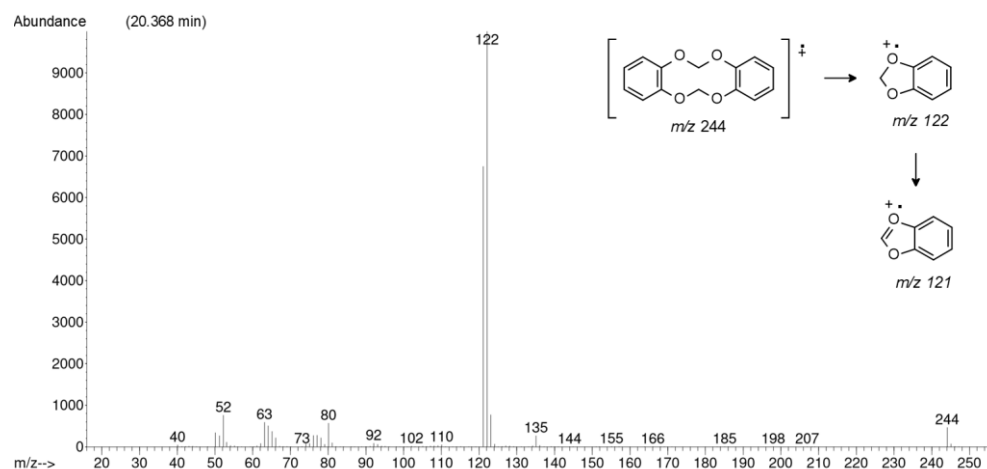


Figure 3-5: Mass spectrum and proposed fragmentation scheme of organic impurity 39

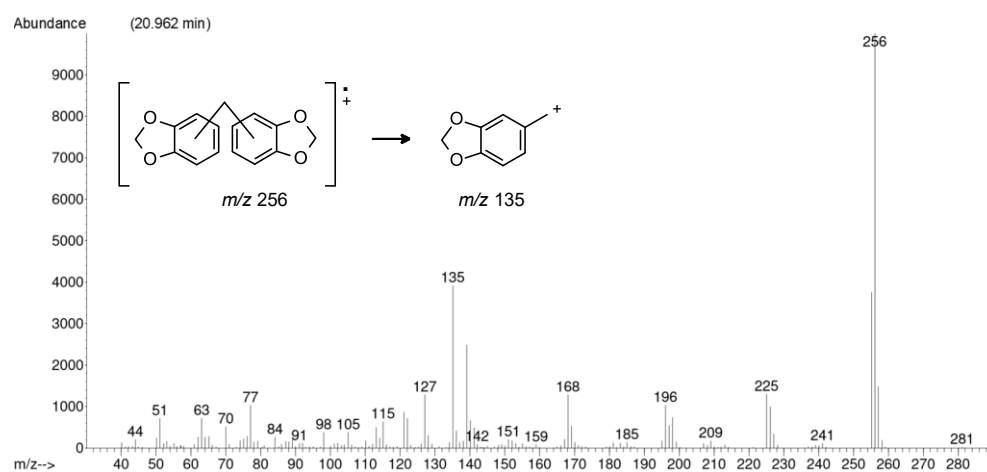
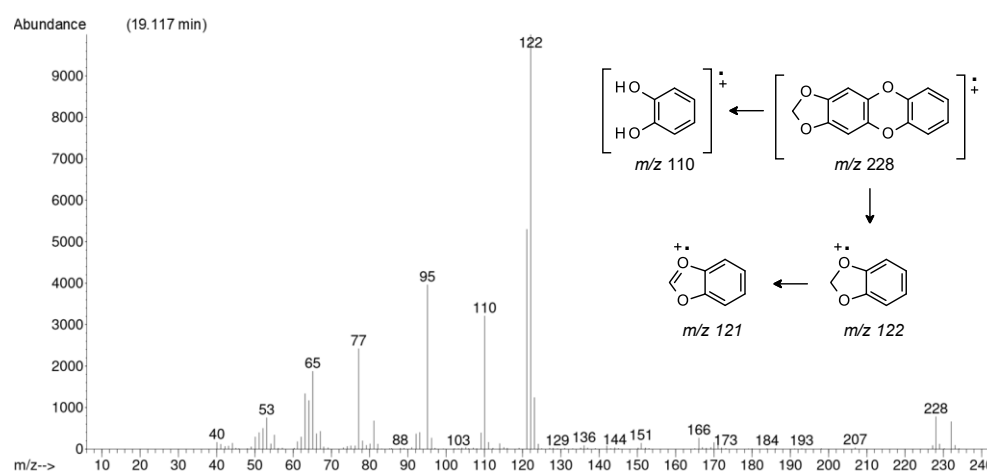


Figure 3-6: Mass spectrum and proposed fragmentation scheme of organic impurities 40 (a-c)



Note: m/z 232 has a low abundance and is likely a result of background interference and/or a contaminant

Figure 3-7: Mass spectrum and proposed fragmentation scheme of organic impurity 46

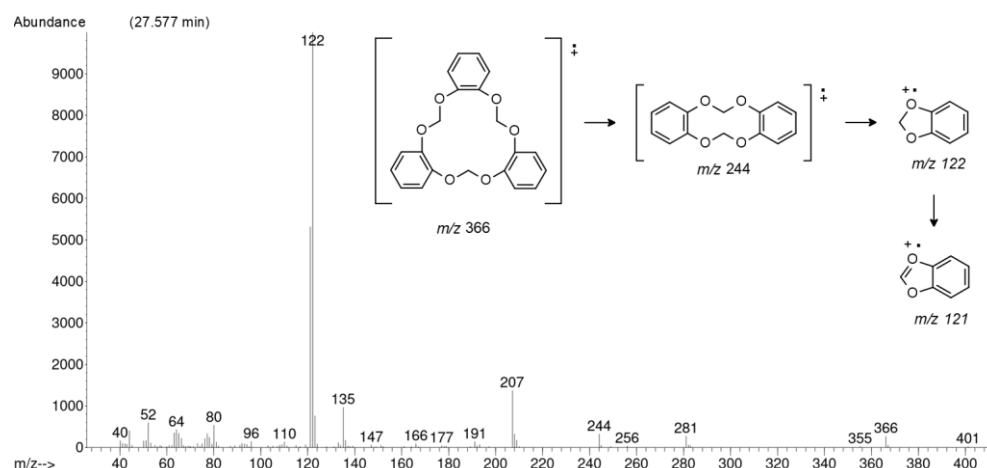
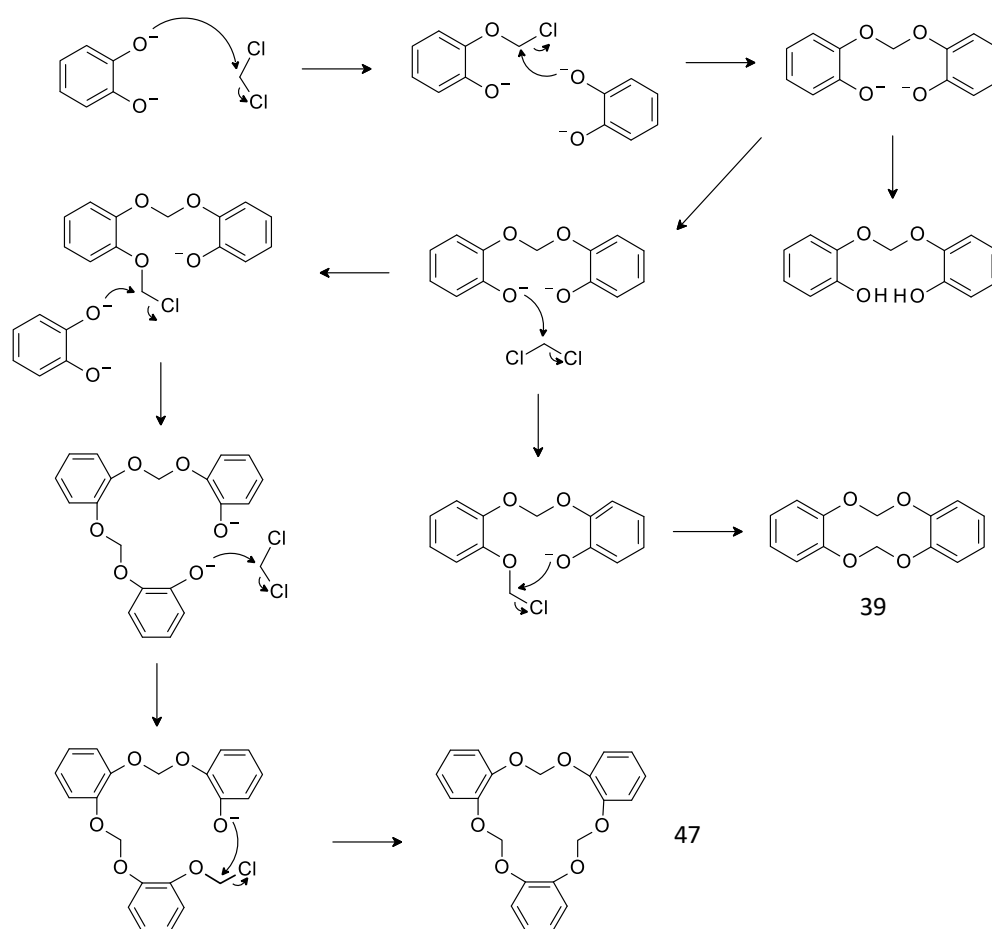


Figure 3-8: Mass spectrum and proposed fragmentation scheme of organic impurity 47

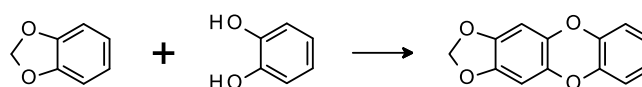
The identity of organic impurities 39 and 40 (a-c) was also confirmed with ^1H NMR spectroscopy, as shown in Figure 3-4. The singlet at 5.69 ppm corresponds to the methylenedioxy protons (a) in organic impurity 39, and a singlet at 7.19 ppm corresponds to the aromatic protons (b) in organic impurity 39. The ^1H NMR spectrum contained distinct signals resulting from organic impurity 39 as it is the most abundant impurity in 1,3-benzodioxole. However, the methylenedioxy and aromatic signals assigned to organic impurities 40 (a-c), 46 and 47 could not be differentiated and assigned. The three signals located within the methylene region of the ^1H NMR spectrum are evidence of the formation of organic impurities 40 (a-c), as they correspond to the methylene groups (c) contained within the three isomers.

Impurities 39 and 47 were formed by the cyclisation of two and three catechoxide dianions, respectively, with dichloromethane. There are three potential mechanisms reported in the literature for the formation of the 1,3-benzodioxole dimer (39) [86]. An additional impurity, 2-[(2-hydroxyphenoxy)methoxy]phenol, was also identified in an incomplete synthesis of 1,3-benzodioxole, where the reaction was heated at reflux for two hours (Figure A2-1). This confirmed that impurities 39 and 47 were formed through the mechanism shown in Scheme 3-6, as it is the only potential mechanism that also results in the formation of impurity 48. This mechanism was also deemed the most feasible in the literature, as the catechoxide dianion is the most reactive of the potential nucleophiles [86].



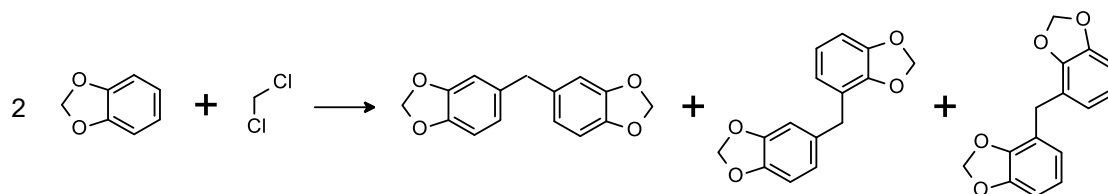
Scheme 3-6: Formation of 2-[(2-hydroxyphenoxy)methoxy]phenol and organic impurities 39 and 47

Impurity 46 was formed by the reaction of the hydroxy functional groups of catechol with the aromatic ring of 1,3-benzodioxole, as shown in Scheme 3-7. This impurity has previously been identified as a reaction by-product of the methylenation reaction, where it was reported to be a result of the formation of a semiquinone radical in the alkaline reaction mixture [91].



Scheme 3-7: Formation of organic impurity 46

Impurities 40 (a-c) were formed through the methylenation reaction across the aromatic ring of two 1,3-benzodioxole molecules, as shown in Scheme 3-8. This reaction can occur on multiple positions of the aromatic ring, giving rise to the three isomers that were detected in 1,3-benzodioxole.



Scheme 3-8: Formation of organic impurities 40 (a-c)

3.3.3 3,4-Methylenedioxypropiofenone from 1,3-benzodioxole

The analysis of the product of the Friedel-Crafts acylation of 1,3-benzodioxole using GC-MS and ^1H NMR spectroscopy confirmed that 3,4-methylenedioxypropiofenone is the principal component. The mass spectrum of the largest peak in the gas chromatogram in Figure 3-9 corresponds to 3,4-methylenedioxypropiofenone based on its fragmentation pattern, as shown in Figure 3-10. The signals that correspond to the proton environments of 3,4-methylenedioxypropiofenone are labelled A – F in the ^1H NMR spectrum of the reaction product, shown in Figure 3-11.

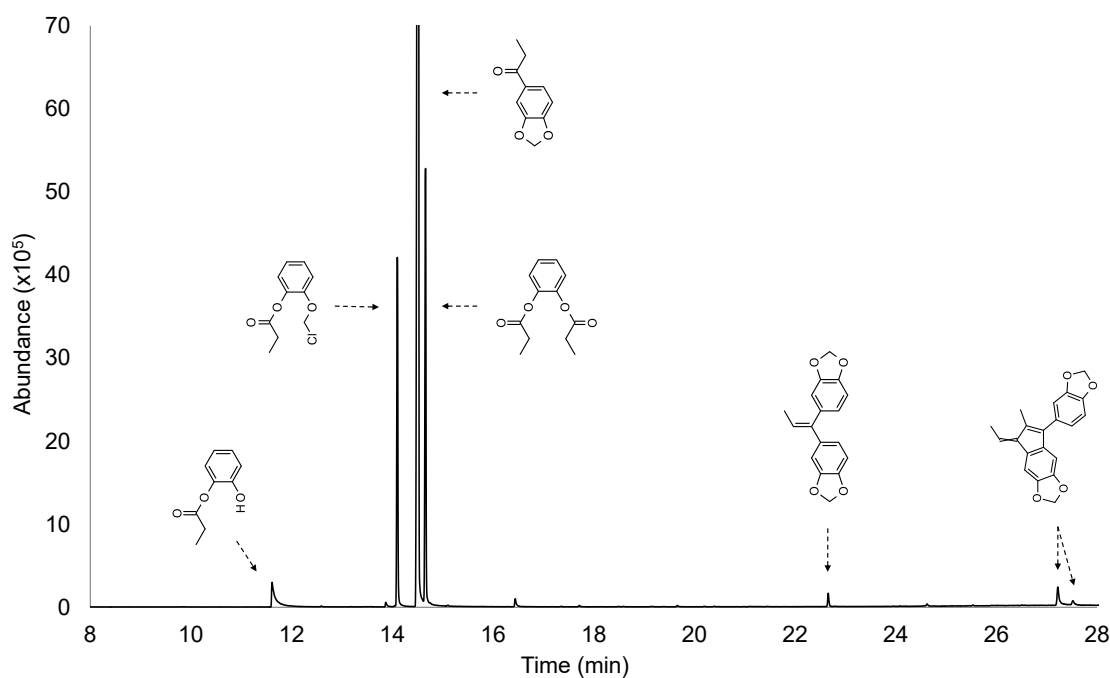


Figure 3-9: GC-MS total ion chromatogram of 3,4-methylenedioxypropiofenone

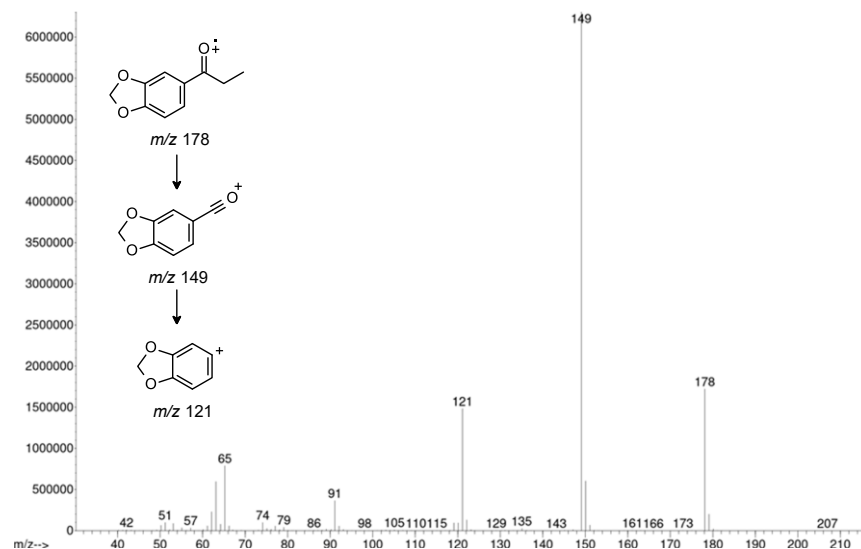


Figure 3-10: Mass spectrum and proposed fragmentation scheme of 3,4-methylenedioxypropiofenone

The gas chromatogram in Figure 3-9 shows the six organic impurities that were identified in the reaction product mixture. Organic impurities 48 - 52 (a-b; two isomers) were consistently identified in the three preparations of 3,4-methylenedioxypropiofenone. The assigned numbers, chemical structures, names, molecular weights, and m/z data of these organic impurities are shown in Table 3-3. A number of exploratory synthetic experiments were conducted to unambiguously determine the identity of organic impurities 48, 50 and 52 (a-b). The identification and formation of organic impurities 48 - 50 and organic impurities 51 - 52 (a-b) are discussed in Sections 3.3.3.1 and 3.3.3.2, respectively.

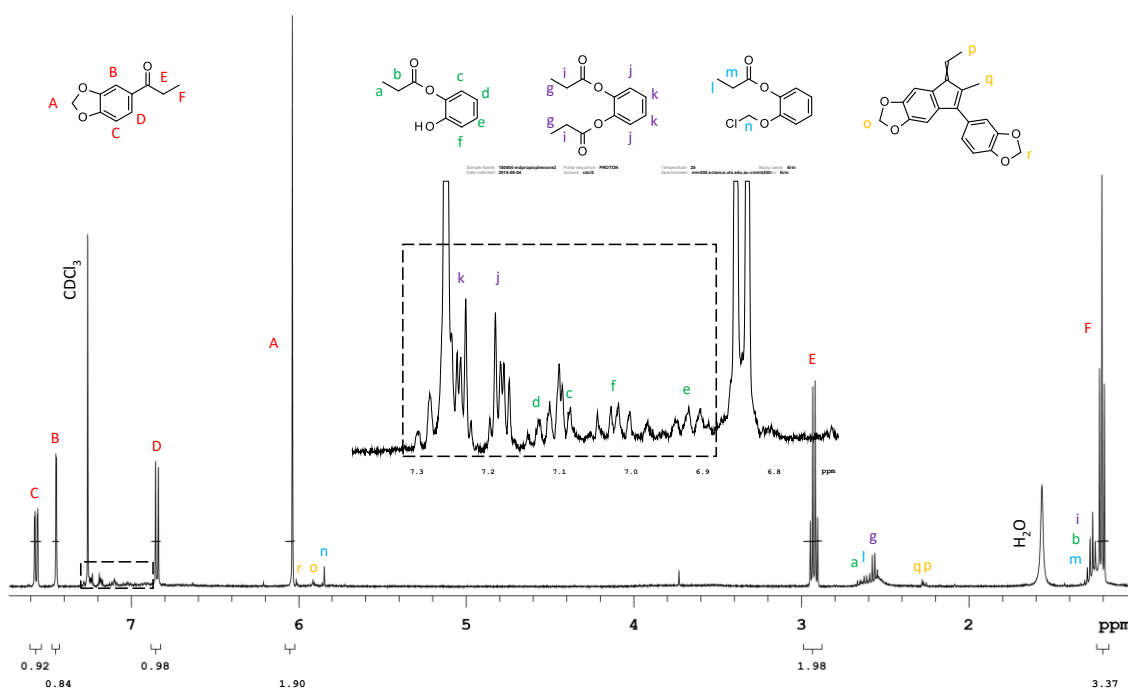


Figure 3-11: ^1H NMR spectrum of 3,4-methylenedioxypropiofenone

Table 3-3: Organic impurities identified in 3,4-methylenedioxypropiphenone

No.	Impurity Structure	Impurity Name	MW (g/mol)	m/z
48		(2-hydroxyphenyl) propanoate	166.2	166, 110, 57
49		[2-(chloromethoxy)phenyl] propanoate	214.6	214, 158, 122/121, 109, 57
50		(2-propanoyloxyphenyl) propanoate	222.2	222, 166, 110, 57
51		5-[1-(1,3-benzodioxol-5-yl)prop-1-enyl]-1,3-benzodioxole	282.3	282, 251, 223, 165, 82
52 (a-b)		(5E)- and (5Z)-7-(1,3-benzodioxol-5-yl)-5-ethylidene-6-methyl-cyclopenta [f][1,3]benzodioxole)	320.3	320, 305, 281, 207, 189, 101, 44

3.3.3.1 Synthesis and identification of organic impurities 48, 49 and 50

Organic impurities 48 and 50 could not be unambiguously identified based on their respective mass spectra and the ^1H NMR spectrum of synthesised 3,4-methylenedioxypropiphenone. The mass spectra of organic impurities 48 and 50 correlated to a number of possible isomers, shown in Figure 3-12, that are feasible reaction by-products of the Friedel-Crafts acylation of 1,3-benzodioxole. The fragmentation pattern of organic impurity 48 consisted of a catechol fragment (m/z 110), a propionyl cation fragment (m/z 56) and molecular ion peak (m/z 166) that could result from either 1-(3,4-dihydroxyphenyl)propan-1-one or (2-hydroxyphenyl) propanoate, as illustrated in Figure 3-13. Similarly, the fragmentation pattern of organic impurity 50 could feasibly result from each of the potential isomers, as shown in Figure 3-14.

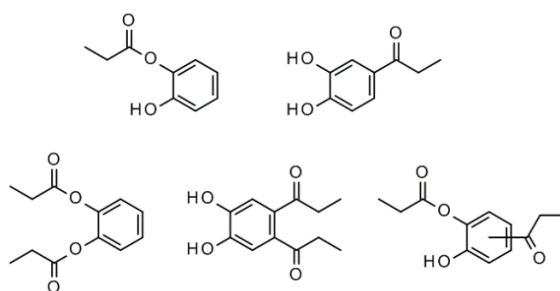


Figure 3-12: Potential chemical structures of organic impurity 48 (top) and organic impurity 50 (bottom)

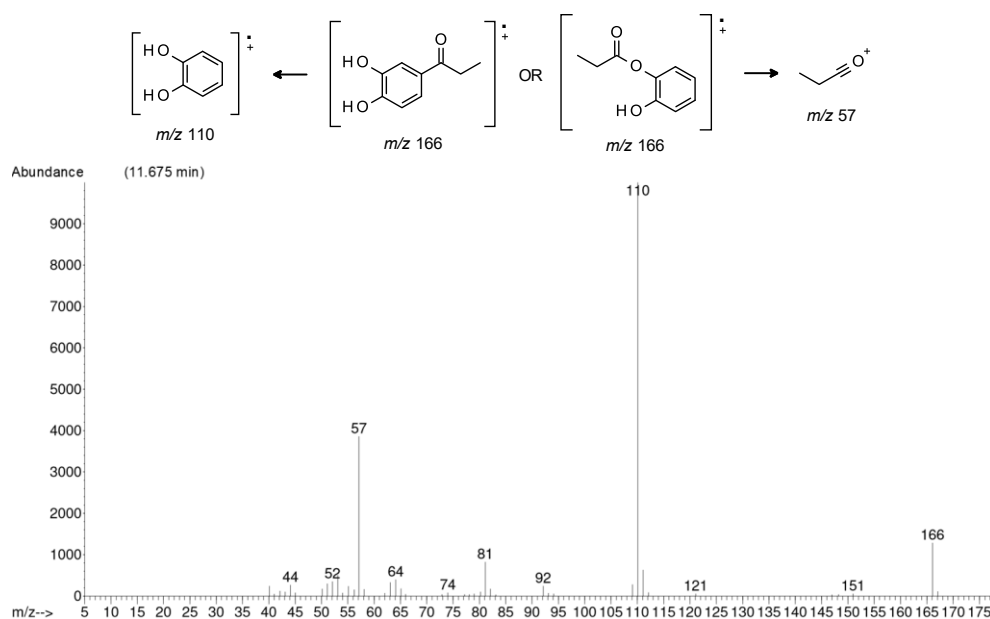


Figure 3-13: Mass spectrum and potential fragmentation pathways of organic impurity 48

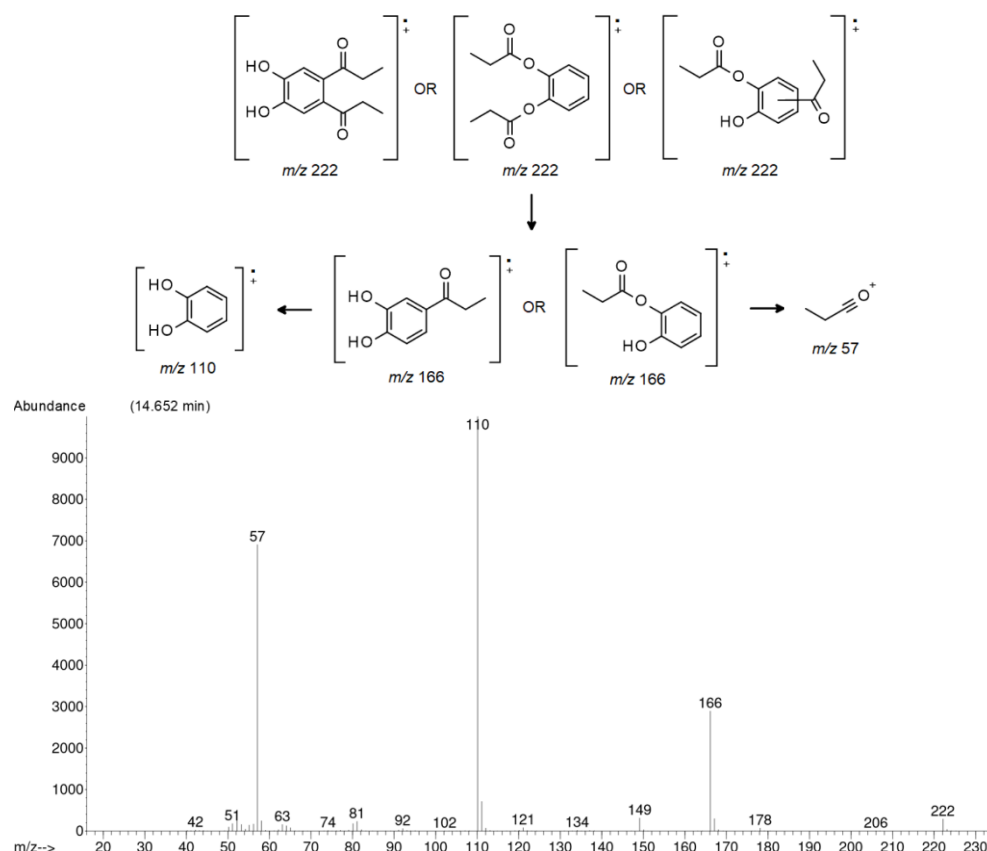
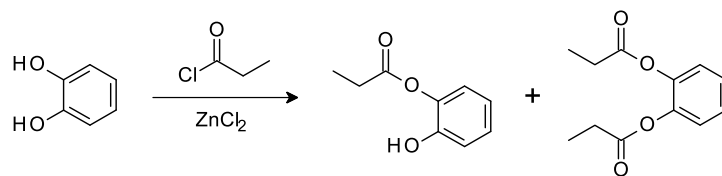


Figure 3-14: Mass spectrum and potential fragmentation pathways of organic impurity 50

The specific chemical structures of organic impurities 48 and 50 could also not be unequivocally determined based on the ^1H NMR spectrum of the synthesised 3,4-methylenedioxypropiofenone, due to the detection of chemical shifts from multiple organic impurities and the low concentration of these signals. The synthesis of these specific chemical compounds was therefore required to provide reference comparisons for organic impurities 48 and 50.

The synthesis of compounds 48 and 50 was performed by the reaction shown in Scheme 3-9, which substituted 1,3-benzodioxole with catechol in the reaction used to synthesise 3,4-methylenedioxypropiofenone. In the reaction of catechol with propionyl chloride and zinc chloride, it was hypothesised that either an aromatic substitution reaction or an esterification reaction could occur. These hypothesised reaction products correlated to the potential chemical structures of organic impurities 48 and 50 shown in Figure 3-12. The reaction resulted in a product mixture containing two compounds with retention times and mass spectra equivalent to those of organic impurities 48 and 50, as shown in Figure 3-15.



Scheme 3-9: The synthesis of (2-hydroxyphenyl) propanoate and (2-propanoyloxyphenyl) propanoate

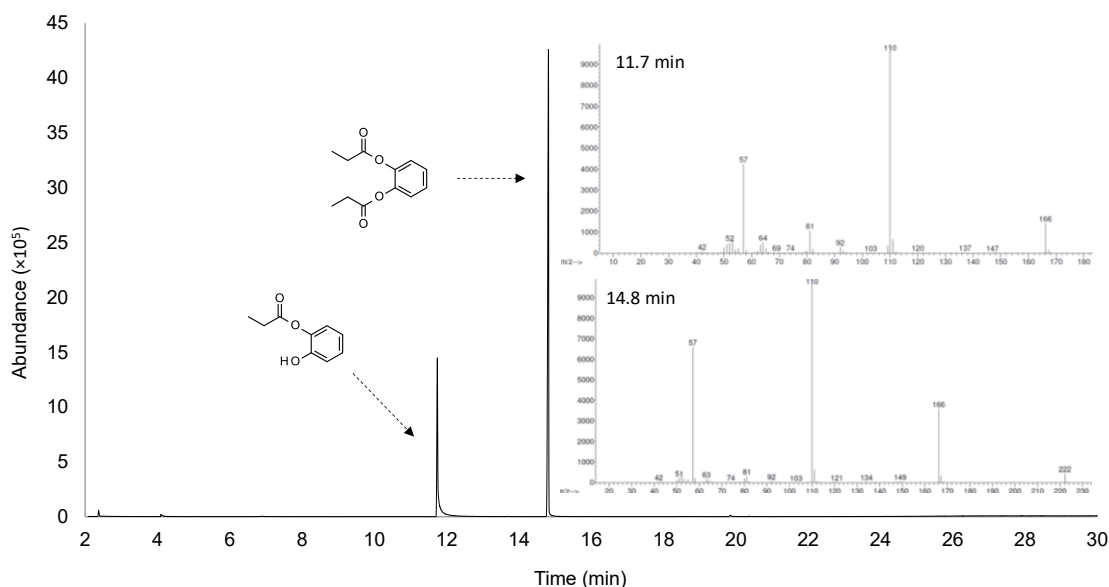


Figure 3-15: Gas chromatogram and mass spectra of synthesised (2-hydroxyphenyl) propanoate and (2-propanoyloxyphenyl) propanoate

The two synthesised compounds were identified using ^1H NMR spectroscopy as (2-hydroxyphenyl)propanoate and (2-propanoyloxyphenyl)propanoate, as shown in Figure 3-16. Analysis of the integration and splitting patterns of the signals within the aromatic region of the ^1H NMR spectrum indicated that no aromatic substitution had occurred. The two aromatic multiplet signals with equivalent integration values were consistent with a symmetrical, 1,2-disubstituted benzene structure, such as (2-propanoyloxyphenyl)propanoate. The two aromatic doublet signals and two aromatic triplet signals with equivalent integration values were also consistent with an unsymmetrical, 1,2-disubstituted benzene structure, such as (2-hydroxyphenyl)propanoate. The ^1H NMR spectrum therefore showed signals that corresponded to products of an esterification reaction.

The signals of (2-hydroxyphenyl)propanoate are labelled a – f and the signals of (2-propanoyloxyphenyl)propanoate are labelled g – k in the ^1H NMR spectrum shown in Figure 3-16. The methylene and methyl signals of these compounds were assigned based on their splitting patterns and integration, relative to the assigned aromatic protons. The quartet at 2.65 ppm corresponded to the two protons in the methylene group and the triplet at 1.26 ppm corresponded to the three protons in the methyl group of (2-hydroxyphenyl)propanoate. The

quartet at 2.57 ppm corresponded to the four protons in the two equivalent methylene groups and the triplet at 1.25 ppm corresponded to the six protons in the two equivalent methyl group of (2-propanoyloxyphenyl)propanoate. The identification of the signals that correspond to (2-hydroxyphenyl)propanoate (organic impurity 48) and (2-propanoyloxyphenyl)propanoate (organic impurity 50) enabled the assignment of their signals in the ^1H NMR spectrum of 3,4-methylenedioxypropiofenone, as shown in Figure 3-11.

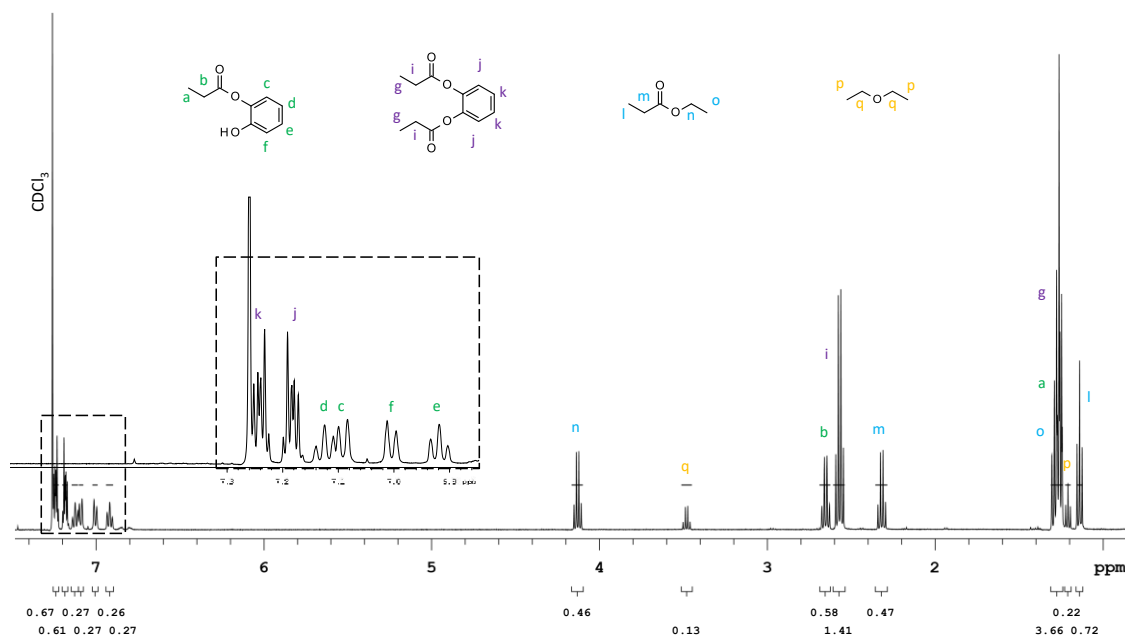
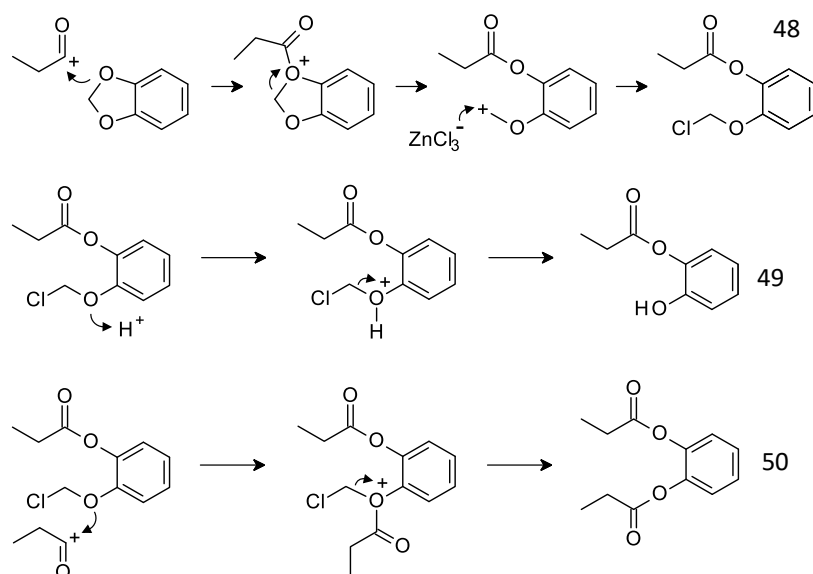


Figure 3-16: ^1H NMR spectrum of (2-hydroxyphenyl) propanoate and (2-propanoyloxyphenyl) propanoate

Organic impurities 48 and 50 could have formed during the synthesis of 3,4-methylenedioxypropiofenone as a result of a catechol impurity in the 1,3-benzodioxole starting material. However, no catechol was detected in the 1,3-benzodioxole that was synthesised and used in this synthetic pathway. This indicated that in the synthesis of 3,4-methylenedioxypropiofenone, organic impurities 48 and 50 were reaction by-products formed by the ether cleavage of 1,3-benzodioxole

The ether cleavage reaction proceeded by the reaction mechanism shown in Scheme 3-10. Propionyl chloride reacted with zinc chloride to form a propionyl cation, which subsequently reacted with the ether functional group in 1,3-benzodioxole to form a chlorinated intermediate. This chlorinated intermediate then reacted with either an acidic hydronium ion to form organic impurity 48, or a second propionyl cation to form organic impurity 50. The chlorinated intermediate in this reaction was also detected in 3,4-methylenedioxypropiofenone as organic impurity 49, further confirming the formation of organic impurities 48 - 50 by this reaction

mechanism. The identification of organic impurity 49 was primarily based on the fragmentation pattern of its mass spectrum, as illustrated in Figure 3-17.



Scheme 3-10: Reaction mechanism for the formation of organic impurities 48, 49 and 50

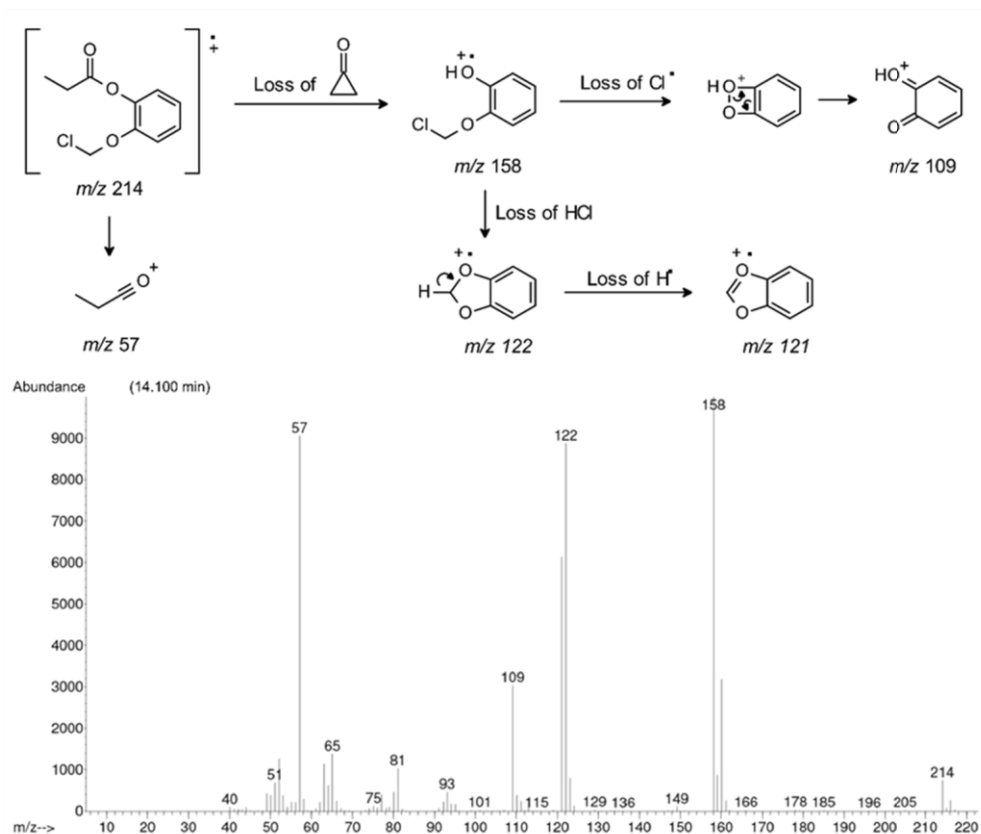
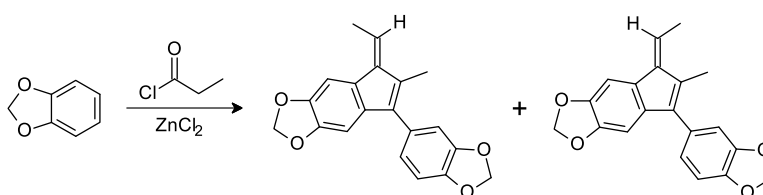


Figure 3-17: Mass spectrum and proposed fragmentation scheme of organic impurity 49

3.3.3.2 Synthesis and identification of organic impurities 51 and 52 (a-b)

The structural elucidation of organic impurities 52 (a-b) was aided by the targeted synthesis of these specific compounds. This synthesis was achieved by the reaction of 1,3-benzodioxole with excess of propionyl chloride and zinc chloride (both at approximately 4.5 molar equivalents) as illustrated in Scheme 3-11. The gas chromatogram of the resulting reaction product is shown in Figure 3-18 and indicates two isomers that have equivalent retention times and mass spectra of impurities 52 (a-b). It is also evident that the reaction product consisted predominantly of the isomer with retention time 27.9 min, while the isomer at 27.8 min was detected at a significantly lower concentration.



Scheme 3-11: The synthesis of (5E)- and (5Z)-7-(1,3-benzodioxol-5-yl)-5-ethylidene-6-methyl-cyclopenta[f][1,3]benzodioxole

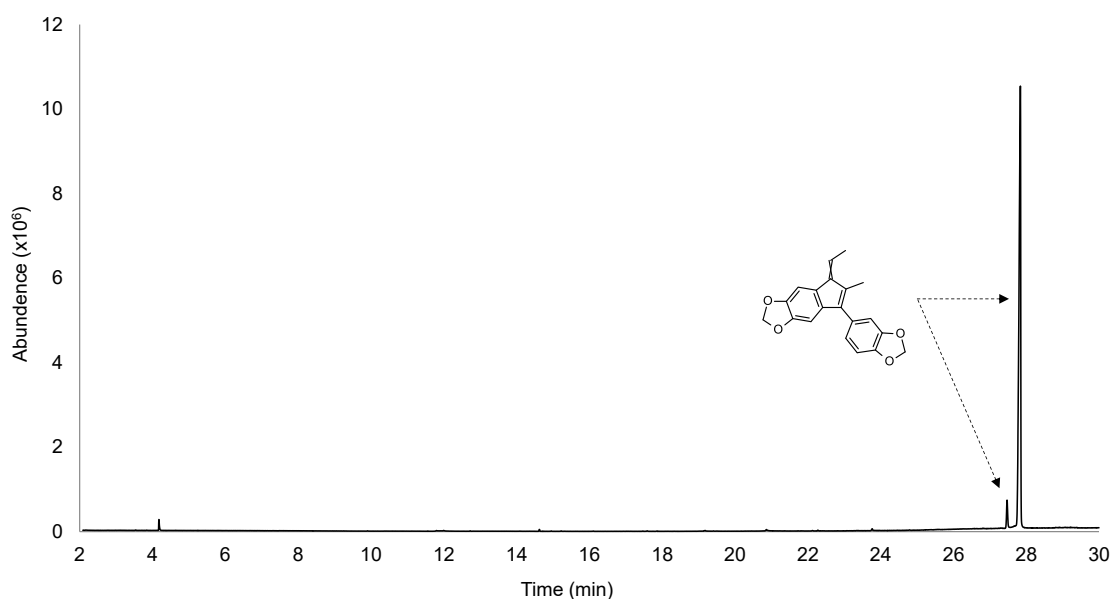


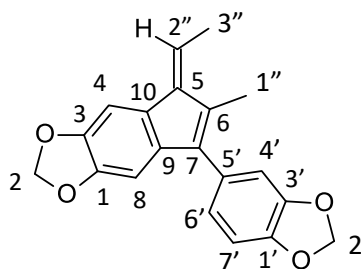
Figure 3-18: Gas chromatogram of (5E) and (5Z)-7-(1,3-benzodioxol-5-yl)-5-ethylidene-6-methyl-cyclopenta[f][1,3]benzodioxole

This reaction product was also analysed using NMR spectroscopy and identified as (5E)- and (5Z)-7-(1,3-benzodioxol-5-yl)-5-ethylidene-6-methyl-cyclopenta[f][1,3]benzodioxole, as shown in Table 3-4. The NMR spectroscopy techniques utilised were proton (Figure 3-20), carbon (Figure A3-2), distortionless enhancement by polarization transfer (DEPT; Figure A3-3), homonuclear correlation spectroscopy (COSY; Figure A3-4) and two-dimensional heteronuclear multiple bond correlation (HMBC; Figure A3-5). The combination of these techniques facilitated the structural

elucidation of organic impurity 52 (a-b), as they respectively generated information regarding the chemical structure's proton environments, carbon environments, carbon–hydrogen coupling over one bond, hydrogen–hydrogen coupling over two bonds and carbon–hydrogen coupling over two and three bonds.

Table 3-4: Summarised NMR data for the structural elucidation of 7-(1,3-benzodioxol-5-yl)-5-ethylidene-6-methyl-cyclopenta[f][1,3]benzodioxole

δ ^1H (ppm)	Correlation to protons at δ (ppm)	Correlation to carbon atoms at δ (ppm)
2.26 (3H, d, H3'')	6.64 (1H, q, H2'')	126.8 (CH, C2''), 140.5 (C5),
2.28 (3H, s, H1'')	-	131.5 (C10), 140.5 (C5), 141.5 (C7)
5.92 (2H, s, H2)	-	145.5 (C1), 146.9 (C3),
6.01 (2H, s, H2')	-	146.9 (C1'), 147.8 (C3')
6.63 (1H, s, H4)	-	131.5 (C10), 136.6 (C9), 140.5 (C5), 145.5 (C1), 146.9 (C3)
6.64 (1H, q, H2'')	2.28 (3H, s, H1'')	15.2 (CH ₃ , C3''), 131.0 (C6), 131.5 (C10), 140.5 (C5)
6.84 (1H, m, H6')	6.91 (1H, d, H7')	128.9 (C5'), 141.5 (C7), 147.8 (C3')
6.85 (1H, m, H4')	-	128.9 (C5'), 141.5 (C7), 146.9 (C1'), 147.8 (C3')
6.91 (1H, d, H7')	6.84 (1H, m, H6')	128.9 (C5'), 146.9 (C1'), 147.8 (C3')
7.03 (1H, s, H4)	-	131.5 (C10), 136.6 (C9), 141.5 (C7), 145.5 (C1), 146.9 (C3),



The mass spectra and associated fragmentation pattern of 7-(1,3-benzodioxol-5-yl)-5-ethylidene-6-methyl-cyclopenta[f][1,3]benzodioxole are consistent with the mass spectra of organic impurities 52 (a-b), shown in Figure 3-19. The identification of the signals in the ^1H NMR spectrum (Figure 3-20) that correspond to (E)- and (Z)-7-(1,3-benzodioxol-5-yl)-5-ethylidene-6-methyl-cyclopenta[f][1,3]benzodioxole enabled the assignment of some of their signals in the ^1H NMR spectrum of 3,4-methylenedioxypropiofenone, as shown in Figure 3-11. This

confirmed the identification of organic impurity 52 (a-b) as (E)- and (Z)-7-(1,3-benzodioxol-5-yl)-5-ethylidene-6-methyl-cyclopenta[f][1,3]benzodioxole.

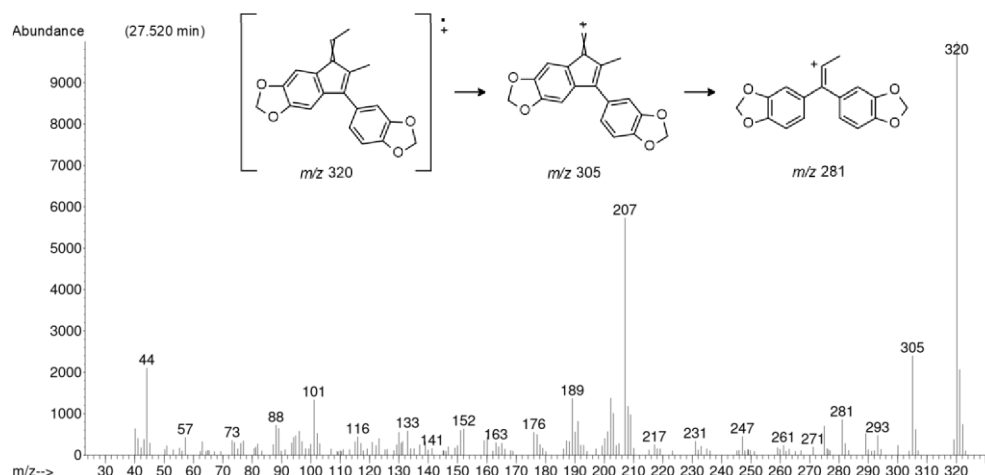


Figure 3-19: Mass spectrum and proposed fragmentation scheme of organic impurity 52

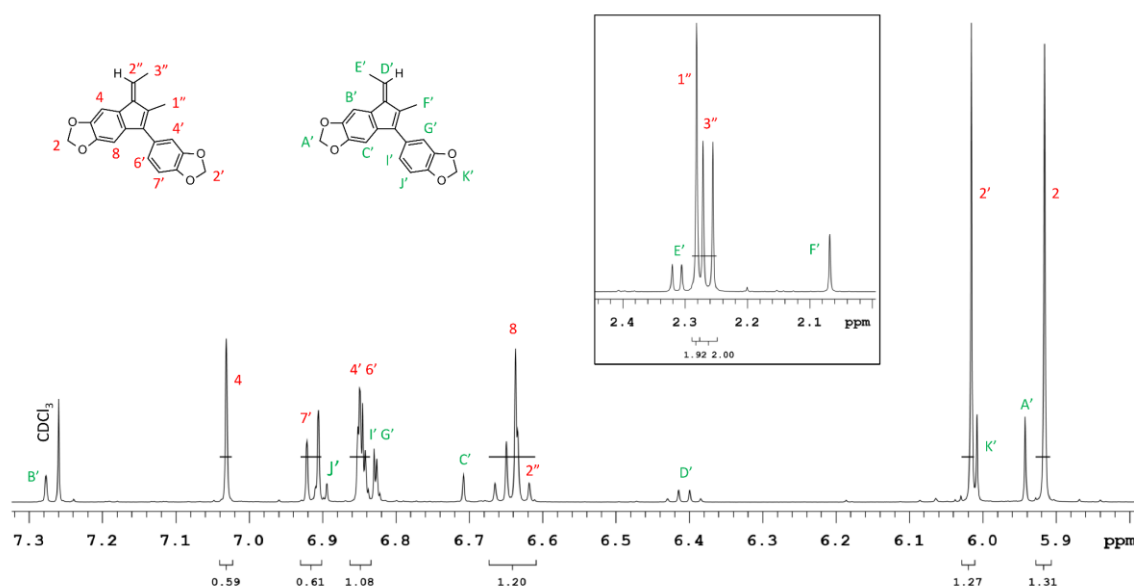


Figure 3-20: ^1H NMR spectrum of (5E) and (5Z)-7-(1,3-benzodioxol-5-yl)-5-ethylidene-6-methyl-cyclopenta[f][1,3]benzodioxole

Organic impurity 51 was identified by the molecular ion observed in the mass spectrum (Figure 3-21) and was formed by a similar reaction mechanism as organic impurities 52 (a-b). Organic impurity 51 was formed by the electrophilic aromatic substitution of 1,3-benzodioxole with 3,4-methylenedioxypropionophenone via the mechanism shown in Scheme 3-12[92]. The aromatic electron pair from 1,3-benzodioxole reacts with the cation formed by the reaction of the zinc(II) chloride and 3,4-methylenedioxypropionophenone. The loss of zinc hydroxychloride and the formation of an alkene bond yielded organic impurity 51. A similar thioether analogue was identified as a reaction by-product of the Friedel-Crafts acylation of ethyl phenyl sulfide [92].

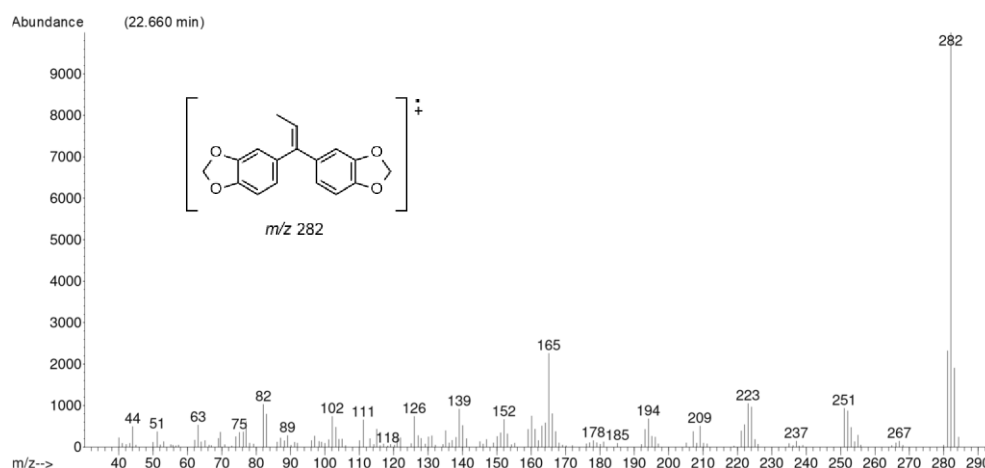
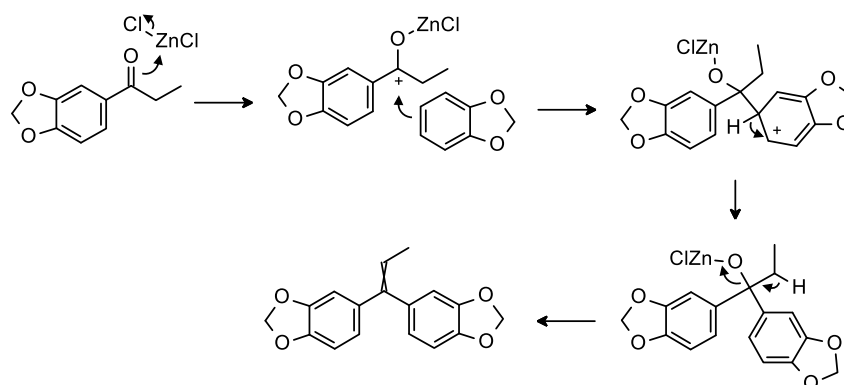
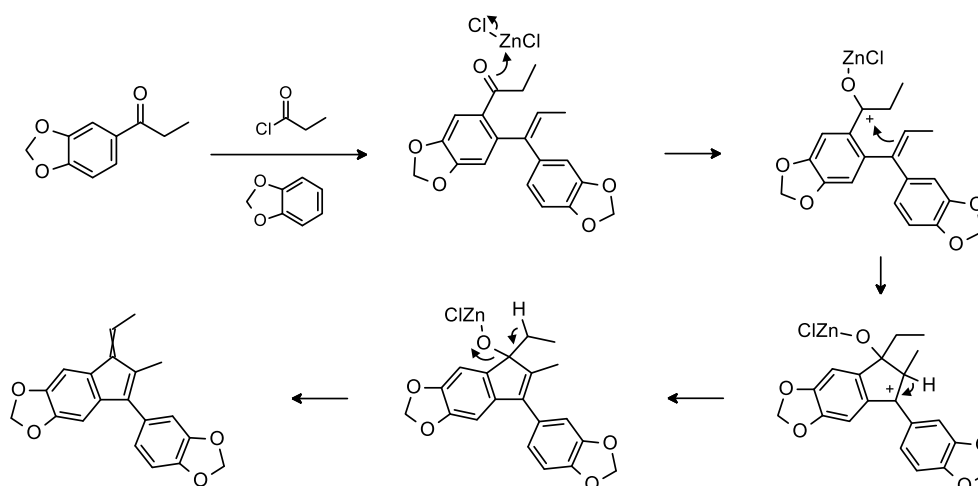


Figure 3-21: Mass spectrum and molecular ion of impurity 51



Scheme 3-12: Reaction mechanism for the formation of organic impurity 51



Scheme 3-13: Reaction mechanism for the formation of organic impurity 52 (a-b)

Organic impurities 52 (a-b) were formed by the reaction of 3,4-methylenedioxypropiophenone with 1,3-benzodioxole and propionyl chloride, as shown in Scheme 3-13. An intermediate compound bearing an alkene and a ketone functional group was formed through a second

Friedel-Crafts acylation reaction and the electrophilic aromatic substitution of 1,3-benzodioxole, though the order in which these reactions occurred is not known. Organic impurities 52 (a-b) were formed through a subsequent intra-molecular ring-forming reaction of the intermediate compound. The intra-molecular ring-forming reaction produced two geometric isomers due to the stereogenic carbons in the alkene group that formed in the final step of the reaction mechanism.

3.3.4 5-Bromo-3,4-methylenedioxypropioiophenone from 3,4-methylenedioxypropioiophenone

The analysis of the product of the bromination of 3,4-methylenedioxypropioiophenone using GC-MS and ^1H NMR spectroscopy confirmed that 5-bromo-3,4-methylenedioxypropioiophenone is the principal component. The mass spectrum of the largest peak in the gas chromatogram in Figure 3-22 corresponds to 5-bromo-3,4-methylenedioxypropioiophenone based on its fragmentation pattern, as shown in Figure 3-23. The signals that correspond to the proton environments of 5-bromo-3,4-methylenedioxypropioiophenone are labelled A–F in the ^1H NMR spectrum of the reaction product, shown in Figure 3-24. These signals are shifted downfield by varying degrees compared to the corresponding signals in the ^1H NMR spectrum of 3,4-methylenedioxypropioiophenone as a result of the de-shielding effect of the bromine atom.

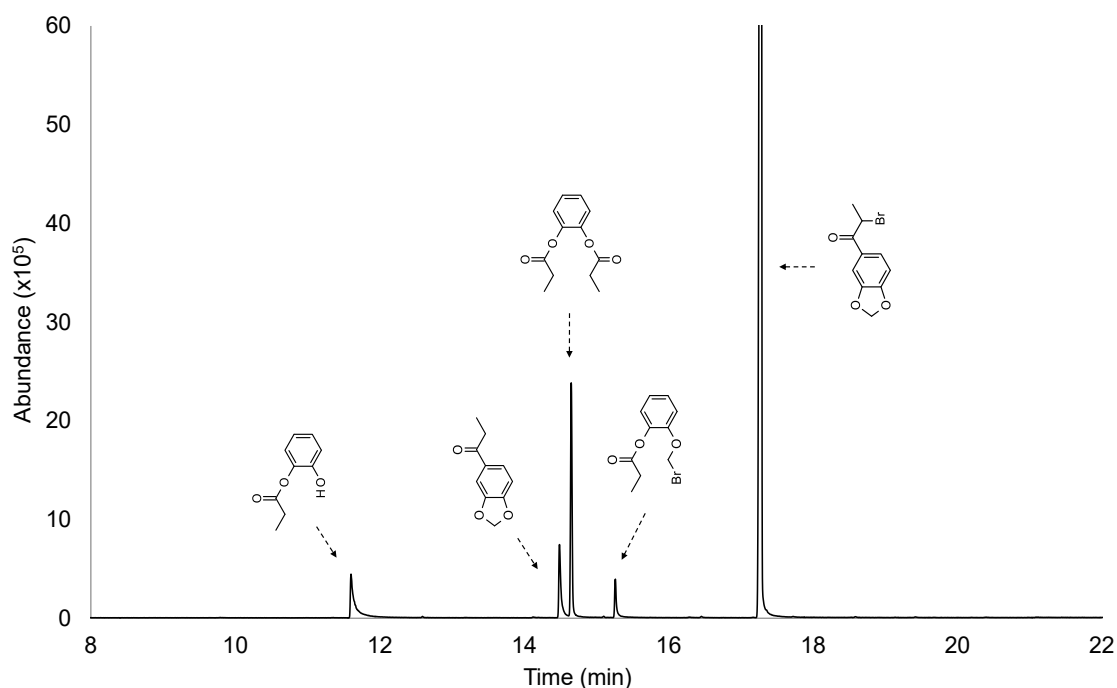


Figure 3-22: GC-MS total ion chromatogram of 5-bromo-3,4-methylenedioxypropioiophenone

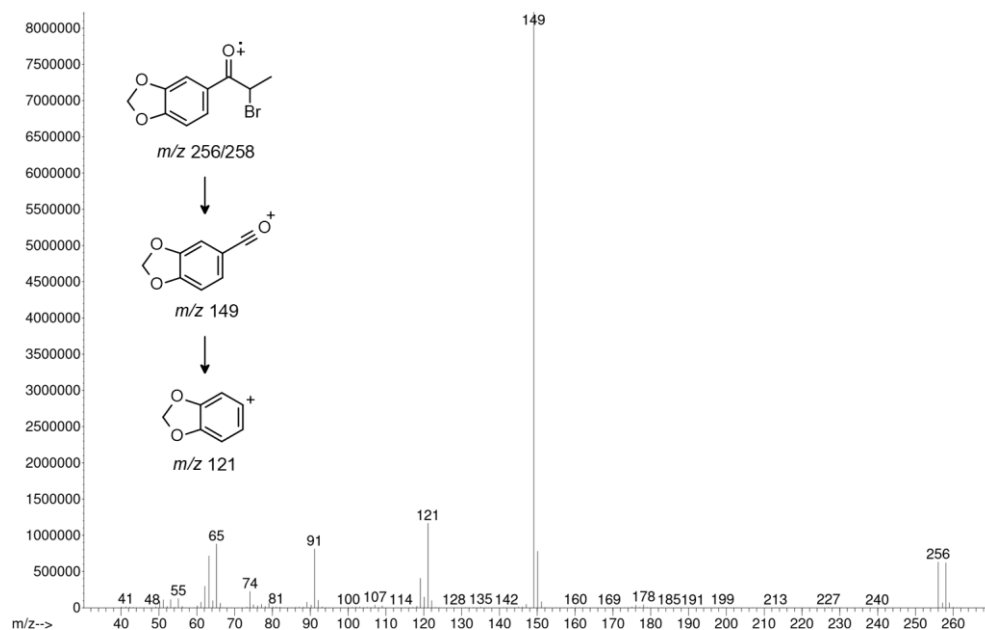


Figure 3-23: Mass spectrum and proposed fragmentation scheme of 5-bromo-3,4-methylenedioxypropiphenone

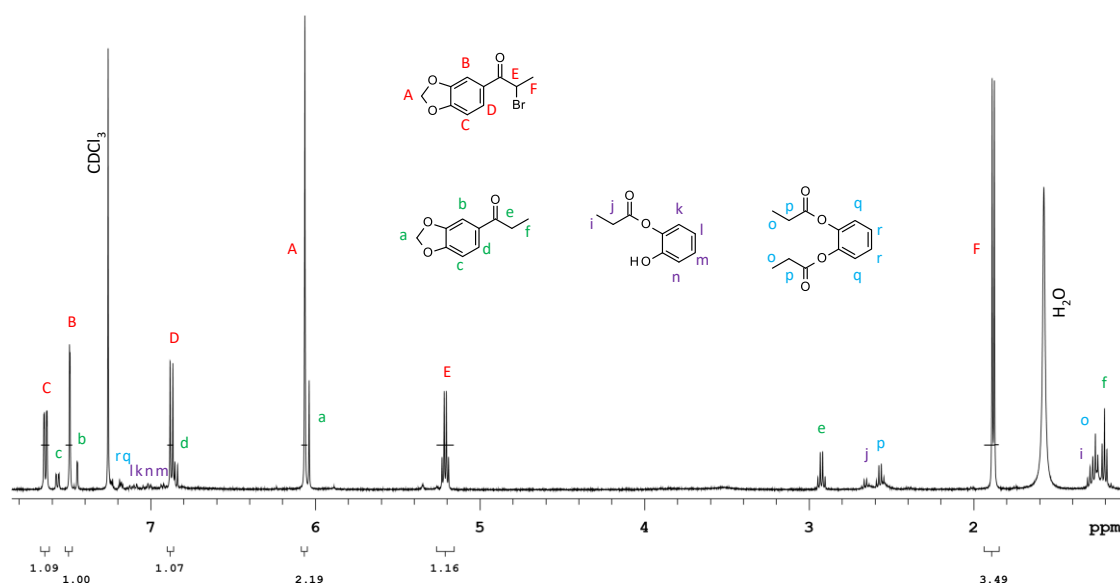


Figure 3-24: ^1H NMR spectrum of 5-bromo-3,4-methylenedioxypropiphenone and identified organic impurities

The gas chromatogram in Figure 3-22 shows the four organic impurities that were identified in the reaction product mixture. Organic impurities 23, 48 and 50 were consistently identified in the three preparations of 5-bromo-3,4-methylenedioxypropiphenone while organic impurity 53 was identified in one preparation. The assigned numbers, chemical structures, names, molecular weights, and m/z data of these organic impurities are shown in Table 3-5. Organic impurity 53 was identified based on the fragmentation pattern of its mass spectra, as shown in Figure 3-25.

Table 3-5: Organic impurities identified in 5-bromo 3,4-methylenedioxypropiofenone

No.	Impurity Structure	Impurity Name	MW (g/mol)	m/z
23		3,4-methylenedioxypropiofenone	178.2	178, 149, 121, 91, 65
48		(2-hydroxyphenyl) propanoate	166.2	166, 110, 57
50		(2-propanoyloxyphenyl) propanoate	222.2	222, 166, 110, 57
53*		[2-(bromomethoxy)phenyl] propanoate	259.1	260/258, 204/202, 122/121, 109, 95, 57

* This organic impurity was only identified in one preparation

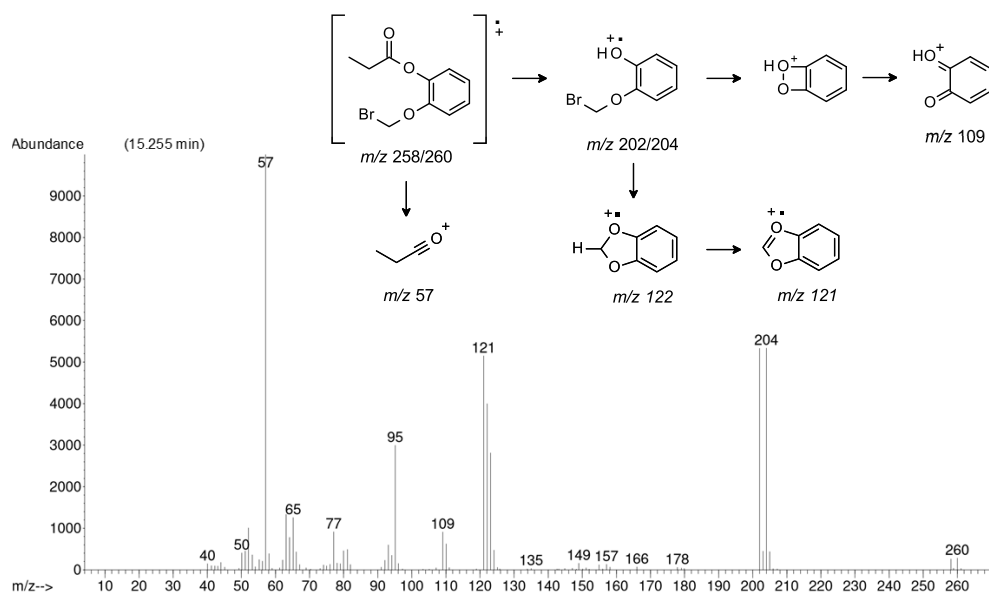
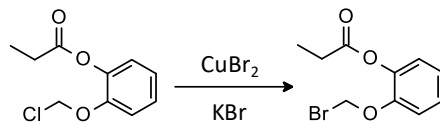


Figure 3-25: Mass spectrum and proposed fragmentation scheme of organic impurity 53

Organic impurities 48 and 50 were carried over, unchanged, from the synthesis of 3,4-methylenedioxypropiofenone, while organic impurities 23 and 53 originated from the preparation of 5-bromo-3,4-methylenedioxypropiofenone. Organic impurity 23 is the reaction starting material (3,4-methylenedioxypropiofenone), and its detection indicated that the bromination reaction did not go to completion. Organic impurity 53 was formed as a result of the bromine substitution reaction of impurity 49, as shown in Scheme 3-14. The detection of

impurity 53 in only one preparation of 5-bromo-3,4-methylenedioxypropiphenone was likely the result of varying concentrations of impurity 49 across the three preparations of 3,4-methylenedioxypropiphenone utilised.



Scheme 3-14: Formation of organic impurity 53

The identity of organic impurities 23, 48 and 50 was confirmed through ^1H NMR spectroscopy, as shown in Figure 3-24. The signals that correspond to these organic impurities were determined in the analysis of the 3,4-methylenedioxypropiphenone reaction product, as shown in Figure 3-11, and are present in the ^1H NMR spectrum of the 5-bromo-3,4-methylenedioxypropiphenone reaction product.

3.3.5 Methylone from 5-bromo-3,4-methylenedioxypropiphenone

The analysis of the product of the amination of 5-bromo-3,4-methylenedioxypropiphenone with GC-MS and ^1H NMR spectroscopy confirmed that methylone is the principal component. The mass spectrum of the largest peak in the gas chromatogram in Figure 3-26 corresponds to methylone based on its fragmentation pattern, as shown in Figure 3-27. The signals that correspond to the proton environments of methylone are labelled A–G in the ^1H NMR spectrum of the reaction product, shown in Figure 3-28.

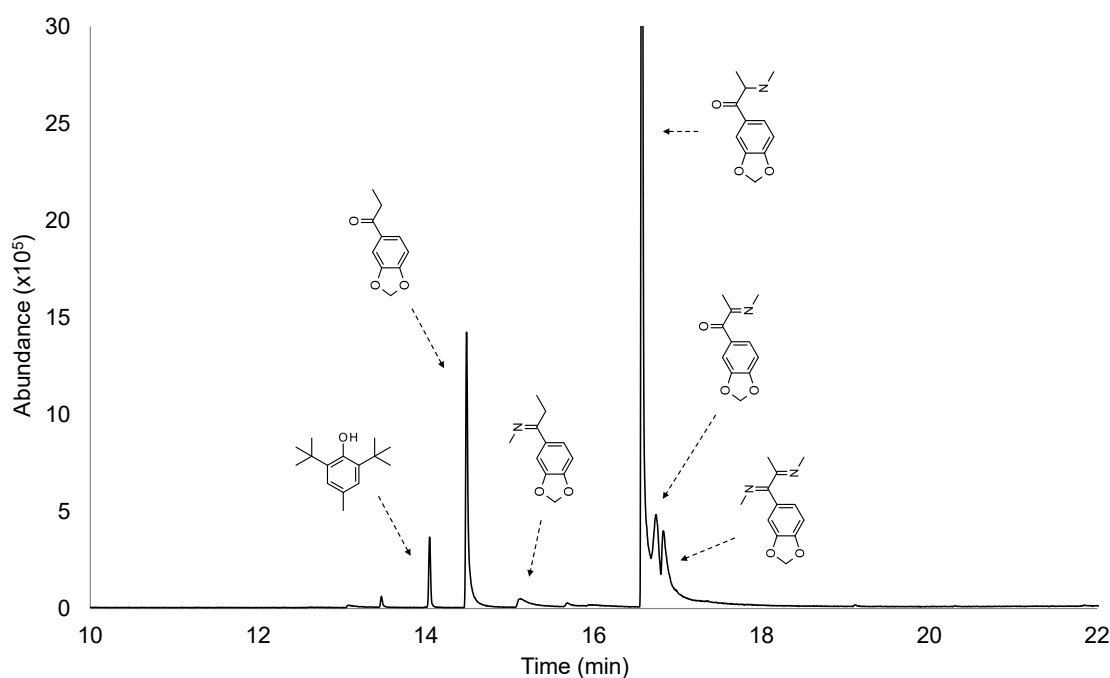


Figure 3-26: GC-MS total ion chromatogram of methylone

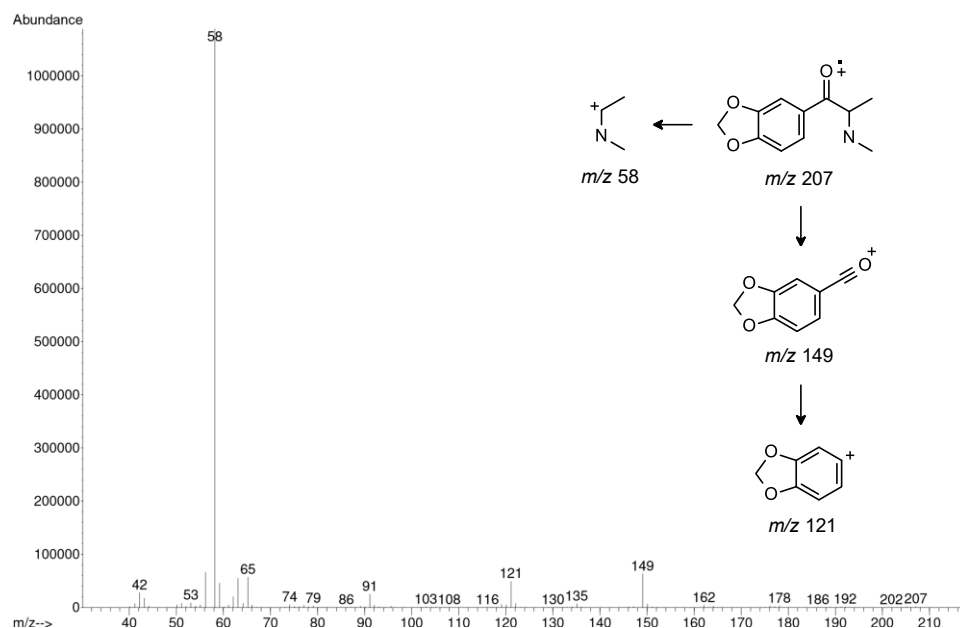


Figure 3-27: Mass spectrum and proposed fragmentation scheme of methylone

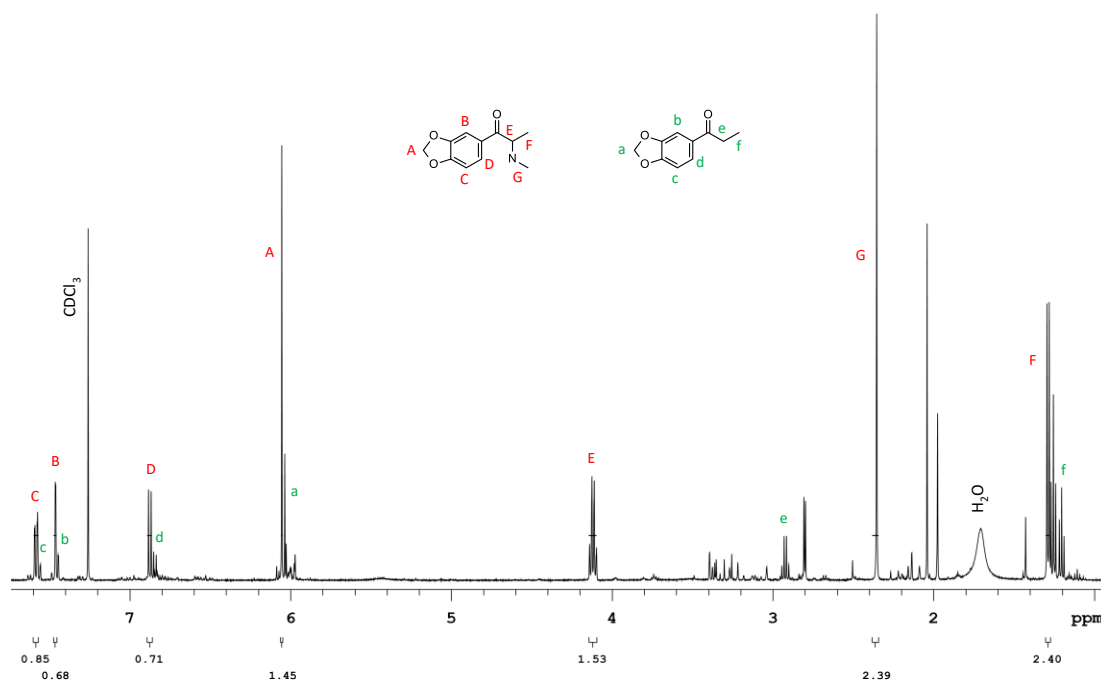


Figure 3-28: ^1H NMR spectrum of methylone

Figure 3-26 shows the five organic impurities that were identified in the reaction product mixture. Organic impurities 23, 43, 54 and 56 were consistently identified in the three preparations of 5-bromo-3,4-methylenedioxypropiofenone while organic impurity 55 was identified in one preparation. The assigned numbers, chemical structures, names, molecular weights, and m/z data of these organic impurities are shown in Table 3-6. Organic impurities 43, 54 and 55 were identified based on the fragmentation pattern of their mass spectra, as shown in Figure 3-29 to Figure 3-31. The mass spectrum of organic impurity 56, shown in Figure 3-32,

corresponds to the library reference mass spectrum of butylated hydroxytoluene with a 98% quality.

Table 3-6: Organic impurities identified in methylone

No.	Impurity Structure	Impurity Name	MW (g/mol)	m/z
23		3,4-methylenedioxy propiophenone	178.2	178, 149, 121, 91, 65
43		1-(1,3-benzodioxol-5-yl)-2-methylimino-propan-1-one	205.2	205, 149, 121, 56
54		1-(1,3-benzodioxol-5-yl)-N-methyl-propan-1-imine	191.2	190/191, 162, 147, 135, 121, 63, 32
55*		1-(1,3-benzodioxol-5-yl)-N1, N2-dimethyl-propane-1,2-diimine	218.3	217, 162, 147, 56
56		butylated hydroxytoluene	220.4	220, 205, 145, 57

* This organic impurity was identified in one preparation

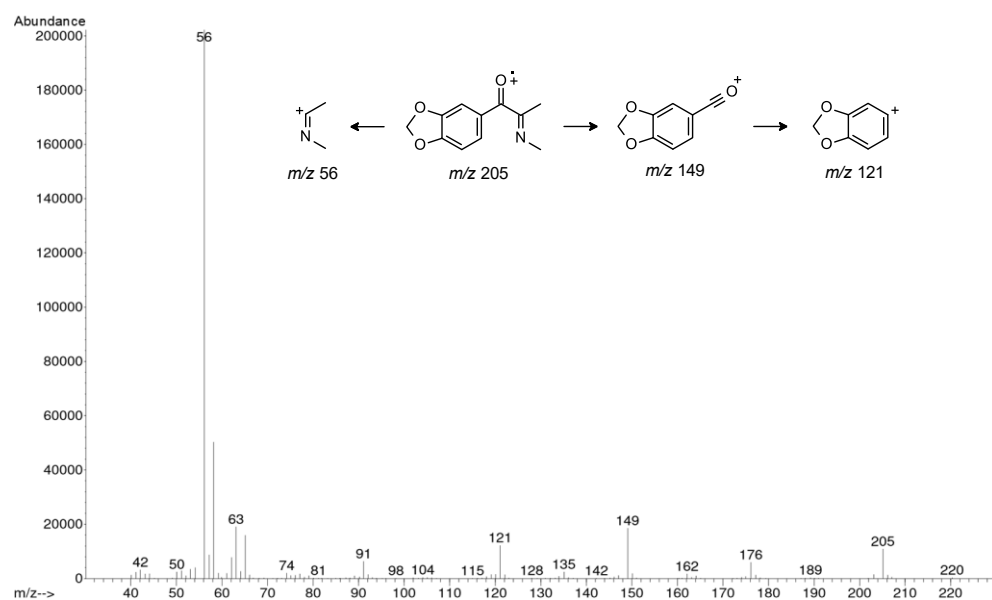


Figure 3-29: Mass spectrum and proposed fragmentation scheme of organic impurity 43

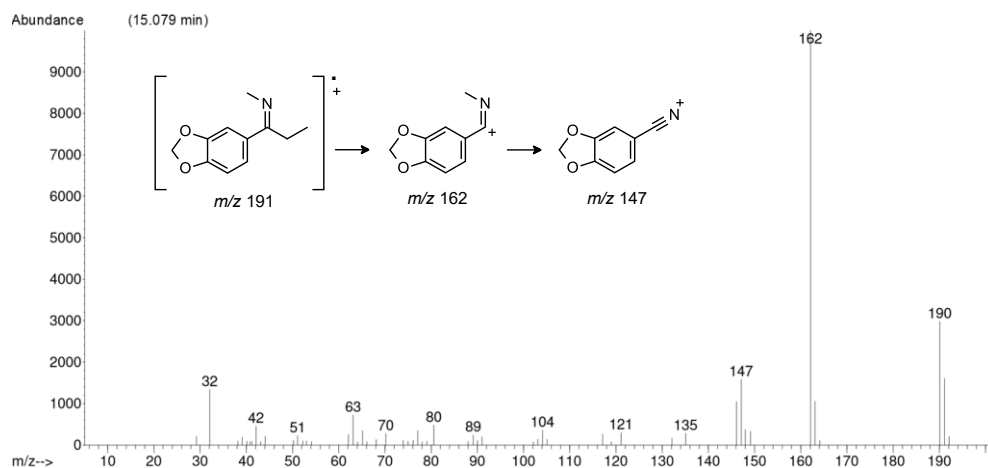


Figure 3-30: Mass spectrum and proposed fragmentation scheme of organic impurity 54

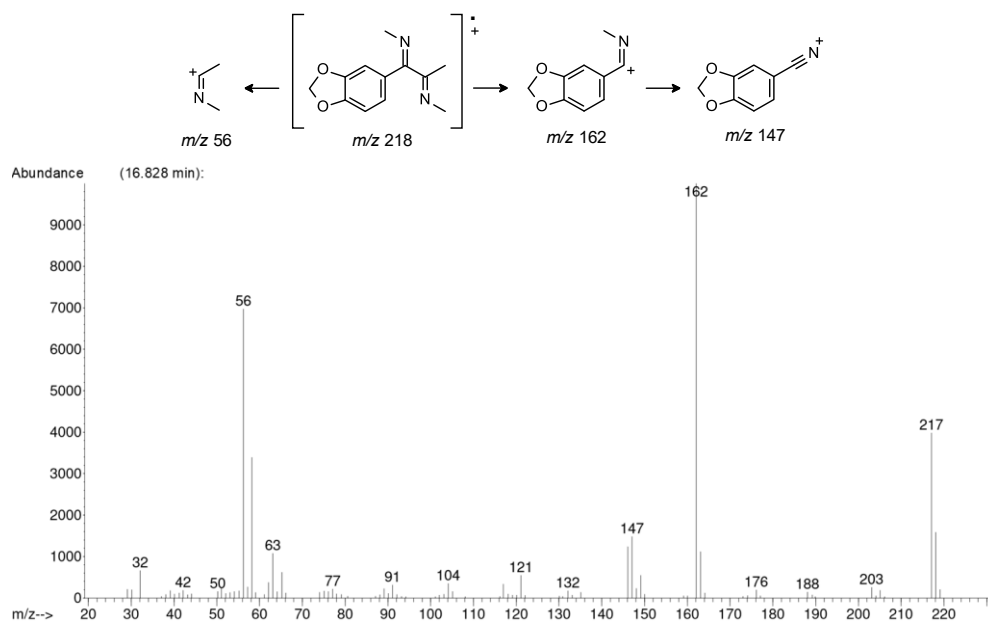


Figure 3-31: Mass spectrum and proposed fragmentation scheme of organic impurity 55

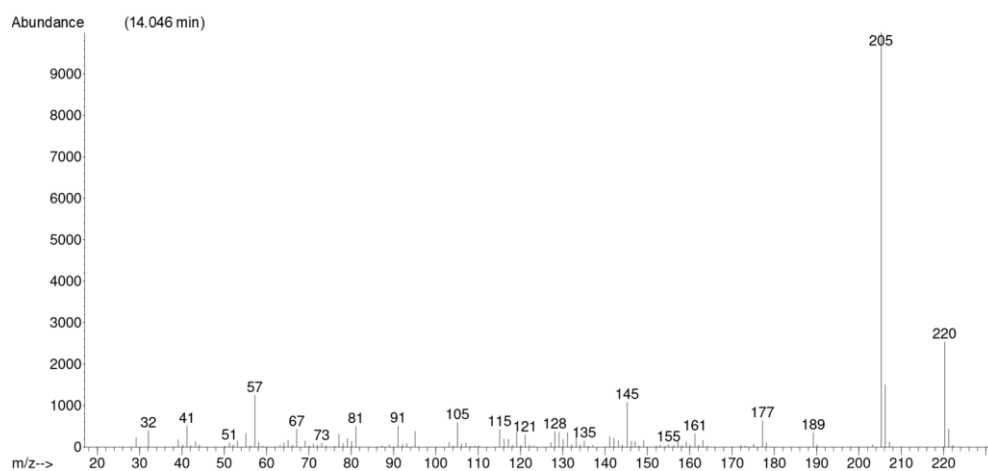
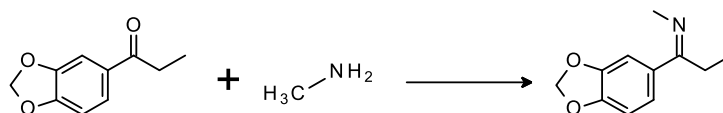


Figure 3-32: Mass spectrum of organic impurity 56 (98% quality for butylated hydroxytoluene)

Organic impurity 23 was carried over unchanged from the previous reaction product, although it may have also formed by decomposition of methylone [68]. Organic impurity 43 is a characteristic artefact that had previously been identified in methylone [8]. Organic impurity 54 was formed by the reaction of the ketone functional group in 3,4-methylenedioxypropionophenone with methylamine, as shown in Scheme 3-15. Organic impurity 55 was formed when both an imine-forming reaction between the ketone functional group and methylamine, and the reaction that formed the characteristic artefact, occurred on the same methylone molecule. Organic impurity 56 is a stabiliser present in the reaction solvent tetrahydrofuran. Trace amounts of 56 were also detected in previous reaction products as it is also a stabiliser in the diethyl ether used in the solvent extraction process.



Scheme 3-15: Formation of organic impurity 54

3.4 Route Specific Organic Impurities

The detection of organic impurities 23 and 54 in methylone is indicative of synthesis from 3,4-methylenedioxypropionophenone, and the detection of organic impurities 43 and 55 in methylone was indicative of synthesis via 5-bromo-3,4-methylenedioxypropionophenone. However, the detection of these organic impurities provided little discriminatory value, as all reported syntheses of racemic cathinones utilised the appropriate ring-substituted propionophenone as a precursor [8, 25]. The detection of organic impurity 56 also had little to no discriminatory value, as it originated from solvents that could be utilised in numerous synthetic pathways. Therefore, no route specific organic impurities were detected or identified in methylone that had been synthesised from catechol.

Organic impurities 39, 40 (a-c), 46 and 47 were characteristic of the methylenation of catechol but were not detected in the products of subsequent syntheses during the preparation of methylone. The removal of these methylenation reaction by-products demonstrated a limitation of the organic impurity profiling of methylone, as the use of catechol as a precursor could not be determined based on analysis of the methylone final product under the conditions used. This is consistent with the study by Bortz *et al.* [29], where similarly no organic impurities that signified the use of catechol as a precursor were detected in methylone.

Impurities 48 - 52 (a-b) are characteristic of the Friedel-Crafts acylation of 1,3-benzodioxole but were not detected in the products of the subsequent bromination and amination reactions. This

demonstrated that the synthesis of methylone via the 1,3-benzodioxole intermediate could not be determined through the analysis of the methylone final product under the conditions used. In the study by Bortz *et al.* [29], these organic impurities were similarly not detected in the methylone final product. However, Bortz *et al.* reported that organic impurity 45 was identified which indicated synthesis from 1,3-benzodioxole, as its formation in methylone is dependent on remaining propionyl chloride reactant from the Friedel-Crafts acylation of 1,3-benzodioxole [29]. This route specific impurity was not identified in this work, presumably as there was no remaining propionyl chloride in the 5-bromo-3,4-methylenedioxypropiofenone used in the amination reaction.

The inability to detect route specific impurities in subsequent reaction product mixtures meant that the organic impurity profiling techniques used here could provide no evidence of the use of the catechol precursor or the 1,3-benzodioxole intermediate, even when relatively unsophisticated purification techniques were used. This demonstrates the significant limitations of organic impurity profiling of methylone in the determination of precursor chemicals and synthetic pathways used. It is feasible, however, that these route specific organic impurities could be detected if methylone was analysed using a more sensitive GC-MS technique or liquid chromatography tandem mass spectrometry (LC-MS/MS).

Finally, 3,4-methylenedioxyphenyl-1,2-propanedione and an imidazolium by-product, which have been previously identified as organic impurities in synthetic cathinones [63, 68], were not identified in the synthesised methylone. 3,4-Methylenedioxyphenyl-1,2-propanedione may form by decomposition of methylone under a variety of conditions [68]. In the context of the current work, its presence (or otherwise) does not provide any additional information about the synthetic pathway. The reaction of two cathinone molecules during synthesis and/or storage may form an imidazolium compound [63] which, similarly, might not offer unambiguous insights into the precursors used during synthesis. The potential detection and identification of these compounds through alternate analytical techniques was therefore not pursued.

3.5 Conclusions

Methylone was synthesised from the uncontrolled precursor catechol via a four-step synthetic pathway that is feasible in a reasonably equipped clandestine laboratory. This synthesis involved the methylenation of catechol, Friedel-Crafts acylation of 1,3-benzodioxole, the bromination of 3,4-methylenedioxypropiofenone and the nucleophilic substitution of bromine in 5-bromo-3,4-methylenedioxypropiofenone with methylamine.

The reaction products of each step in the synthetic pathway were analysed using GC-MS and ^1H NMR spectroscopy and the chemical structure and origin of organic impurities was determined. Six organic impurities (39, 40 (a-c), 46 and 47) were identified in 1,3-benzodioxole, six organic impurities (48, 49, 50, 51 and 52 (a-b)) were identified in 3,4-methylenedioxypropiofenone, four organic impurities (23, 48, 50 and 53) were identified in 5-bromo-3,4-methylenedioxypropiofenone and five organic impurities (23, 43, 54, 55 and 56) were identified in methylone. Exploratory synthetic experiments were also conducted to unambiguously identify organic impurities 48, 50, and 52 (a-b).

An important issue identified in this work is that neither the catechol precursor or 1,3-benzodioxole intermediate could be identified by the organic impurity profiling techniques used here. Some route specific impurities, indicating the synthetic pathway used to prepare 3,4-methylenedioxypropiofenone, were identified in the synthesised intermediate compounds but the organic impurities (or their reaction products) were not detected in the subsequent reaction mixtures, even when using relatively unsophisticated purification techniques. This inability to determine the precursor and synthetic pathway used through analysis of the methylone final product demonstrated a significant limitation in the organic impurity profiling of methylone.

Chapter 4: Safrole

Chapter 4: Safrole

4.1 Introduction

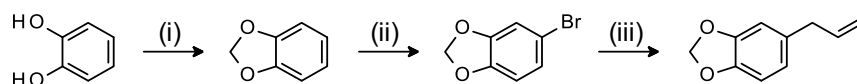
This chapter discusses the synthesis and organic impurity profiling of safrole that was synthesised from the 'pre-precursor' catechol via two synthetic routes and the 'pre-precursor' eugenol via one synthetic route. The reactions utilised in these three synthetic routes are described in detail in Section 4.2. The reaction products of each step in the synthetic routes were analysed using GC-MS and ^1H NMR spectroscopy. The chemical structures and origins of the detected organic impurities are detailed in Section 4.3. The organic impurity profiles of the safrole synthesised by the three synthetic routes were compared against each other and the relevant literature. The significance of the identified organic impurities was analysed, and route specific impurities are discussed in Section 4.4.

4.2 Synthesis of Safrole

Safrole was synthesised from catechol via two synthetic routes and from eugenol via one synthetic route. The synthesis of safrole was performed at minimum in duplicate for each synthetic route, using synthetic methods that are feasible in a reasonably equipped clandestine laboratory. All products were purified by unsophisticated purification techniques, such as liquid-liquid extraction and filtration, to mimic a clandestine laboratory setting.

4.2.1 Route 1: Safrole from Catechol

Safrole was synthesised from catechol via the reaction pathway shown in Scheme 4-1, which was designated as Route 1. This reaction pathway has three steps: the methylenation of catechol, the bromination of 1,3-benzodioxole and a Grignard reaction using 5-bromo-1,3-benzodioxole and allyl bromide.



Scheme 4-1: Synthesis of safrole from catechol via Route 1

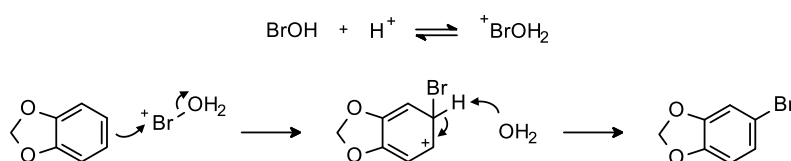
(i) CH_2Cl_2 , NaOH (ii) HBr, HOOH , CH_3COOH (iii) 1. Mg, DIBAL-H 2. $\text{CH}_2=\text{CHCH}_2\text{Br}$

4.2.1.1 1,3-Benzodioxole from Catechol

1,3-Benzodioxole was synthesised by the methylenation of catechol with dichloromethane (Reaction i, Scheme 4-1), which was discussed in detail in Section 3.2.1. There are multiple reagents and solvents that are viable options for the methylenation reaction [12, 33]. In the synthesis of safrole via Route 1, the methylenation reaction was performed using sodium hydroxide as base and the polar, aprotic solvent dimethyl sulfoxide.

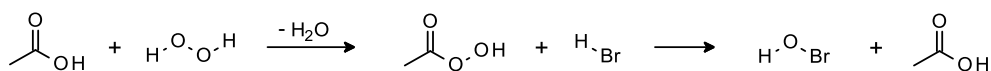
4.2.1.2 5-Bromo-1,3-benzodioxole from 1,3-Benzodioxole

The bromination of 1,3-benzodioxole (Reaction ii, Scheme 4-1) in hypobromous acid is an electrophilic aromatic substitution reaction. The reaction mechanism for the synthesis of 5-bromo-1,3-benzodioxole from 1,3-benzodioxole is shown in Scheme 4-2. In the acidic reaction conditions used, hypobromous acid is in equilibrium with ${}^+\text{BrOH}_2$ [93], which reacts with 1,3-benzodioxole to form a resonance stabilised intermediate. Subsequent deprotonation yields 5-bromo-1,3-benzodioxole.



Scheme 4-2: Reaction mechanism for the formation of the 5-bromo-1,3-benzodioxole

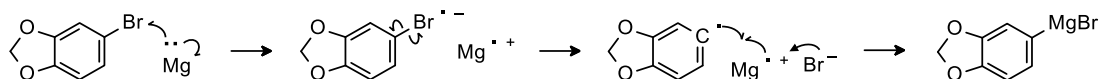
Hypobromous acid was generated *in situ* by the reactions of hydrobromic acid, acetic acid and hydrogen peroxide, as shown in the reaction mechanism in Scheme 4-3. The dehydration reaction of acetic acid and hydrogen peroxide yields peracetic acid, which reacts with hydrobromic acid to form hypobromous acid and regenerate acetic acid. The strong oxidant peracetic acid was required to effectively oxidise the bromide in hydrobromic acid to bromine that is in the +1 oxidation state in hypobromous acid [94].



Scheme 4-3: The *in situ* formation of hypobromous acid

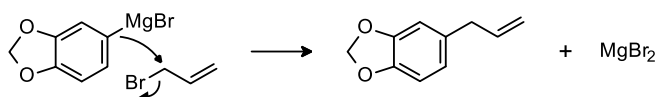
4.2.1.3 Safrole from 5-Bromo-1,3-benzodioxole

The synthesis of safrole from 5-bromo-1,3-benzodioxole was achieved by a Grignard reaction with allyl bromide (Reaction iii, Scheme 4-1). The first step in the Grignard reaction was the formation of the Grignard reagent by the reaction of 5-bromo-1,3-benzodioxole and magnesium with DIBAH as an activating agent. The reaction mechanism for the formation of the Grignard reagent is shown in Scheme 4-4, which involves the formation of radical intermediates [95]. The use of DIBAH as an activating agent was advantageous as it permits the safe synthesis of the Grignard reagent with reaction initiation at or below room temperature, and the formation of the Grignard reagent when trace levels of water are contained within the reaction mixture [96].



Scheme 4-4: Reaction mechanism for the synthesis of the Grignard reagent

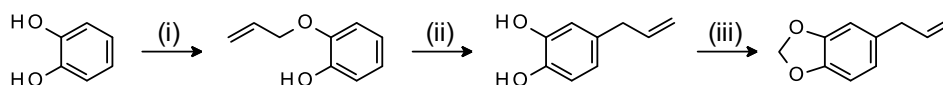
The second step was the reaction of the prepared Grignard reagent with allyl bromide, as shown by the reaction mechanism in Scheme 4-5. The carbon in the carbon-magnesium bond of the Grignard reagent is basic and nucleophilic [88], and substitutes the bromine in allyl bromide to form safrole. A Grignard reagent will decompose in the presence of water or react with atmospheric oxygen, and therefore Grignard reaction was performed with oven-dried glassware, anhydrous solvent, and under nitrogen gas.



Scheme 4-5: Reaction mechanism for the synthesis of safrole from the Grignard reagent and allyl bromide

4.2.2 Route 2: Safrole from Catechol

Safrole was synthesised from catechol via the reaction pathway shown in Scheme 4-6, which was designated as Route 2. This reaction pathway included three steps: the etherification of catechol and allyl bromide, the Claisen Rearrangement of 2-allyloxyphenol and the methylenation of 4-allylcatechol.

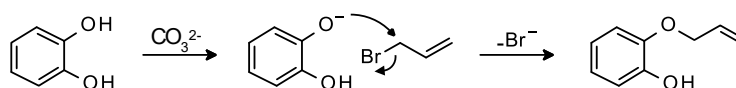


Scheme 4-6: The synthesis of safrole from catechol via Route 2.

(i) $\text{CH}_2\text{CHCH}_2\text{Br}$, K_2CO_3 (ii) NaOC_2H_5 , Δ (iii) CH_2Cl_2 , NaOH

4.2.2.1 2-Allyloxyphenol from Catechol

The etherification of catechol with allyl bromide to form 2-allyloxyphenol (Reaction i, Scheme 4-6) was achieved through the Williamson ether synthesis. The mechanism for the etherification reaction using catechol and allyl bromide is shown in Scheme 4-7. The base, potassium carbonate, first deprotonates catechol to form a catechoxide anion. The Williamson ether synthesis then occurs by the $\text{S}_{\text{N}}2$ reaction of the catechoxide anion with allyl bromide to form 2-allyloxyphenol.



Scheme 4-7: Reaction mechanism for the synthesis of 2-allyloxyphenol from catechol

4.2.2.2 4-Allylcatechol from 2-Allyloxyphenol

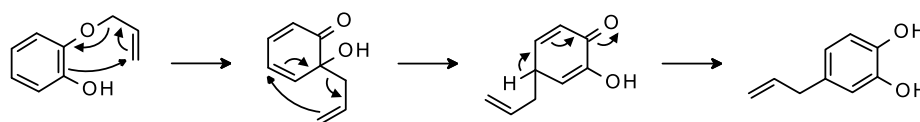
The Claisen rearrangement of 2-allyloxyphenol (Reaction ii, Scheme 4-6) is a base-catalysed thermal rearrangement reaction. The competing *ortho*- and *para*- Claisen rearrangements are sensitive to pH, and the use of sodium ethoxide base favours the desired *para*- Claisen

rearrangement [46]. The approximate reaction progress was determined through the analysis of quenched reaction aliquots at intervals using GC-MS. The gas chromatograms and gas chromatogram area data for the analysed aliquots are shown in Appendix 2. The peak areas of the starting material 2-allyloxyphenol (10.5 min) and the reaction products 3-allylcatechol (12.5 min) and 4-allylcatechol (13.7 min) were compared to determine the percentage reaction completion, as shown in Table 4-1. This also demonstrated that under the reaction conditions utilised, the desired product 4-allylcatechol and the reaction by-product 3-allylcatechol were synthesised in an approximate 5:1 ratio.

Table 4-1: Reaction progress of the Claisen rearrangement of 2-allyloxyphenol

Reaction Time (Hours)	Relative Percentage (%) in Reaction Aliquot of:			Reaction Completion (%)
	2-Allyloxyphenol	3-Allylcatechol	4-Allylcatechol	
3	96	1	3	4
8	86	2	11	14
24	71	5	24	29
48	23	13	64	77
72	7	15	78	93
96	1	16	83	99

The reaction mechanism for the synthesis of 4-allylcatechol from 2-allyloxyphenol through *para*-Claisen rearrangement is shown in Scheme 4-8. The bonding electrons in 2-allyloxyphenol undergo rearrangement through a pericyclic mechanism to form a cyclohexadienone intermediate [88, 95]. As the *ortho*- position is substituted by a phenol group, a second rearrangement occurs that yields a *para*-substituted cyclohexadienone intermediate [47, 95]. This intermediate then isomerises to form 4-allylcatechol [88].

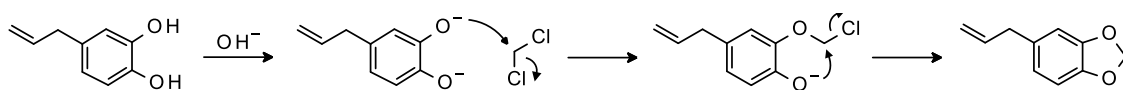


Scheme 4-8: Reaction mechanism for the synthesis of 4-allylcatechol from 2-allyloxyphenol

4.2.2.3 Safrole from 4-Allylcatechol

The methylenation of 4-allylcatechol (Reaction iii, Scheme 4-6) is a ring-forming reaction with dichloromethane under alkaline conditions. The reaction mechanism for the methylenation of 4-allylcatechol to yield safrole is shown in Figure 4-10. The sodium hydroxide base first

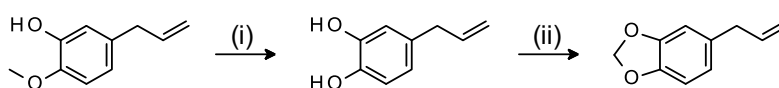
deprotonates 4-allylcatechol to form 4-allylbenzene-1,2-diolate. This intermediate then reacts with dichloromethane in a ring-forming reaction to form safrole.



Scheme 4-9: Reaction mechanism for the synthesis of safrole from 4-allylcatechol

4.2.3 Route 3: Safrole from Eugenol

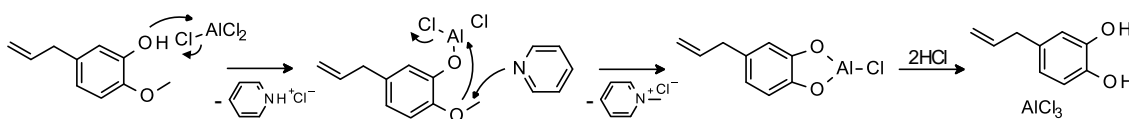
Safrole was synthesised from eugenol via the reaction pathway shown in Scheme 4-10, which was designated as Route 3. This reaction pathway included two steps: the demethylation of eugenol and the methylenation of 4-allylcatechol.



Scheme 4-10: The synthesis of safrole from eugenol via Route 3
(i) AlCl_3 , pyridine (ii) CH_2Cl_2 , NaOH

4.2.3.1 4-Allylcatechol from Eugenol

The demethylation of eugenol (Reaction i, Scheme 4-10) is an ether cleavage reaction that utilised aluminium chloride, pyridine and hydrochloric acid. The reaction conditions used were similar to the conditions used for demethylation of vanillin to form 3,4-dihydroxybenzaldehyde by Gallagher *et al.* [31]. The reaction mechanism for the synthesis of 4-allylcatechol from eugenol is shown in Scheme 4-11. Eugenol reacts with aluminium chloride to form an aluminium phenolate intermediate, which undergoes nucleophilic displacement with pyridine to form a five-membered cyclic intermediate [97, 98]. The five-membered cyclic intermediate is then hydrolysed with hydrochloric acid to yield 4-allylcatechol [97].



Scheme 4-11: Reaction mechanism for the synthesis of 4-allylcatechol from eugenol

4.2.3.2 Safrole from 4-Allylcatechol

The synthesis of safrole in Route 3 was achieved by a methylenation of 4-allylcatechol with dichloromethane (Reaction ii, Scheme 4-10). The reaction conditions utilised were the same as those used for the synthesis of safrole from 4-allylcatechol in Route 2, as discussed in detail in Section 4.2.2.3.

4.3 Organic Impurity Profiling

Safrole was synthesised from the 'pre-precursor' catechol via two synthetic routes and from the 'pre-precursor' eugenol via one synthetic route. The reaction products of each step in the synthetic pathways were analysed using GC-MS and ^1H NMR spectroscopy. The detected organic impurities were identified by analysis of the mass fragmentation pattern in their mass spectrum. The mass spectra and proposed fragmentation schemes of the reaction products and identified organic impurities are shown in Appendix 1 and Section 3.3.2. The identification of these organic impurities was also confirmed with ^1H NMR spectroscopy when the organic impurity was sufficiently concentrated to produce distinct ^1H NMR signals. The formation of the identified organic impurities during the relevant reactions in the synthesis of safrole was also investigated.

4.3.1 Route 1: Safrole from Catechol

In Route 1, safrole was synthesised from catechol via three steps: a methylenation reaction to yield 1,3-benzodioxole, a bromination reaction to yield 5-bromo-1,3-benzodioxole, and a Grignard reaction to yield safrole. The catechol starting material used did not contain any significant amount of organic impurities, as shown in Figure 3-1. The chemical structures and origin of the organic impurities detected in the 1,3-benzodioxole and 5-bromo-1,3-benzodioxole intermediates and the safrole product were investigated.

4.3.1.1 1,3-Benzodioxole from Catechol

Analysis of the product of the methylenation of catechol using GC-MS and ^1H NMR spectroscopy confirmed that 1,3-benzodioxole is the principal component. The largest peak in the gas chromatogram in Figure 4-1 was identified as a 1,3-benzodioxole. The signals that correspond to proton environments of 1,3-benzodioxole are labelled A - B in the ^1H NMR spectrum of the reaction product shown in Figure 4-2. The gas chromatogram in Figure 4-1 shows the five organic impurities that were consistently identified in the reaction product mixture. Organic impurities 39, 40 (a-c) and 47 (see Table 3-2) were identified in 1,3-benzodioxole synthesised from catechol during the preparation of methylone and the identification and formation of these organic impurities was discussed in detail in Section 3.3.2.

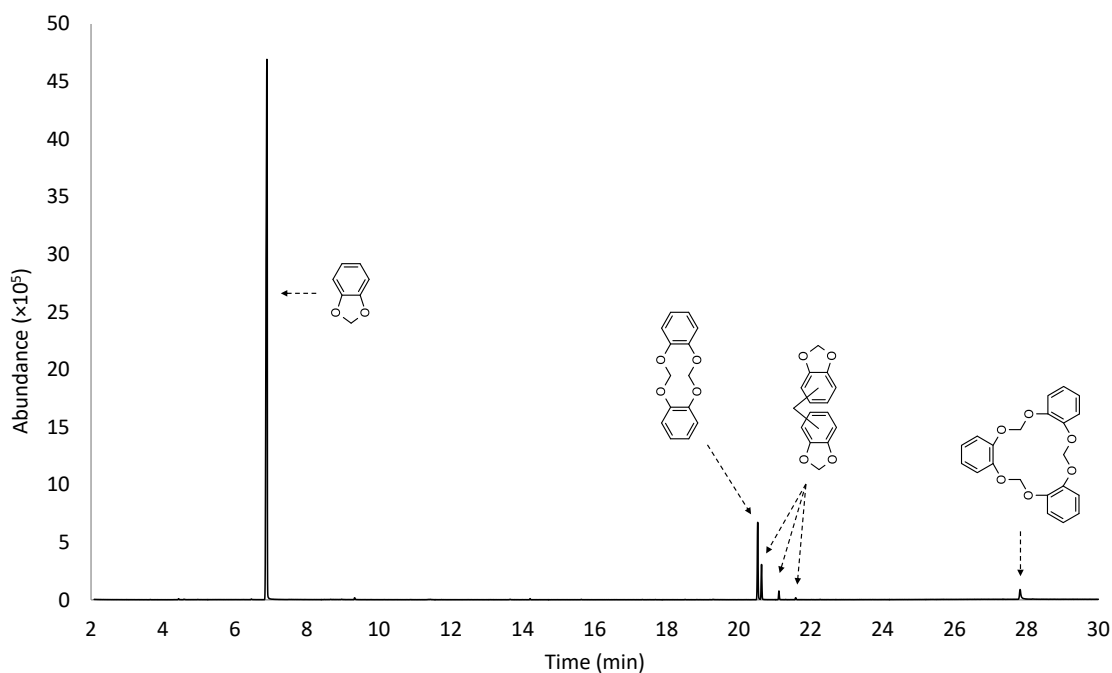


Figure 4-1: GC-MS total ion chromatogram of 1,3-benzodioxole synthesised via Route 1

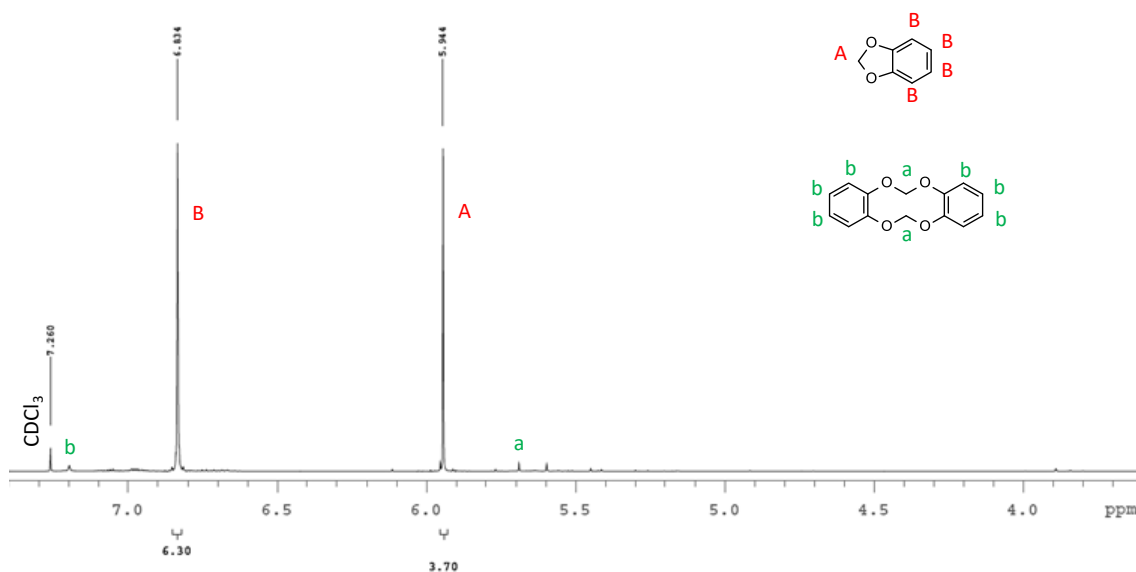


Figure 4-2: ^1H NMR spectrum of 1,3-benzodioxole synthesised via Route 1

4.3.1.2 5-Bromo-1,3-benzodioxole from 1,3-Benzodioxole

Analysis of the product of the bromination of 1,3-benzodioxole using GC-MS and ^1H NMR spectroscopy confirmed that 5-bromo-1,3-benzodioxole is the principal component. The largest peak in the gas chromatogram in Figure 4-3 was assigned to a brominated 1,3-benzodioxole. The signals that correspond to proton environments of 5-bromo-1,3-benzodioxole are labelled A - D in the ^1H NMR spectrum of the reaction product shown in Figure 4-4. The two aromatic doublets at 6.94 ppm and 6.69 ppm (C and D, respectively) and the aromatic singlet at 6.96 ppm (B) are

consistent with an unsymmetrical 1,2,4-trisubstituted benzene structure. This confirmed that the bromination reaction occurred on the fifth carbon to form 5-bromo-1,3-benzodioxole.

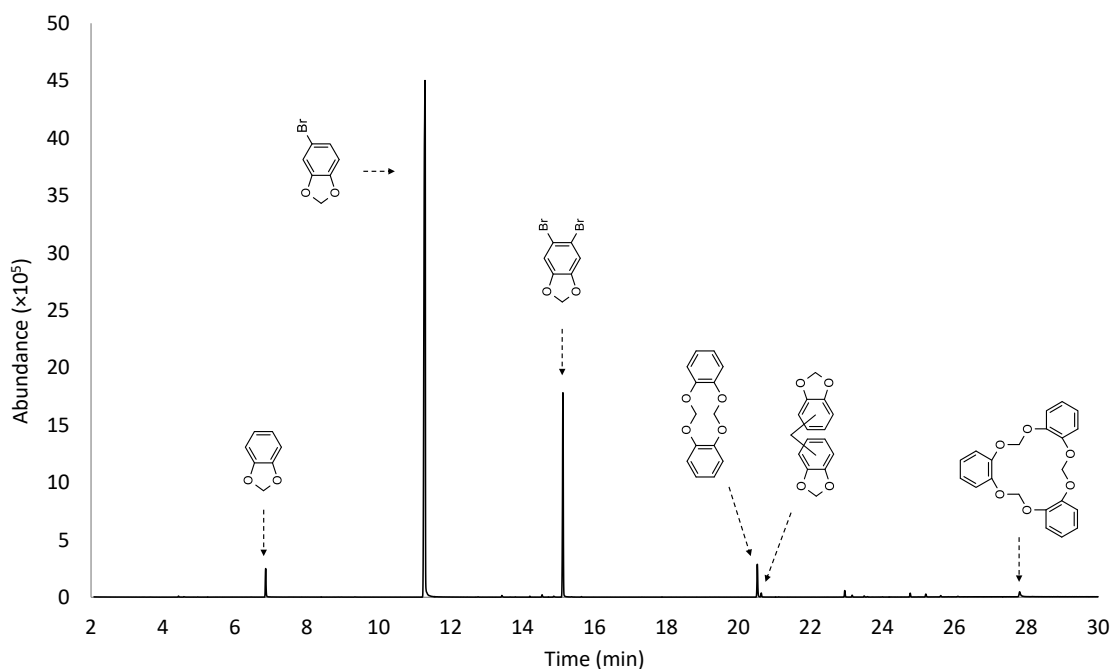


Figure 4-3: GC-MS total ion chromatogram of 5-bromo-1,3-benzodioxole synthesised via Route 1

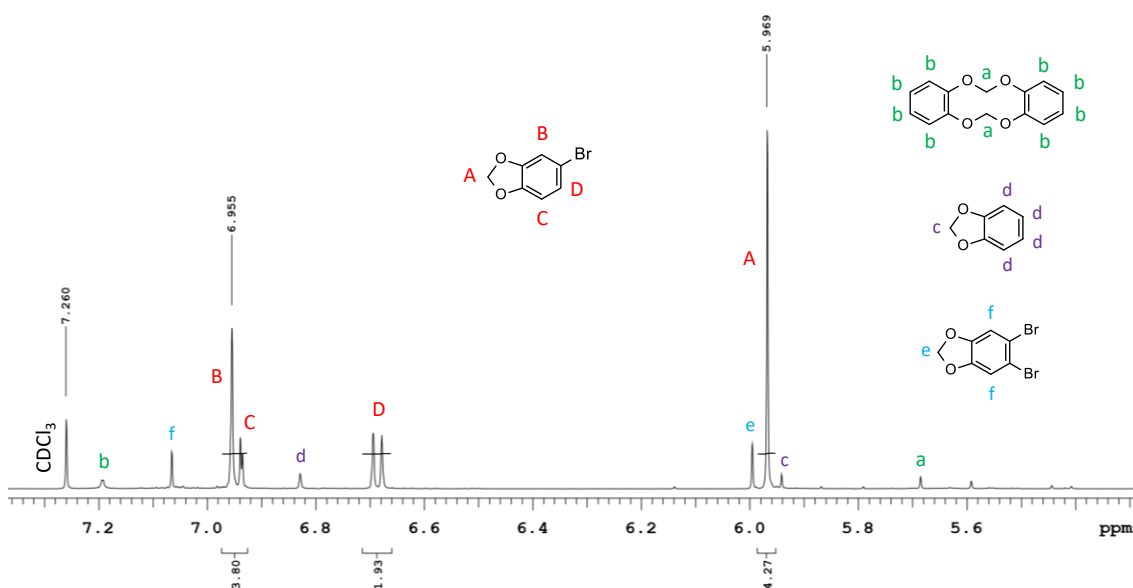
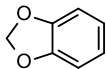
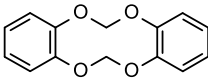

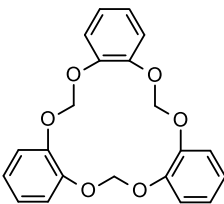
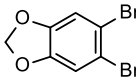


Figure 4-4: ^1H NMR spectrum of 5-bromo-1,3-benzodioxole synthesised via Route 1

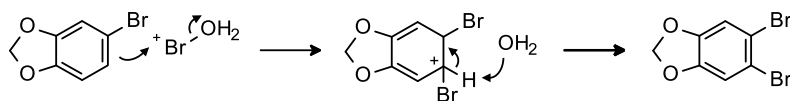
The gas chromatogram in Figure 4-3 shows the five organic impurities that were consistently identified in the reaction product mixture. Organic impurities 39, 40 and 47 were carried over, unchanged, from the synthesised 1,3-benzodioxole, while organic impurities 5 and 57 originated from the preparation of 5-bromo-1,3-benzodioxole. The assigned numbers, chemical structures, names, molecular weights, and m/z data of organic impurities 5, 39, 40, 47 and 57 are shown in Table 4-2.

Table 4-2: Organic impurities identified in 5-bromo-1,3-benzodioxole synthesised via Route 1

No.	Impurity Structure	Impurity Name	MW (g/mol)	m/z
5		1,3-benzodioxole	122.1	122/121, 63
39		1,3-benzodioxole dimer	244.2	244, 135, 122/121, 63
40		4,4'-, 4,5'-, or 5,5'-methylenebis-1,3-benzodioxole	256.3	256, 225, 196, 168, 135, 77
47		1,3-benzodioxole trimer	366.4	366, 244, 135, 122/121
57		5,6-dibromo-1,3-benzodioxole	279.9	282/280/278, 143/141, 62

Organic impurity 5 is the starting material of the reaction, and its detection therefore indicated that the bromination reaction did not proceed to completion. The identity of organic impurities 5 and 39 was confirmed through ^1H NMR spectroscopy, as shown in Figure 4-4. The signals that correspond to these organic impurities were determined in the analysis of the 1,3-benzodioxole reaction product, as shown in Figure 3-4, and are present in the ^1H NMR spectrum of the 5-bromo-1,3-benzodioxole reaction product.

Organic impurity 57 was formed through a subsequent bromination reaction of 5-bromo-1,3-benzodioxole via the mechanism shown in Scheme 4-12. The identity of organic impurity 57 was also confirmed with ^1H NMR spectroscopy, as shown in Figure 4-4. The singlet at 6.0 ppm corresponds to the methylene protons (e), which are shifted downfield in comparison to the methylene protons of 5-bromo-1,3-benzodioxole due to the de-shielding effect of the second bromine atom. The aromatic singlet at 7.07 ppm (f) is consistent with a symmetrical 1,2,4,5-tetrasubstituted benzene structure, which confirmed that the second bromination occurred on the sixth carbon to form 5,6-dibromo-1,3-benzodioxole.



Scheme 4-12: Formation of organic impurity 57

4.3.1.3 Safrole from 5-Bromo-1,3-benzodioxole

Analysis of the product of the Grignard reaction between 5-bromo-1,3-benzodioxole and allyl bromide with GC-MS and ^1H NMR spectroscopy confirmed that safrole is the principal component. The largest peak in the gas chromatogram in Figure 4-5 was identified as a safrole. The signals that correspond to proton environments of safrole are labelled A - G in the ^1H NMR spectrum of the reaction product shown in Figure 4-6.

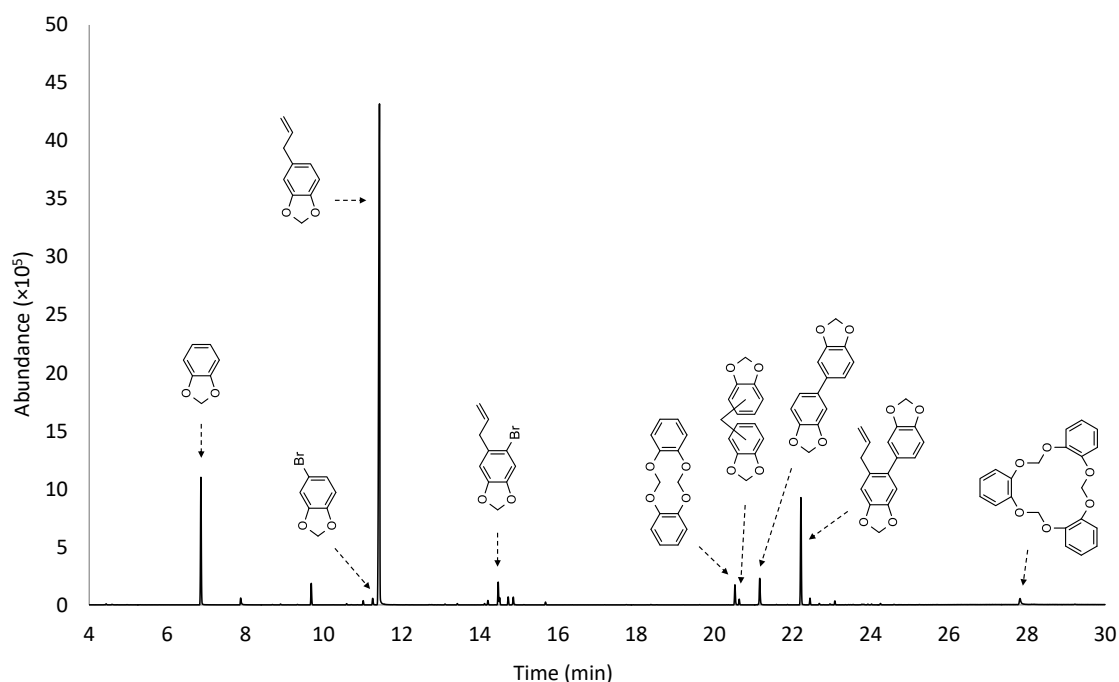


Figure 4-5: GC-MS total ion chromatogram of safrole synthesised via Route 1

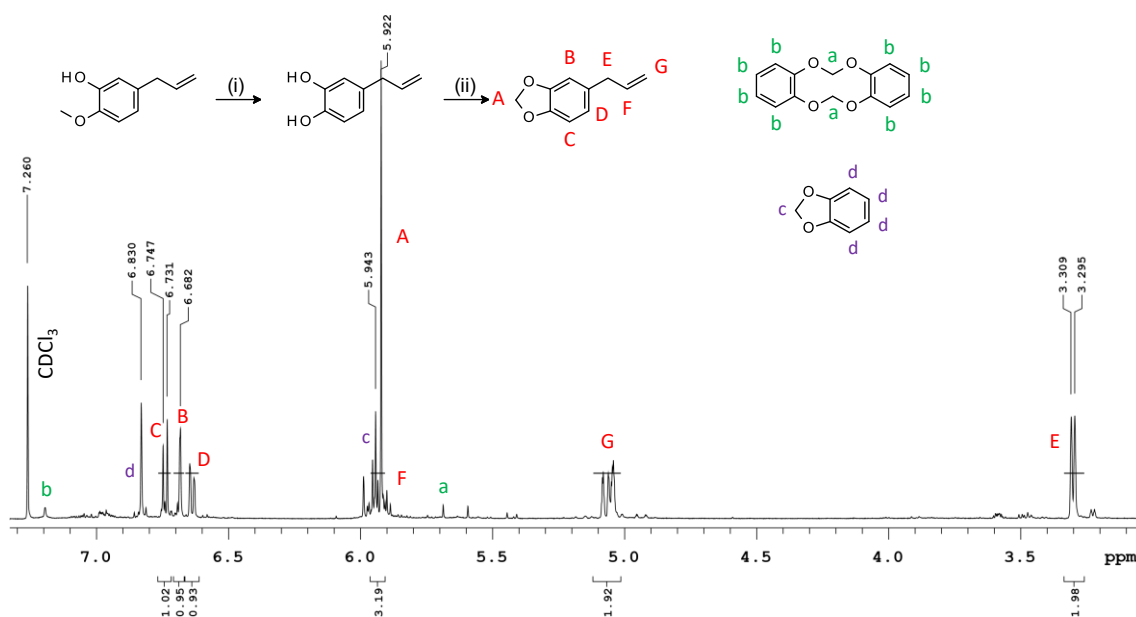
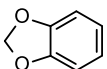
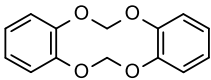
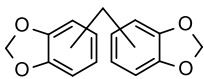
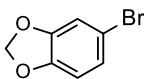
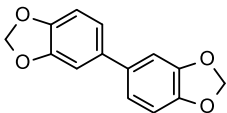
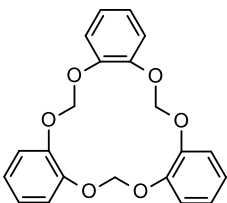
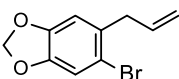
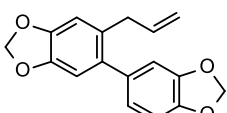


Figure 4-6: ^1H NMR spectrum of safrole synthesised via Route 1

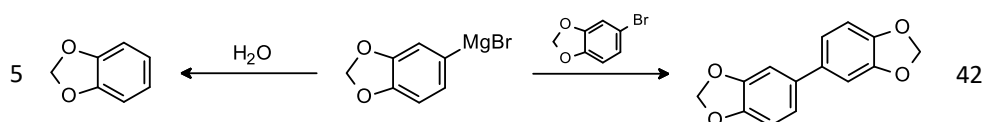
The gas chromatogram in Figure 4-5 shows the eight organic impurities that were consistently identified in the reaction product mixture. Organic impurities 39, 40 and 47 were carried over, unchanged, from the synthesised 5-bromo-1,3-benzodioxole, while organic impurities 41, 42, 58 and 59 originated from the preparation of safrole. Organic impurity 5 may have been carried over from the synthesised 5-bromo-1,3-benzodioxole, however, may have also formed during the synthesis of safrole. The assigned numbers, chemical structures, names, molecular weights, and m/z data of organic impurities 5, 39, 40, 41, 42, 47, 58 and 59 are shown in Table 4-3.

Table 4-3: Organic impurities identified in safrole synthesised via Route 1

No.	Impurity Structure	Impurity Name	MW (g/mol)	m/z
5		1,3-benzodioxole	122.1	122/121, 63
39		1,3-benzodioxole dimer	244.2	244, 135, 122/121, 63
40		4,4', 4,5', and 5,5'-methylenebis-1,3-benzodioxole	256.3	256, 225, 196, 168, 135, 77
41		5-bromo-1,3-benzodioxole	201.0	202/200, 121, 63
42		5,5'-bi-1,3-benzodioxole	242.2	242, 126, 121/120, 63
47		1,3-benzodioxole trimer	366.4	366, 244, 135, 122/121
58		5-bromo-6-(2-propenyl)-1,3-benzodioxole	241.1	242/240, 199, 131, 103, 77
59		5-allyl-6-(1,3-benzodioxol-5-yl)-1,3-benzodioxole	282.3	282, 267, 237, 209, 165, 139

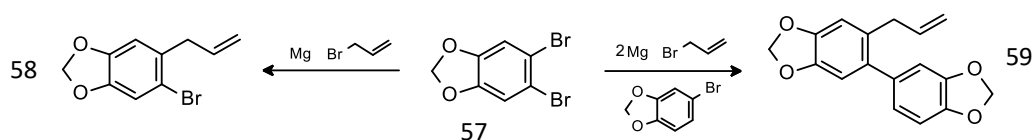
Organic impurity 41 is the starting material of the reaction, and its detection therefore indicated that the Grignard reaction did not proceed to completion. Organic impurities 5 and 42 are reaction by-products of the Grignard reaction that were formed through side reactions of the

Grignard reagent, as shown in Scheme 4-13. It is highly likely that the Grignard reagent reacted with water to form impurity 5 during the synthesis of safrole, as the relative concentration of impurity 5 increased in safrole compared to 5-bromo-1,3-benzodioxole. This decomposition reaction could have occurred due to water contamination in the reactant set-up or an incomplete reaction when the reaction mixture was quenched. Organic impurity 42 formed through the reaction of the Grignard reagent with 5-bromo-1,3-benzodioxole, the starting material of the Grignard reaction.



Scheme 4-13: Formation of organic impurities 5 and 42

Organic impurities 58 and 59 were formed through side Grignard reactions of impurity 57, the bromination reaction by-product identified in 5-bromo-1,3-benzodioxole, as shown in Scheme 4-14. Organic impurity 58 was synthesised through the reaction of allyl bromide and the Grignard reagent formed by the reaction of impurity 57 with magnesium. In the formation of organic impurity 59, impurity 57 reacted with magnesium and allyl bromide as well as with magnesium and 5-bromo-1,3-benzodioxole.



Scheme 4-14: Formation of organic impurities 58 and 59

4.3.2 Route 2: Safrole from Catechol

In Route 2, safrole was synthesised from catechol via three steps: an etherification reaction to yield 2-allyloxyphenol, a Claisen rearrangement reaction to yield 4-allylcatechol and a methylenation reaction to yield safrole. The catechol starting material used did not contain any significant organic impurities, as shown in Figure 3-1. The chemical structures and origin of the organic impurities detected in the 2-allyloxyphenol and 4-allylcatechol intermediates and the safrole product were investigated.

4.3.2.1 2-Allyloxyphenol from Catechol

The analysis of the product of the etherification of catechol with allyl bromide using GC-MS confirmed that 2-allyloxyphenol is the principal component, with the largest peak in the gas chromatogram in Figure 4-7 identified as 2-allyloxyphenol. The gas chromatogram in Figure 4-7 also shows the two organic impurities that were consistently identified in the reaction product

mixture. Organic impurities 60 and 61 originated from the preparation of 2-allyloxyphenol. The assigned numbers, chemical structures, names, molecular weights, and m/z data of organic impurities 60 and 61 are shown in Table 4-4.

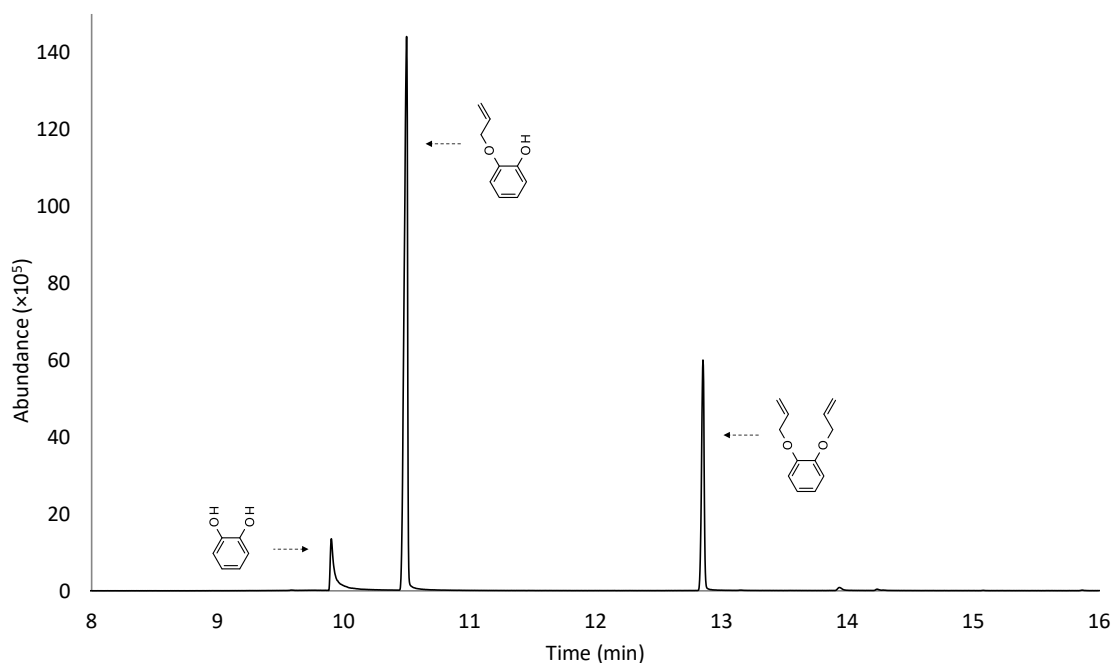


Figure 4-7: GC-MS total ion chromatogram of 2-allyloxyphenol synthesised via Route 2

Table 4-4: Organic impurities identified in 2-allyloxyphenol via Route 2

No.	Impurity Structure	Impurity Name	MW (g/mol)	m/z
60		catechol	110.1	110, 92, 81, 64/63, 53
61		1,2-diallyloxybenzene	190.2	190, 149, 121, 119, 81, 52, 41

The identification of 2-allyloxyphenol as the principal component in the reaction product using ^1H NMR spectroscopy was not definitive due to the similarity in the 2-allyloxyphenol and 1,2-diallyloxybenzene (61) proton environments. The signals that correspond to proton environments of 2-allyloxyphenol are labelled A – F and the signals that correspond to impurity 61 are labelled a - d in the ^1H NMR spectrum of the reaction product shown in Figure 4-8.

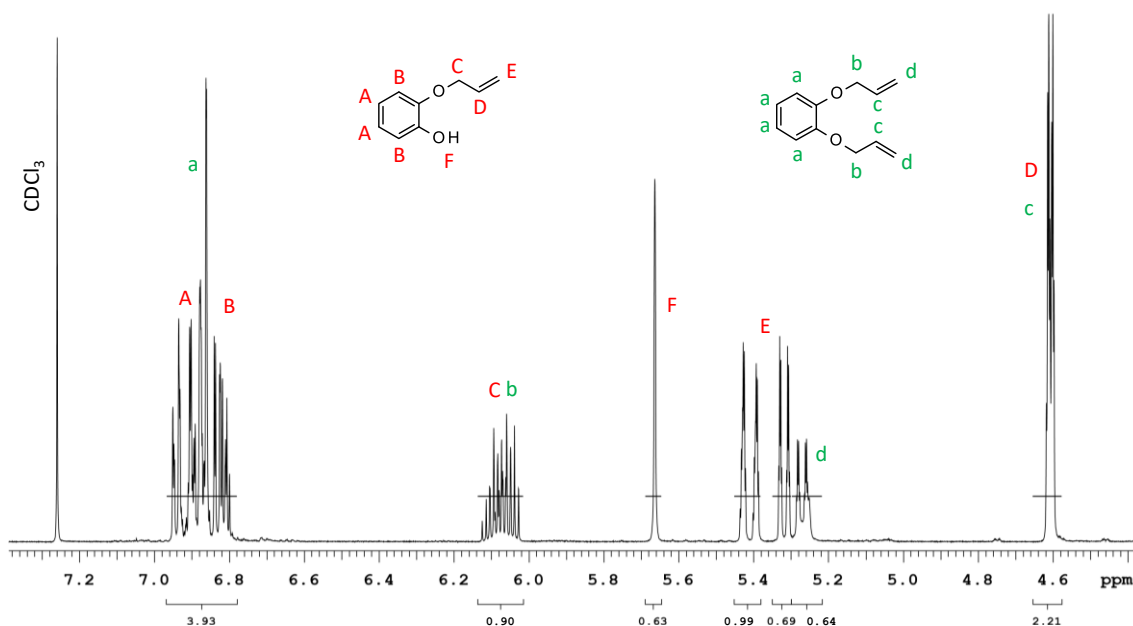
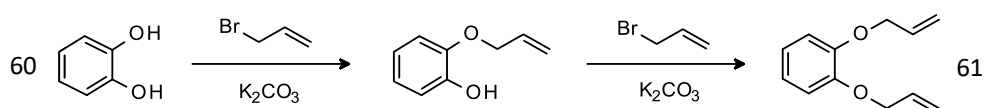


Figure 4-8: ^1H NMR spectrum of 2-allyloxyphenol synthesised via Route 2

The multiplet at 6.08 ppm and the doublet at 4.61 ppm, respectively, correspond to the methylene (C, b) and methine (D, c) proton environments of both 2-allyloxyphenol and organic impurity 61. The overlapping doublet of doublets at 5.37 ppm and 5.34 ppm correspond to the vinyl methylene proton environments of 2-allyloxyphenol (E) and impurity 61 (d), respectively. The aromatic protons of 2-allyloxyphenol produce two multiplets at 6.91 ppm (A) and 6.83 ppm (B), whereas the aromatic protons of organic impurity 61 produce a single doublet at 6.86 ppm (a). The singlet at 5.66 ppm corresponds to the phenol (F) proton environment of 2-allyloxyphenol.

Organic impurities 60 and 61 are, respectively, the starting material and a reaction by-product of the etherification of catechol, as shown in Scheme 4-15. In the etherification reaction, catechol and allyl bromide were reacted in a one-to-one molar ratio. However, some disubstitution with allyl bromide occurred, which resulted in formation of organic impurity 61. Catechol (60) was therefore also identified in 2-allyloxyphenol, due to the allyl bromide being consumed before the reaction reached completion.



Scheme 4-15: Origin of organic impurities 60 and 61

4.3.2.2 4-Allylcatechol from 2-Allyloxyphenol

Analysis of the product of the Claisen rearrangement of 2-allyloxyphenol with GC-MS and ^1H NMR spectroscopy confirmed that 4-allylcatechol is the principal component. The largest peak in the gas chromatogram in Figure 4-9 was identified as 4-allylcatechol. The signals that correspond to proton environments of 4-allylcatechol are labelled A - F in the ^1H NMR spectrum of the reaction product shown in Figure 4-10.

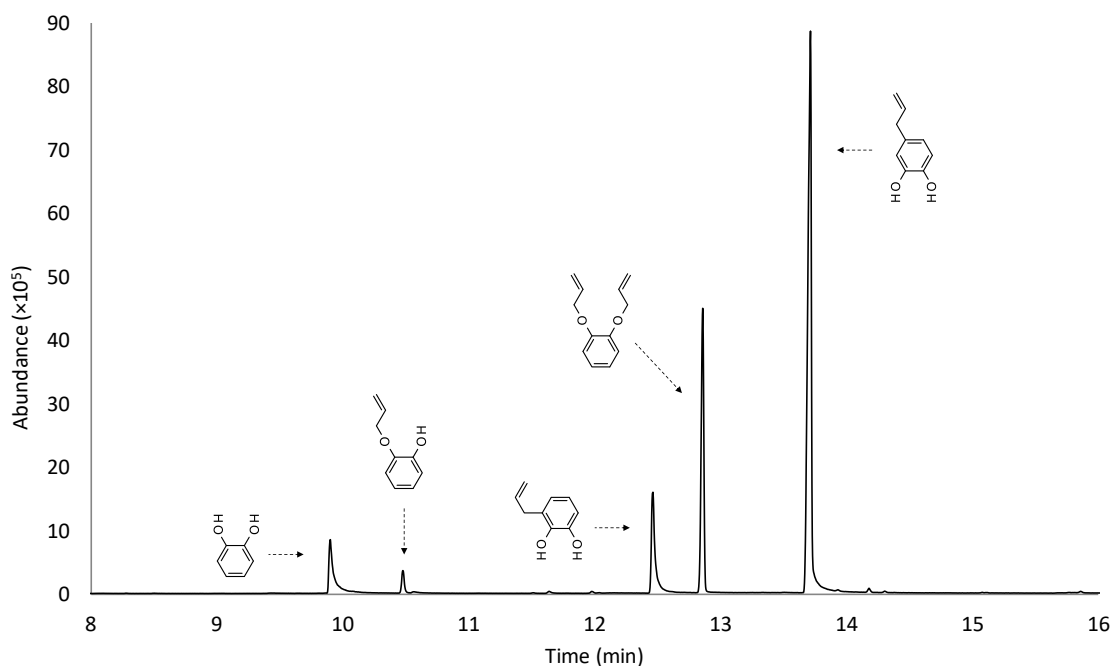


Figure 4-9: GC-MS total ion chromatogram of 4-allylcatechol synthesised via Route 2

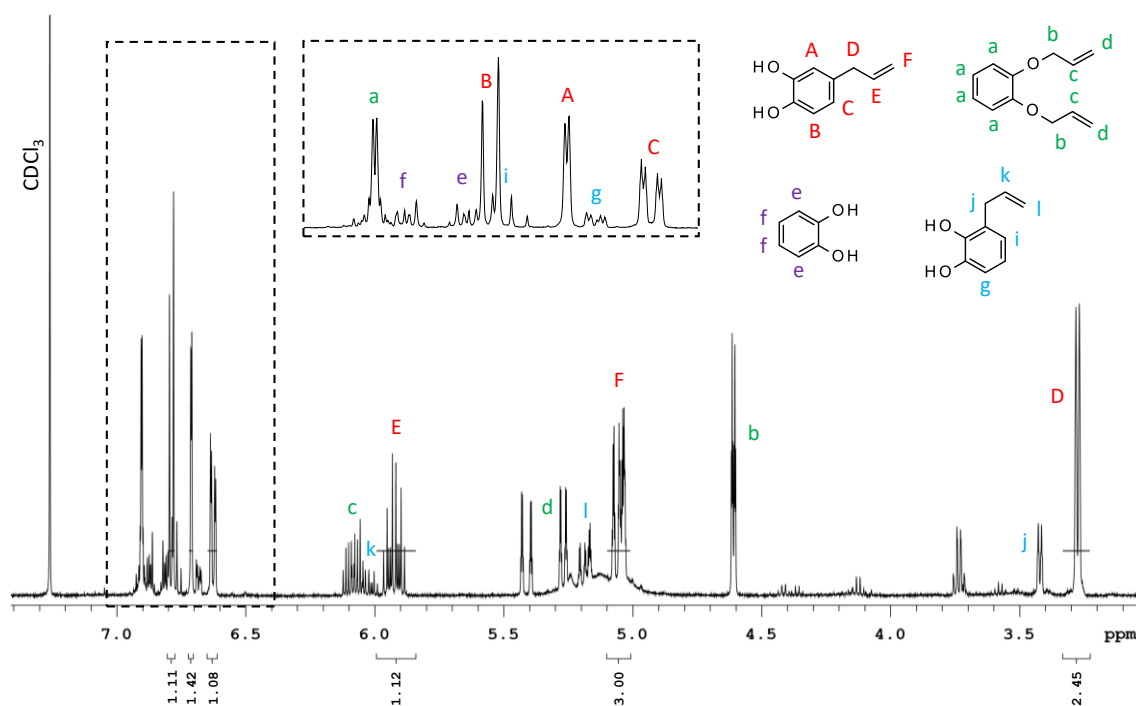
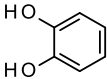
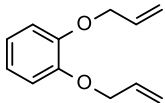
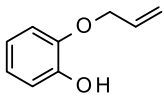
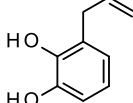


Figure 4-10: ^1H NMR spectrum of 4-allylcatechol synthesised via Route 2

The gas chromatogram in Figure 4-9 shows the four organic impurities that were consistently identified in the reaction product mixture. Organic impurities 60 and 61 were carried over, unchanged, from the synthesised 2-allyloxyphenol, while organic impurities 62 and 63 originated from the preparation of 4-allylcatechol. The assigned numbers, chemical structures, names, molecular weights, and m/z data of organic impurities 60, 61, 62 and 63 are shown in Table 4-5.

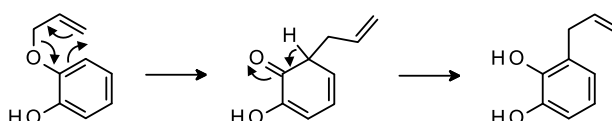
Table 4-5: Organic impurities identified in 4-allylcatechol synthesised via Route 2

No.	Impurity Structure	Impurity Name	MW (g/mol)	m/z
60		catechol	110.1	110, 92, 81, 64/63, 53
61		1,2-diallyloxybenzene	190.2	190, 149, 121, 119, 81, 52, 41
62		2-allyloxyphenol	150.2	150, 109, 81, 53, 41
63		3-allylcatechol	150.2	150, 131, 122, 104/103, 91, 77, 51

The identity of organic impurities 60, 61 and 63 was confirmed using ^1H NMR spectroscopy, as shown in Figure 4-10. The signals that correspond to organic impurities 60 and 61 were determined in the analysis of the catechol starting material and the 2-allyloxyphenol reaction product, as shown in Figure 3-1 and Figure 4-8 respectively. These signals are present in the ^1H NMR spectrum of the 4-allylcatechol reaction product and are labelled a - d (61) and e - f (60).

The signals that correspond to the proton environments of organic impurity 63 are labelled g - l in the ^1H NMR spectrum shown in Figure 4-10. The multiplet at 6.02 ppm, the doublet of doublets at 5.18 ppm, and the doublet at 3.42 ppm correspond, respectively, to the methine (k), vinyl methylene (l) and methylene (j) proton environments of 3-allylcatechol (63). These signals are shifted downfield in comparison to the related signals of 4-allylcatechol due to their closer proximity to the electronegative oxygen. The doublet at 6.78 ppm (i) and the doublet of doublets at 6.68 ppm (g) correspond to two of the aromatic proton environments of impurity 63, however, the third aromatic proton did not produce a distinct, differentiable signal.

Organic impurity 62 is the starting material of the Claisen rearrangement reaction, and its detection therefore indicated that the reaction did not proceed to completion. Organic impurity 63 is a reaction by-product of the Claisen rearrangement reaction, formed through the *ortho*-Claisen rearrangement of 2-allyloxyphenol. The reaction mechanism for the *ortho*-Claisen rearrangement of 2-allyloxyphenol is shown in Scheme 4-16. The bonding electrons in 2-allyloxyphenol undergo rearrangement through a pericyclic mechanism to form a cyclohexadienone intermediate, which then isomerises to form organic impurity 63 [88, 95].



Scheme 4-16: Reaction mechanism for the formation of organic impurity 63

4.3.2.3 Safrole from 4-Allylcatechol

Analysis of the product of the methylenation of 4-allylcatechol using GC-MS and ^1H NMR spectroscopy confirmed that safrole is the principal component. The largest peak in the gas chromatogram in Figure 4-11 was identified as a safrole. The signals that correspond to proton environments of safrole are labelled A - G in the ^1H NMR spectrum of the reaction product shown in Figure 4-12.

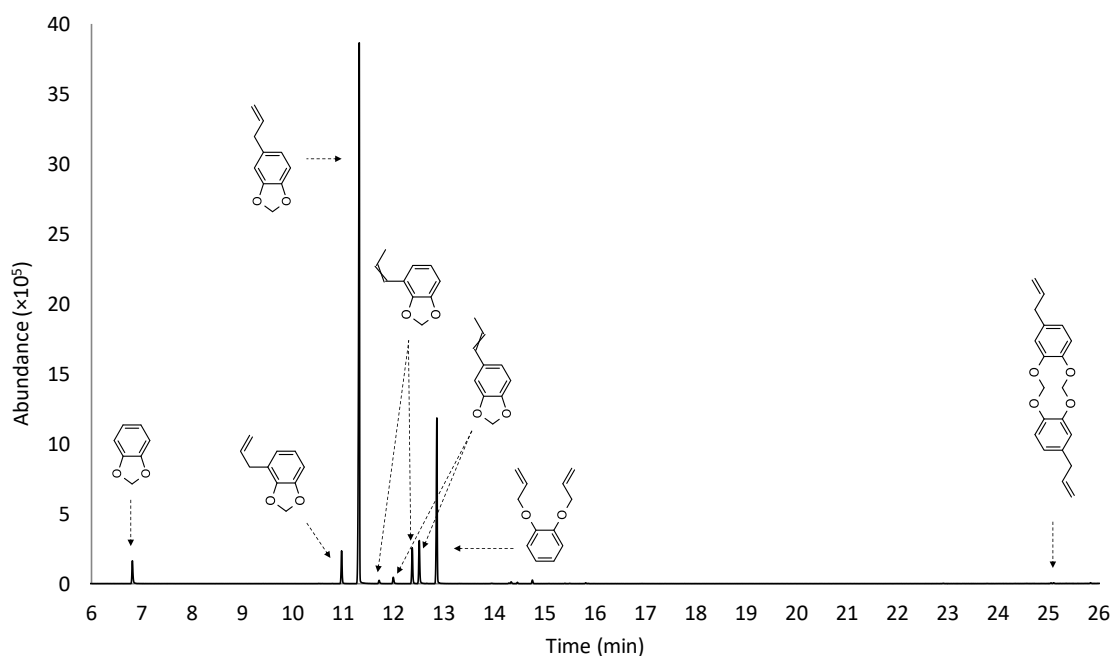
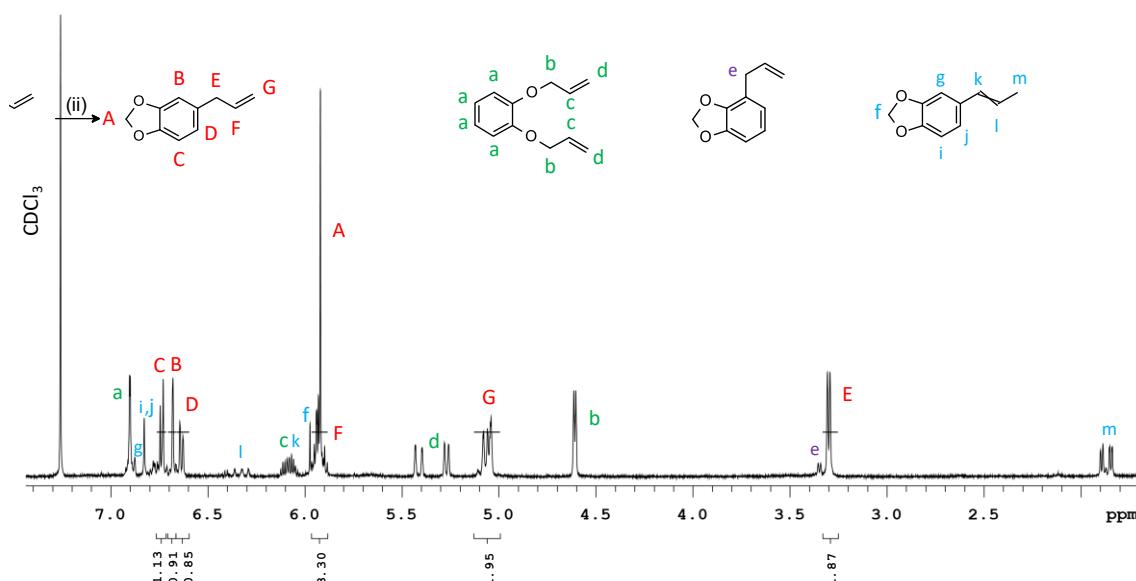


Figure 4-11: GC-MS total ion chromatogram of safrole synthesised via Route 2

Figure 4-12: ^1H NMR spectrum of safrole synthesised via Route 2

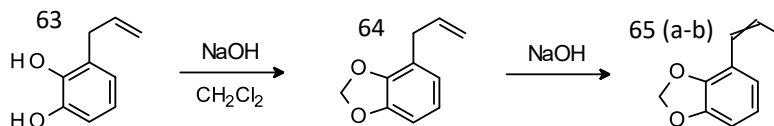
The gas chromatogram in Figure 4-11 shows the eight organic impurities that were consistently identified in the reaction product mixture. Organic impurities 61 was carried over, unchanged, from 4-allylcatechol, while organic impurities 3 (a-b), 5, 64, 65 (a-b), and 66 originated from the preparation of safrole. The assigned numbers, chemical structures, names, molecular weights, and m/z data of organic impurities 3 (a-b), 5, 61, 64, 65 (a-b), and 66 are shown in Table 4-6.

Table 4-6: Organic impurities identified in safrole synthesised via Route 2

No.	Impurity Structure	Impurity Name	MW (g/mol)	m/z
3 (a-b)		isosafrole	162.2	162, 135, 131, 104/103, 91, 77, 63, 51
5		1,3-benzodioxole	122.1	122/121, 63
61		1,2-diallyloxybenzene	190.2	190, 149, 121, 119, 81, 52, 41
64		4-allyl-1,3-benzodioxole	162.2	162, 135, 131, 119, 104/103, 91, 77, 63, 51
65 (a-b)		4-propen-1-enyl-1,3-benzodioxole	162.2	162, 131, 119, 104/103, 91, 77, 63, 51
66		safrole dimer	324.4	324, 281, 253, 225, 207, 162, 147, 135, 115, 104/103, 91, 73, 65, 44

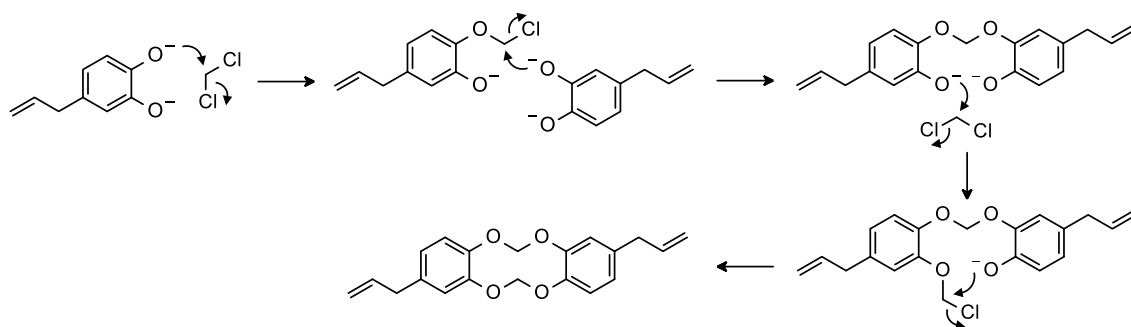
The identity of organic impurities 3 (a-b), 61 and 64 was confirmed through ^1H NMR spectroscopy, as shown in Figure 4-12. The doublet at 3.35 ppm corresponds to the methylene (e) proton environment of organic impurity 64, which is shifted downfield compared to the related signal in safrole due to its closer proximity to the electronegative oxygen. The remaining proton environments of organic impurity 64 did not produce distinct, differentiable signals. The signals that correspond to organic impurities 61 were determined in the analysis of 2-allyloxyphenol reaction product, as shown in Figure 4-8. Similarly, the signals that correspond to isosafrole (3 (a-b)) were determined in the analysis of the isosafrole reaction product in Section 5.3.2.1. These signals are present in the ^1H NMR spectrum of the safrole reaction product and are labelled a - d (61) and f - m (3 (a-b)) .

Organic impurities 5, 64 and 65 (a-b) were formed through side reactions of organic impurities identified in 4-allylcatechol. The reactions that lead to impurities 64 and 65 (a-b) are shown in Scheme 4-17. Organic impurities 5 and 64 were formed by the methylenation of, respectively, organic impurities 60 and 63 with dichloromethane. A proportion of impurity 64 then underwent an isomerisation process, facilitated by sodium hydroxide used in the methylenation reaction, to form organic impurities 65 (a-b).



Scheme 4-17: Formation of organic impurities 64 and 65 (a-b)

Organic impurities 3 (a-b) and 66 are reaction by-products of the methylenation of 4-allylcatechol. A proportion of the safrole product underwent a sodium hydroxide facilitated isomerisation process to form impurities 3 (a-b). Sodium hydroxide also deprotonated 4-allylcatechol to yield 4-allylbenzene-1,2-diolate. Organic impurity 66 was then formed through the cyclisation of two 4-allylbenzene-1,2-diolate molecules with two dichloromethane molecules, as shown in Scheme 4-18. This reaction mechanism could have feasibly resulted in the formation of a *cis*- and a *trans*- isomer. However, only one peak with a mass spectrum that corresponded to organic impurity 66 was identified in the gas chromatogram. The *trans*- isomer shown in Scheme 4-18 was the most likely to have formed [91], although formation of the *cis*- isomer cannot be discounted.



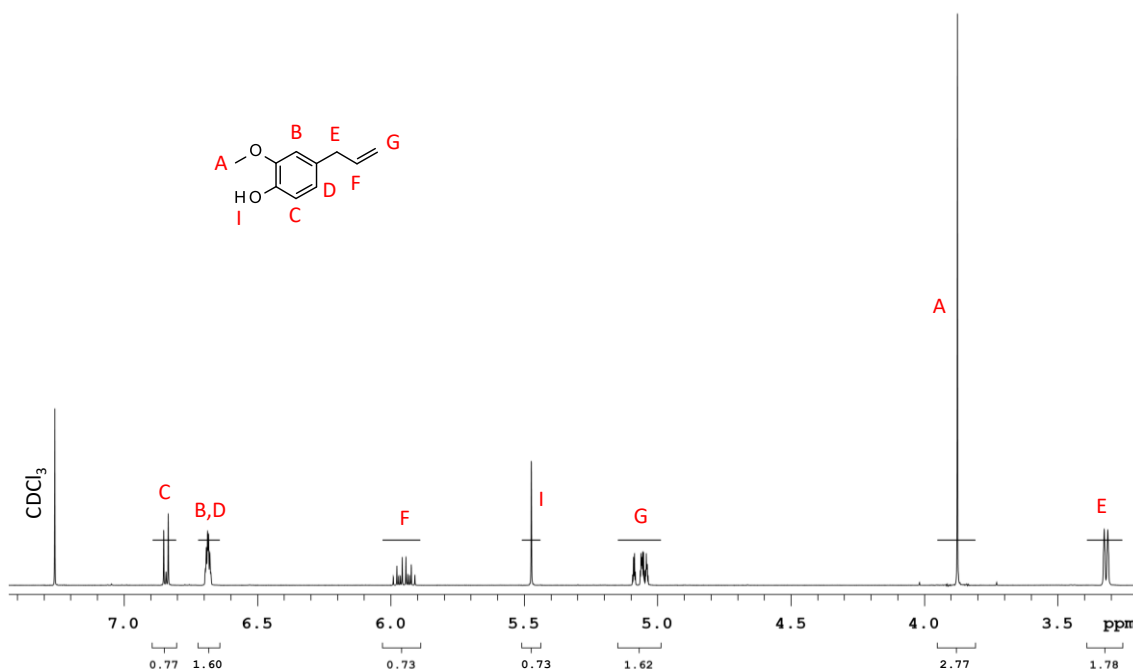
Scheme 4-18: Formation of organic impurity 66

4.3.3 Route 3: Safrole from Eugenol

In Route 3, safrole was synthesised from eugenol in two steps: a demethylation reaction to yield 4-allylcatechol and a methylenation reaction to yield safrole. The chemical structures and origin of the organic impurities detected in the 4-allylcatechol intermediate and the safrole product were investigated.

4.3.3.1 Eugenol

The eugenol utilised as a starting material for the synthesis of safrole was analysed via ^1H NMR spectroscopy. The signals that correspond to proton environments of eugenol are labelled A - I in the ^1H NMR spectrum shown in Figure 4-13. There are no additional significant signals within the ^1H NMR spectrum of eugenol, which demonstrated that there were no significant organic impurities contained within the eugenol starting material.

Figure 4-13: ^1H NMR spectrum of eugenol

4.3.3.2 4-Allylcatechol from Eugenol

The product of the demethylation reaction of eugenol was analysed using GC-MS and ^1H NMR spectroscopy and 4-allylcatechol was found to be the principal component. The largest peak in the gas chromatogram in Figure 4-14 was assigned to 4-allylcatechol. The signals that correspond to proton environments of 4-allylcatechol are labelled A - G in the ^1H NMR spectrum of the reaction product shown in Figure 4-15.

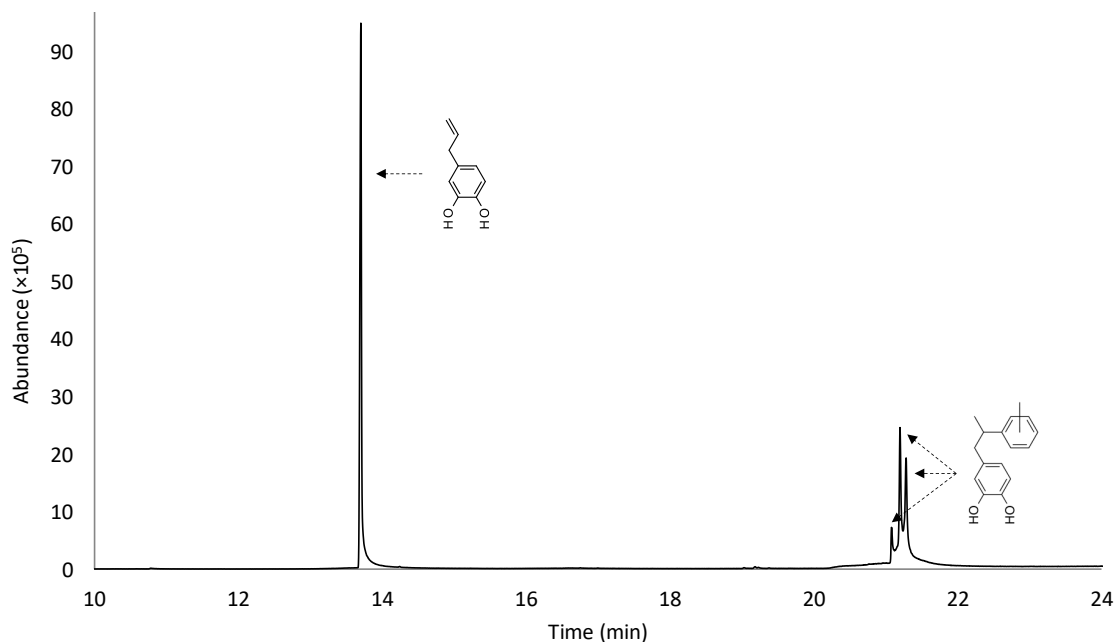


Figure 4-14: GC-MS total ion chromatogram of 4-allylcatechol synthesised via Route 3

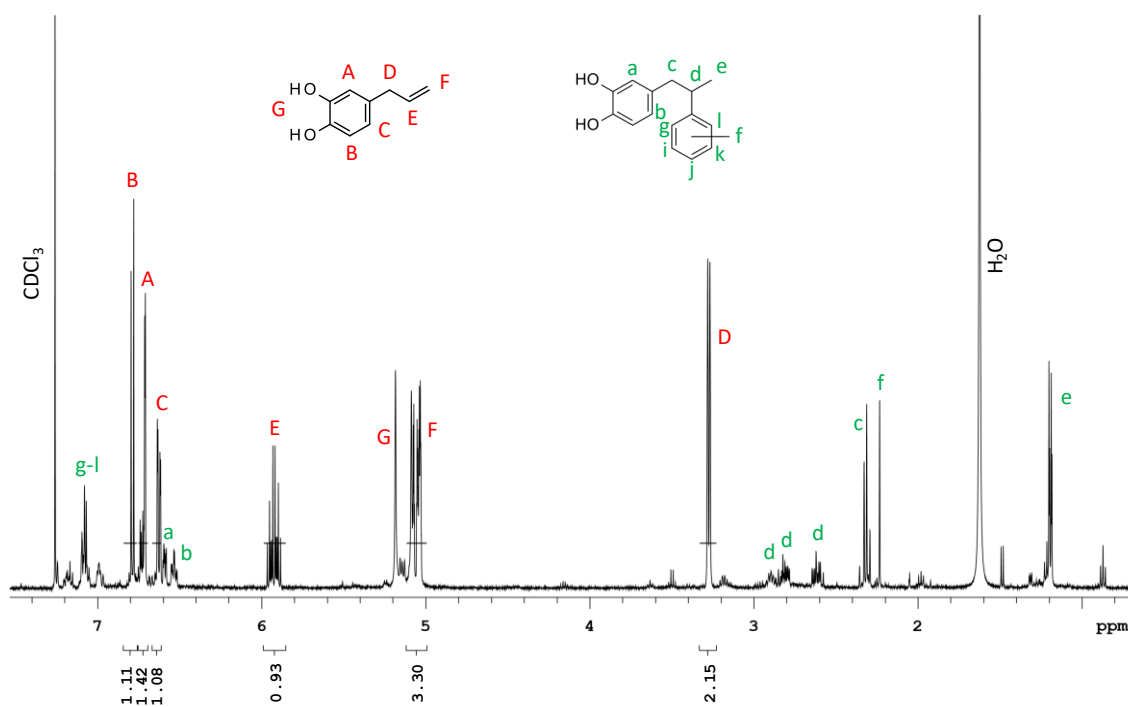
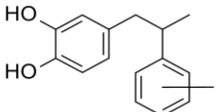


Figure 4-15: ^1H NMR spectrum of 4-allylcatechol synthesised via Route 3

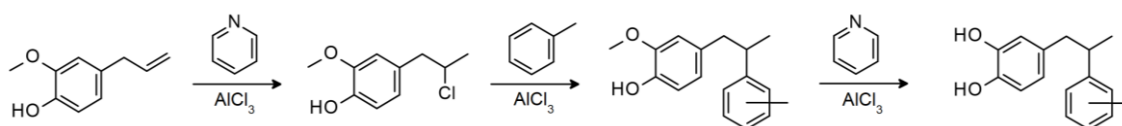
The gas chromatogram in Figure 4-14 shows the three organic impurities that were consistently identified in the reaction product mixture. Organic impurities 67 (a-c) originated from the preparation of 4-allylcatechol. The assigned numbers, chemical structures, names, molecular weights, and m/z data of organic impurities 67 (a-c) are shown in Table 4-7.

Table 4-7: Organic impurities identified in 4-allylcatechol synthesised via Route 3

No.	Impurity Structure	Impurity Name	MW (g/mol)	m/z
67 (a-c)		4-[2-(<i>o</i> , <i>p</i> and <i>m</i> -tolyl)propyl]benzene-1,2-diol	242.3	242, 179, 123, 119, 91, 77, 65, 51

The identities of the organic impurities 67 (a-c) were confirmed using ^1H NMR spectroscopy, as shown in Figure 4-15. The three multiplets in the 6.97 ppm – 7.20 ppm region of the ^1H NMR spectrum correspond to the aromatic (g-l) proton environments of the *ortho*-, *para*- or *meta*-substituted methyl benzene groups of the three isomers. The doublet at 2.32 ppm, the singlet at 2.23 ppm, and the doublet at 1.20 ppm, respectively, correspond to the equivalent methylene (c), benzylic (f) and methyl (e) proton environments of organic impurities 67 (a-c). The multiplets at 2.90 ppm, 2.82 ppm and 2.61 ppm arise from the three methine (d) proton environments within the three isomers. The doublet at 6.59 ppm (a) and the doublet of doublets at 6.54 ppm (b) are assigned to two of the aromatic proton environments of the 1,2-dihydroxybenzene structure, however, the third proton in the 1,2-dihydroxybenzene moiety did not produce a distinct, differentiable signal.

Organic impurities 67 (a-c) are reaction by-products of the demethylation of eugenol, formed by the reactions shown in Scheme 4-19. The demethylation of eugenol utilised an aluminium chloride reagent, which resulted in a halogenation side reaction that produced a chlorinated intermediate [99]. The chlorinated intermediate can react with the solvent toluene by a Friedel-Crafts alkylation reaction in the *ortho*, *para* and *meta* positions to form three isomers, which underwent demethylation of the ether group to yield organic impurities 67 (a-c).



Scheme 4-19: Formation of organic impurities 67 (a-c)

4.3.3.3 Safrole from 4-Allylcatechol

The product formed by the methylenation of 4-allylcatechol was mostly safrole, as determined by GC-MS and ^1H NMR spectroscopy. Figure 4-16 shows that the largest peak in the gas chromatogram was due to safrole. The signals that correspond to proton environments of safrole are labelled A - G in the ^1H NMR spectrum of the reaction product shown in Figure 4-17.

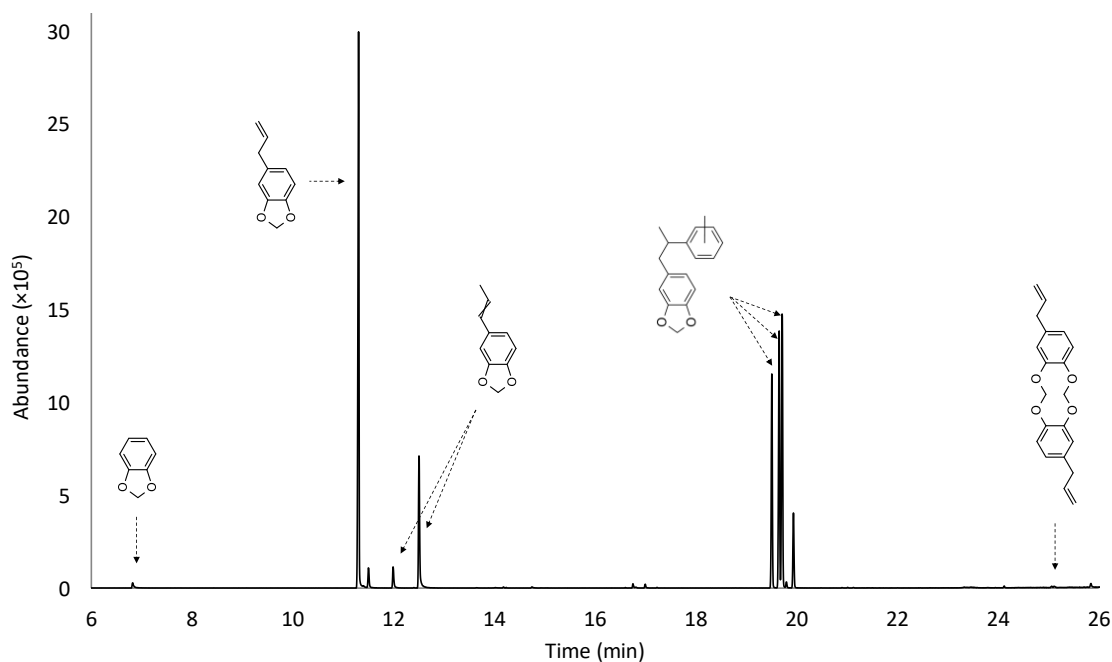


Figure 4-16: GC-MS total ion chromatogram of safrole synthesised via Route 3

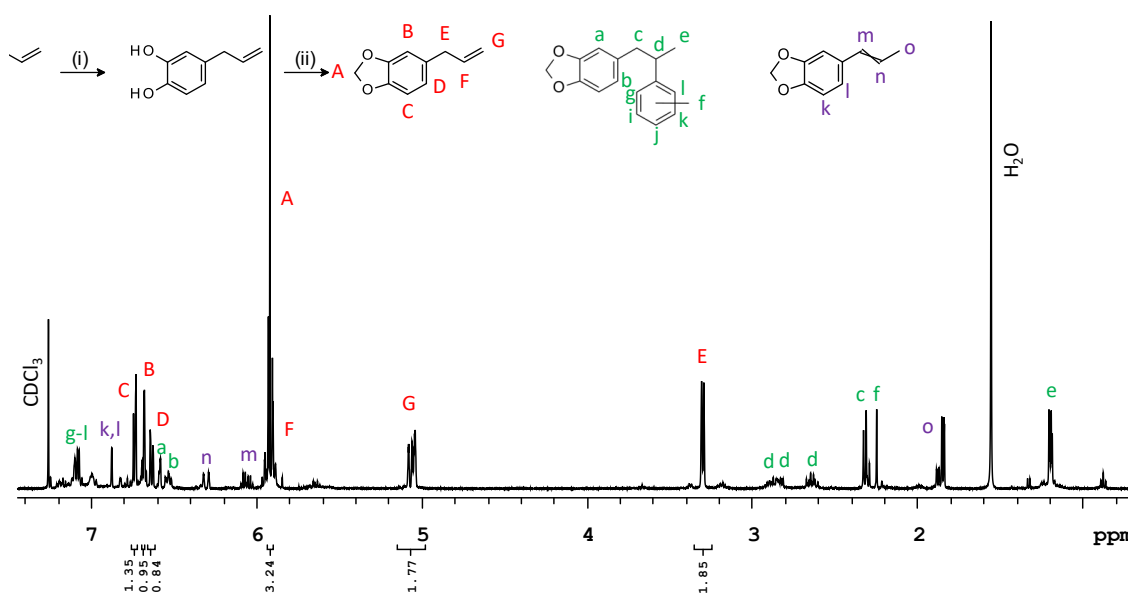
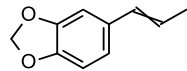
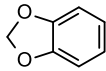
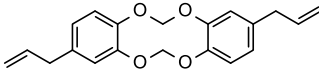
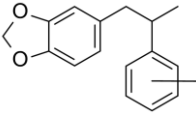


Figure 4-17: ^1H NMR spectrum of safrole synthesised via Route 3

The gas chromatogram in Figure 4-16 shows the seven organic impurities that were consistently identified in the reaction product mixture. Organic impurities 3 (a-b), 5, 66, and 68 (a-c) originated from the preparation of safrole. The assigned numbers, chemical structures, names, molecular weights, and m/z data of organic impurities 3 (a-b), 5, 66, and 68 (a-c) are shown in Table 4-8.

Table 4-8: Organic impurities identified in safrole synthesised via Route 3

No.	Impurity Structure	Impurity Name	MW (g/mol)	m/z
3 (a-b)		isosafrole	162.2	162, 135, 131, 104/103, 91, 77, 63, 51
5		1,3-benzodioxole	122.1	122/121, 63
66		safrole dimer	324.4	324, 281, 253, 225, 207, 162, 147, 135, 115, 104/103, 91, 73, 65, 44
68 (a-c)		4-[2-(<i>o</i> , <i>p</i> and <i>m</i> -tolyl)propyl] 1,3-benzodioxole	254.3	254, 135, 119, 91, 77, 65, 51

Organic impurities 68 (a-c) were formed in side reactions by the methylenation of organic impurities 67 (a-c). The identity of organic impurities 68 (a-c) was confirmed through ^1H NMR spectroscopy, with signals that correspond to the proton environments labelled a-f in ^1H NMR spectrum in Figure 4-17. The distinct signals produced from organic impurities 68 (a-c) were consistent with the signals produced from organic impurities 67 (a-c) in the ^1H NMR spectrum of the 4-allylcatechol reaction product, as shown in Figure 4-15. The methylene protons from the methylenedioxy ring in organic impurities 68 (a-c) did not produce a distinct, differentiable signal in the ^1H NMR spectrum of the safrole reaction product.

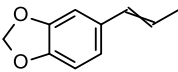
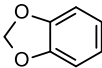
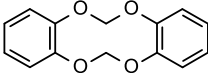

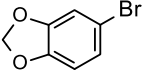
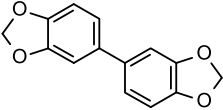
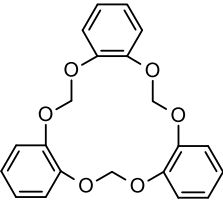
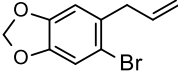
Organic impurities 3 (a-b) and 66 are reaction by-products of the methylenation of 4-allylcatechol. A proportion of the safrole product underwent a sodium hydroxide facilitated isomerisation process to form impurities 3 (a-b). The ^1H NMR signals that correspond to isosafrole (3 (a-b)) were determined in the analysis of the isosafrole reaction product in Section 5.3.2.1, and these signals are present and labelled k-o in the ^1H NMR spectrum of the safrole reaction product shown in Figure 4-17. Organic impurity 66 arose through the cyclisation of two 4-allylbenzene-1,2-diolate molecules, formed by the deprotonation of 4-allylcatechol, with dichloromethane. Organic impurity 5 likely resulted from the decomposition of safrole or a

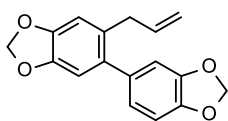
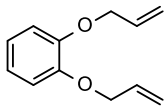
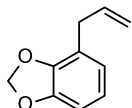
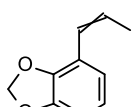
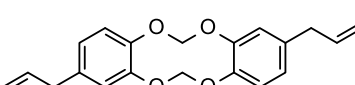
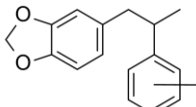
safrole impurity, noting that no catechol was detected in the 4-allylcatechol intermediate used in the methylenation reaction.

4.4 Route Specific Organic Impurities

The organic impurities identified in the catechol-derived safrole from Routes 1 and 2 and eugenol-derived safrole from Route 3 are listed in Table 4-9. Route specific impurities were identified by comparing the organic impurity profiles of safrole synthesised via the three synthetic routes, and the literature organic impurity profiles of synthetic safrole and safrole prepared from sassafras oil [21, 35, 100].

Table 4-9: Comparison of organic Impurities identified in safrole synthesised via Route 1, 2 and 3.

No.	Impurity	Identified in safrole synthesised via Route:		
		1	2	3
3 (a-b)		X	✓	✓
5		✓	✓	✓
39		✓	X	X
40		✓	X	X
41		✓	X	X
42		✓	X	X
47		✓	X	X
58		✓	X	X

No.	Impurity	Identified in safrole synthesised via Route:		
		1	2	3
59		✓	X	X
61		X	✓	X
64		X	✓	X
65 (a-b)		X	✓	X
66		X	✓	✓
68 (a-c)		X	X	✓

Organic impurities 39, 40, 41, 42, 47, 58, and 59 were detected only in safrole prepared by Route 1 and have not previously been identified in safrole produced from sassafras oil [21, 100]. Organic impurities 39, 40, 41, 42, 47, and 58 (but not 59) were previously identified in synthetic, catechol-derived safrole that was prepared by an equivalent synthetic pathway to Route 1 [35]. Organic impurities 39, 40, 41, 42, 47, 58, and 59 are thus route specific for the synthesis of safrole via Route 1. In the study by Heather *et al.* [35], the synthetic, catechol-derived safrole also contained a sesamol impurity due to the reaction of the Grignard reagent with atmospheric oxygen. This impurity was not identified in safrole prepared by Route 1, as the Grignard reaction was performed under a nitrogen atmosphere.

Organic impurities 39, 40, and 47 are characteristic by-products of the methylenation of catechol, and their detection is therefore indicative of synthetic, catechol-derived safrole. Organic impurity 41 is an intermediate in the synthetic route, and its detection is therefore indicative of the bromination reaction used in the second step. The Grignard reaction can be

inferred from the detection of organic impurity 42, which is a characteristic reaction by-product formed when the Grignard reagent is prepared from 5-bromo-1,3-benzodioxole. Impurities 58, and 59 result from a Grignard reaction of a characteristic bromination impurity, and thus their detection in safrole indicate the synthetic route used in its preparation.

Organic impurities 61, 64, and 65 (a-b) were only identified in catechol-derived safrole from Route 2 and have not been previously identified in safrole [21, 100]. Thus, they are route specific for the synthesis of safrole from catechol via Route 2. Impurity 61 is a characteristic by-product of the etherification of catechol, and its detection is therefore indicative of synthetic, catechol-derived safrole. Impurities 64 and 65 (a-b) result from the methylenation of a characteristic Claisen rearrangement reaction by-product, and thus their detection in safrole indicate the synthetic pathway used in its preparation.

Organic impurities 68 (a-c) were only identified in eugenol-derived safrole from Route 3 and have not been previously identified in safrole [21, 100]. Thus, they are route specific for the synthesis of safrole from eugenol via Route 3. The formation of organic impurities 68 (a-c) is dependent on the reagents and solvents utilised in the demethylation reaction (in this case, aluminium(III) chloride and toluene, respectively). The demethylation of eugenol can be performed utilising a variety of different reaction conditions, with experimental procedures available on websites dedicated to the synthesis of illicit drugs [33, 34, 42]. Thus, impurities 68 (a-c) will likely not be detected in safrole synthesised from eugenol if alternate reagents and/or solvents are used in its preparation.

Organic impurity 66 is not a route specific impurity, as it was detected in safrole synthesised by Routes 2 and 3. This is because it is a characteristic by-product of the methylenation of 4-allylcatechol, which was used in the synthesis of safrole via both Routes 2 and 3. However, organic impurity 66 has not been previously identified in safrole [21, 100] and its detection in safrole indicates that it is synthetically derived.

Organic impurity 5 was identified in safrole synthesised by all routes, and has previously been detected in synthetic, catechol-derived safrole and safrole produced from sassafras oil [21, 62, 100]. Organic impurities 3 (a-b) were identified in safrole synthesised by Routes 2 and 3, and have previously been identified in safrole produced from sassafras oil [21, 100]. The detection of impurities 3 (a-b) and 5 in safrole therefore has little to no discriminatory value.

4.5 Conclusions

Safrole was synthesised from the 'pre-precursor' catechol via Route 1 in three steps: the methylenation of catechol, the bromination of 1,3-benzodioxole and a Grignard reaction using 5-bromo-1,3-benzodioxole and allyl bromide. Safrole was synthesised from the 'pre-precursor' catechol via Route 2 in three steps: the etherification of catechol, the Claisen rearrangement of 2-allyloxyphenol, and the methylenation of 4-allylcatechol. Safrole was synthesised from the 'pre-precursor' eugenol via Route 3 in two steps: the demethylation of eugenol, and the methylenation of 4-allylcatechol.

The products of each step in the synthetic routes were analysed by GC-MS and ^1H NMR spectroscopy, and a number of detected organic impurities were identified. Eight organic impurities (5, 39, 40, 41, 42, 47, 58, and 59) were identified in safrole from catechol via Route 1, eight organic impurities (3 (a-b), 5, 61, 64, 65 (a-b), and 66) were identified in safrole synthesised from catechol via Route 2, and seven organic impurities (3 (a-b), 5, 66, 68 (a-c)) were identified in safrole synthesised from eugenol via Route 3. Importantly, nine organic impurities (59, 61, 64, 65 (a-b), 66, and 68 (a-c)) were identified in safrole that have not previously been reported.

Route specific organic impurities were identified in safrole that indicated the 'pre-precursors' catechol and eugenol were used in the respective synthetic pathways. Route specific organic impurities were also identified that indicated the route used to synthesise safrole from the respective 'pre-precursor'. Thus, the use of the 'pre-precursors' catechol and eugenol and the synthetic routes that were used in its preparation could be ascertained by the organic impurity profiling of safrole under the conditions used here.

Chapter 5: MDMA

Chapter 5: MDMA

5.1 Introduction

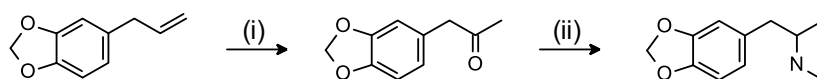
This chapter discusses the synthesis and organic impurity profiling of MDMA that was prepared from synthetic safrole via two routes. The reactions utilised in these two synthetic routes are described in detail in Section 5.2. Synthetic safrole was prepared from the ‘pre-precursor’ catechol via two synthetic routes and the ‘pre-precursor’ eugenol via one synthetic route, resulting in the synthesis of MDMA from catechol by four routes and from eugenol by two routes. The reaction products of each step in the six synthetic routes were analysed using GC-MS and ^1H NMR spectroscopy. The chemical structures and origins of the detected organic impurities are detailed in Section 5.3. A proportion of the detected organic impurities resulted from organic impurities that are present in the synthetic safrole used, as discussed in Chapter 4. The removal, persistence, or subsequent reactions of these organic impurities during the preparation of MDMA was discussed. The organic impurity profiles of MDMA synthesised by the six synthetic routes were compared against each other and the relevant literature. The significance of the identified organic impurities was analysed, and route specific impurities are discussed in Section 5.4.

5.2 Synthesis

Synthetic safrole, prepared from catechol by two routes and eugenol by one route, was used to synthesise MDMA via two synthetic routes. This resulted in the synthesis of MDMA by a total of six synthetic routes: four from the ‘pre-precursor’ catechol and two from the ‘pre-precursor’ eugenol. The synthesis of MDMA was performed at minimum in duplicate for each synthetic route, using synthetic methods that are feasible in a clandestine laboratory. All products were purified by unsophisticated purification techniques, such as liquid-liquid extraction and filtration, to mimic a reasonably equipped clandestine laboratory setting.

5.2.1 Route A: MDMA from Safrole

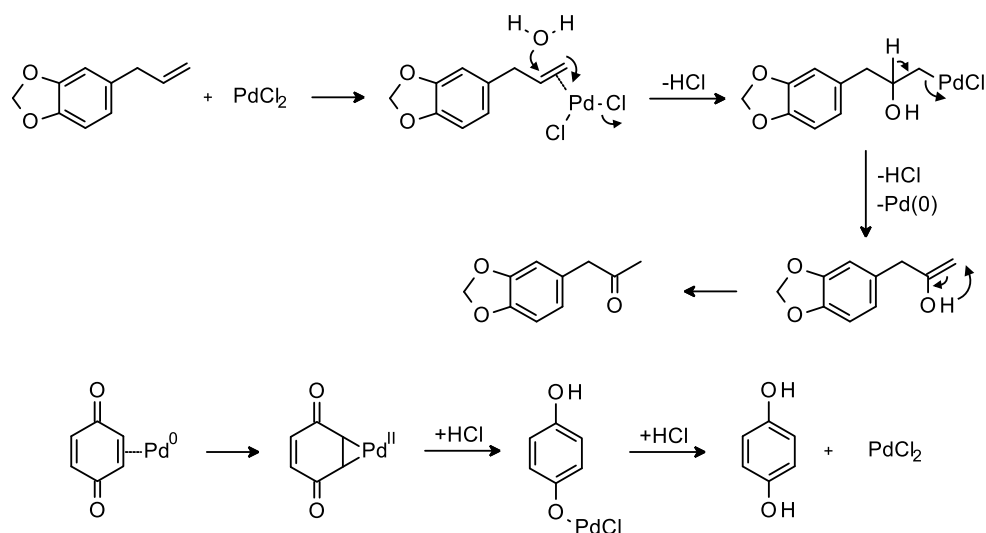
MDMA was synthesised from synthetic safrole via the reaction pathway shown in Scheme 5-1, which was designated as Route A. This is a common reaction pathway utilised by clandestine laboratories [17, 19, 21] and has two steps: the Wacker oxidation of safrole, and the reductive amination of MDP2P.



Scheme 5-1: Synthesis of MDMA from safrole via Route A
(i) H_2O , *p*-benzoquinone, PdCl_2 (ii) $\text{Al}(\text{Hg})$, CH_3NO_2

5.2.1.1 MDP2P from Safrole

The Wacker oxidation of safrole (Reaction i, Scheme 5-1) utilises water and *p*-benzoquinone as reagents, and a palladium chloride catalyst [19]. The reaction mechanism for the synthesis of MDP2P from safrole is shown in Scheme 5-2 [101-103]. A complexation reaction occurs between the alkene group in safrole and palladium chloride, and the resulting intermediate reacts with water and undergoes hydroxypalladation. β -Hydride elimination and tautomerisation yields MDP2P, and the palladium chloride catalyst is regenerated *in situ* via an oxidation reaction with *p*-benzoquinone.

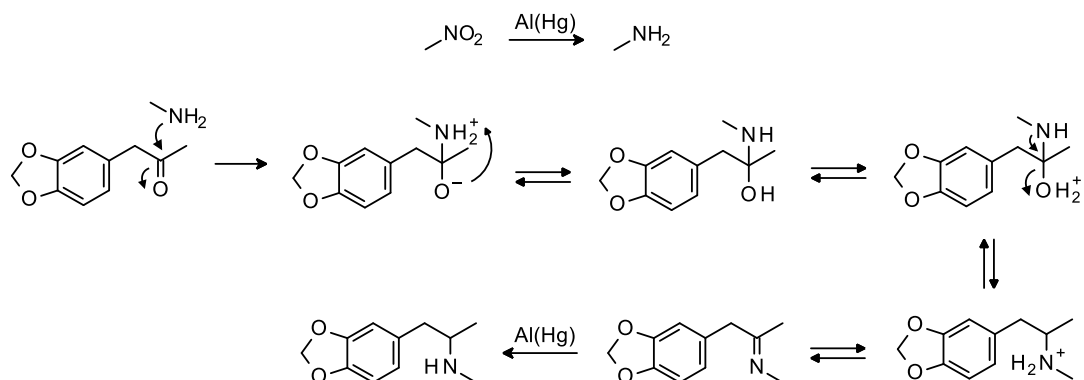


Scheme 5-2: Reaction mechanism for the synthesis of MDP2P from safrole

5.2.1.2 MDMA from MDP2P

The synthesis of MDMA was achieved by the reductive amination of MDP2P using nitromethane and an aluminium/mercury amalgam (Reaction ii, Scheme 5-1). The reductive amination of MDP2P is typically performed using the reagent methylamine [17], which is monitored under Category II of the *Code of Practice for the Supply Diversion into Illicit Drug Manufacture* [28]. Nitromethane is a feasible alternative in the synthesis of MDMA, as it eliminates the need for clandestine laboratory operators to procure a reagent used for the synthesis of numerous ATSS, and is reduced *in situ* by the aluminium/mercury amalgam to form methylamine [17, 104].

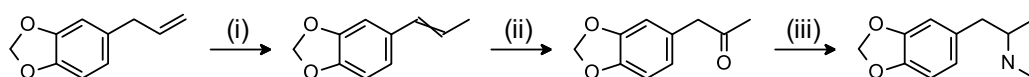
The reaction mechanism for the synthesis of MDMA from MDP2P is shown in Scheme 5-3 [88]. The ketone group in MDP2P and the primary amine reagent, methylamine, undergo a nucleophilic addition reaction to form an imine intermediate. Subsequent reduction of the imine intermediate by the aluminium/mercury amalgam yields MDMA.



Scheme 5-3: Reaction mechanism for the synthesis of MDMA from MDP2P

5.2.2 Route B: MDMA from safrole

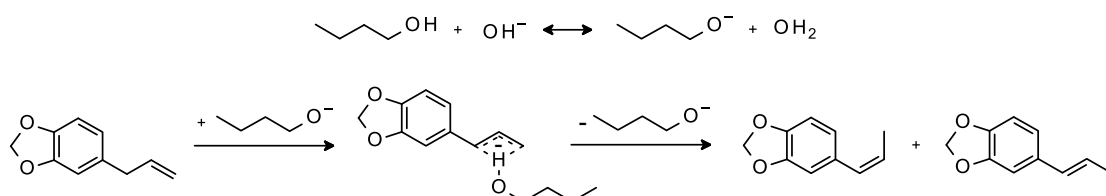
MDMA was synthesised from synthetic safrole via the reaction pathway shown in Scheme 5-4, which was designated as Route B. This is a common reaction pathway utilised by clandestine laboratories [4, 17, 20, 21] and has three steps: the isomerisation of safrole, peracid oxidation and acidic dehydration of isosafrole and the reductive amination of MDP2P.



Scheme 5-4: Synthesis of MDMA from safrole via Route B
(i) KOH, C₄H₉OH (ii) 1. HOOH, HCOOH 2. H₂SO₄ (iii) Al(Hg), CH₃NO₂

5.2.2.1 Isosafrole from Safrole

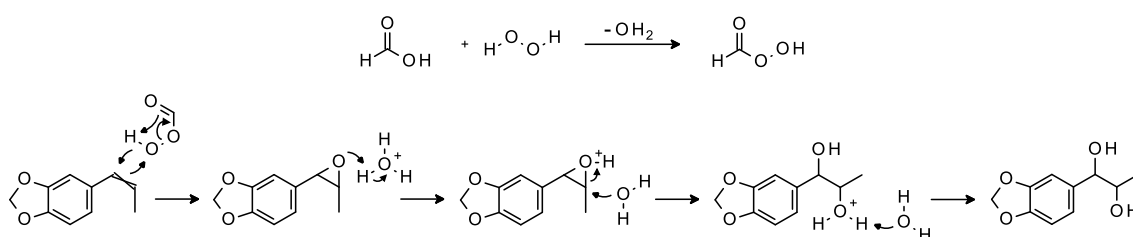
The isomerisation of safole (Reaction i, Scheme 5-4) is a base-catalysed rearrangement reaction. The reaction mechanism for the synthesis of *cis*- and *trans*- isosafrole from safole is shown in Scheme 5-5 [105]. Potassium hydroxide and 1-butanol first react to form butoxide, which reacts with safole and removes a benzylic proton. The results in an anionic allylic intermediate, where the allylic carbons and the hydrogen in butanol are hydrogen bonded. *Cis*- and *trans*- isosafrole are then formed by the collapse of this intermediate.



Scheme 5-5: Reaction mechanism for the synthesis of cis- and trans- isosafrole from safrole

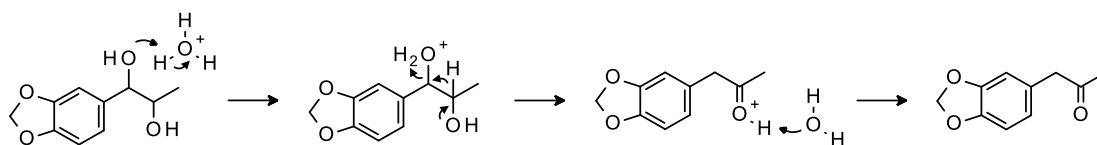
5.2.2.2 MDP2P from Isosafrole

The synthesis of MDP2P from isosafrole (Reaction ii, Scheme 5-4) was achieved by peracid oxidation and acidic dehydration, via an isosafrole glycol intermediate. The reaction mechanism for the peracid oxidation of isosafrole to form isosafrole glycol is shown in Scheme 5-6 [88]. Formic acid and hydrogen peroxide undergo a dehydration reaction to yield peroxy acid. The alkene group in isosafrole reacts with peroxy acid to form an epoxide intermediate, which is then protonated by acid. The nucleophilic addition of water to the protonated epoxide yields isosafrole glycol.



Scheme 5-6: Reaction mechanism for the peracid oxidation of isosafrole

The acidic dehydration of isosafrole glycol is a pinacol rearrangement reaction [95]. The reaction mechanism for the synthesis of MDP2P from isosafrole glycol is shown in Scheme 5-7. The benzylic hydroxide of isosafrole glycol is protonated under the acidic reaction conditions. Electron migration from the adjacent hydroxide group and subsequent deprotonation of the resulting ketone carbocation yields MDP2P.



Scheme 5-7: Reaction mechanism for the acidic dehydration of isosafrole glycol to form MDP2P

5.2.2.3 MDMA from MDP2P

The synthesis of MDMA via Route B was achieved by a reductive amination of MDP2P with nitromethane and an aluminium/mercury amalgam (Reaction iii, Scheme 5-4). The reaction conditions utilised were the same as those used to synthesise MDMA from MDP2P in Route A, as discussed in detail in Section 5.2.1.2.

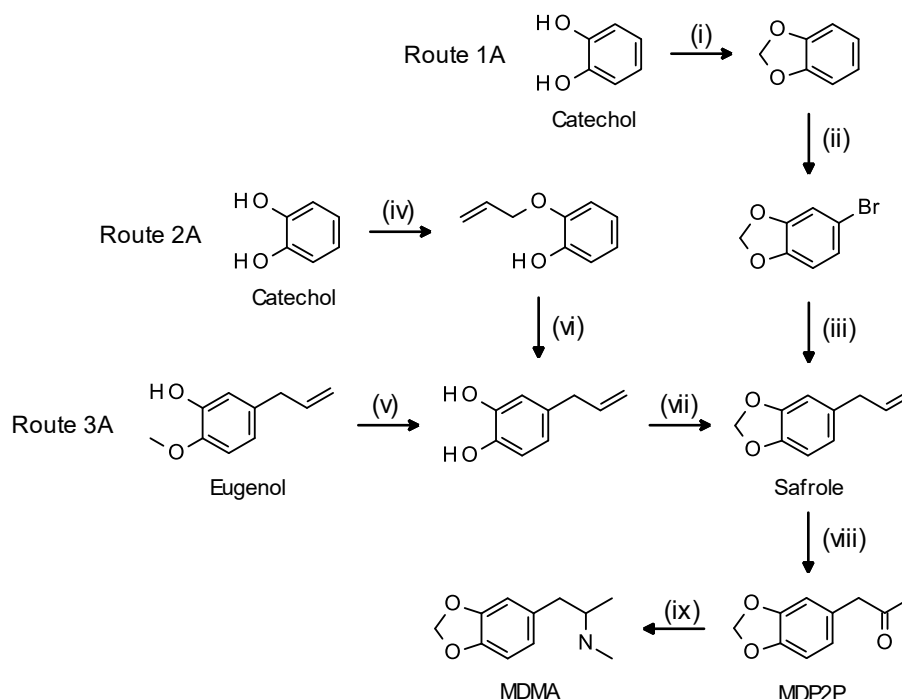
5.3 Organic Impurity Profiling

MDMA was prepared via a synthetic safrole intermediate by six routes; four from the 'pre-precursor' catechol and two from the 'pre-precursor' eugenol. The reaction products of each step in the synthesis of MDMA from safrole were analysed using GC-MS and ^1H NMR

spectroscopy. The detected organic impurities were identified by analysis of the mass fragmentation pattern in their mass spectrum. Due to the significant number of organic impurities detected in reaction products, the overlapping ^1H NMR signals of organic impurities formed during the synthesis of MDMA from safrole could not be differentiated and assigned. The mass spectra and fragmentation patterns of the reaction products and identified organic impurities are shown in Appendix 1, and the ^1H NMR spectra of reaction product mixtures are shown in Appendix 3. The formation of the identified organic impurities during the relevant reactions in the synthesis of MDMA was also investigated.

5.3.1 Routes 1A, 2A and 3A

In Route A, MDMA was synthesised from synthetic safrole via two steps: Wacker oxidation to yield MDP2P, and reductive amination to yield MDMA. The synthetic safrole used had been prepared from catechol by two routes (Routes 1 and 2) and eugenol by one route (Route 3). This resulted in the synthesis of MDMA from catechol via two routes (Routes 1A and 2A) and from eugenol via one route (Route 3A), as shown in Scheme 5-8. The chemical structures and origin of the organic impurities detected in the MDP2P intermediates and the MDMA products prepared by Routes 1A, 2A and 3A were investigated.



Scheme 5-8: Synthesis of MDMA from catechol and eugenol via safrole by Routes 1A, 2A and 3A

(i) CH_2Cl_2 , NaOH (ii) HBr, HCOOH , CH_3COOH (iii) 1. Mg, DIBAL 2. $\text{CH}_2\text{CHCH}_2\text{Br}$ (iv) $\text{CH}_2\text{CHCH}_2\text{Br}$, K_2CO_3 (v) NaOC_2H_5 , Δ (vi) AlCl_3 , pyridine (vii) CH_2Cl_2 , NaOH (viii) H_2O , *p*-benzoquinone, PdCl_2 (ix) $\text{Al}(\text{Hg})$, CH_3NO_2

5.3.1.1 MDP2P from Safrole

The gas chromatogram in Figure 5-1 shows the fifteen organic impurities that were consistently identified in the MDP2P prepared by Route 1A. The gas chromatogram in Figure 5-2 shows the twelve organic impurities that were consistently identified in the MDP2P prepared by Route 2A. The gas chromatogram in Figure 5-3 shows the eleven organic impurities that were consistently identified in the MDP2P prepared by Route 3A. The assigned numbers, chemical structures, names, molecular weights, and m/z data of the organic impurities identified in the MDP2P synthesised via Routes 1A, 2A and 3A, and the route in which they were identified, are shown in Table 5-1.

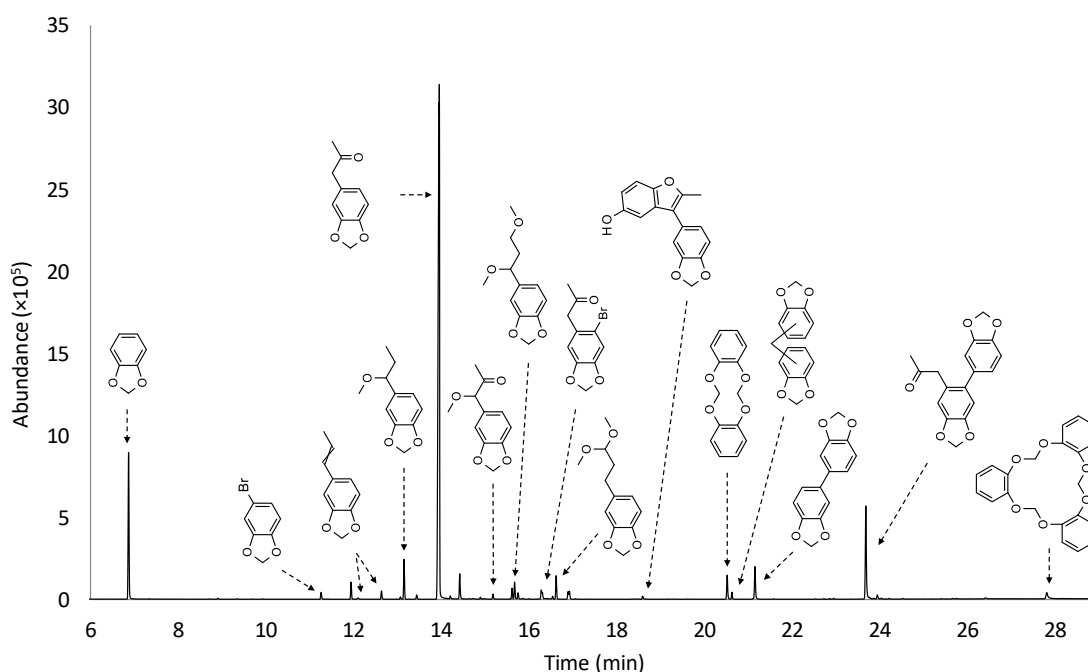


Figure 5-1: GC-MS total ion chromatogram of MDP2P synthesised via Route 1A

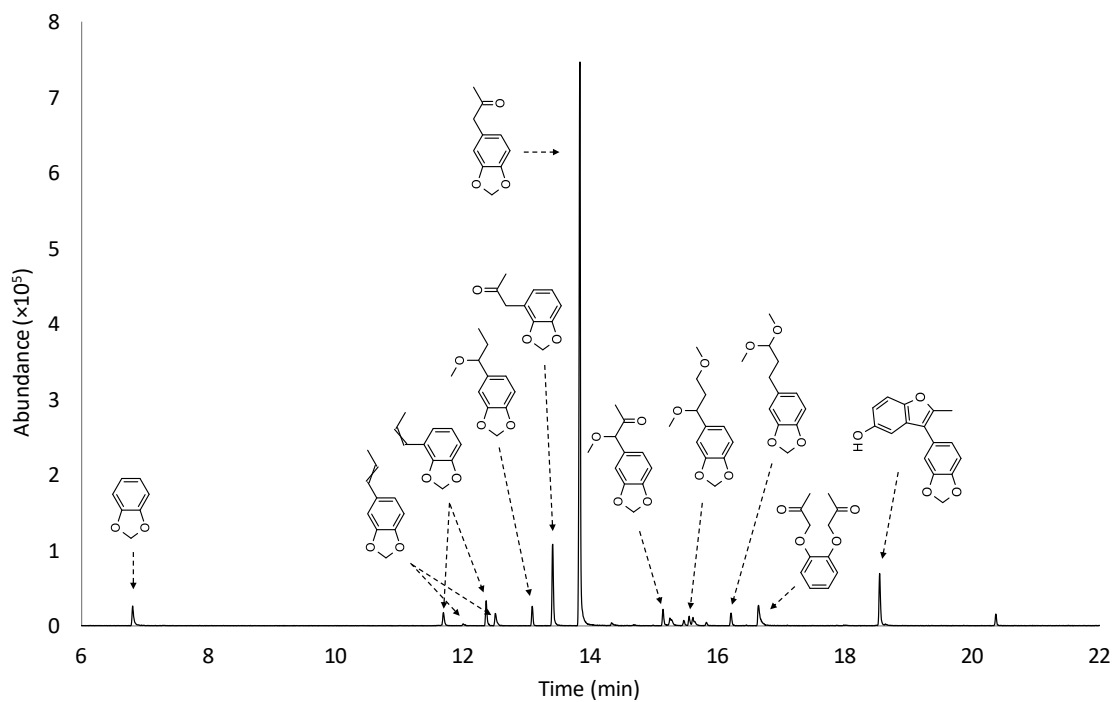


Figure 5-2: GC-MS total ion chromatogram of MDP2P synthesised via Route 2A

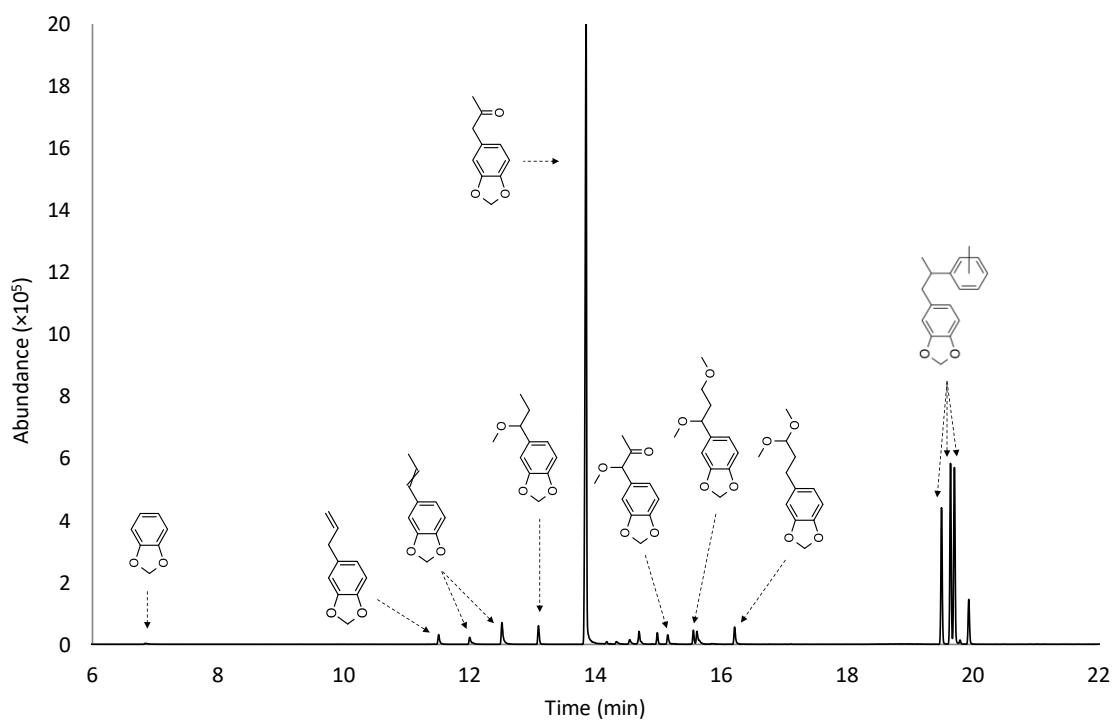
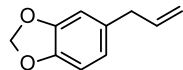
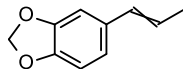
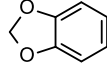
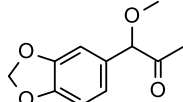
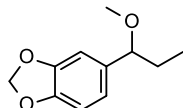
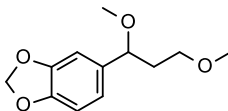
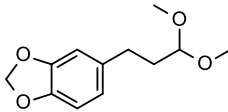
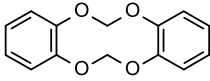
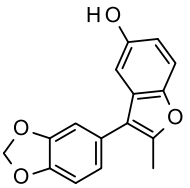
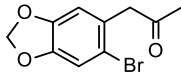
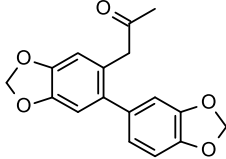
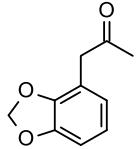
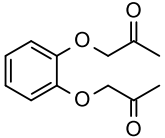


Figure 5-3: GC-MS total ion chromatogram of MDP2P synthesised via Route 3A

Table 5-1: Organic impurities identified in MDP2P synthesised via Route 1A, 2A and 3A

No.	Impurity Structure	Impurity Name	MW (g/mol)	m/z	Identified in MDP2P synthesised via Route:		
					1A	2A	3A
2		safrole	162.2	162, 131, 119, 104/103, 91, 77, 63, 51, 44	X	X	✓
3 (a-b)		<i>cis</i> - and <i>trans</i> - isosafrole	162.2	162, 131, 104/103, 77, 44	✓	✓	✓
5		1,3-benzodioxole	122.1	122/121, 63	✓	✓	✓
25		1-(3,4-Methylenedioxyphenyl)-1-methoxypropan-2-one	208.2	208, 165, 150/149, 135, 119, 77, 44/43	✓	✓	✓
26		1-(3,4-methylenedioxyphenyl)-1-methoxypropane	194.2	194, 165, 150/149, 135, 77	✓	✓	✓
28		1-(3,4-methylenedioxyphenyl)-1,3-dimethoxypropane	224.3	224, 192, 161, 135, 75	✓	✓	✓
29		3-(3,4-methylenedioxyphenyl)-1,1-dimethoxypropane	224.3	224, 192, 161, 135, 75	✓	✓	✓
39		1,3-benzodioxole dimer	244.2	244, 135, 122/121, 63	✓	X	X

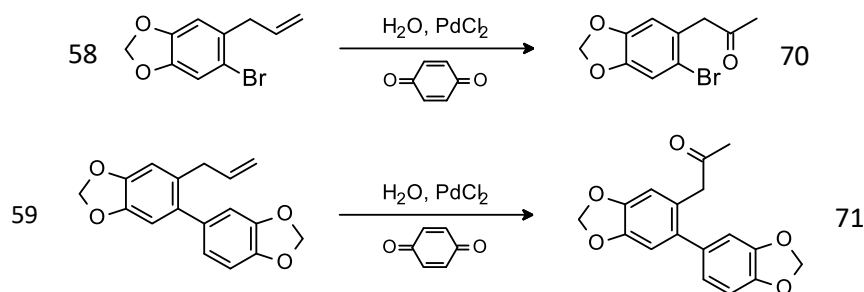
No.	Impurity Structure	Impurity Name	MW (g/mol)	m/z	Identified in MDP2P synthesised via Route:		
					1A	2A	3A
40		4,4', 4,5'- or 5,5'-methylenebis-1,3-benzodioxole	256.3	256, 225, 196, 168, 135, 77	✓	X	X
41		5-bromo-1,3-benzodioxole	201.0	202/200, 121, 63	✓	X	X
42		5,5'-bi-1,3-benzodioxole	242.2	242, 126, 121/120, 63	✓	X	X
47		1,3-benzodioxole trimer	366.4	366, 244, 135, 122/121	✓	X	X
65 (a-b)		4-prop-1-enyl-1,3-benzodioxole	166.2	162, 131, 119, 104/103, 91, 77, 63, 51	X	✓	X
68 (a-c)		4-[2-(<i>o</i> , <i>p</i> and <i>m</i> -tolyl)propyl] 1,3-benzodioxole	254.3	254, 135, 119, 91, 77, 65, 51	X	X	✓

No.	Impurity Structure	Impurity Name	MW (g/mol)	m/z	Identified in MDP2P synthesised via Route:		
					1A	2A	3A
69		3-(1,3-benzodioxol-5-yl)-2-methyl-benzofuran-5-ol	268.3	268, 205, 166, 149, 135, 121, 103, 75, 71, 65, 57, 45, 43	✓	✓	X
70		1-(6-bromo-1,3-benzodioxol-5-yl)propan-2-one	257.1	258/256, 215/213, 177, 157, 147, 135, 78, 43	✓	X	X
71		1-[6-(1,3-benzodioxol-5-yl)-1,3-benzodioxol-5-yl]propan-2-one	298.3	298, 255, 225, 195, 167, 139, 63, 43	✓	X	X
72		1-(1,3-benzodioxol-4-yl)propan-2-one	178.2	178, 135, 105, 77, 65, 51, 43	X	✓	X
73		1-(2-acetonyloxyphenoxy)propan-2-one	222.2	222, 179, 149, 135, 122/121, 107, 92, 77, 65, 57, 51, 43	X	✓	X

Organic impurities 3 (a-b), 5, 25, 26, 28, and 29 were identified in MDP2P synthesised by Routes 1A, 2A and 3A, and organic impurity 69 was identified in MDP2P synthesised by Routes 1A and 2A. Organic impurities 26, 28, and 29 are characteristic by-products of the Wacker oxidation of safrole in methanol solvent [19]. Organic impurity 25 is also a reaction by-product of the Wacker oxidation of safrole in methanol solvent, but is not characteristic as it has been identified in MDP2P prepared by peracid oxidation of isosafrole [19, 61]. Organic impurity 69 is a Wacker oxidation by-product that was formed by the reaction of MDP2P with *p*-benzoquinone [106].

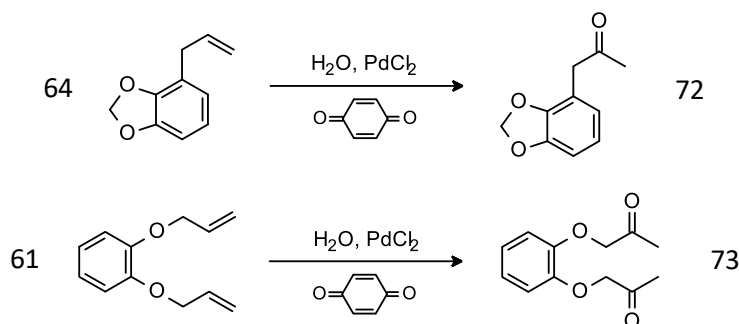
Organic impurities 3 (a-b) were identified in safrole synthesised by Routes 2 and 3, and organic impurity 5 was identified in safrole synthesised by all three routes. Organic impurities 3 (a-b) are reaction by-products of the Wacker oxidation of safrole, however, may also have been carried over, unchanged, from safrole in Routes 2A and 3A. Organic impurity 5 was carried over, unchanged, from the safrole in Routes 1A, 2A, and 3A.

Organic impurities 39, 40, 41, 42, 47, 70, and 71 were identified in MDP2P synthesised by Route 1A. Organic impurities 39, 40, 41, 42, and 47 were identified in safrole synthesised by Route 1 and have been carried over, unchanged, in the Wacker oxidation reaction. As shown in Scheme 5-9, the Wacker oxidation of organic impurities 58 and 59, identified in safrole synthesised by Route 1, yielded organic impurities 70 and 71.



Scheme 5-9: Formation of organic impurities 70 and 71 in Route 1A

Organic impurities 65 (a-b), 72, and 73 were identified in MDP2P synthesised by Routes 2A. Organic impurities 65 (a-b) were identified in safrole synthesised by Route 2 and have been carried over, unchanged, in the Wacker oxidation reaction. Organic impurities 64 and 61, identified in safrole synthesised by Route 2, undergo Wacker oxidation to respectively form organic impurities 72 and 73 as shown in Scheme 5-10.



Scheme 5-10: Formation of organic impurities 72 and 73 in Route 2A

Organic impurities 2 and 68 (a-c) were identified in MDP2P synthesised by Routes 3A. Safrole (organic impurity 2) is the starting material of the Wacker oxidation reaction, and its detection therefore indicated that this reaction did not proceed to completion in Route 3A. Organic impurities 68 (a-c) were identified in safrole synthesised by Route 3 and have been carried over, unchanged, in the Wacker oxidation of safrole.

5.3.1.2 MDMA from MDP2P

The gas chromatogram in Figure 5-4 shows the thirteen organic impurities that were consistently identified in the MDMA prepared by Route 1A. The gas chromatogram in Figure 5-5 shows the twelve organic impurities that were consistently identified in the MDMA prepared by Route 2A. The gas chromatogram in Figure 5-6 shows the eleven organic impurities that were consistently identified in the MDMA prepared by Route 3A. The assigned numbers, chemical structures, names, molecular weights, and m/z data of the organic impurities identified in the MDMA synthesised via Route 1A, 2A and 3A, and route in which they were identified, are shown in Table 5-2.

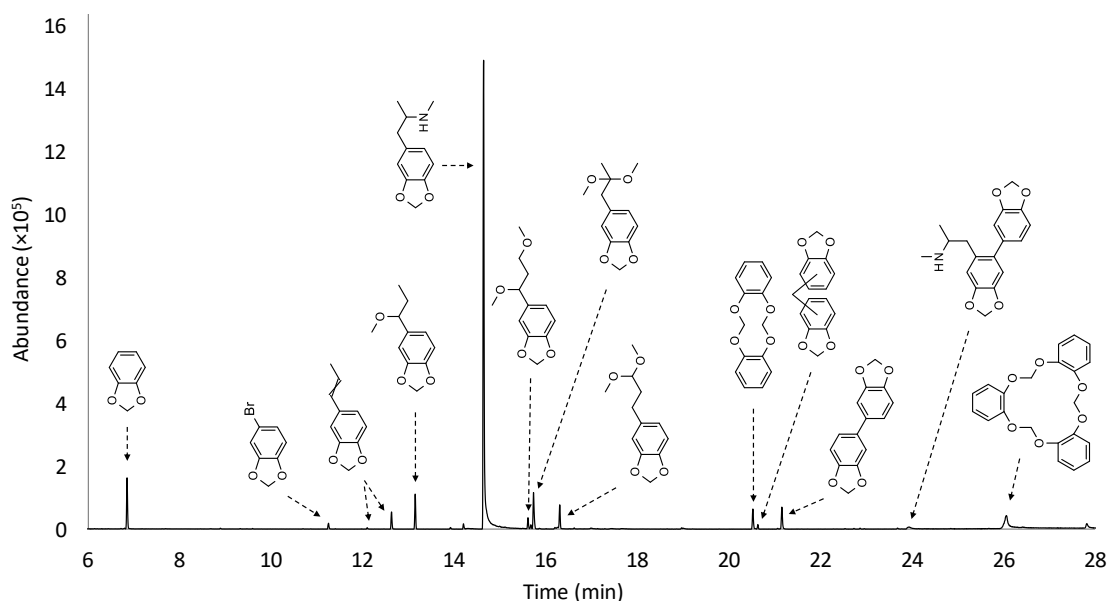


Figure 5-4: GC-MS total ion chromatogram of MDMA synthesised via Route 1A

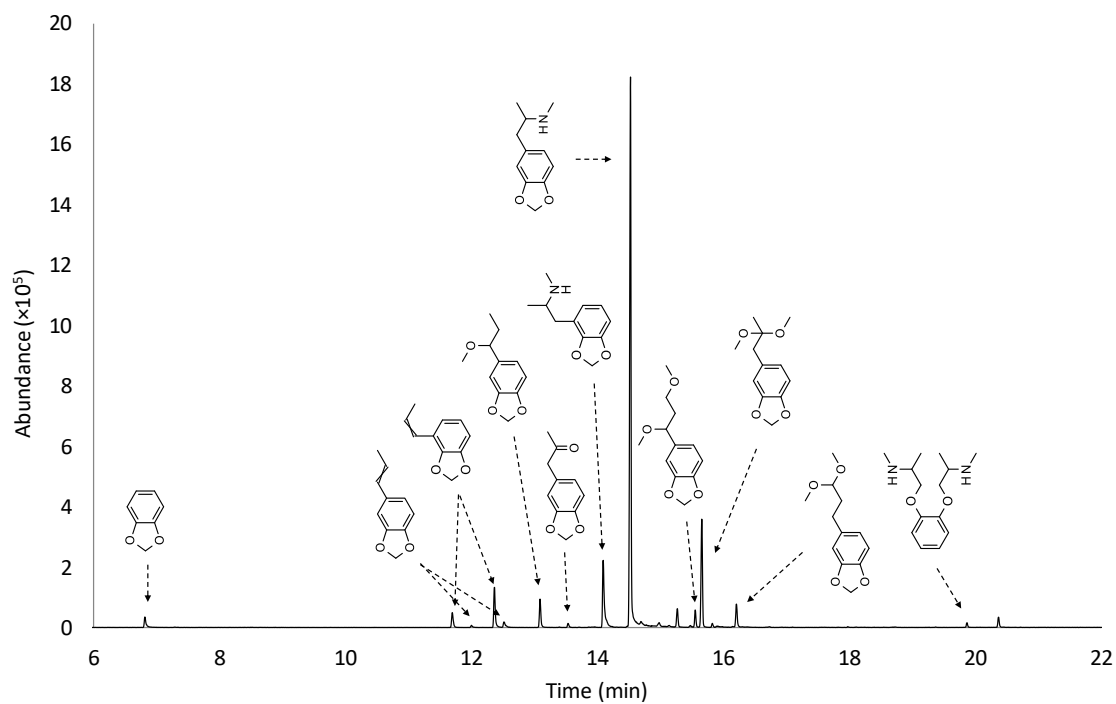


Figure 5-5: GC-MS total ion chromatogram of MDMA synthesised via Route 2A

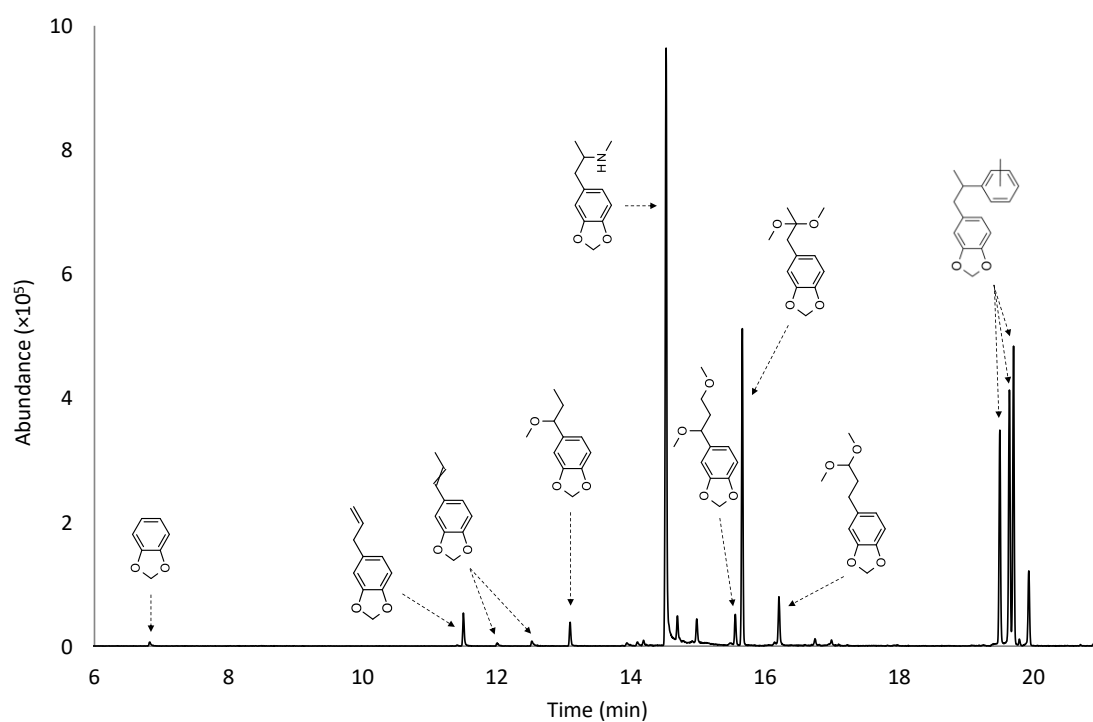
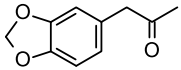
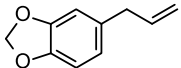
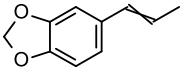
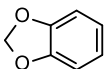
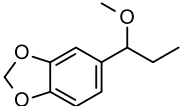
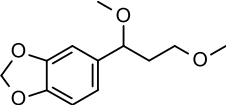
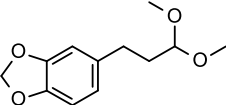
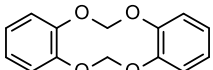
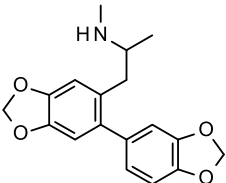
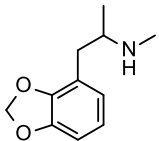
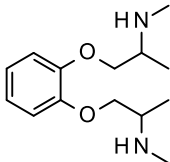
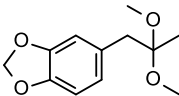


Figure 5-6: GC-MS total ion chromatogram of MDMA synthesised via Route 3A

Table 5-2: Organic impurities identified in MDMA synthesised via Route 1A, 2A and 3A

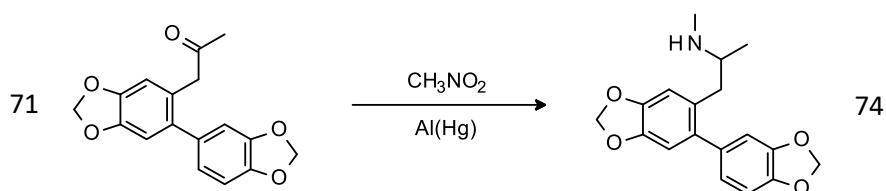
No.	Impurity Structure	Impurity Name	MW (g/mol)	m/z	Identified in MDMA synthesised via Route:		
					1A	2A	3A
1		MDP2P	178.2	178, 135, 105, 77, 63, 51, 43	X	✓	X
2		Safrole	162.2	162, 131, 119, 104/103, 91, 77, 63, 51, 44	X	X	✓
3 (a-b)		<i>cis</i> - and <i>trans</i> - isosafrole	162.2	162, 135, 131, 104/103, 91, 77, 63, 51	✓	✓	✓
5		1,3-benzodioxole	122.1	122/121, 63	✓	✓	✓
26		1-(3,4-methylenedioxyphenyl) -1-methoxypropane	194.2	194, 165, 150/149, 135, 77	✓	✓	✓
28		1-(3,4-methylenedioxyphenyl) -1,3-dimethoxypropane	224.3	224, 192, 161, 135, 75	✓	✓	✓
29		3-(3,4-methylenedioxyphenyl) -1,1-dimethoxypropane	224.3	224, 192, 161, 135, 75	✓	✓	✓
39		1,3-benzodioxole dimer	244.2	244, 135, 122/121, 63	✓	X	X

No.	Impurity Structure	Impurity Name	MW (g/mol)	m/z	Identified in MDMA synthesised via Route:		
					1A	2A	3A
40		4,4', 4,5'- or 5,5'-methylenebis-1,3-benzodioxole	256.3	256, 225, 196, 168, 135, 77	✓	X	X
41		5-bromo-1,3-benzodioxole	201.0	202/200, 121, 63	✓	X	X
42		5,5'-bi-1,3-benzodioxole	242.2	242, 126, 121/120, 63	✓	X	X
47		1,3-benzodioxole trimer	366.4	366, 244, 135, 122/121	✓	X	X
65 (a-b)		4-prop-1-enyl-1,3-benzodioxole	162.2	162, 131, 119, 104/103, 91, 77, 63, 51	X	✓	X
68 (a-c)		4-[2-(<i>o</i> , <i>p</i> and <i>m</i> -tolyl)propyl] 1,3-benzodioxole	254.3	254, 135, 119, 91, 77, 65, 51	X	X	✓

No.	Impurity Structure	Impurity Name	MW (g/mol)	m/z	Identified in MDMA synthesised via Route:		
					1A	2A	3A
74		1-[6-(1,3-benzodioxol-5-yl)-1,3-benzodioxol-5-yl]-N-methyl-propan-2-amine	313.3	256, 58, 44	✓	X	X
75		1-(1,3-benzodioxol-4-yl)-N-methyl-propan-2-amine	193.2	192, 178, 151, 135, 105, 93, 77, 58, 51	X	✓	X
76		N-methyl-1-[2-[2-(methilamino)propoxy]phenoxy]propan-2-amine	252.4	251, 219, 149, 121, 110, 89, 72, 43	X	✓	X
77		MDP2P dimethyl acetal	224.3	224, 193, 135, 89	✓	✓	✓

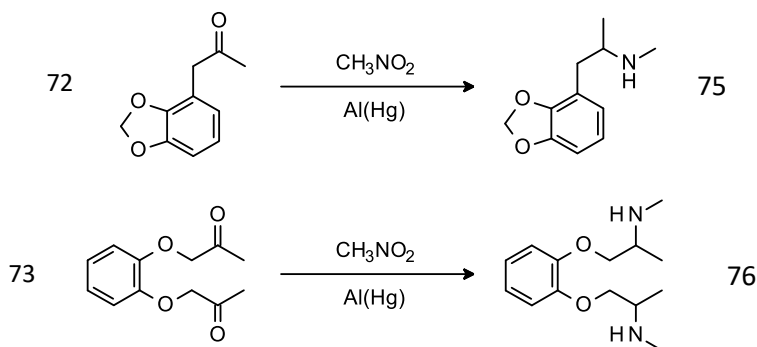
Organic impurities 3 (a-b), 5, 26, 28, 29, and 77 were identified in MDMA synthesised by Routes 1A, 2A and 3A. Organic impurities 3 (a-b), 5, 26, 28 and 29 were identified in MDP2P and have been carried over, unchanged, in the reductive amination reaction. Organic impurity 77 is a characteristic by-product of the reductive amination of MDP2P in methanol solvent [31].

Organic impurities 39, 40, 41, 42, 47, and 74 were identified in MDMA synthesised by Route 1A. Organic impurities 39, 40, 41, 42, and 47 were identified in both safrole synthesised by Route 1 and MDP2P synthesised by Route 1A, and have been carried over, unchanged, in the reductive amination reaction. As shown in Scheme 5-11, the reductive amination of organic impurity 71, identified in MDP2P synthesised by Route 1A, yielded organic impurity 74.



Scheme 5-11: Formation of organic impurity 74 in Route 1A

Organic impurities 1, 65 (a-b), 75, and 76 were identified in MDMA synthesised by Route 2A. MDP2P (organic impurity 1) is the starting material of the reductive amination reaction, and its detection therefore indicated this reaction did not proceed to completion in Route 2A. Organic impurities 65 (a-b) were identified in both safrole synthesised by Route 2 and MDP2P synthesised by Route 2A, and have been carried over, unchanged, in the reductive amination reaction. Organic impurities 72 and 73, identified in MDP2P synthesised by Route 2A, underwent reductive amination to respectively form organic impurities 75 and 76 as shown in Scheme 5-12.

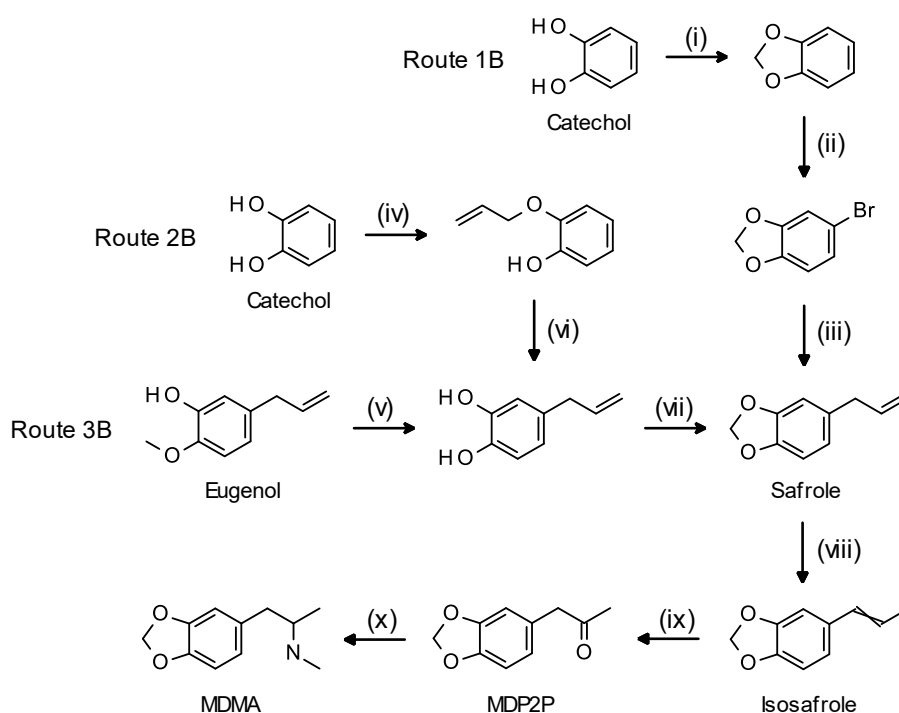


Scheme 5-12: Formation of organic impurities 75 and 76 in Route 2A

Organic impurities 2 and 68 (a-c) were identified in MDMA synthesised by Route 3A. Organic impurities 2 and 68 (a-c) were identified in MDP2P synthesised by Route 3A, and have been carried over, unchanged, in the subsequent reductive amination reaction.

5.3.2 Routes 1B, 2B and 3B

In Route B, MDMA was synthesised from synthetic safrole via three steps: isomerisation to yield isosafrole, peracid oxidation and acidic dehydration to yield MDP2P, and reductive amination to yield MDMA. The synthetic safrole used had been prepared from catechol by two routes (Route 1 and 2) and eugenol by one route (Route 3). This resulted in the synthesis of MDMA from catechol via two routes (Route 1B and 2B) and from eugenol via one route (Route 3B), as shown in Scheme 5-13. The chemical structures and origin of the organic impurities detected in the isosafrole and MDP2P intermediates and the MDMA products prepared by Routes 1B, 2B and 3B were investigated.



Scheme 5-13: Synthesis of MDMA from catechol and eugenol via safrole by Routes 1B, 2B and 3B

(i) CH_2Cl_2 , NaOH (ii) HBr, HCOOH, CH_3COOH (iii) 1. Mg, DIBAL 2. $\text{CH}_2\text{CHCH}_2\text{Br}$ (iv) $\text{CH}_2\text{CHCH}_2\text{Br}$, K_2CO_3 (v) NaOC_2H_5 , Δ (vi) AlCl_3 , pyridine (vii) CH_2Cl_2 , NaOH (viii) KOH, $\text{C}_4\text{H}_9\text{OH}$ (ix) 1. HOOH, HCOOH 2. H_2SO_4 (x) $\text{Al}(\text{Hg})$, CH_3NO_2

5.3.2.1 Isosafrole from Safrole

The gas chromatogram in Figure 5-7 shows the eleven organic impurities that were consistently identified in the isosafrole prepared by Route 1B. The gas chromatogram in Figure 5-8 shows the nine organic impurities that were consistently identified in the isosafrole prepared by Route 2B. The gas chromatogram in Figure 5-9 shows the six organic impurities that were consistently identified in the isosafrole prepared by Route 3B. The assigned numbers, chemical structures, names, molecular weights, and m/z data of the organic impurities identified in the isosafrole

synthesised via Route 1B, 2B and 3B, and the route in which they were identified, are shown in Table 5-3.

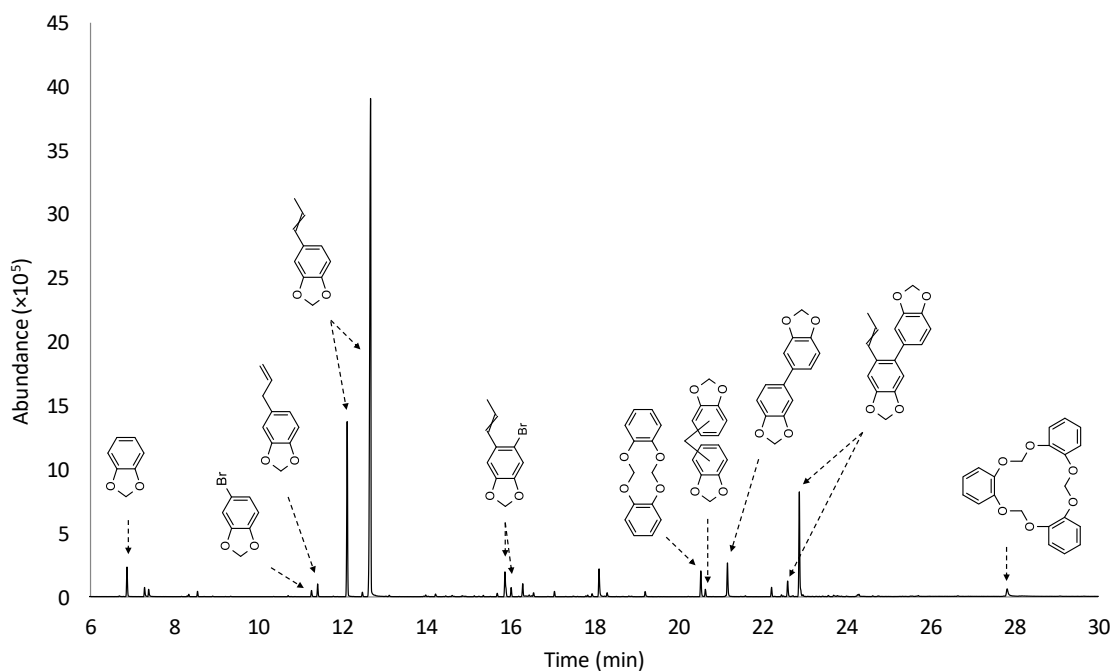


Figure 5-7: GC-MS total ion chromatogram of isosafrole synthesised via Route 1B

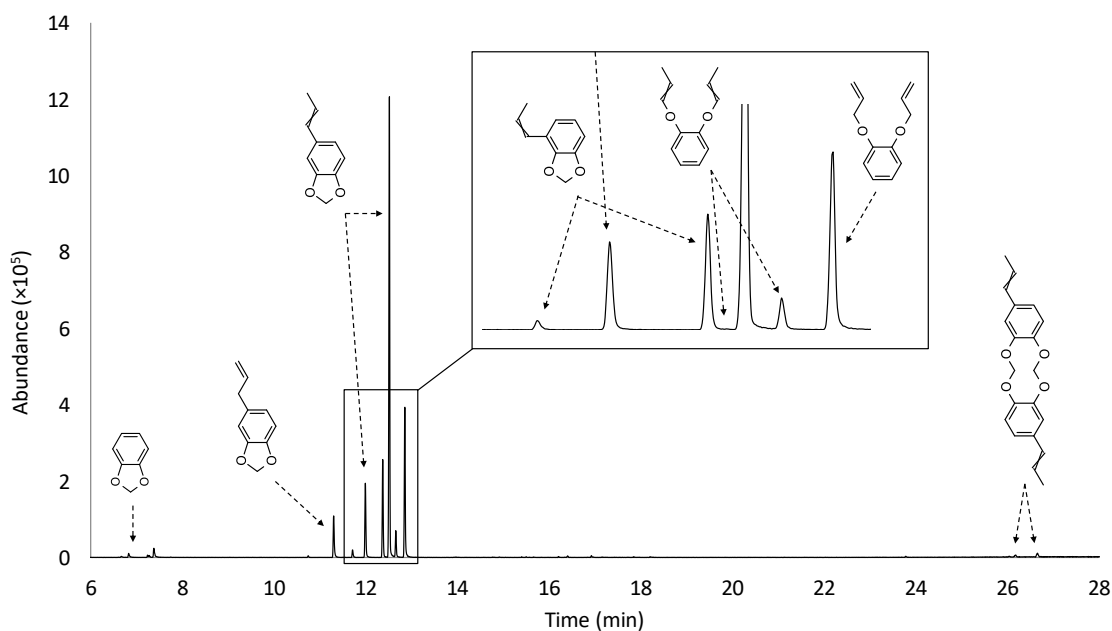


Figure 5-8: GC-MS total ion chromatogram of isosafrole synthesised via Route 2B

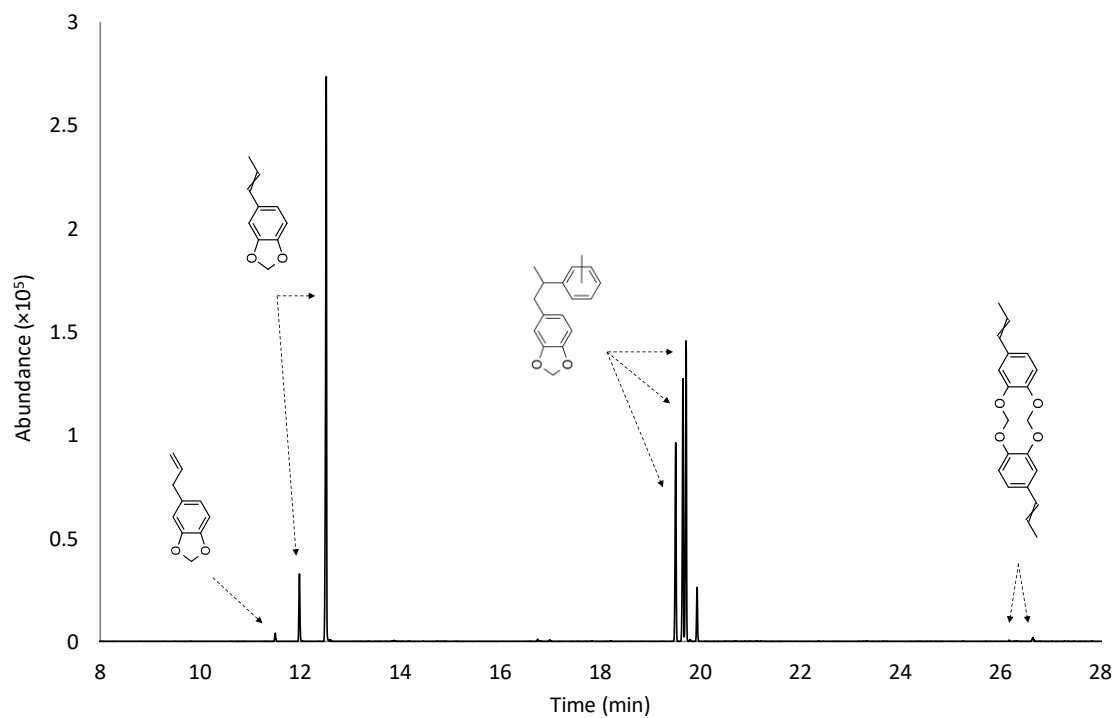
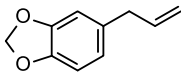
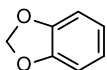
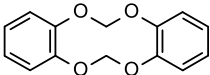
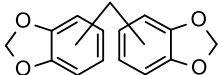
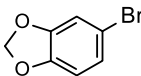
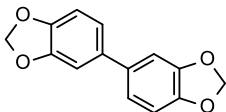
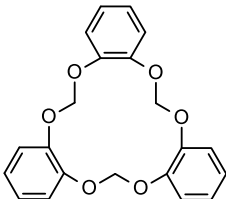
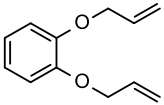
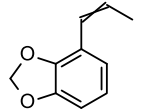
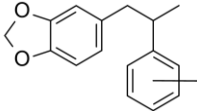
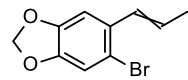
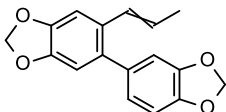
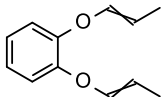
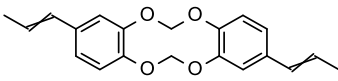


Figure 5-9: GC-MS total ion chromatogram of isosafrole synthesised via Route 3B

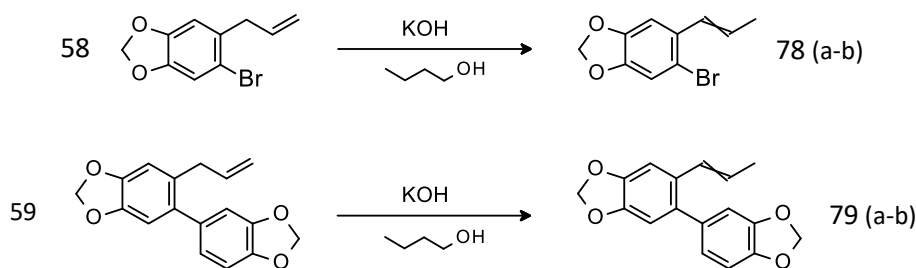
Table 5-3: Organic impurities identified in isosafrole synthesised via Route 1B, 2B and 3B

No.	Impurity Structure	Impurity Name	MW (g/mol)	m/z	Identified in isosafrole synthesised via Route:		
					1B	2B	3B
2		Safrole	162.2	162, 131, 119, 104/103, 91, 77, 63, 51, 44	✓	✓	✓
5		1,3-benzodioxole	122.1	122/121, 63	✓	✓	X
39		1,3-benzodioxole dimer	244.2	244, 135, 122/121, 63	✓	X	X
40		4,4'-, 4,5'- or 5,5'- methylenebis-1,3- benzodioxole	256.3	256, 225, 196, 168, 135, 77	✓	X	X
41		5-bromo-1,3- benzodioxole	201.0	202/200, 121, 63	✓	X	X
42		5,5'-bi-1,3- benzodioxole	242.2	242, 126, 121/120, 63	✓	X	X
47		1,3-benzodioxole trimer	366.4	366, 244, 135, 122/121	✓	X	X

No.	Impurity Structure	Impurity Name	MW (g/mol)	m/z	Identified in isosafrole synthesised via Route:		
					1B	2B	3B
61		1,2-diallyloxybenzene	190.2	190, 149, 121/119, 81, 52, 41	X	✓	X
65 (a-b)		4-prop-1-enyl-1,3-benzodioxole	162.2	162, 131, 119, 104/103, 91, 77, 63, 51	X	✓	X
68 (a-c)		4-[2-(<i>o</i> , <i>p</i> and <i>m</i> -tolyl)propyl]1,3-benzodioxole	254.3	254, 135, 119, 91, 77, 65, 51	X	X	✓
78 (a-b)		5-bromo-6-prop-1-enyl-1,3-benzodioxole	241.1	242/240, 131, 103, 77, 63, 51	✓	X	X
79 (a-b)		5-(1,3-benzodioxol-5-yl)-6-prop-1-enyl-1,3-benzodioxole	282.3	282, 267, 253, 237, 224 209, 165, 139, 115, 82, 63	✓	X	X
80 (a-b)		1,2-dipropoxybenzene	190.2	190, 149, 121, 109, 81, 63, 52, 41	X	✓	X
81 (a-b)		isosafrole dimer	324.4	324, 281, 253, 207, 162, 131, 115, 104/103, 91, 77	X	✓	✓

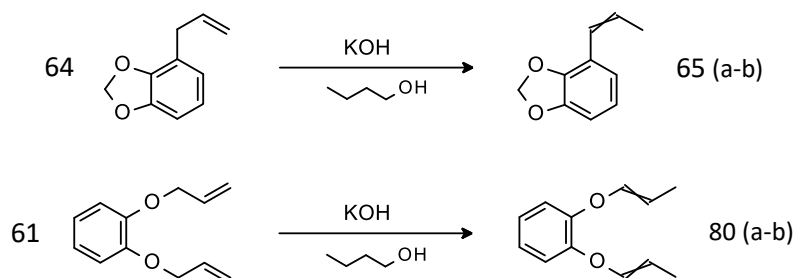
Organic impurity 2 was identified in isosafrole synthesised by Routes 1B, 2B and 3B and organic impurity 5 was identified in isosafrole synthesised by Routes 1B and 2B. Safrole (organic impurity 2) is the starting material for the isomerisation reaction, and its detection therefore indicated that this reaction did not proceed to completion in the three routes. Organic impurity 5 was identified in safrole synthesised by all three routes, and was carried over, unchanged, from the safrole in Routes 1B and 2B.

Organic impurities 39, 40, 41, 42, 47, 78 (a-b), and 79 (a-b) were identified in isosafrole synthesised by Route 1B. Organic impurities 39, 40, 41, 42, and 47 were identified in safrole synthesised by Route 1 and have been carried over, unchanged, in the isomerisation reaction. As shown in Scheme 5-14, the isomerisation of organic impurities 58 and 59, identified in safrole synthesised by Route 1, yielded organic impurities 78 (a-b), and 79 (a-b).



Scheme 5-14: Formation of organic impurities 78 and 79 in Route 1B

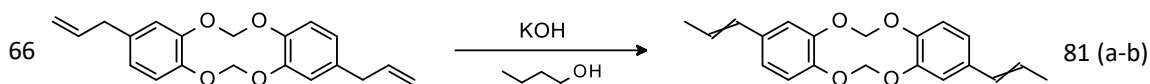
Organic impurities 61, 65 (a-b), and 80 (a-b) were identified in isosafrole synthesised by Route 2B. Organic impurities 61 and 65 (a-b) were identified in safrole synthesised by Route 2 and have been carried over in the isomerisation reaction. As shown in Scheme 5-15, a proportion of organic impurity 61 also underwent isomerisation to form organic impurities 80 (a-b). Organic impurities 65 (a-b) were also formed during the isomerisation reaction by the isomerisation of organic impurity 64, identified in safrole synthesised by Route 2.



Scheme 5-15: Formation of organic impurities 65 and 80 in Route 2B

Organic impurities 81 (a-b) were identified in isosafrole synthesised by Routes 2B and 3B, and organic impurities 68 (a-c) were identified in isosafrole synthesised by Route 3B. The

isomerisation of organic impurity 66, identified in safrole synthesised by both Routes 2 and 3, yielded organic impurities 81 (a-b) as shown in Scheme 5-16. Organic impurities 68 (a-c) were identified in safrole synthesised by Route 3, and were carried over, unchanged, in the isomerisation reaction.



Scheme 5-16: Formation of organic impurities 81 (a-b) in Route 2B and 3B

5.3.2.2 MDP2P from Isosafrole

The gas chromatogram in Figure 5-10 shows the nine organic impurities that were consistently identified in the MDP2P prepared by Route 1B. The gas chromatogram in Figure 5-11 shows the eleven organic impurities that were consistently identified in the MDP2P prepared by Route 2B. The gas chromatogram in Figure 5-12 shows the ten organic impurities that were consistently identified in the MDP2P prepared by Route 3B. The assigned numbers, chemical structures, names, molecular weights, and m/z data of the organic impurities identified in the MDP2P synthesised via Route 1B, 2B and 3B, and route in which they were identified, are shown in Table 5-4.

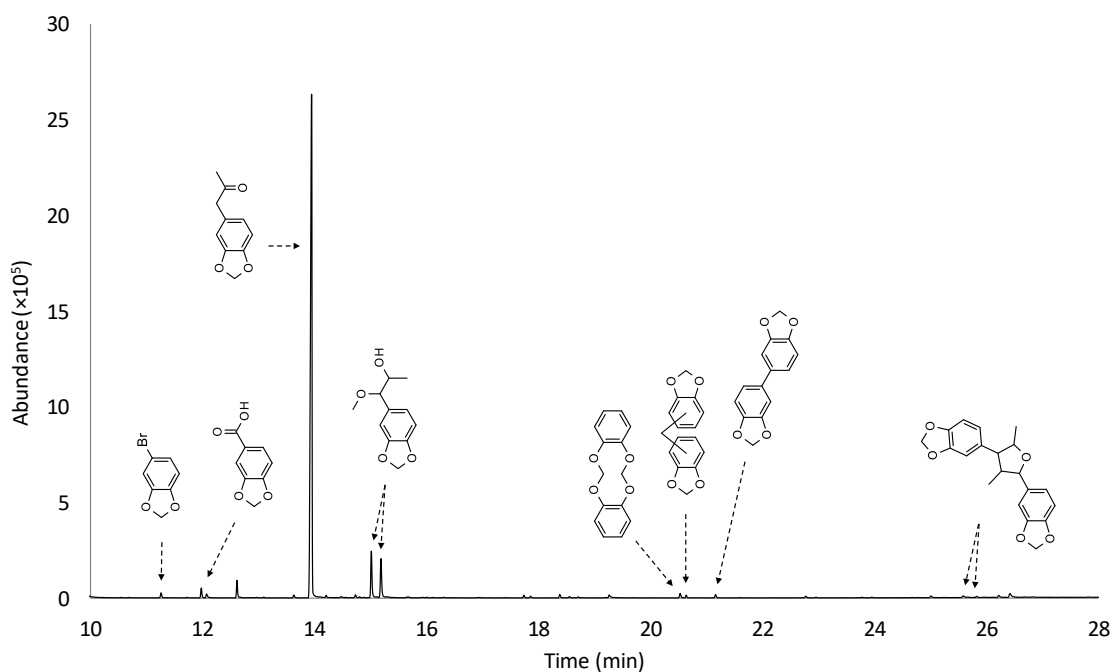


Figure 5-10: GC-MS total ion chromatogram of MDP2P synthesised via Route 1B

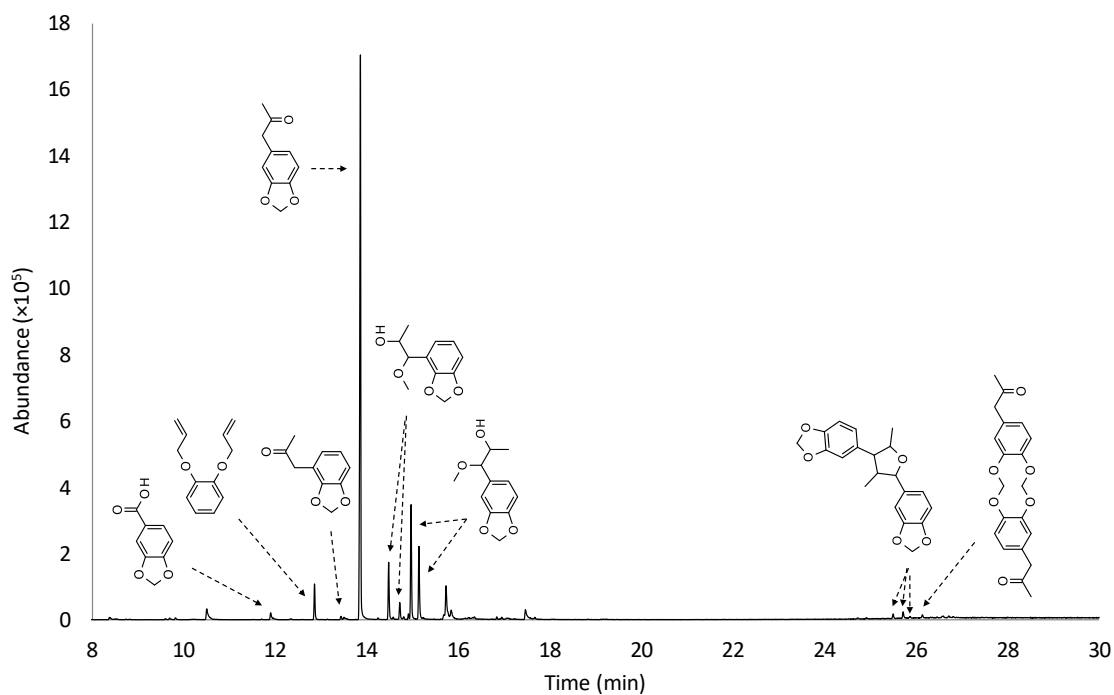


Figure 5-11: GC-MS total ion chromatogram of MDP2P synthesised via Route 2B

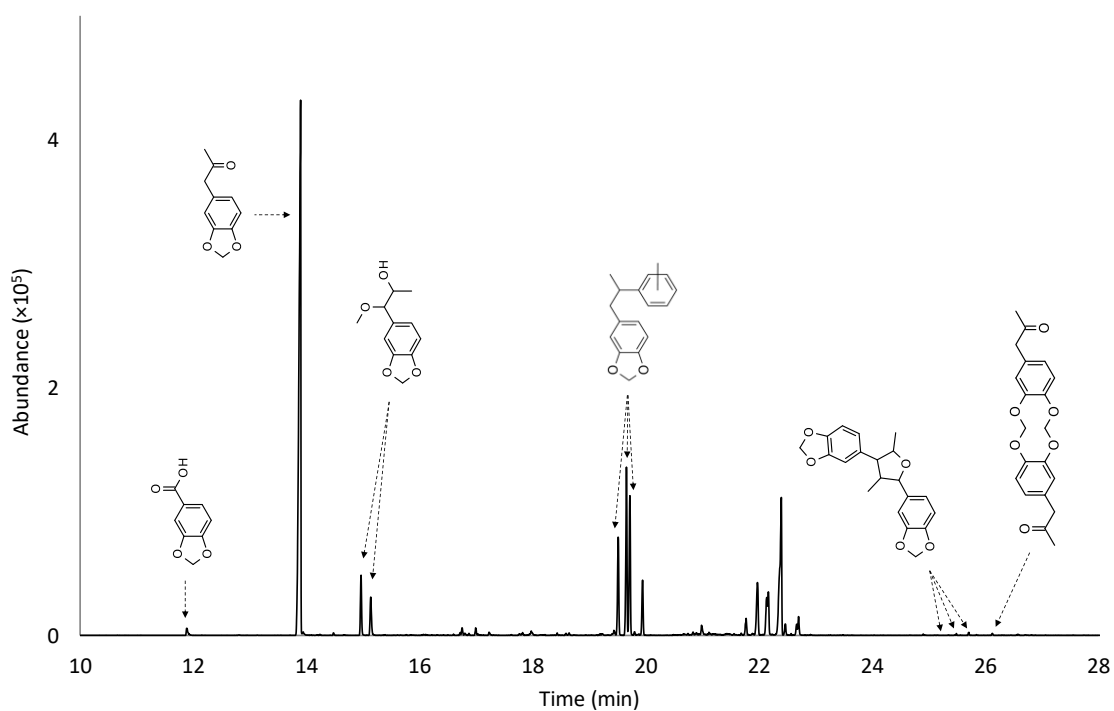
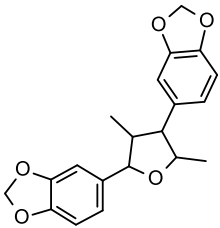
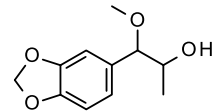
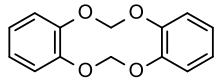
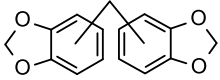
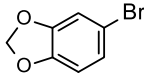
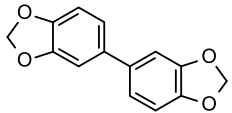
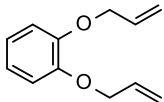
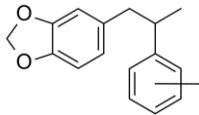
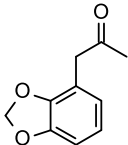
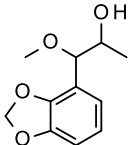
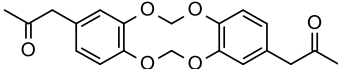
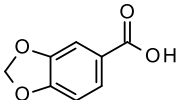


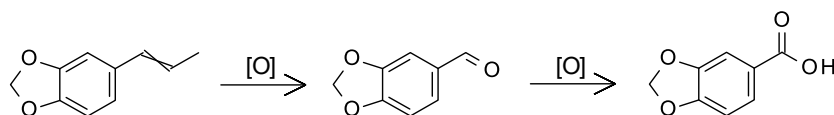
Figure 5-12: GC-MS total ion chromatogram of MDP2P synthesised via Route 3B

Table 5-4: Organic impurities identified in MDP2P synthesised via Route 1B, 2B and 3B

No.	Impurity Structure	Impurity Name	MW (g/mol)	m/z	Identified in MDP2P synthesised via Route:		
					1B	2B	3B
22 (a-c)		2,4-dimethyl-3,5-bis(3,4-methylenedioxyphenyl) tetrahydrofuran	340.2	340, 296, 281, 207, 44	✓	✓	✓
24 (a-b)		1-(1,3-benzodioxol-5-yl)-1-methoxy-propan-2-ol	210.2	210, 165, 150/149, 135, 77	✓	✓	✓
39		1,3-benzodioxole dimer	244.2	244, 135, 122/121, 63	✓	X	X
40		4,4'-, 4,5'- or 5,5'-methylenebis-1,3-benzodioxole	256.3	256, 225, 196, 168, 135, 77	✓	X	X
41		5-bromo-1,3-benzodioxole	201.0	202/200, 121, 63	✓	X	X
42		5,5'-bi-1,3-benzodioxole	242.2	242, 126, 121/120, 63	✓	X	X

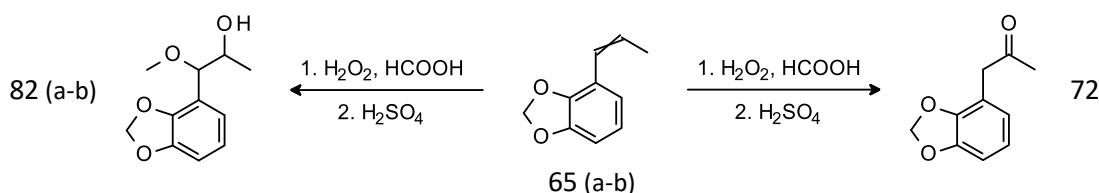
No.	Impurity Structure	Impurity Name	MW (g/mol)	m/z	Identified in MDP2P synthesised via Route:		
					1B	2B	3B
61		1,2-diallyloxybenzene	190.2	190, 149, 121/119, 81, 52, 41	X	✓	X
68 (a-c)		4-[2-(<i>o</i> , <i>p</i> and <i>m</i> -tolyl)propyl] 1,3-benzodioxole	254.3	254, 135, 119, 91, 77, 65, 51	X	X	✓
72		1-(1,3-benzodioxol-4-yl)propan-2-one	178.2	178, 135, 105, 77, 65, 51, 43	X	✓	X
82 (a-b)		1-(1,3-benzodioxol-4-yl)-1-methoxy-propan-2-ol	210.2	210, 165, 150/149, 135, 77	X	✓	X
83		MDP2P dimer	356.4	356, 341, 331, 281, 207, 162, 149, 131, 104/103, 91, 73, 43	X	✓	✓
84		1,3-benzodioxole-5-carboxylic acid	166.1	166, 150/149, 135, 121, 77	✓	✓	✓

Organic impurities 22 (a-c), 24 (a-b), and 84 were identified in MDP2P synthesised by Routes 1B, 2B and 3B. Organic impurities 22 (a-c) and 24 (a-b) are characteristic by-products of the peracid oxidation and acid dehydration of isosafrole [20]. Organic impurity 84 was synthesised by the oxidation of isosafrole, as shown in Scheme 5-17, during the peracid oxidation reaction.



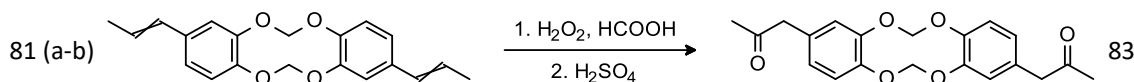
Scheme 5-17: Formation of organic impurity 84

Organic impurities 39, 40, 41, and 42 were identified in MDP2P synthesised by Route 1B, and organic impurities 61, 72, and 82 (a-b) were identified in MDP2P synthesised by Route 2B. Organic impurities 39, 40, 41, 42, and 61 were identified in both safrole and isosafrole in their respective routes, and were carried over, unchanged, in the peracid oxidation and acidic dehydration reaction. As shown in Scheme 5-14, the peracid oxidation and acidic dehydration of organic impurities 65 (a-b), identified in isosafrole synthesised by Route 2B, yielded organic impurity 72. A proportion of organic impurities 65 (a-b) also reacted to form organic impurities 82 (a-b), derivatives of known reaction by-products of the peracid oxidation and acidic dehydration reaction [20].



Scheme 5-18: Formation of organic impurities 72 and 82 (a-b) in Route 1B

Organic impurity 83 was identified in MDP2P synthesised by Routes 2B and 3B, and organic impurities 68 (a-c) were identified in MDP2P synthesised by Route 3B. As shown in Scheme 5-19, the peracid oxidation and acidic dehydration of organic impurities 81 (a-b), identified in isosafrole synthesised by Routes 2B and 3B, yielded organic impurity 83. Organic impurities 68 (a-c) were identified in both safrole synthesised by Route 3 and isosafrole synthesised by Route 3B, and were carried over, unchanged, in the peracid oxidation and acidic dehydration reaction.



Scheme 5-19: Formation of organic impurity 83 in Route 2B and 3B

5.3.2.3 MDMA from MDP2P

The gas chromatogram in Figure 5-13 shows the ten organic impurities that were consistently identified in the MDMA prepared by Route 1B. The gas chromatogram in Figure 5-14 shows the twelve organic impurities that were consistently identified in the MDMA prepared by Route 2B. The gas chromatogram in Figure 5-15 shows the eleven organic impurities that were consistently identified in the MDMA prepared by Route 3B. The assigned numbers, chemical structures, names, molecular weights, and m/z data of the organic impurities identified in the MDMA synthesised via Route 1B, 2B and 3B, and route in which they were identified, are shown in Table 5-5.

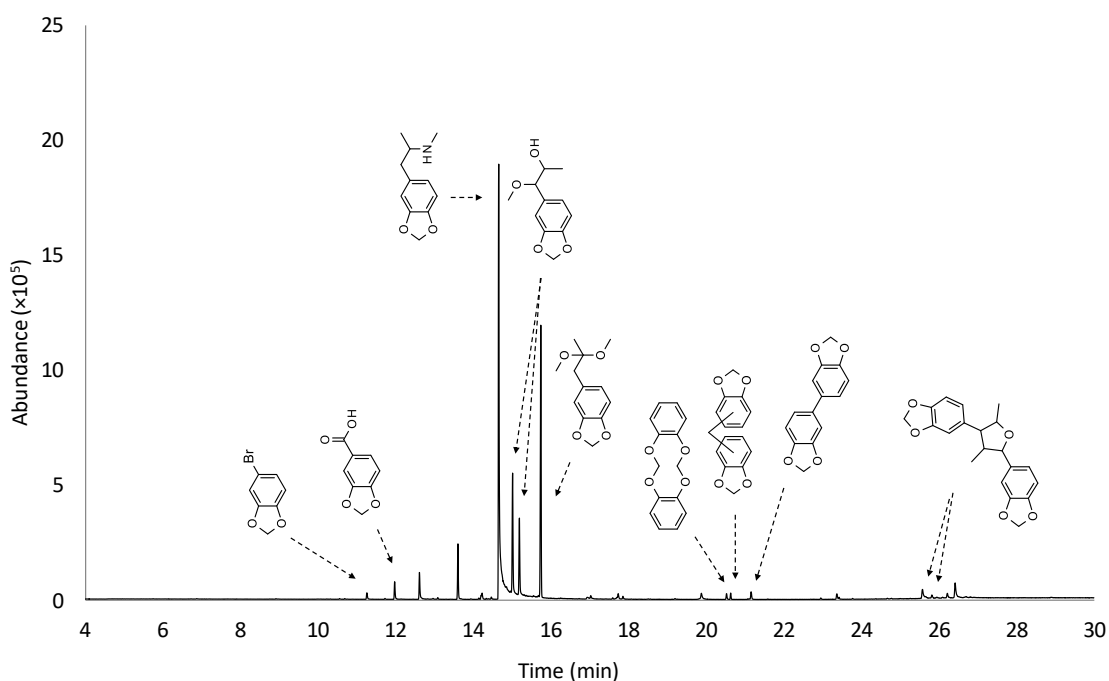


Figure 5-13: GC-MS total ion chromatogram of MDMA synthesised via Route 1B

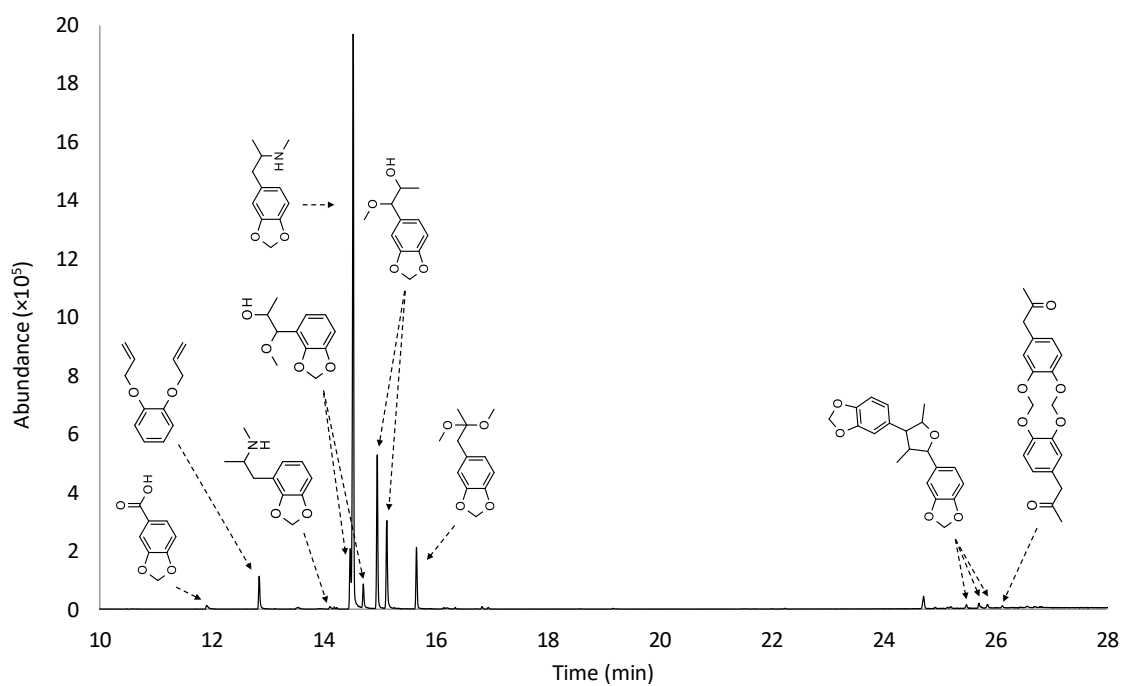


Figure 5-14: GC-MS total ion chromatogram of MDMA synthesised via Route 2B

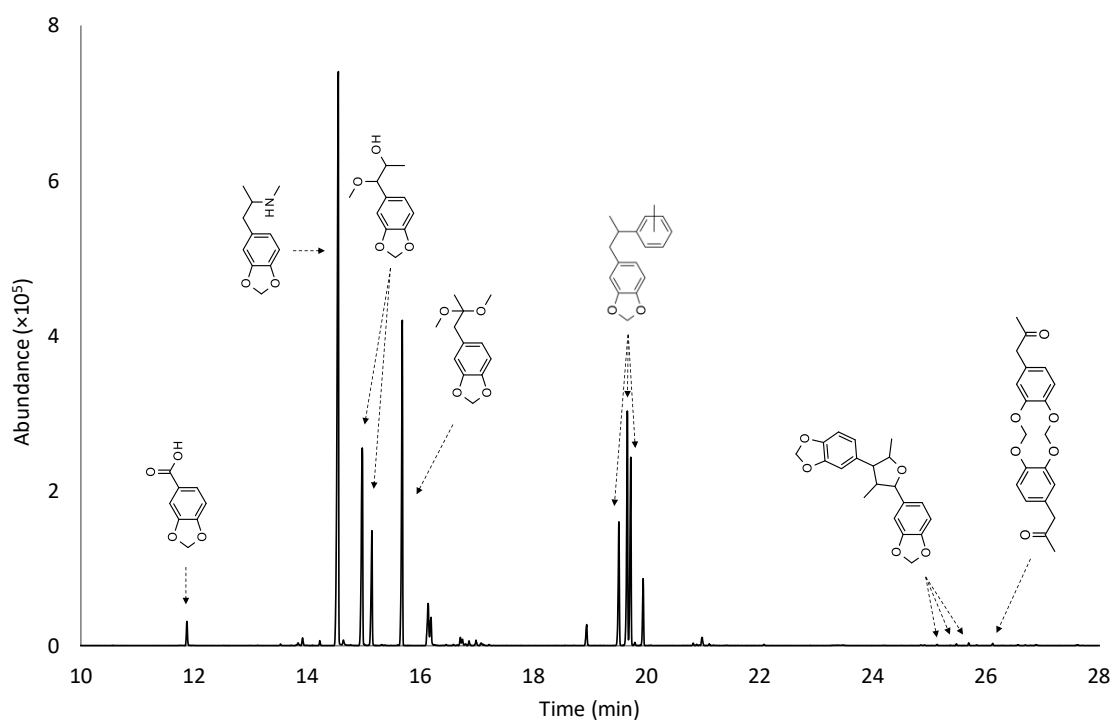
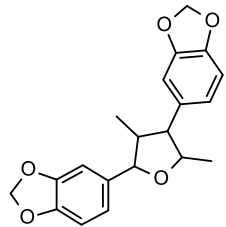
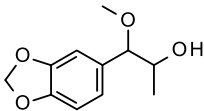
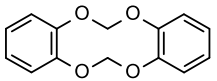

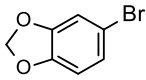
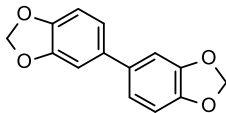
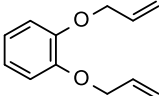
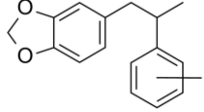
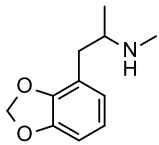
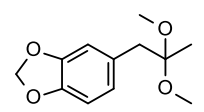
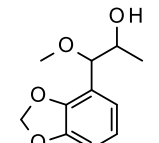
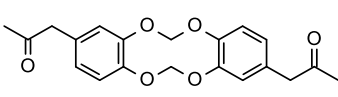
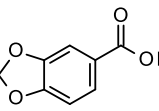


Figure 5-15: GC-MS total ion chromatogram of MDMA synthesised via Route 3B

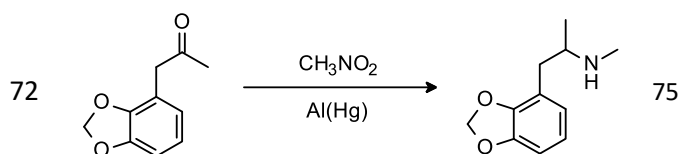
Table 5-5: Organic impurities identified in MDMA synthesised via Route 1B, 2B and 3B

No.	Impurity Structure	Impurity Name	MW (g/mol)	m/z	Identified in MDMA synthesised via Route:		
					1B	2B	3B
22 (a-c)		2,4-dimethyl-3,5-bis(3,4-methylenedioxyphenyl) tetrahydrofuran	340.4	340, 296, 281, 207, 44	✓	✓	✓
24 (a-b)		1-(1,3-benzodioxol-5-yl)-1-methoxy-propan-2-ol	210.2	210, 165, 150/149, 135, 77	✓	✓	✓
39		1,3-benzodioxole dimer	244.2	244, 135, 122/121, 63	✓	X	X
40 (a-c)		4,4', 4,5' - or 5,5' - methylenebis-1,3-benzodioxole	256.3	256, 225, 196, 168, 135, 77	✓	X	X
41		5-bromo-1,3-benzodioxole	201.0	202/200, 121, 63	✓	X	X
42		5,5'-bi-1,3-benzodioxole	242.2	242, 126, 121/120, 63	✓	X	X

No.	Impurity Structure	Impurity Name	MW (g/mol)	m/z	Identified in MDMA synthesised via Route:		
					1B	2B	3B
61		1,2-diallyloxybenzene	190.2	190, 149, 121/119, 81, 52, 41	X	✓	X
68 (a-c)		4-[2-(<i>o</i> , <i>p</i> and <i>m</i> -tolyl)propyl] 1,3-benzodioxole	254.3	254, 135, 119, 91, 77, 65, 51	X	X	✓
75		1-(1,3-benzodioxol-4-yl)-N-methyl-propan-2-amine	193.2	192, 178, 151, 135, 105, 93, 77, 58, 51	X	✓	X
77		MDP2P dimethyl acetal	224.3	224, 193, 135, 89	✓	✓	✓
82 (a-b)		1-(1,3-benzodioxol-4-yl)-1-methoxy-propan-2-ol	210.2	210, 165, 150/149, 135, 77	X	✓	X
83		MDP2P dimer	356.4	356, 341, 331, 281, 207, 162, 149, 131, 104/103, 91, 73, 43	X	✓	✓
84		1,3-benzodioxole-5-carboxylic acid	166.1	166, 150/149, 135, 121, 77	✓	✓	✓

Organic impurities 22 (a-c), 24 (a-b), 77, and 84 were identified in MDMA synthesised by Routes 1B, 2B and 3B. Organic impurities 22 (a-c), 24 (a-b), and 84 were reaction by-products of the peracid oxidation and acidic dehydration reaction to form MDP2P, and in all three routes were carried over, unchanged, in the reductive amination reaction. Organic impurity 77 is a characteristic by-product of the reductive amination of MDP2P in methanol solvent [31].

Organic impurities 39, 40, 41, and 42 were identified in MDMA synthesised by Route 1B, and organic impurities 61, 75, and 82 (a-b) were identified in MDMA synthesised by Route 2B. Organic impurities 39, 40, 41, 42, 61, and 82 (a-b) were identified in MDP2P in their respective routes and were carried over, unchanged, in the reductive amination reaction. As shown in Scheme 5-20, the reductive amination of organic impurity 72, identified in MDP2P synthesised by Route 2B, yielded organic impurity 75.



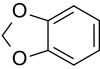
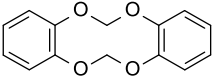
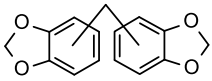
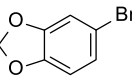
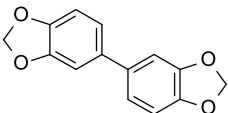
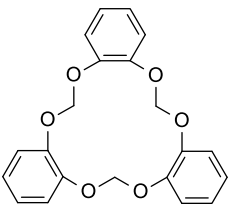
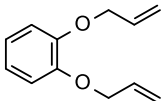
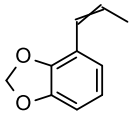
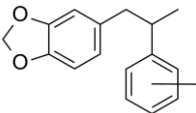
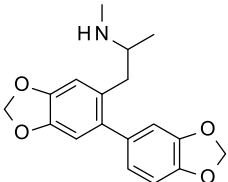
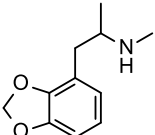
Scheme 5-20: Formation of organic impurity 75 in Route 2B

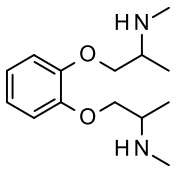
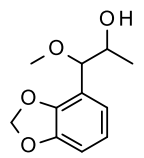
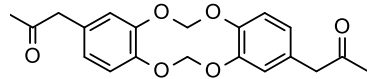
Organic impurity 83 was identified in MDMA synthesised by Routes 2B and 3B, and organic impurities 68 (a-c) were identified in MDMA synthesised by Route 3B. Organic impurities 68 (a-c) and 83 were identified in MDP2P in their respective routes and were carried over, unchanged, in the reductive amination reaction.

5.4 Route Specific Organic Impurities

The organic impurities identified in the catechol-derived MDMA from Routes 1A, 1B, 2A, and 2B and eugenol-derived MDMA from Routes 3A and 3B that resulted from the use of the relevant ‘pre-precursor’ are listed in Table 5-6. Route specific impurities were identified by comparing the organic impurity profiles of MDMA synthesised via the six synthetic routes, and the literature organic impurity profiles MDMA.

Table 5-6: Organic impurities identified in MDMA that result from use of the 'pre-precursors' catechol and eugenol

No.	Impurity	Identified is MDMA synthesised via Route:					
		1A	1B	2A	2B	3A	3B
5		✓	X	✓	X	✓	X
39		✓	✓	X	X	X	X
40		✓	✓	X	X	X	X
41		✓	✓	X	X	X	X
42		✓	✓	X	X	X	X
47		✓	X	X	X	X	X
61		X	X	X	✓	X	X
65 (a-b)		X	X	✓	X	X	X
68 (a-c)		X	X	X	X	✓	✓
74		✓	X	X	X	X	X
75		X	X	✓	✓	X	X

No.	Impurity	Identified in MDMA synthesised via Route:					
		1A	1B	2A	2B	3A	3B
76		X	X	✓	X	X	X
82 (a-b)		X	X	X	✓	X	X
83		X	X	X	✓	X	✓

Organic impurities 39, 40, 41, and 42 were identified in MDMA prepared by Routes 1A and 1B, and organic impurities 47 and 74 were only detected in MDMA prepared by Route 1A. Organic impurities 39, 40, 41, and 42 (but not 47 nor 74) have previously been identified in catechol-derived MDMA that was prepared by an equivalent synthetic pathway to Route 1B [35]. However, these organic impurities have not been identified in MDMA prepared from any other precursor or by any other synthetic route [17, 19-21, 23, 24, 31, 41, 54, 61, 62]. While organic impurities 47 and 74 were not identified in MDMA synthesised by Route 1B, they could feasibly be detected if alternate synthetic or purification conditions were used or if MDMA was analysed by a more sensitive GC-MS or LC-MS/MS technique. Thus, organic impurities 39, 40, 41, 42, 47, and 74 are specific to the synthesis of MDMA from synthetic, catechol-derived safrole prepared via Route 1.

Organic impurities 39, 40, and 47 are characteristic by-products of the methylenation of catechol, and the detection of any of these impurities in MDMA therefore indicates that catechol was used as a 'pre-precursor'. Organic impurity 41 is an intermediate in the synthesis of safrole from catechol by Route 1, and its detection is therefore indicative of the bromination reaction. The Grignard reaction can be inferred from the detection of organic impurity 42, which is a characteristic by-product formed when the Grignard reagent is prepared from 5-bromo-1,3-benzodioxole. Impurity 74 is the subsequent reaction product of both a bromination and Grignard reaction by-product, and its detection in MDMA is indicative of safrole prepared via Route 1. As such, the use of the 'pre-precursor' catechol and synthetic Route 1 could be ascertained from the organic impurity profiling of MDMA under the conditions used here.

Organic impurities 61 and 76, detected in MDMA prepared by Routes 2A and 2B respectively, are characteristic by-products of the etherification of catechol. Their detection in MDMA therefore indicates that catechol was used as a 'pre-precursor'. Organic impurities 65 (a-b), 75, and 82 (a-b) are subsequent reaction products of a characteristic Claisen rearrangement by-product, and their detection in MDMA is indicative of safrole prepared via Route 2. Organic impurities 65 (a-b) and 75 were detected in MDMA prepared by Route 2A and organic impurities 75 and 82 (a-b) were detected in MDMA prepared by Route 2B. Thus, the use of the 'pre-precursor' catechol and synthetic Route 2 could be ascertained from the organic impurity profiling of MDMA under the conditions used here.

Organic impurities 61, 65 (a-b), 75, 76, and 82 (a-b) have not previously been identified in MDMA [17, 19-21, 23, 24, 31, 35, 41, 54, 61, 62] and are specific to the synthesis of MDMA from synthetic, catechol-derived safrole prepared via Route 2. While organic impurity 61 was not identified in MDMA from Route 1A and organic impurities 65 (a-b) and 76 were not identified in MDMA from Route 1B, they could feasibly be detected if alternate synthetic or purification conditions were used or if MDMA was analysed by a more sensitive GC-MS or LC-MS/MS technique. Conversely, organic impurities 82 (a-b) are peracid oxidation and acidic dehydration by-products of a Claisen rearrangement by-product, and therefore are route specific for the synthesis of MDMA from catechol by Route 1B.

Organic impurities 68 (a-c) were identified in MDMA prepared by Routes 3A and 3B and have not previously been identified in MDMA [17, 19-21, 23, 24, 31, 35, 41, 54, 61, 62]. Thus, organic impurities 68 (a-c) are specific to the synthesis of MDMA from synthetic, eugenol-derived safrole prepared via Route 3. Organic impurities 68 (a-c) resulted from a reaction by-product of the demethylation of eugenol, and therefore the use of the 'pre-precursor' eugenol and synthetic Route 3 could be ascertained by the organic impurity profiling of MDMA under the conditions used here. However, organic impurities 68 (a-c) would likely not be detected if alternate reagents and/or solvents were used in the preparation of safrole from eugenol.

Organic impurity 5 was identified in MDMA synthesised via Routes 1A, 2A and 3A, and organic impurity 83 was identified in MDMA synthesised via Routes 2B and 3B. Organic impurity 5 has previously been identified in MDMA prepared by multiple routes [17, 21, 62] and its detection in MDMA therefore has little to no discriminatory value. A dimer of MDMA has previously been identified as an impurity in MDMA synthesised from vanillin, and the MDP2P dimer (organic impurity 83) was an intermediate in its formation [31]. It is unclear why organic impurity 83 did not undergo reductive amination in this work to form the MDMA dimer. The detection of organic

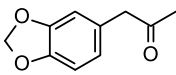
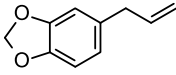
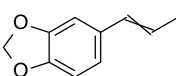
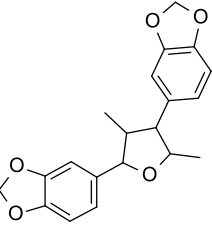
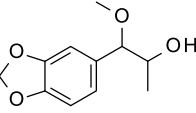
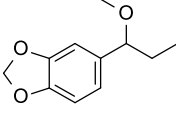
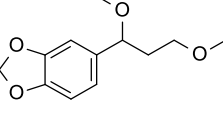
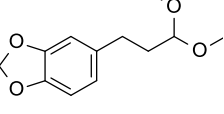
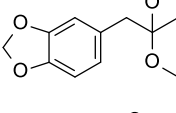
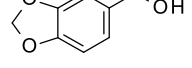
impurity 83 in MDMA indicates that either synthetic safrole or piperonal were used but does not identify a specific 'pre-precursor'.

Organic impurities were also identified in MDMA that resulted from its preparation via safrole, a traditional MDMA precursor. The organic impurities identified in the catechol-derived MDMA from Routes 1A, 1B, 2A, and 2B and eugenol-derived MDMA from Routes 3A and 3B that resulted from synthesis from safrole are listed in Table 5-7. The formation of these organic impurities in MDMA under the conditions used here was not related to the use of the 'pre-precursors' catechol or eugenol. Route specific impurities were identified by comparing the organic impurity profiles of MDMA synthesised via the six synthetic routes, and the literature organic impurity profiles MDMA.

Organic impurities 26, 28, and 29, detected in MDMA prepared by Routes 1A, 2A and 3A, are specific to the synthesis of MDMA from safrole by Route A as they are characteristic by-products of the Wacker oxidation of safrole in methanol solvent [19]. Organic impurities 22 (a-c) and 24 (a-b), detected in MDMA prepared by Route 1B, 2B and 3B, are specific to the synthesis of MDMA from isosafrole by Route B as they are characteristic by-products of the peracid oxidation and acid dehydration of isosafrole [20]. Therefore, the synthesis of MDMA from safrole via Route A or Route B could be determined based on the organic impurity profiling of MDMA under the conditions used here.

Organic impurity 77, detected in all routes, is characteristic of the reductive amination of MDP2P in methanol solvent [31]. Organic impurities 1, 2, and 3 (a-b) are traditional MDMA precursors and organic impurity 84 arises from the oxidation of isosafrole (3 (a-b)). Traditional MDMA precursors detected in MDMA could have resulted from an impurity in a precursor, a reaction by-product, an intermediate, or a precursor in a synthetic route [21, 24]. The detection of organic impurities 1, 2, 3 (a-b), 77, and/or 84 in MDMA therefore has little to no discriminatory value, as they can be detected in MDMA prepared by multiple synthetic pathways [17, 24, 31].

Table 5-7: Organic Impurities identified in MDMA that result from synthesis from safrole

No.	Impurity	Identified is MDMA synthesised via Route:					
		1A	1B	2A	2B	3A	3B
1		X	X	✓	X	X	X
2		X	X	X	X	✓	X
3 (a-b)		✓	X	✓	X	✓	X
22 (a-c)		X	✓	X	✓	X	✓
24 (a-b)		X	✓	X	✓	X	✓
26		✓	X	✓	X	✓	X
28		✓	X	✓	X	✓	X
29		✓	X	✓	X	✓	X
77		✓	✓	✓	✓	✓	✓
84		X	✓	X	✓	X	✓

5.5 Conclusions

MDMA was synthesised from synthetic safrole via Route A in two steps: the Wacker oxidation of safrole and the reductive amination of MDP2P. MDMA was synthesised from synthetic safrole via Route B in three steps: the isomerisation of safrole, the peracid oxidation and acidic dehydration of isosafrole, and the reductive amination of MDP2P. The synthetic safrole utilised had been prepared from the 'pre-precursor' catechol via Routes 1 and 2 and the 'pre-precursor' eugenol via Route 3. Thus, MDMA was synthesised from 'pre-precursors' by six synthetic routes; four from catechol (Routes 1A, 1B, 2A and 2B) and two from eugenol (Routes 3A and 3B).

The products of each step in the synthetic routes were analysed by GC-MS and ^1H NMR spectroscopy, and a number of detected organic impurities were identified. Thirteen organic impurities were identified in MDMA prepared by Route 1A and ten organic impurities were identified in MDMA prepared by Route 1B; respectively, seven and four of the impurities identified resulted from use of the catechol 'pre-precursor'. Twelve organic impurities were identified in MDMA prepared by both Routes 2A and 2B; respectively, five and four of the impurities identified resulted from use of the catechol 'pre-precursor'. Eleven organic impurities were identified in MDMA prepared by both Routes 3A and 3B; four of the impurities identified in each route resulted from use of the eugenol 'pre-precursor'. Importantly, thirteen organic impurities (47, 61, 65 (a-b), 68 (a-c), 74, 75, 76, 82 (a-b), and 83) were identified in MDMA that have not previously been reported.

Route specific organic impurities were identified in MDMA that indicated the 'pre-precursors' catechol and eugenol were used in the respective synthetic routes. Route specific organic impurities were also identified that indicated the route used to synthesise MDMA from the safrole intermediate, and the route used to synthesise safrole from the respective 'pre-precursor'. Thus, the use of the 'pre-precursors' catechol and eugenol and the synthetic routes that were used in its preparation could be ascertained by the organic impurity profiling of MDMA under the conditions used here.

Chapter 6: Conclusions and Future Research Recommendations

Chapter 6: Conclusions and Future Research Recommendations

The use of uncontrolled 'pre-precursors' has gained popularity with clandestine laboratory operators for the synthesis of ATS [6], however, there has been limited research into the chemical profiles of MDMA and analogues synthesised from 'pre-precursors'. Law enforcement agencies require ongoing, relevant research to adapt to the changing manufacturing techniques in the illicit drug market [50]. Therefore, the work presented in this thesis examined the organic impurity profiles of methylone, safrole and MDMA that were synthesised from the 'pre-precursors' catechol and eugenol.

Methylone, safrole and MDMA were synthesised from 'pre-precursors' using synthetic methods that were feasible in a reasonably equipped clandestine laboratory. Methylone was synthesised from the 'pre-precursor' catechol via a four-step synthetic route that involved the methylenation of catechol, Friedel-Crafts acylation of 1,3-benzodioxole, the bromination of 3,4-methylenedioxypropiophenone and the nucleophilic substitution of 5-bromo-3,4-methylenedioxypropiophenone with methylamine.

Safrole was synthesised from the 'pre-precursor' catechol via two three-step synthetic routes (Routes 1 and 2), and from the 'pre-precursor' eugenol via a two-step synthetic route (Route 3). These synthetic routes involved the following reactions:

- Route 1 - The methylenation of catechol, the bromination of 1,3-benzodioxole and a Grignard reaction using 5-bromo-1,3-benzodioxole and allyl bromide.
- Route 2 - The etherification of catechol, the Claisen rearrangement of 2-allyloxyphenol, and the methylenation of 4-allylcatechol.
- Route 3 - The demethylation of eugenol, and the methylenation of 4-allylcatechol.

MDMA was then synthesised from the synthetic safrole via a two-step synthetic route (Route A) and a three-step synthetic route (Route B). These routes involved the following reactions:

- Route A - The Wacker oxidation of safrole and the reductive amination of MDP2P.
- Route B - The isomerisation of safrole, the peracid oxidation and acidic dehydration of isosafrole, and the reductive amination of MDP2P.

Thus, MDMA was synthesised from 'pre-precursors' by a total of six synthetic routes: four from the 'pre-precursor' catechol (Routes 1A, 1B, 2A and 2B) and two from the 'pre-precursor' eugenol (Routes 3A and 3B).

Importantly, future research into the use of 'pre-precursors' to manufacture MDMA and analogues should utilise intelligence current at the time, due to the consistently changing

manufacturing techniques used in the illicit drug market. Further research into the use of the 'pre-precursor' catechol could investigate the synthesis of MDMA from catechol via a piperonal intermediate [16, 33]. However, the organic impurity profiles of piperonal prepared from catechol would need to be compared to a wide array of commercially obtained piperonal in order to ascertain the significance of the identified organic impurities. This is because piperonal is industrially synthesised from catechol [16], and therefore MDMA prepared from diverted commercial piperonal may also feasibly contain these catechol-related impurities.

In the synthesis of methylone from catechol, the organic impurity profiles of the reaction products of each step in the synthetic route were analysed. Six organic impurities (39, 40 (a-c), 46 and 47) were identified in 1,3-benzodioxole, six organic impurities (48, 49, 50, 51 and 52 (a-b)) were identified in 3,4-methylenedioxypropiophenone, four organic impurities (23, 48, 50 and 53) were identified in 5-bromo-3,4-methylenedioxypropiophenone and five organic impurities (23, 43, 54, 55 and 56) were identified in methylone.

An important issue identified by the organic impurity profiling of methylone was that neither the catechol 'pre-precursor' or the 1,3-benzodioxole intermediate could be identified by the techniques used here. Some characteristic impurities were identified in intermediate compounds but these characteristic impurities (or their reaction products) were not detected in methylone, even though relatively unsophisticated purification techniques were used. While recent research indicates that the analysis of organic impurities alone can provide sufficient information for intelligence purposes [51], the inability to determine the precursor or synthetic pathway used through analysis of the methylone organic impurity profile demonstrated a significant limitation with the standard techniques used here.

Future research into the chemical profiling of high purity ATS (including MDMA analogues) should therefore focus on sensitive organic impurity profiling techniques, and the analysis of isotope ratios. It is feasible that route specific impurities, not identified by the techniques used here, could have been detected if more sensitive GC-MS technique or LC-MS/MS was used to analyse methylone. Additionally, unlike with the analysis of impurity profiles, all synthetic drugs contain a ratio of isotopes, which is dependent on the starting materials and synthetic pathway used. While piperonal is industrially synthesised from catechol [16], methylone prepared from piperonal or from catechol via 1,3-benzodioxole would likely have varied isotope ratios due to the different production processes used. Therefore, high purity ATS with a common source could be identified, or high purity ATS that do not have a common source could be differentiated, through the analysis of isotope ratios using IRMS.

In the synthesis of safrole from catechol via Routes 1 and 2, and from eugenol via Route 3, the organic impurity profiles of the reaction products from each step in the synthetic routes were analysed. Importantly, nine organic impurities (59, 61, 64, 65 (a-b), 66, and 68 (a-c)) were identified in safrole synthesised from 'pre-precursors' that have not previously been reported in literature. The following organic impurities were identified in synthetic safrole:

- Route 1 - Eight organic impurities (5, 39, 40, 41, 42, 47, 58, and 59) were identified; seven (39, 40, 41, 42, 47, 58, and 59) of which were route specific.
- Route 2 - Eight organic impurities (3 (a-b), 5, and 66) were identified; four (61, 64, 65 (a-b)) of which were route specific.
- Route 3 - Seven organic impurities (3 (a-b), 5, 66, 68 (a-c)) were identified; three (68 (a-c)) of which were route specific.

The route specific organic impurities that were identified in safrole indicated both the use of the 'pre-precursors' catechol and eugenol, and the route that was used to synthesise safrole from the respective 'pre-precursor'. Thus, the use of the 'pre-precursors' catechol and eugenol, and respective routes used to synthesise safrole, could be ascertained by the organic impurity profiling of safrole under the conditions used here.

Further research into the chemical profiling of safrole could also investigate isotope ratio analysis. The ratio of isotopes of natural safrole from sassafras oil is dependent on biochemical and environmental factors, whereas the ratio of isotopes in synthetic safrole is dependent on starting materials and synthetic pathway utilised. Therefore, isotope ratio analysis could differentiate synthetic safrole from 'pre-precursors' and natural safrole from sassafras oil. While synthetic safrole could be identified by organic impurity profiling techniques in this work, the use of isotope ratio analysis would be advantageous for the analysis of high purity safrole, or subsequent MDMA, prepared in an industrial scale clandestine laboratory.

The organic impurity profiles of the reaction products from each step in the synthesis of MDMA were also analysed. Importantly, thirteen organic impurities (47, 61, 65 (a-b), 68 (a-c), 74, 75, 76, 82 (a-b), and 83) were identified in MDMA synthesised from 'pre-precursors' that have not previously been reported in literature. The following organic impurities were identified in MDMA prepared from catechol via Routes 1A, 1B, 2A and 2B, and from eugenol via Route 3A and 3B:

- Route 1A - Thirteen (3 (a-b), 5, 26, 28, 29, 39, 40, 41, 42, 47, 74, and 77) organic impurities were identified; six (39, 40, 41, 42, 47, and 74) of which were specific to the use of catechol-derived safrole prepared via Route 1.

- Route 1B - Ten (22 (a-b), 24 (a-b), 39, 40, 41, 42, 77, and 84) organic impurities were identified; four (39, 40, 41, and 42) of which were specific to the use of catechol-derived safrole prepared via Route 1.
- Route 2A - Twelve (1, 3 (a-b), 5, 26, 28, 29, 65 (a-b), 75, and 76 and 77) organic impurities were identified; four (65 (a-b), 75, and 76) of which were specific to the use of catechol-derived safrole prepared via Route 2.
- Route 2B - Twelve (22 (a-c), 24 (a-b), 61, 75, 77, 82 (a-b), 83, and 84) organic impurities were identified; four (61, 75, and 82 (a-b)) of which were specific to the use of catechol-derived safrole prepared via Route 2.
- Route 3A - Eleven (2 and 3 (a-b), 5, 26, 28, 29, 68 (a-c), and 77) organic impurities were identified; three (68 (a-c)) of which were specific to the use of eugenol-derived safrole prepared via Route 3.
- Route 3B - Eleven (22 (a-c), 24 (a-b), 68 (a-c), 77, 83, and 84) organic impurities were identified; three (68 (a-c)) of which were specific to the use of eugenol-derived safrole prepared via Route 3.

The route specific organic impurities that were identified in MDMA indicated that the ‘pre-precursors’ catechol and eugenol were used in the respective synthetic pathways. The route specific organic impurities that were identified in MDMA also indicated the route used to synthesise safrole from the respective ‘pre-precursor’, and the route used to synthesise MDMA from the safrole intermediate. Thus, the use of the ‘pre-precursors’ catechol and eugenol, and the synthetic routes that were used in its preparation, could be ascertained by the organic impurity profiling of MDMA under the conditions used here.

This work focused on analysis and identification of organic impurities that could be detected in MDMA that has been synthesised from the ‘pre-precursors’ catechol and eugenol. Further research should ascertain which organic impurities are most likely to be detected in seized MDMA that has been manufactured by these methodologies. This would involve numerous repeat syntheses with systematic variations to reaction conditions, reaction scale, and reagent purities, in order to determine the effect on the resulting organic impurity profile of MDMA. The conversion of MDMA into the corresponding salt, and subsequent extraction of MDMA base for analysis, using the methodologies most common in laboratories would also indicate the persistence of the identified organic impurities. Additionally, further research could involve the analysis of seized MDMA samples to determine whether any identified organic impurities are detected.

Overall, MDMA was synthesised from the 'pre-precursors' catechol and eugenol, and the analogue methylone was synthesised from the 'pre-precursor' catechol, via synthetic routes that are viable in reasonably equipped clandestine laboratories. Organic impurities were identified in the reaction products of each step in the synthetic routes that were investigated. The origin of these organic impurities was also ascertained, which provided valuable insights into the chemical profiles of safrole, MDMA, methylone, and the intermediate compounds. Neither the use of the catechol precursor nor the 1,3-benzodioxole intermediate could be ascertained based on the organic impurities identified in methylone, which demonstrated the limitations of organic impurity profiling using standard techniques. Conversely, under the conditions used here, route specific organic impurities were identified in safrole and MDMA prepared by all routes which indicated both that the respective 'pre-precursors' catechol and eugenol were used, and the synthetic pathways that were utilised.

Appendices

Appendix 1: Mass Spectra

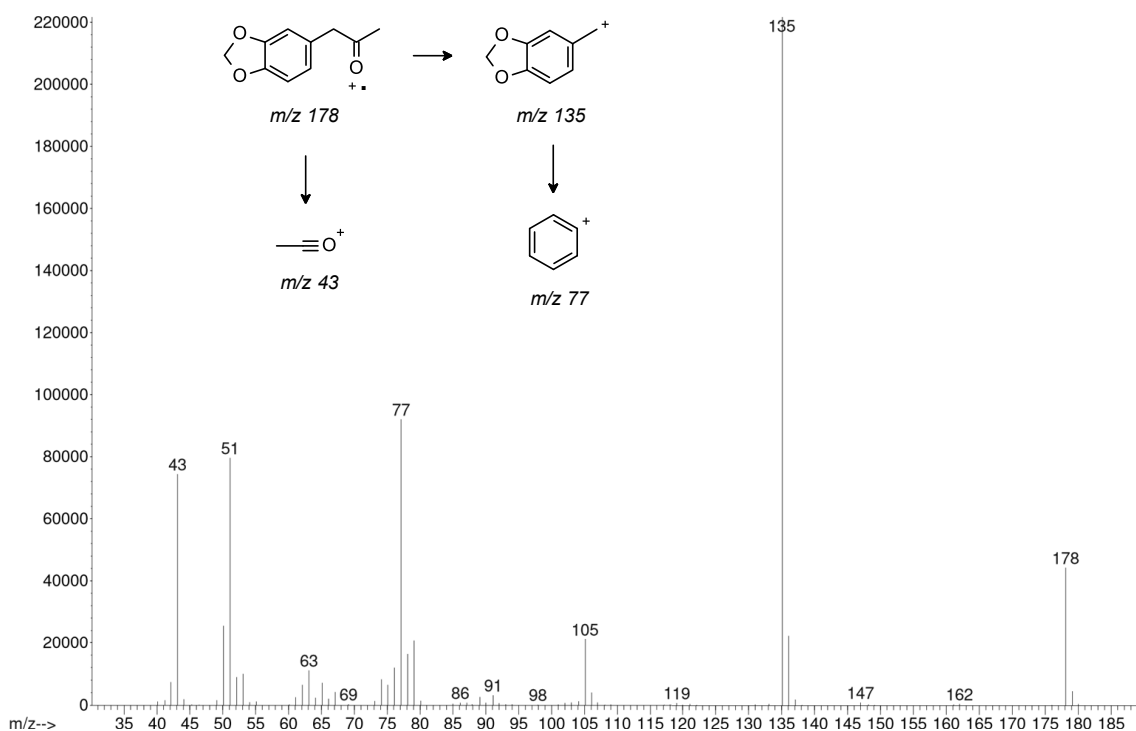


Figure A1-1: Mass spectrum and proposed fragmentation scheme of MDP2P (organic impurity 1)

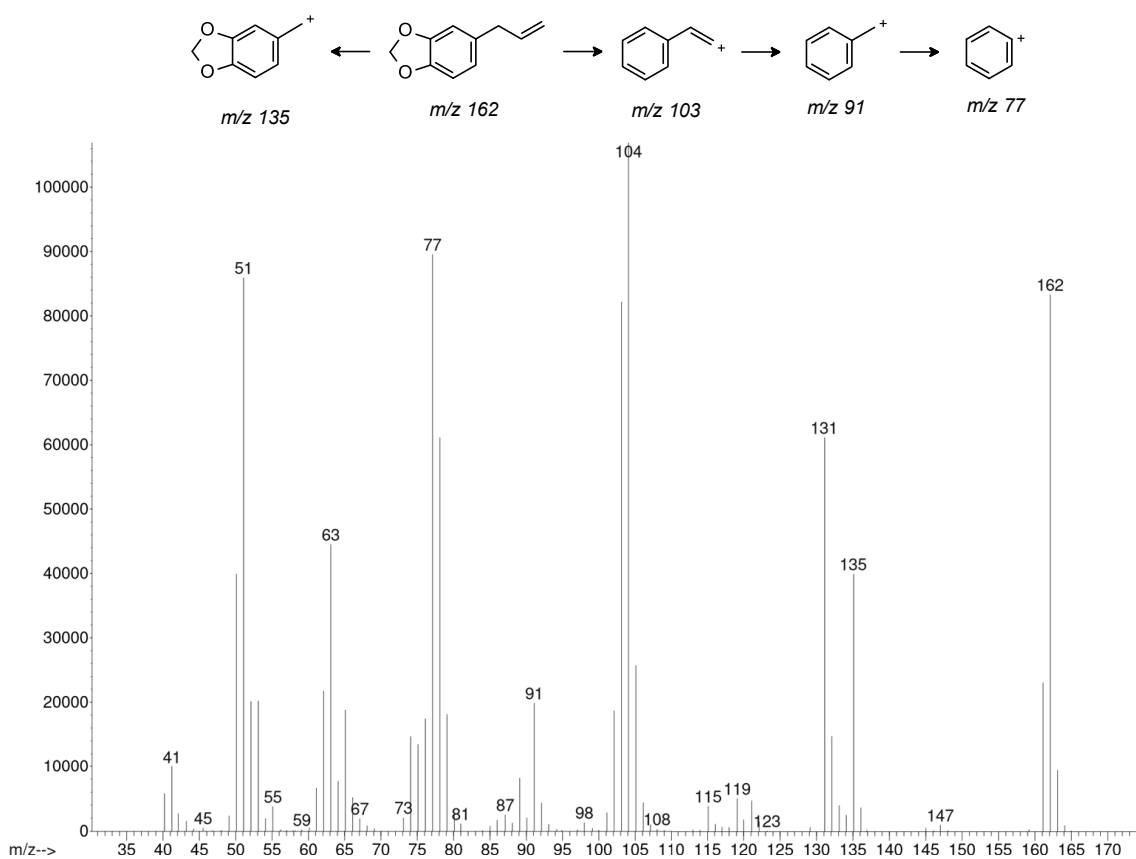


Figure A1-2: Mass spectrum and proposed fragmentation scheme of safrole (organic impurity 2)

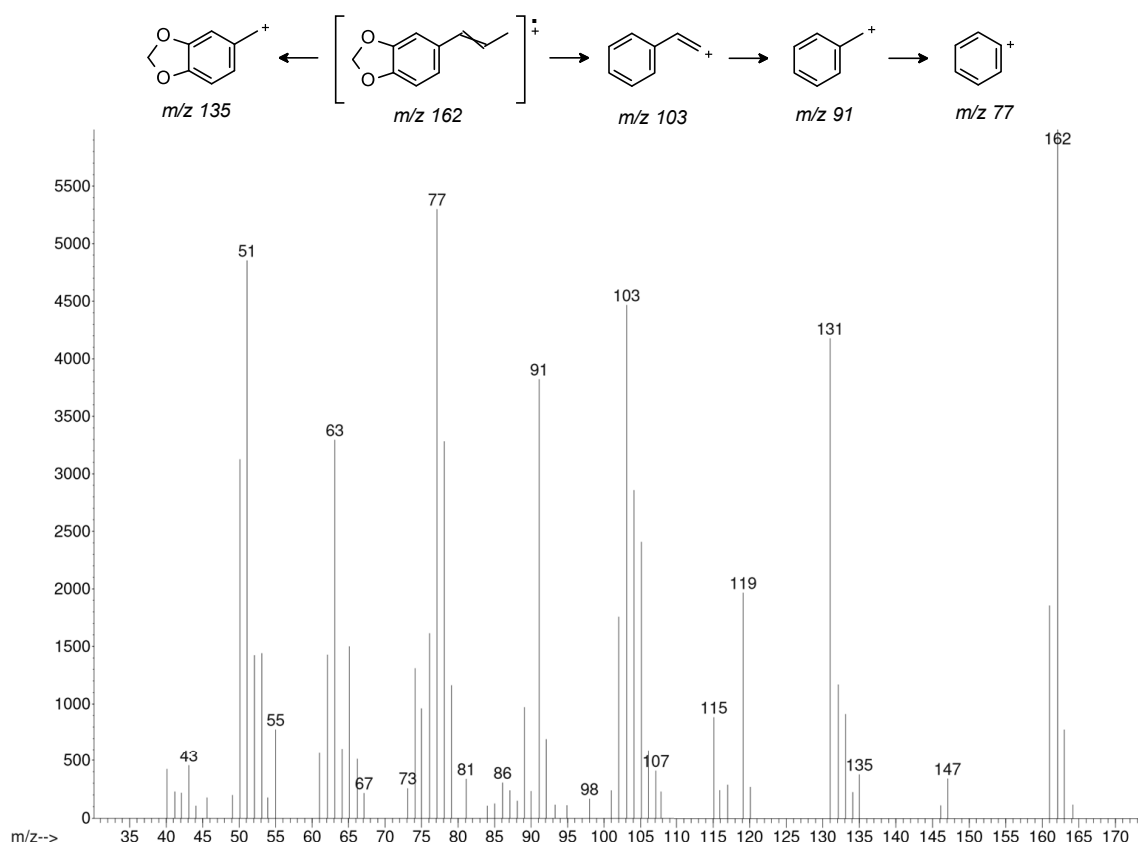


Figure A1-3: Mass spectrum and proposed fragmentation scheme of isosafrole (organic impurity 3)



Note: m/z 207 is attributed to column bleed

Figure A1-4: Mass spectrum and proposed fragmentation scheme of organic impurity 22

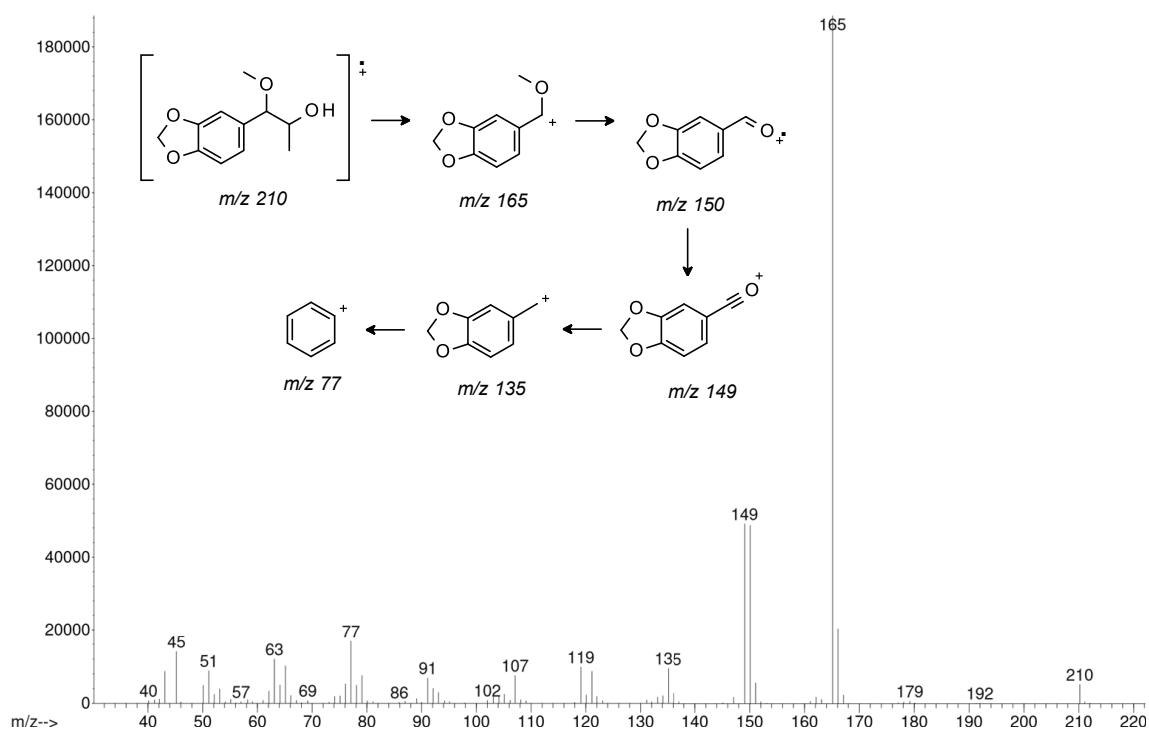


Figure A1-5: Mass spectrum and proposed fragmentation scheme of organic impurity 24

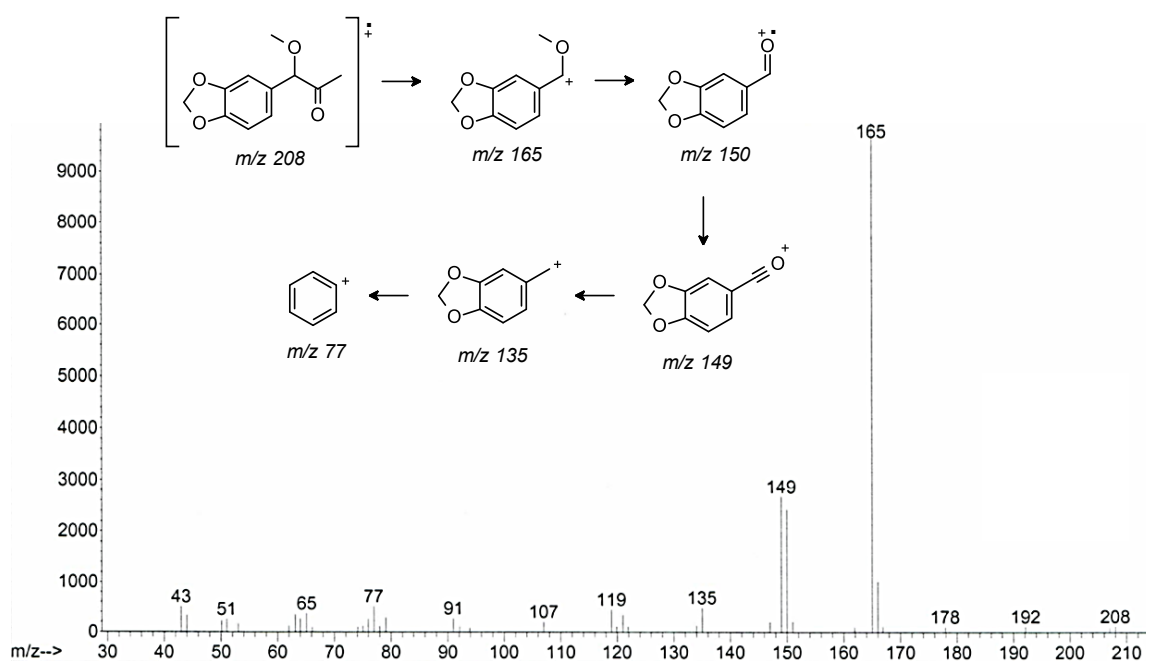


Figure A1-6: Mass spectrum and proposed fragmentation scheme of organic impurity 25

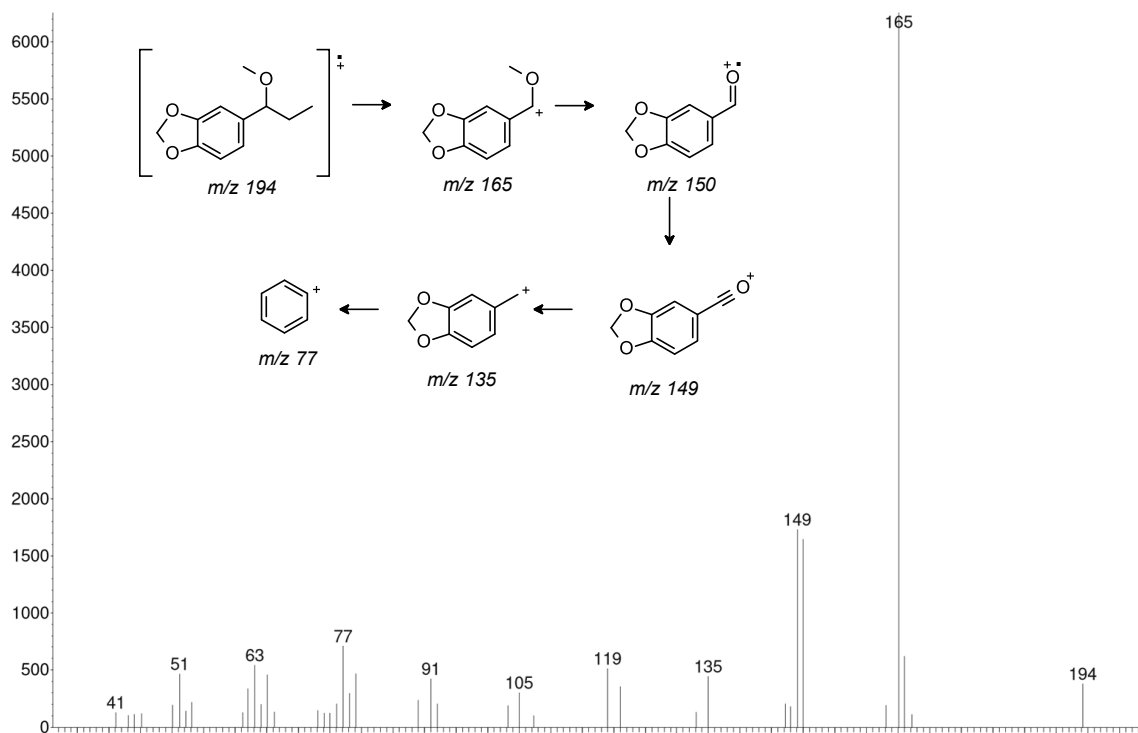


Figure A1-7: Mass spectrum and proposed fragmentation scheme of organic impurity 26

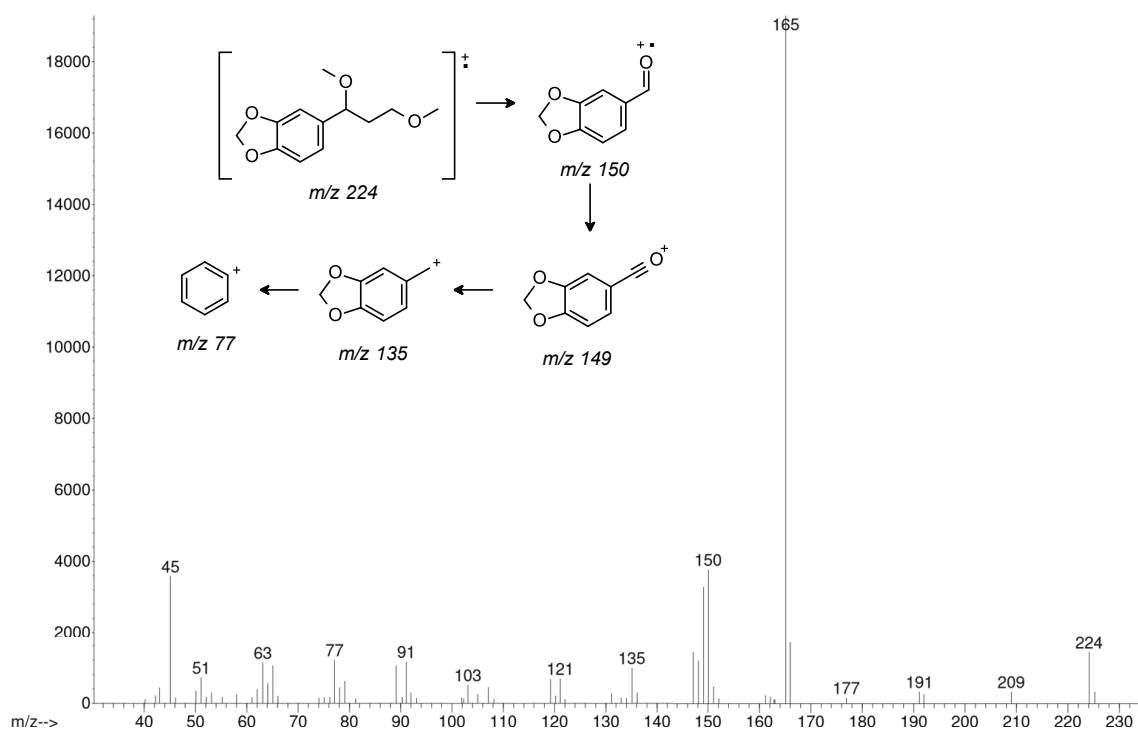


Figure A1-8: Mass spectrum and proposed fragmentation scheme of organic impurity 28

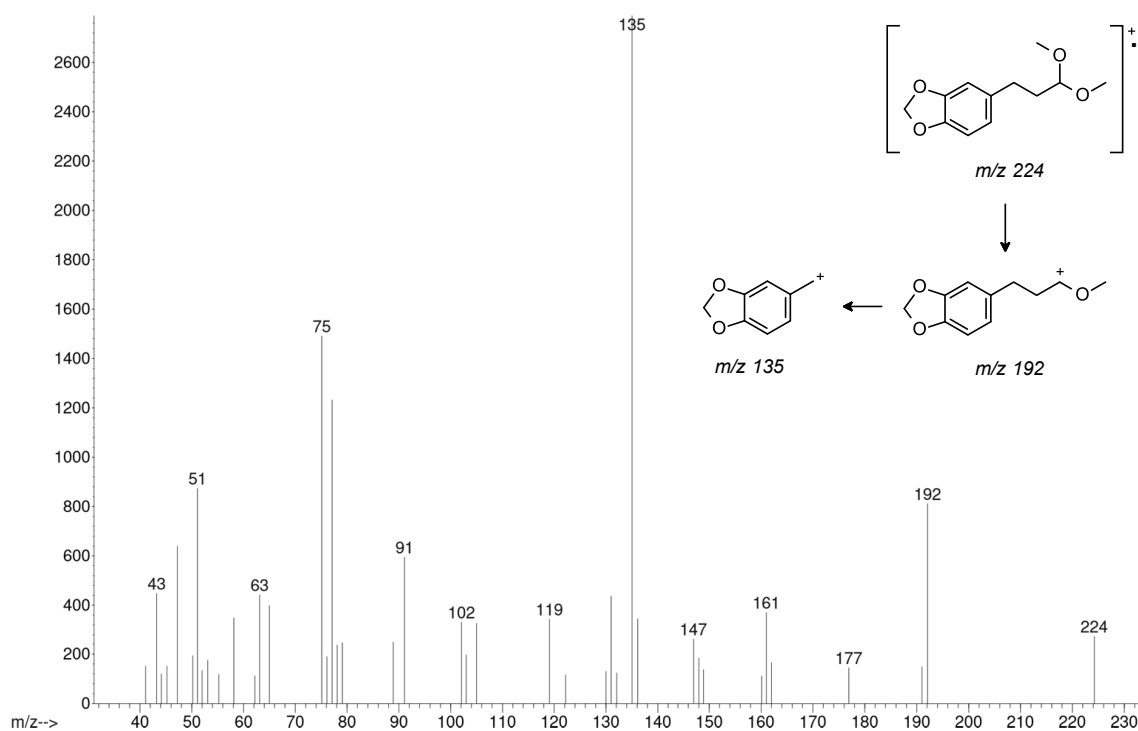


Figure A1-9: Mass spectrum and proposed fragmentation scheme of organic impurity 29

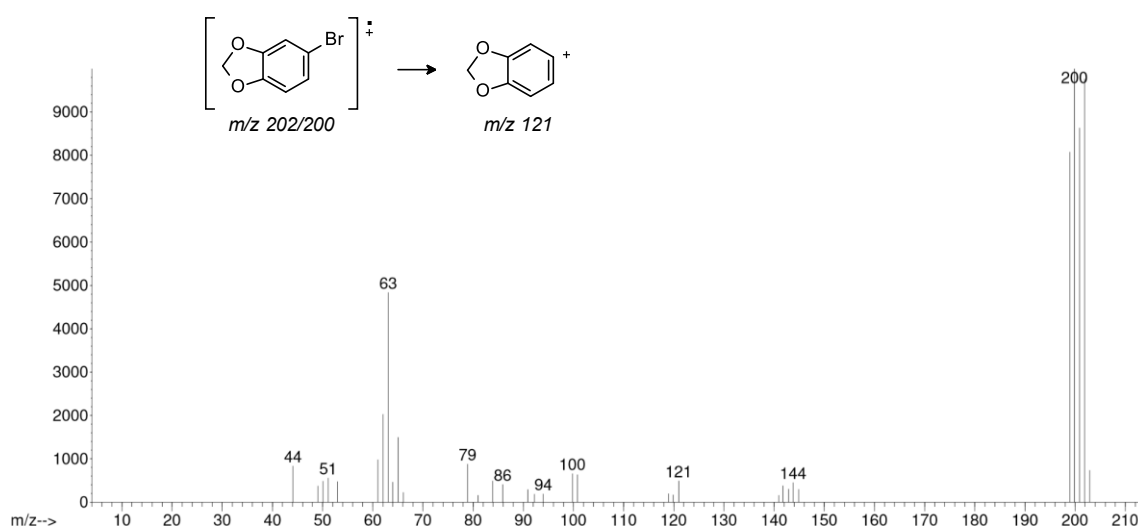


Figure A1-10: Mass spectrum and proposed fragmentation scheme of 5-bromo-1,3-benzodioxole (organic impurity 41)

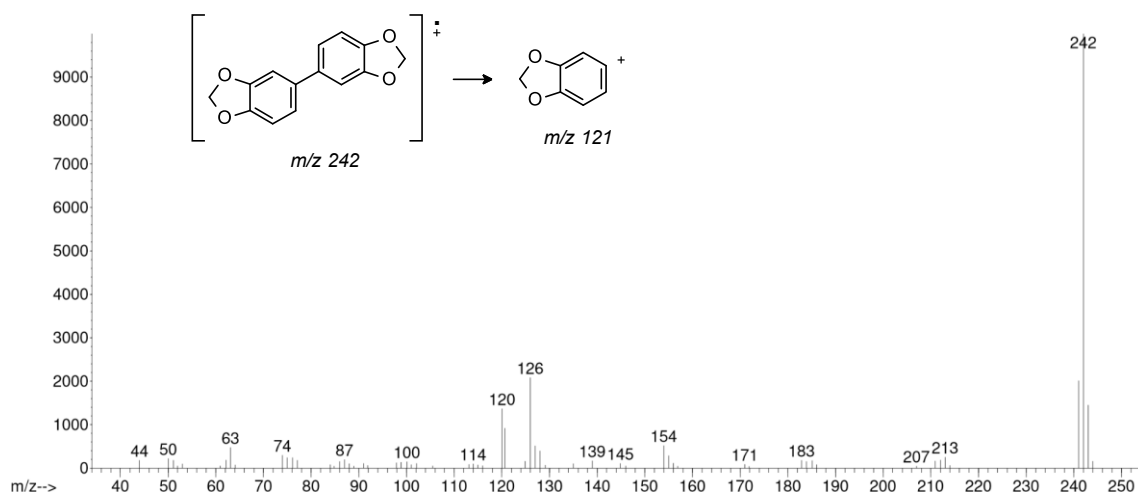


Figure A1-11: Mass spectrum and proposed fragmentation scheme of organic impurity 42

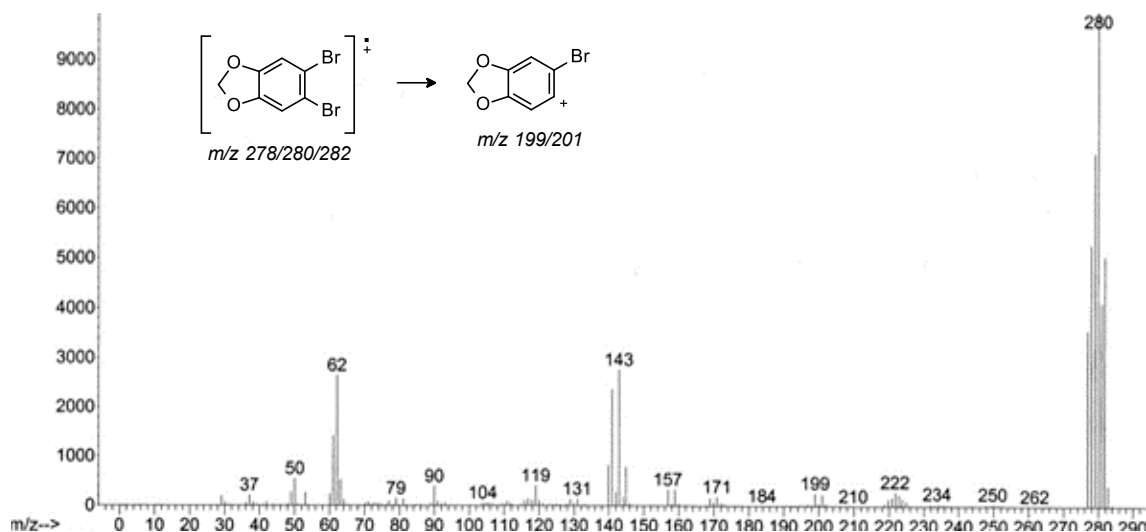


Figure A1-12: Mass spectrum and proposed fragmentation scheme of organic impurity 57

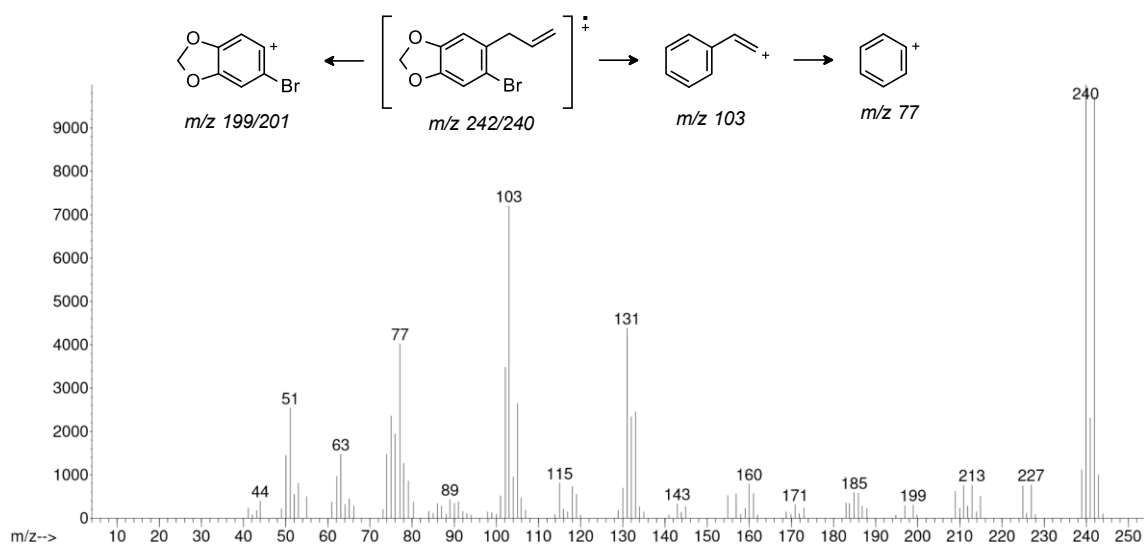


Figure A1-13: Mass spectrum and proposed fragmentation scheme of organic impurity 58

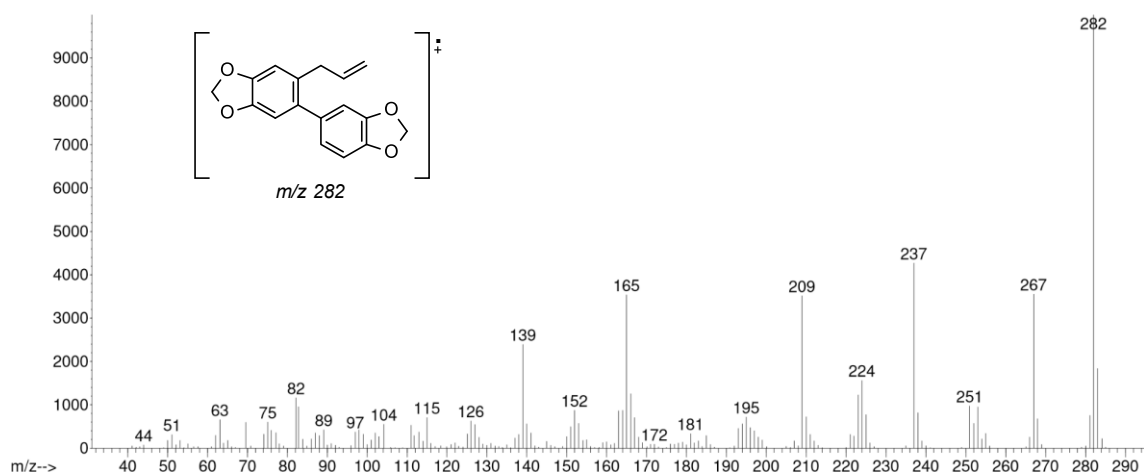


Figure A1-14: Mass spectrum and molecular ion of organic impurity 59

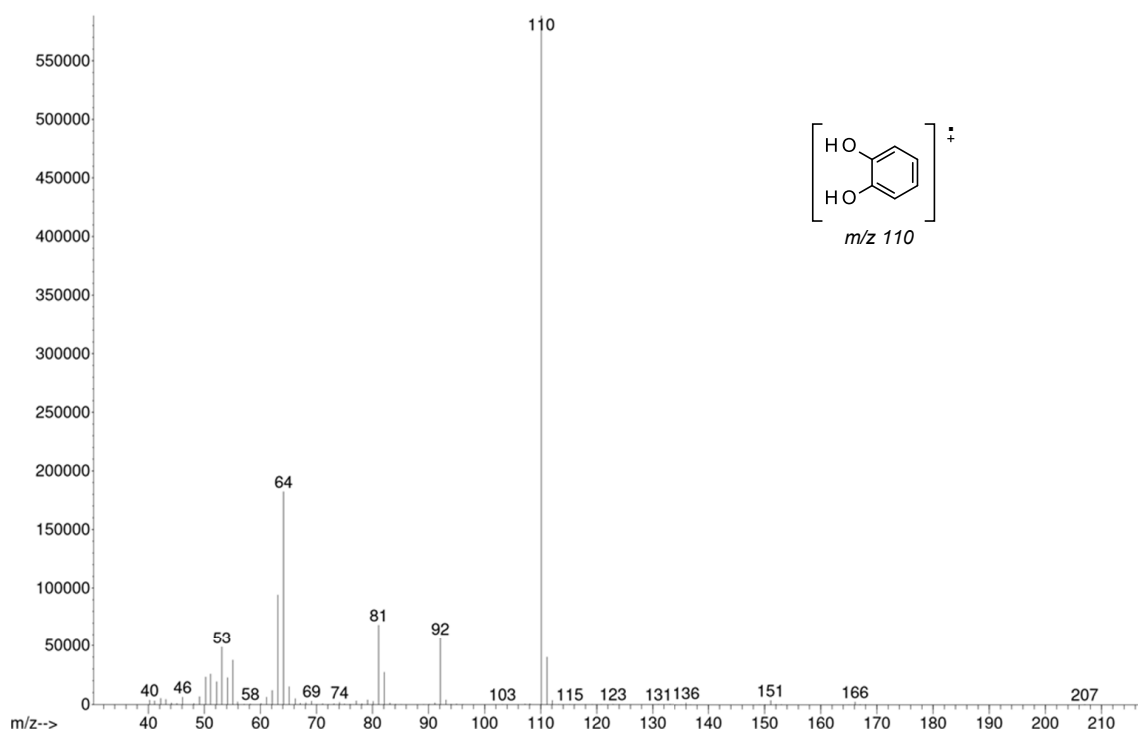


Figure A1-15: Mass spectrum and molecular ion of catechol (organic impurity 60)

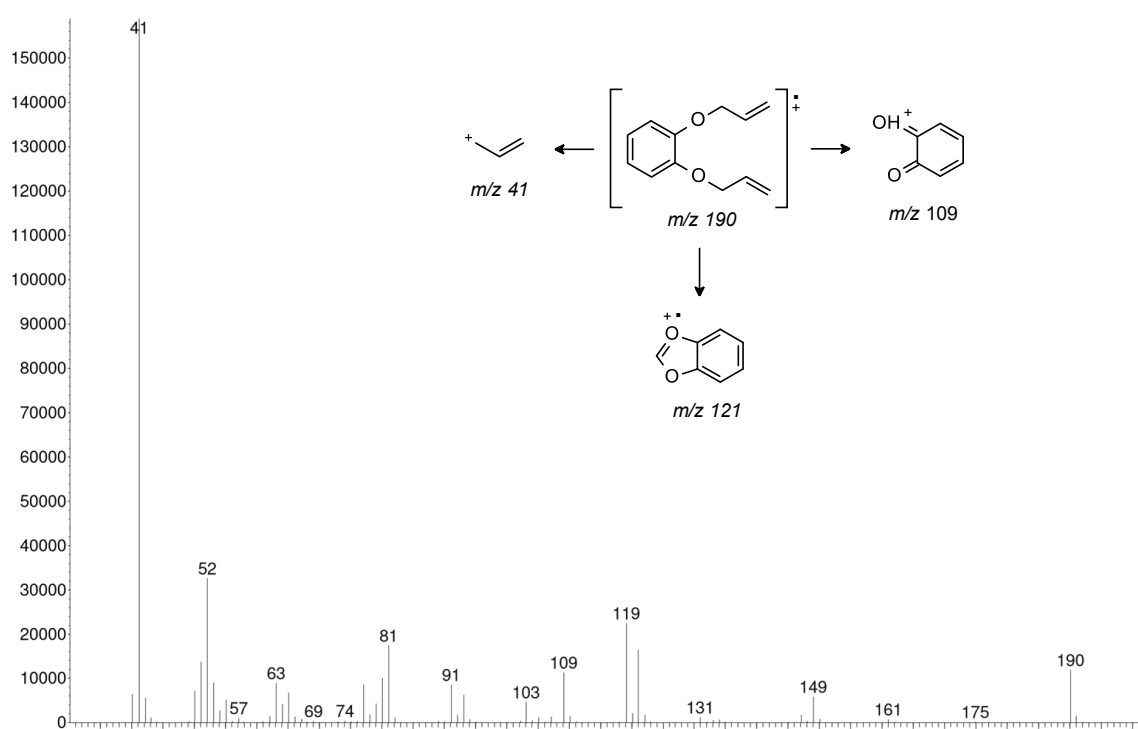


Figure A1-16: Mass spectrum and proposed fragmentation scheme of organic impurity 61

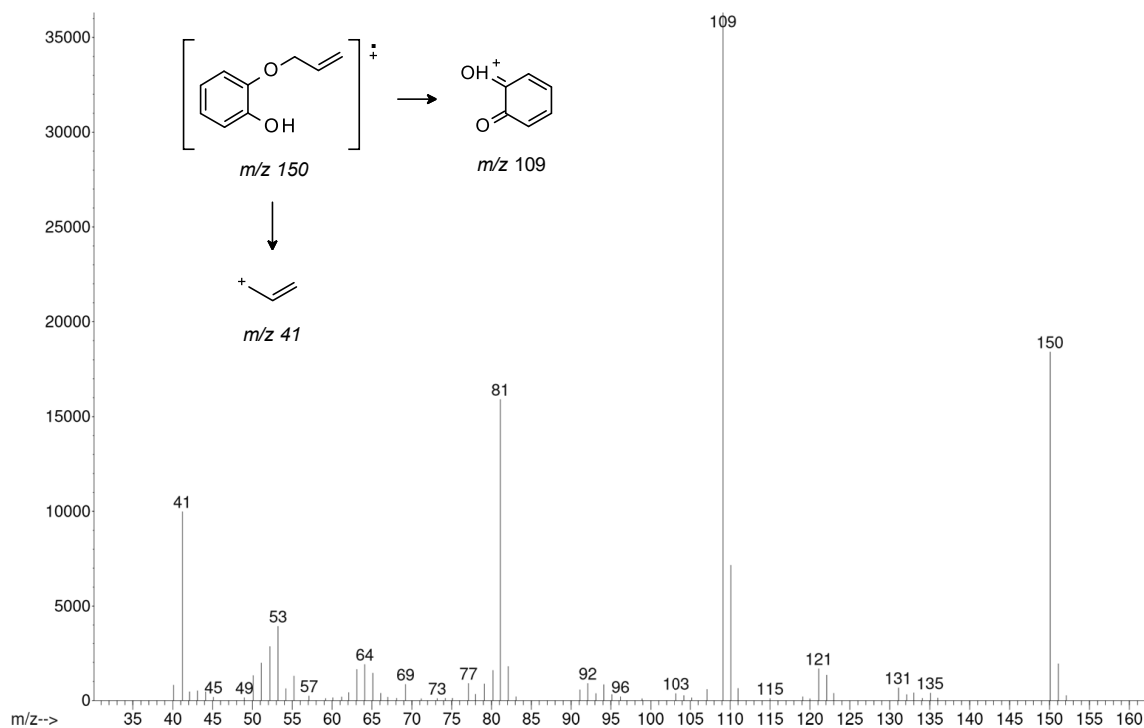


Figure A1-17: Mass spectrum and proposed fragmentation scheme of 2-allyloxyphenol (organic impurity 62)

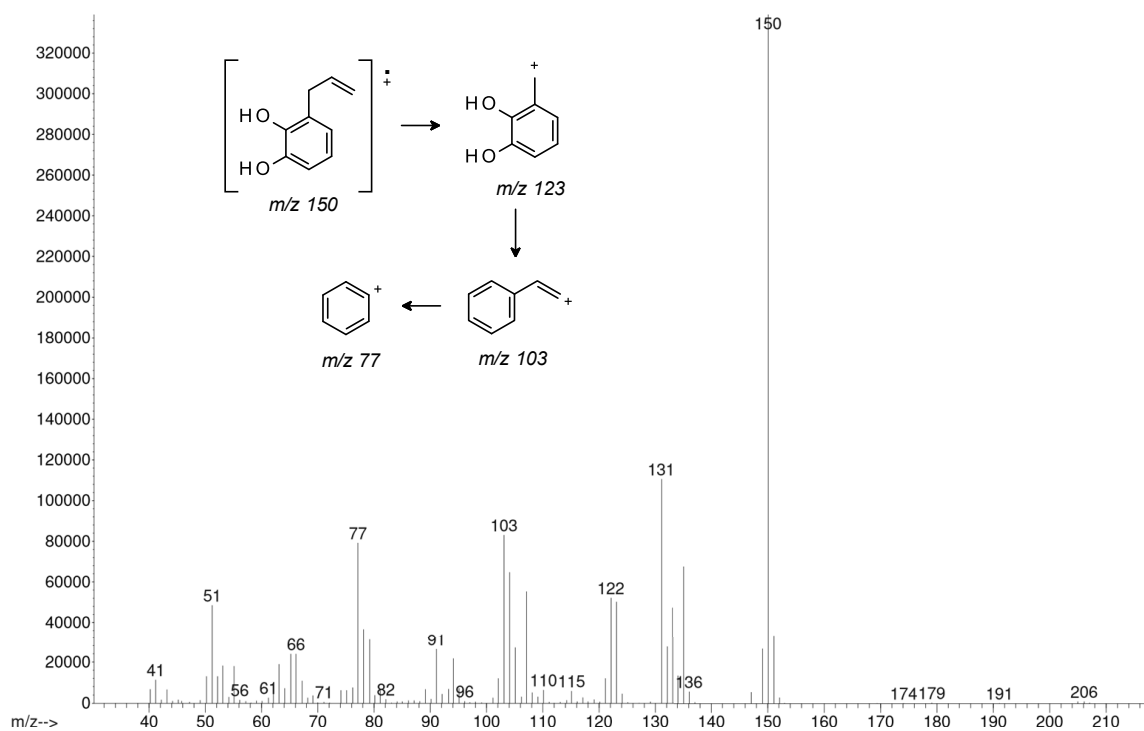


Figure A1-18: Mass spectrum and proposed fragmentation scheme of organic impurity 63

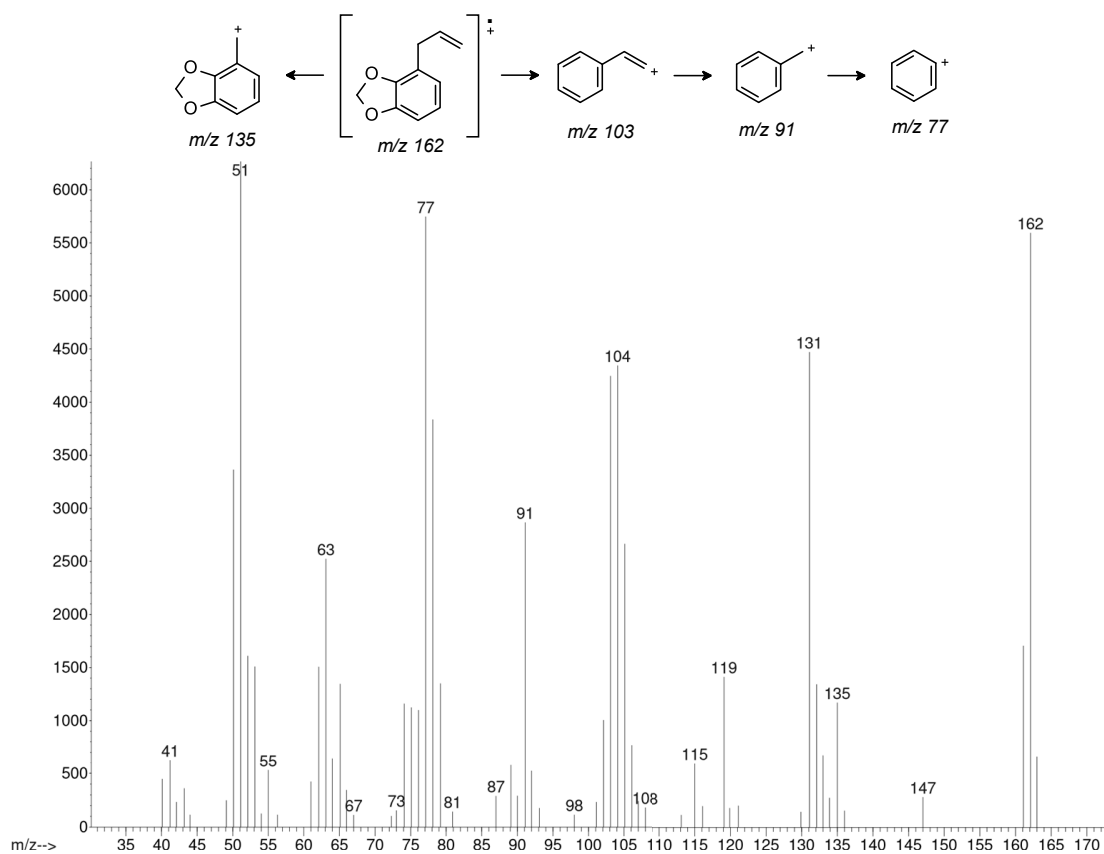


Figure A1-19: Mass spectrum and proposed fragmentation scheme of organic impurity 64

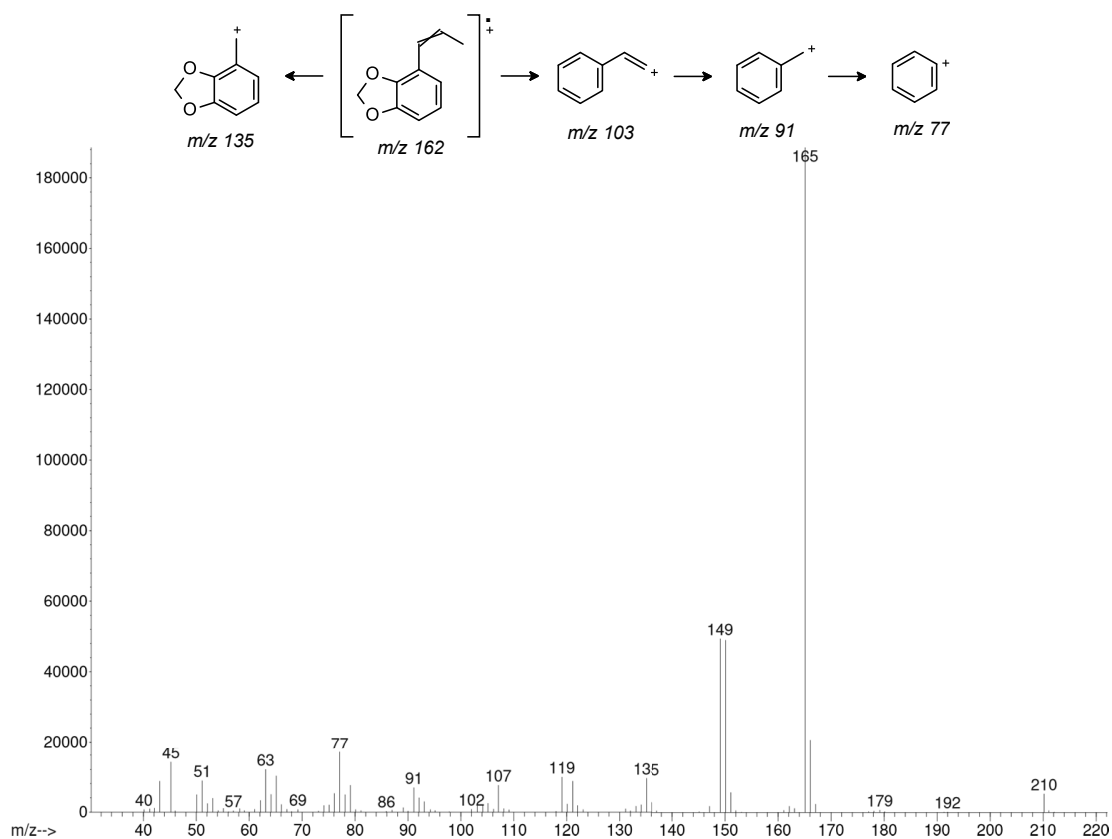


Figure A1-20: Mass spectrum and proposed fragmentation scheme of organic impurity 65

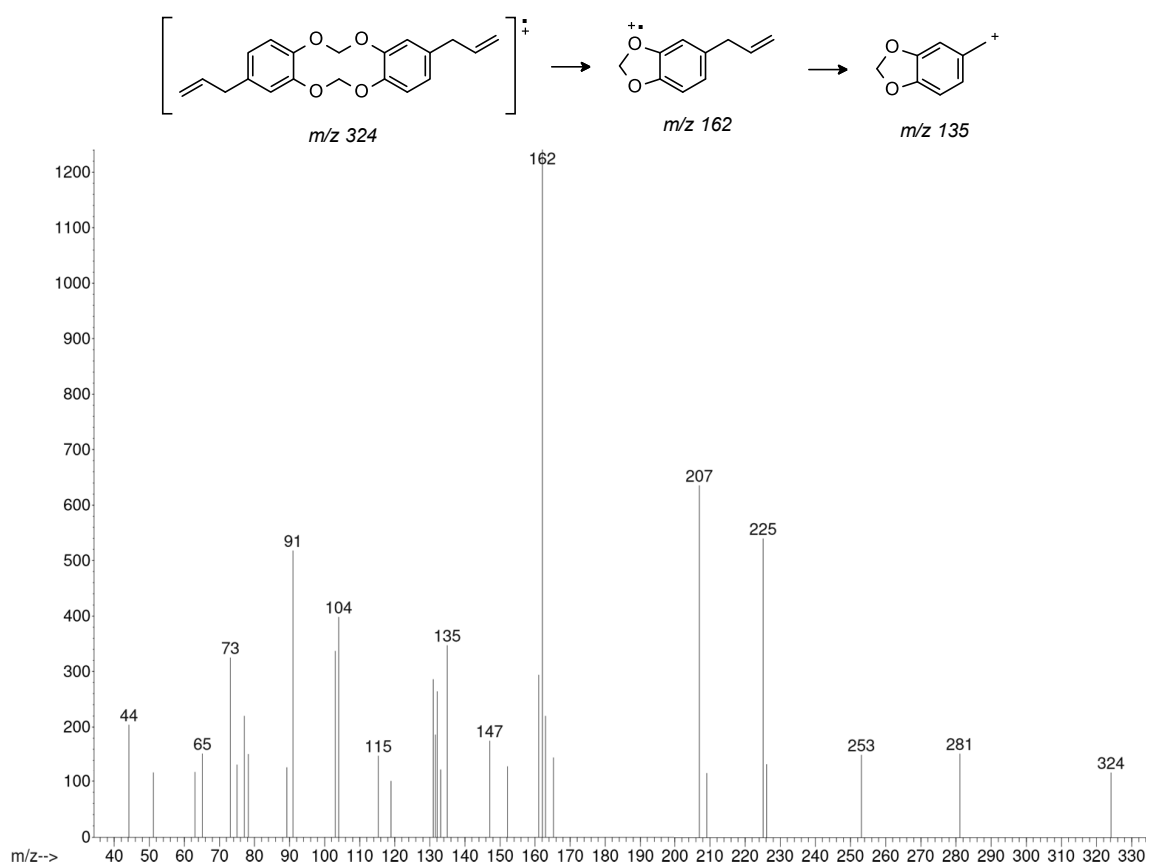


Figure A1-21: Mass spectrum and proposed fragmentation scheme of organic impurity 66

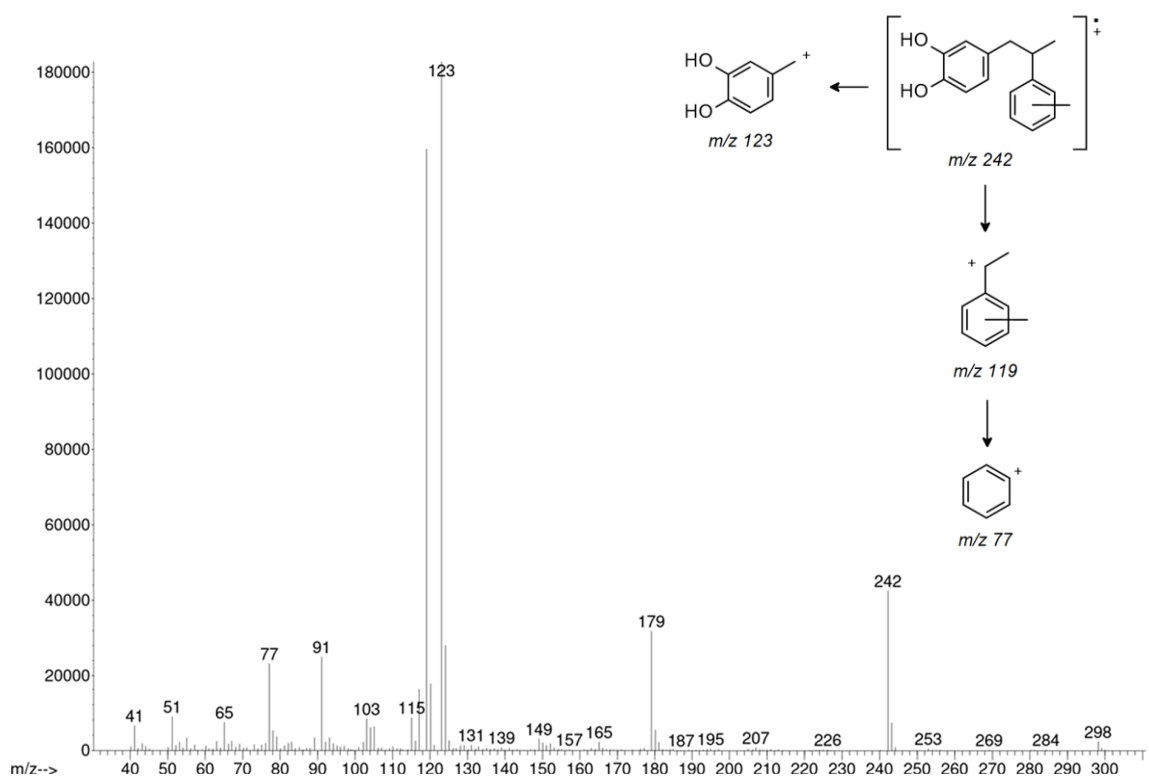


Figure A1-22: Mass spectrum and proposed fragmentation scheme of organic impurity 67 (a-c)

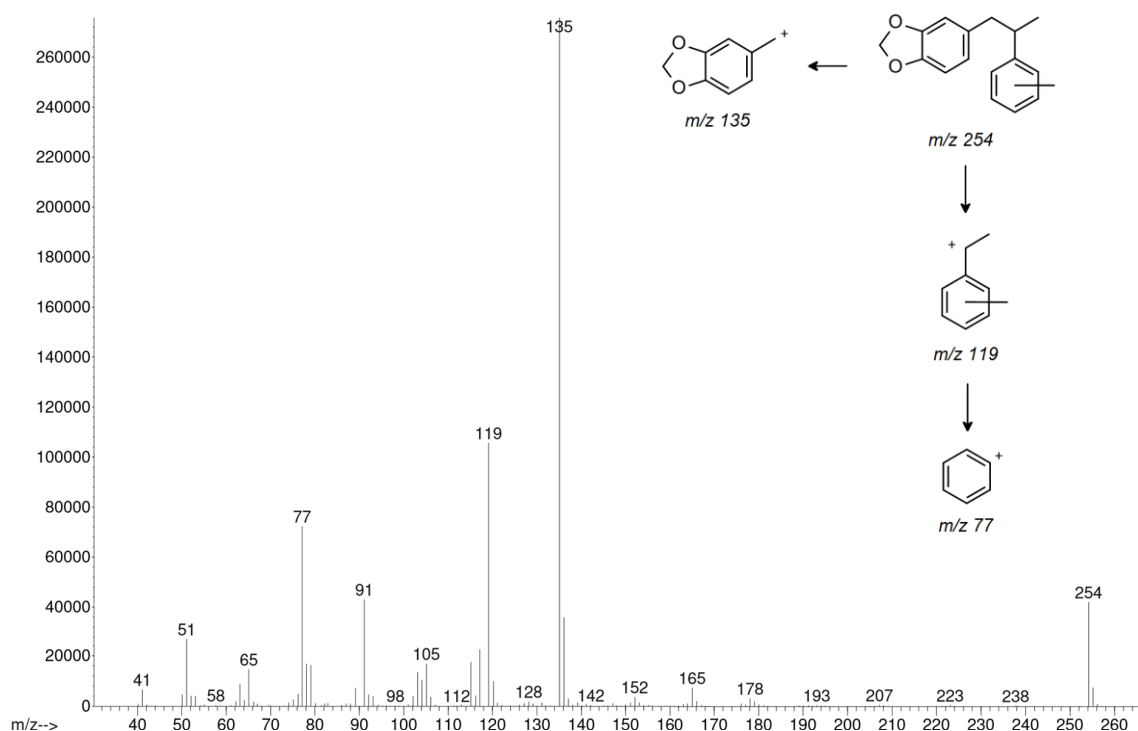


Figure A1-23: Mass spectrum and proposed fragmentation scheme of organic impurity 68 (a-c)

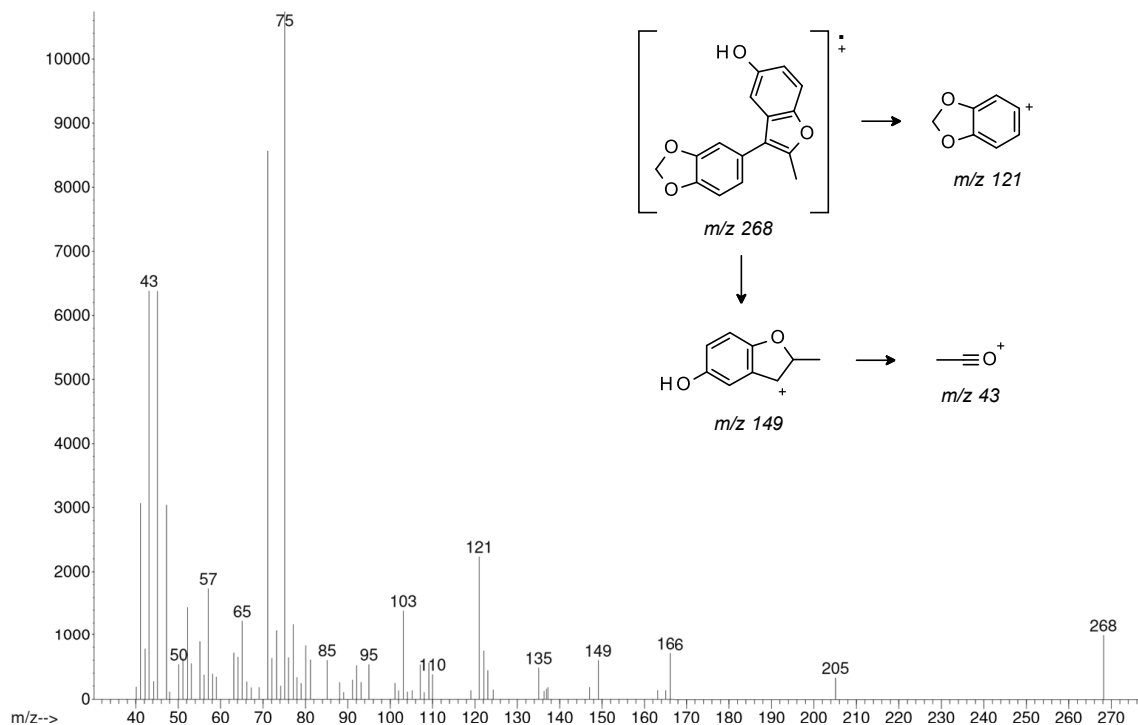


Figure A1-24: Mass spectrum and proposed fragmentation scheme of organic impurity 69

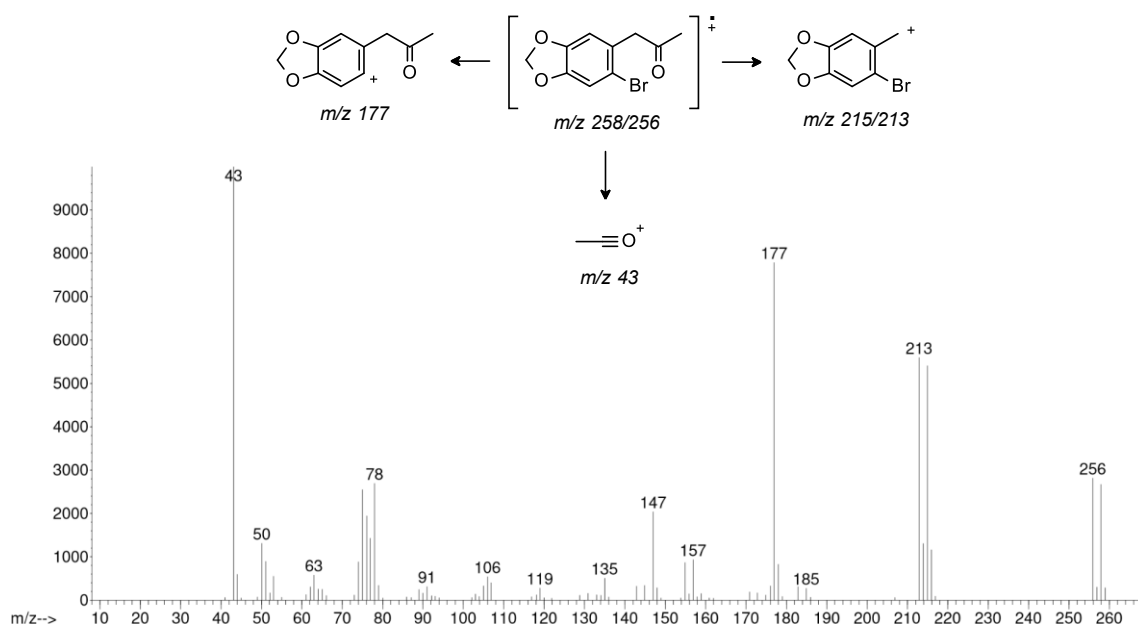


Figure A1-25: Mass spectrum and proposed fragmentation scheme of organic impurity 70

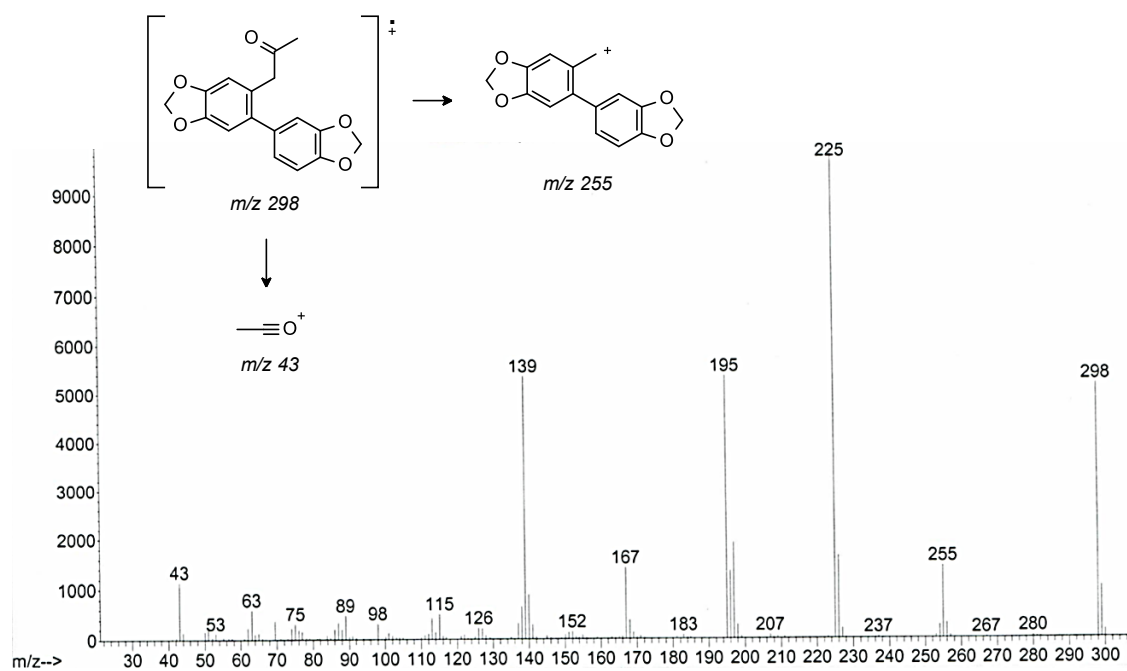


Figure A1-26: Mass spectrum and proposed fragmentation scheme of organic impurity 71

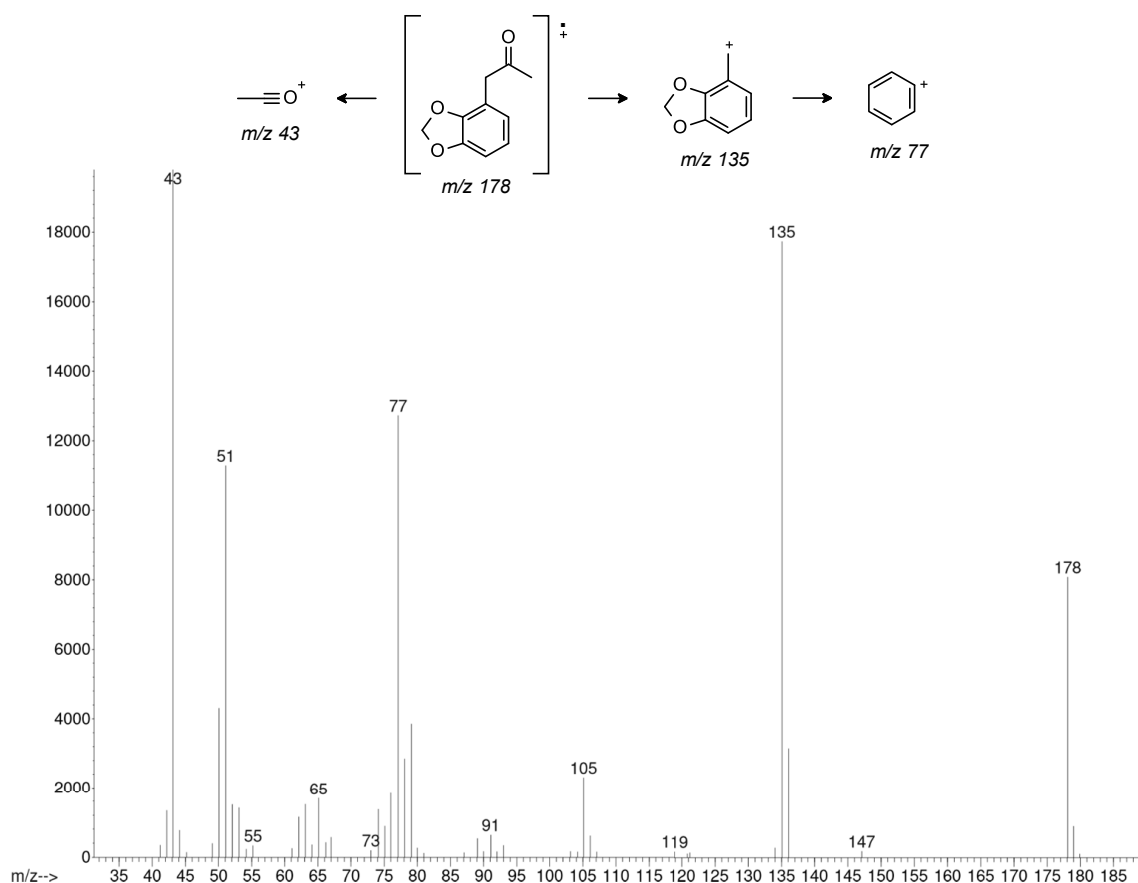


Figure A1-27: Mass spectrum and proposed fragmentation scheme of organic impurity 72

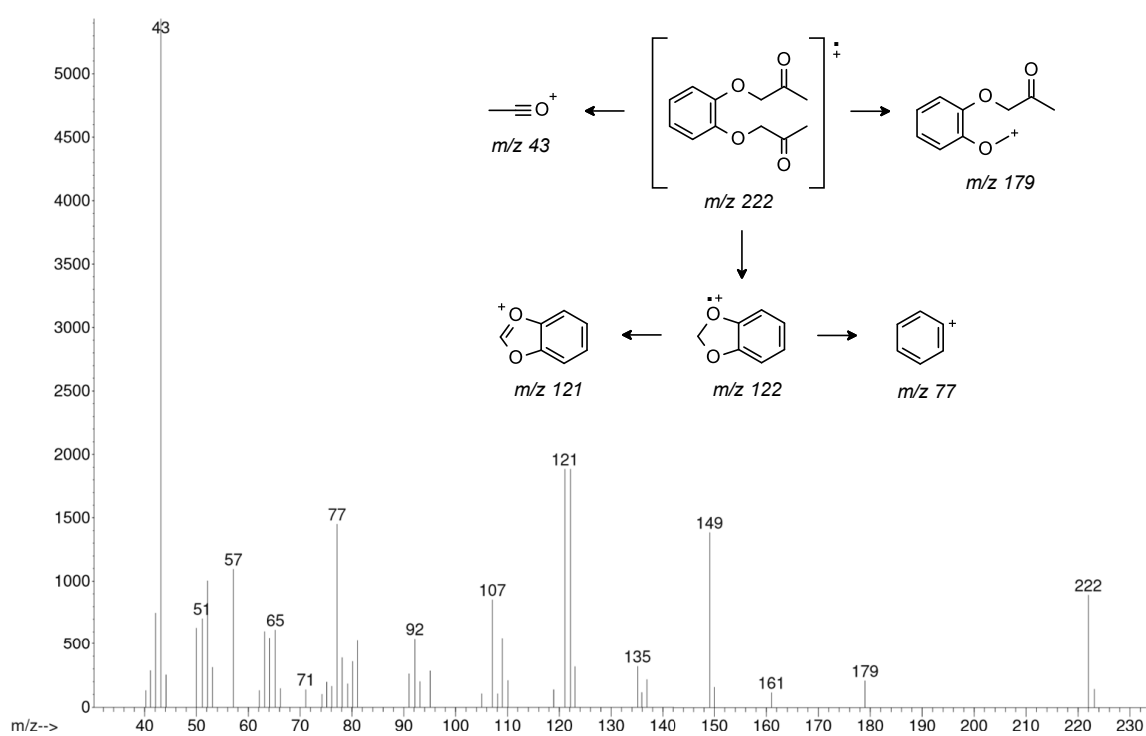


Figure A1-28: Mass spectrum and proposed fragmentation scheme of organic impurity 73



Figure A1-29: Mass spectrum and proposed fragmentation scheme of organic impurity 74

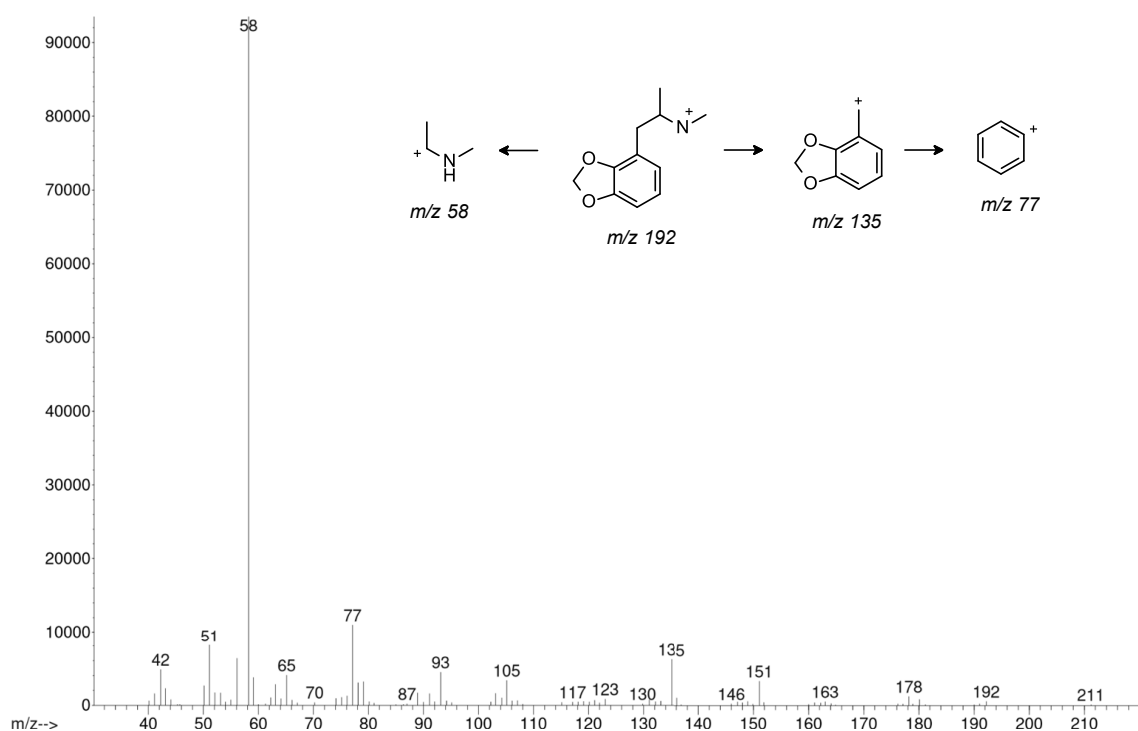


Figure A1-30: Mass spectrum and proposed fragmentation scheme of organic impurity 75

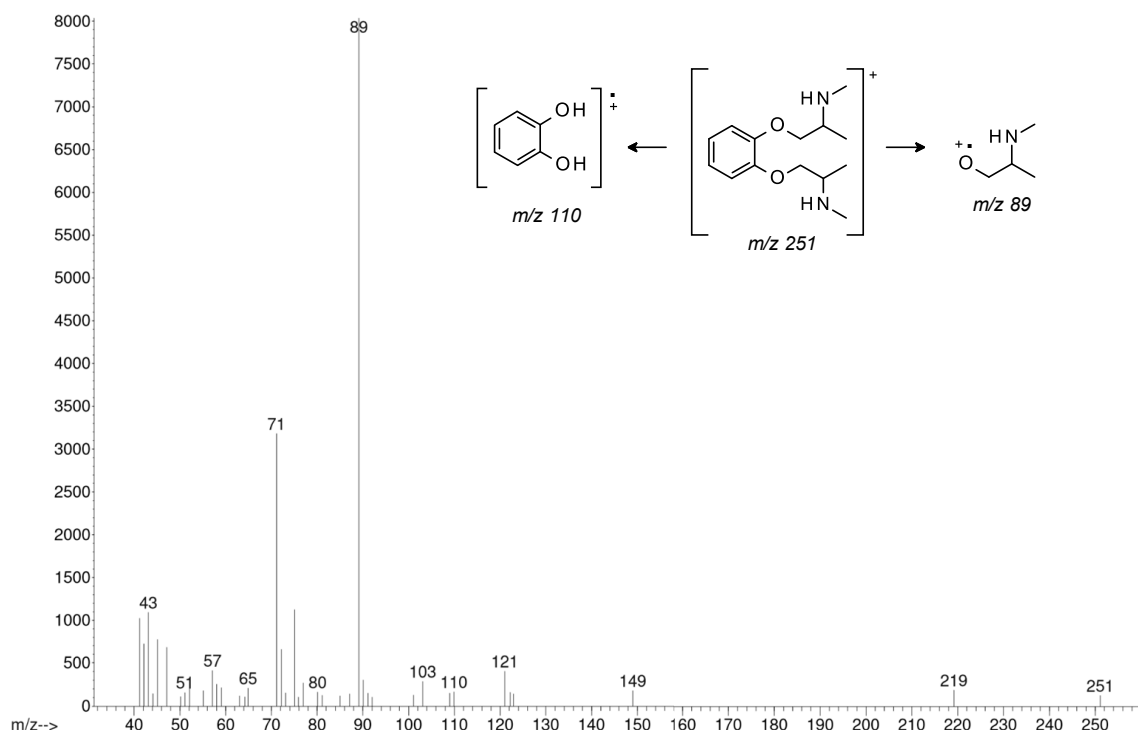


Figure A1-31: Mass spectrum and proposed fragmentation scheme of organic impurity 76

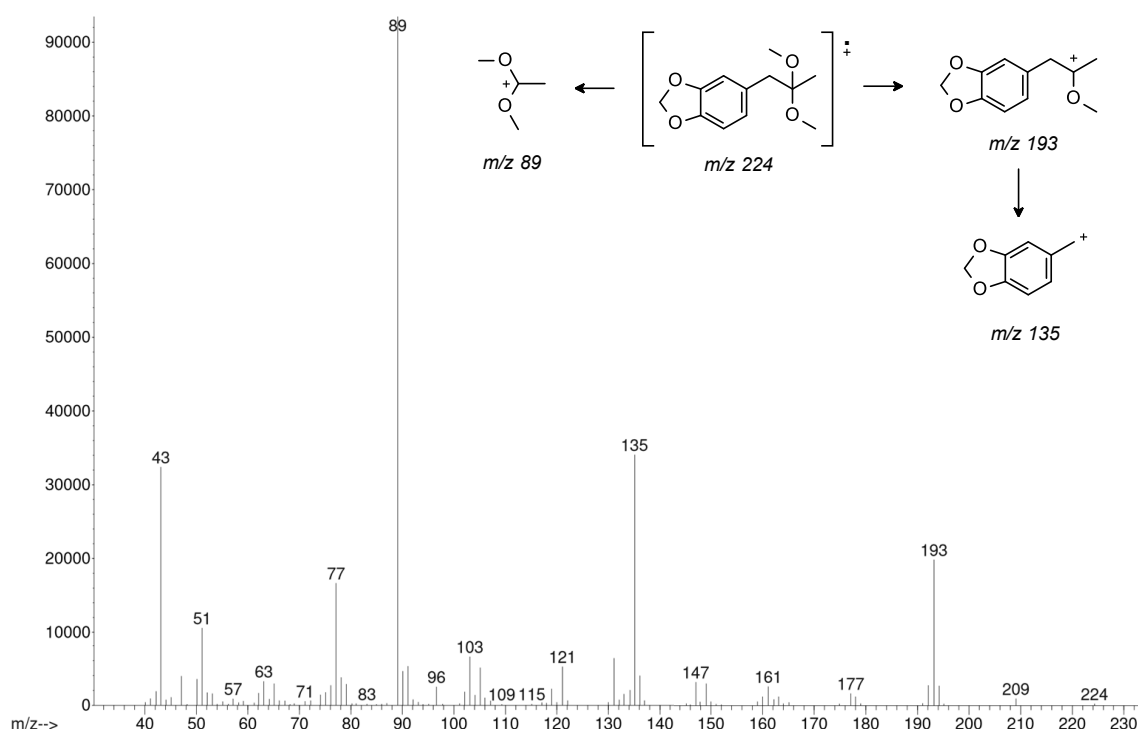


Figure A1-32: Mass spectrum and proposed fragmentation scheme of organic impurity 77

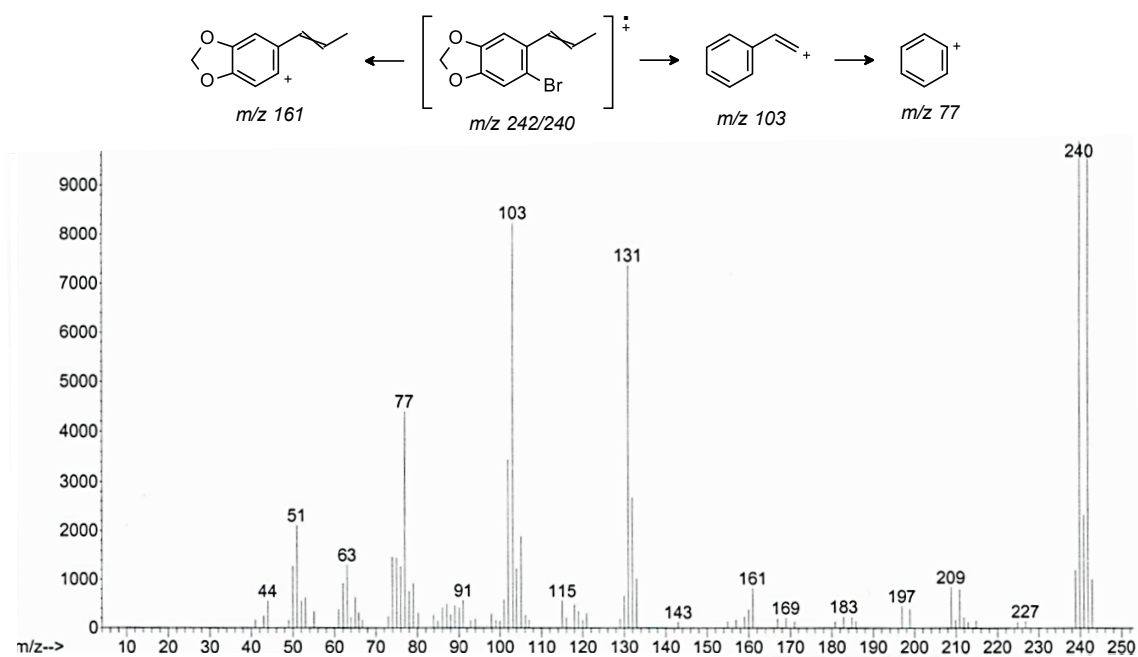


Figure A1-33: Mass spectrum and proposed fragmentation scheme of organic impurity 78 (a-b)

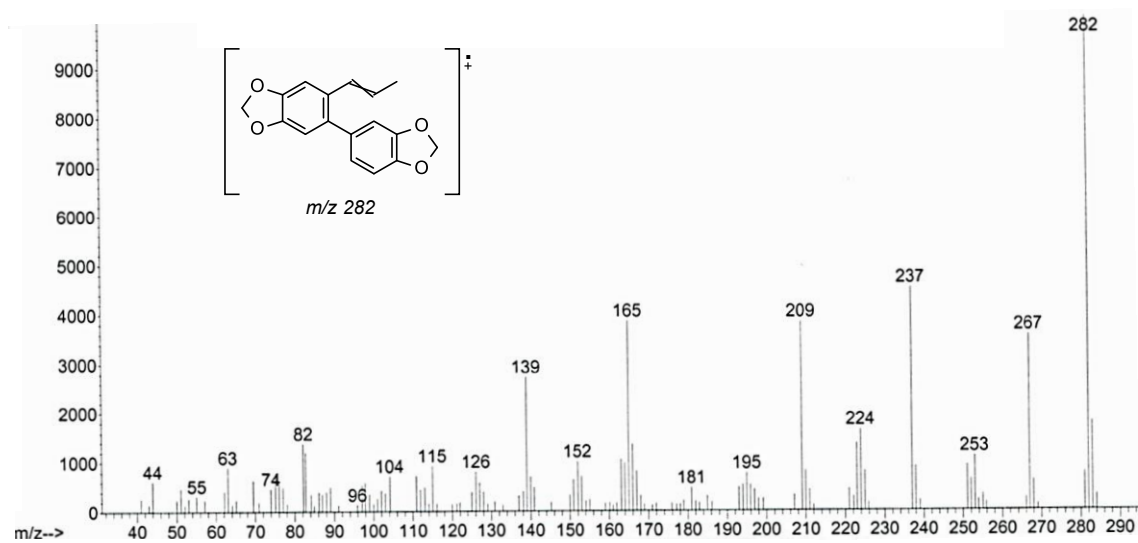


Figure A1-34: Mass spectrum and molecular ion of organic impurity 79 (a-b)

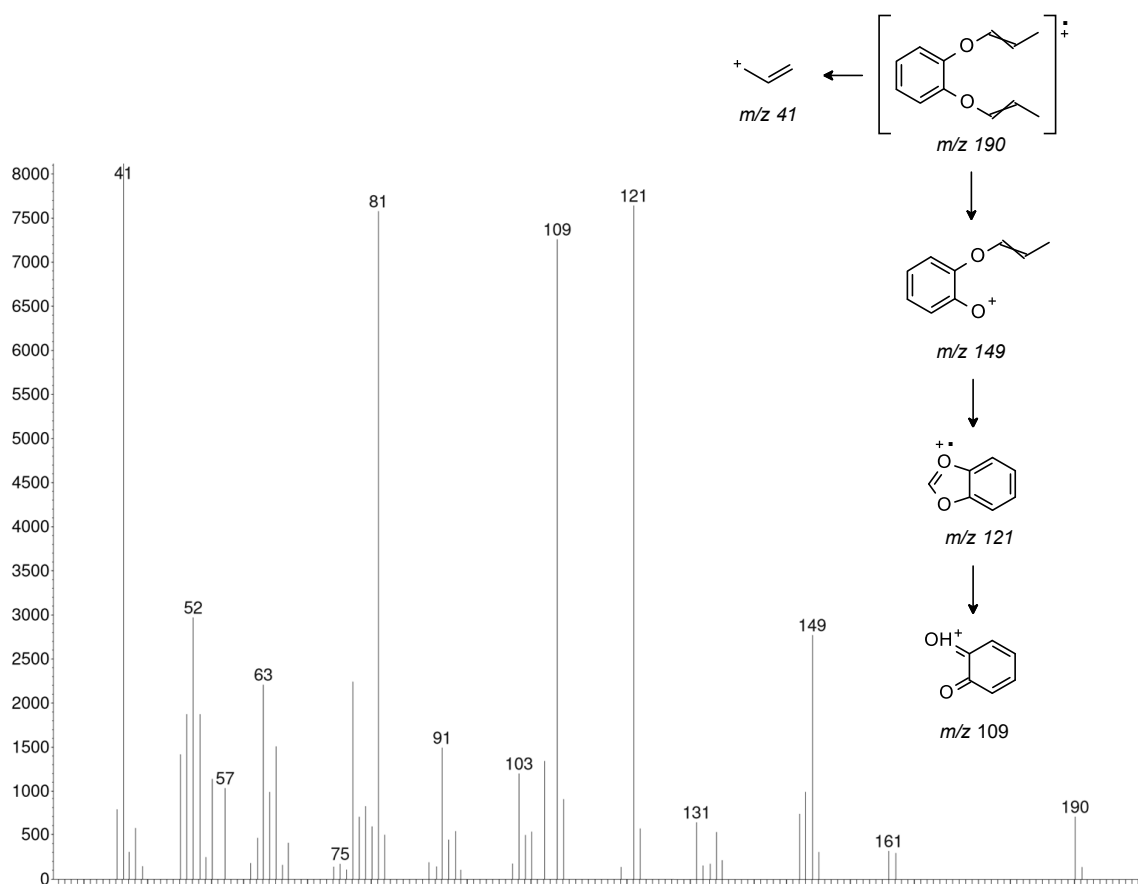


Figure A1-35: Mass spectrum and proposed fragmentation scheme of organic impurity 80

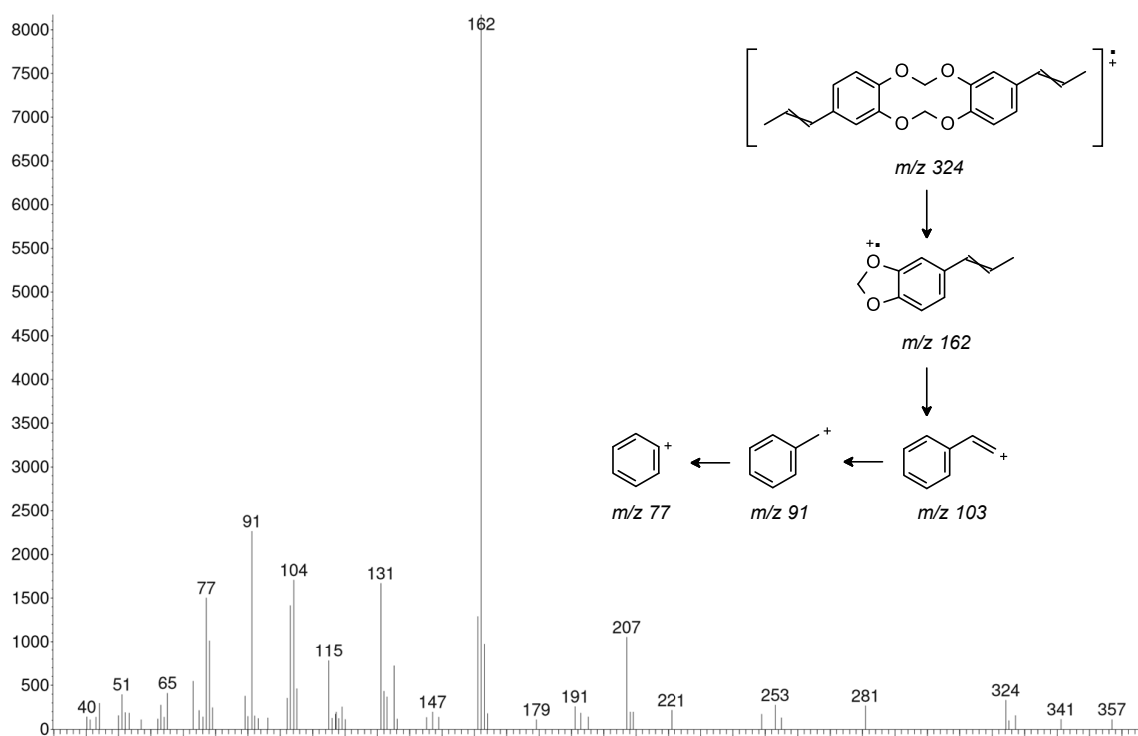


Figure A1-36: Mass spectrum and proposed fragmentation scheme of organic impurity 81

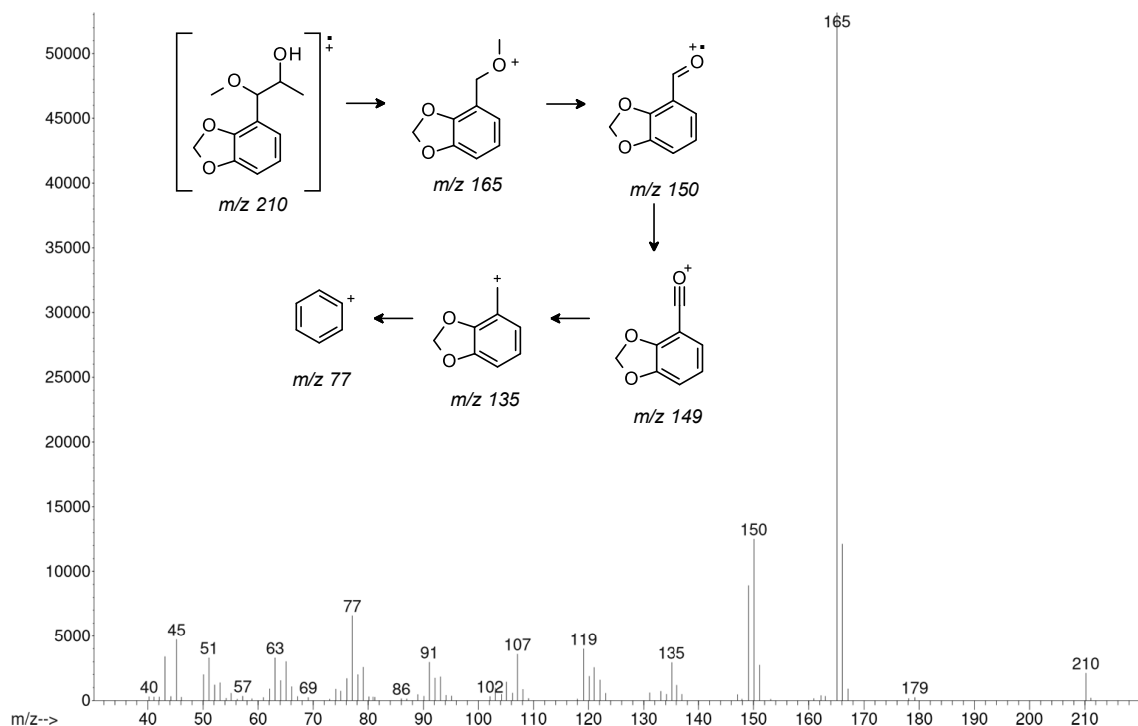


Figure A1-37: Mass spectrum and proposed fragmentation scheme of organic impurity 82

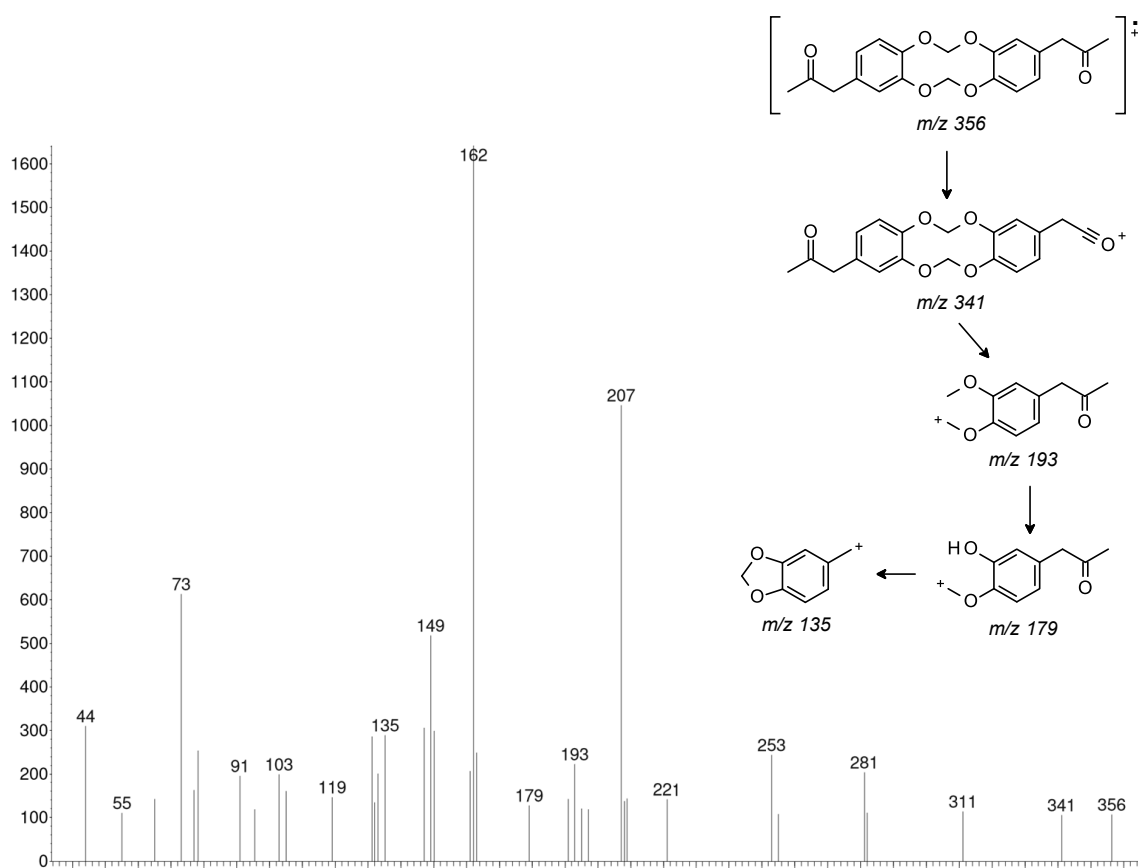


Figure A1-38: Mass spectrum and proposed fragmentation scheme of organic impurity 83

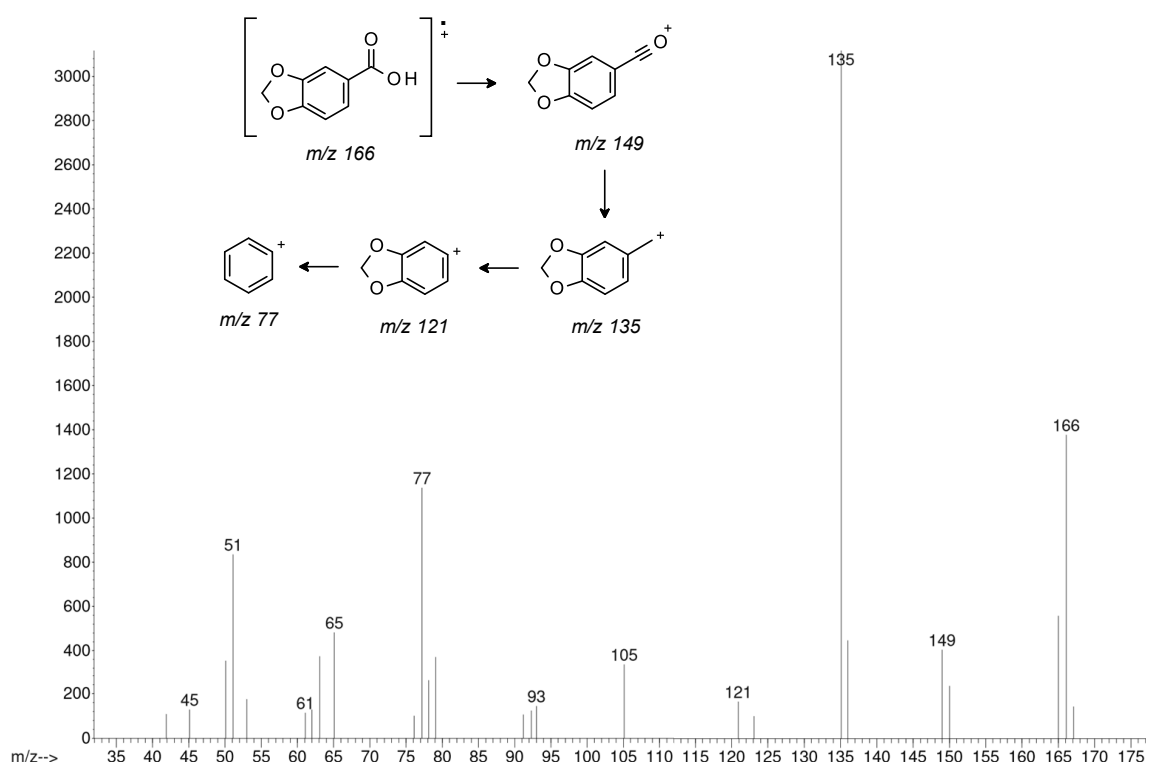


Figure A1-39: Mass spectrum and proposed fragmentation scheme of organic impurity 84

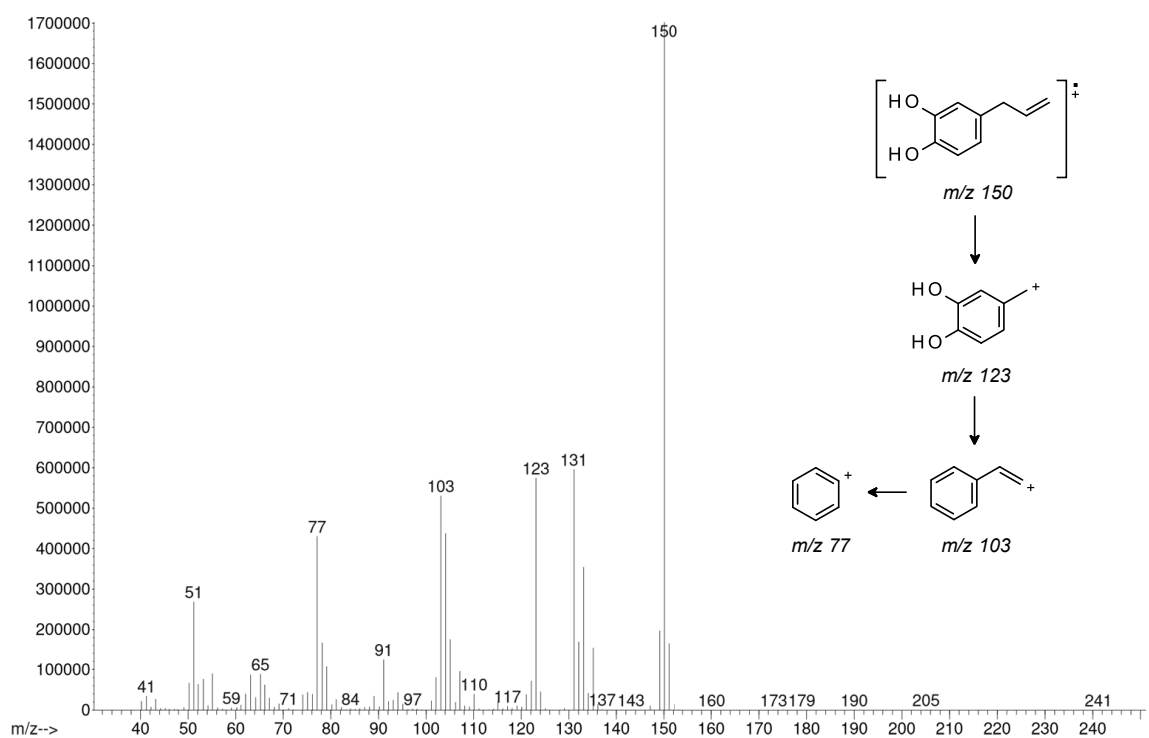


Figure A1-40: Mass spectrum and proposed fragmentation scheme of 4-allylcatechol

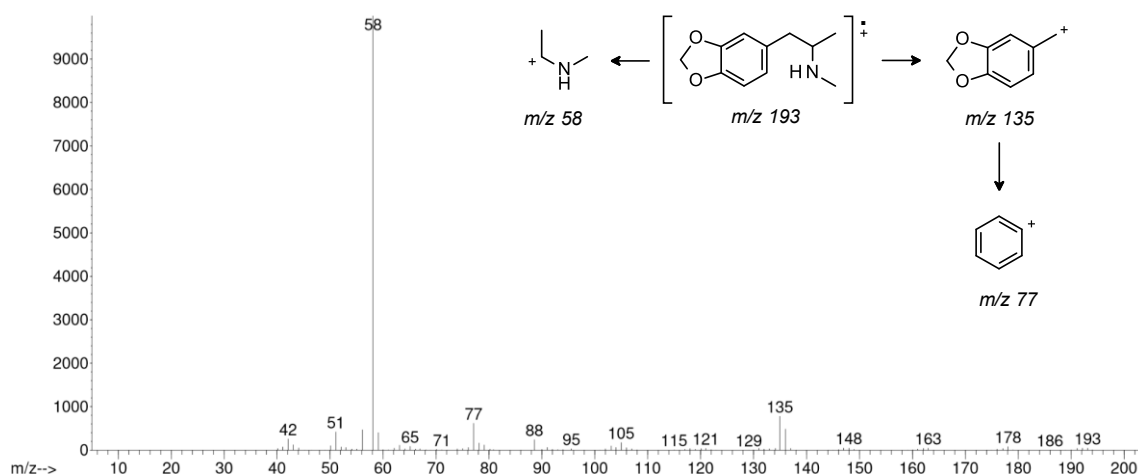


Figure A1-41: Mass spectrum and proposed fragmentation scheme of MDMA

Appendix 2: Gas Chromatograms

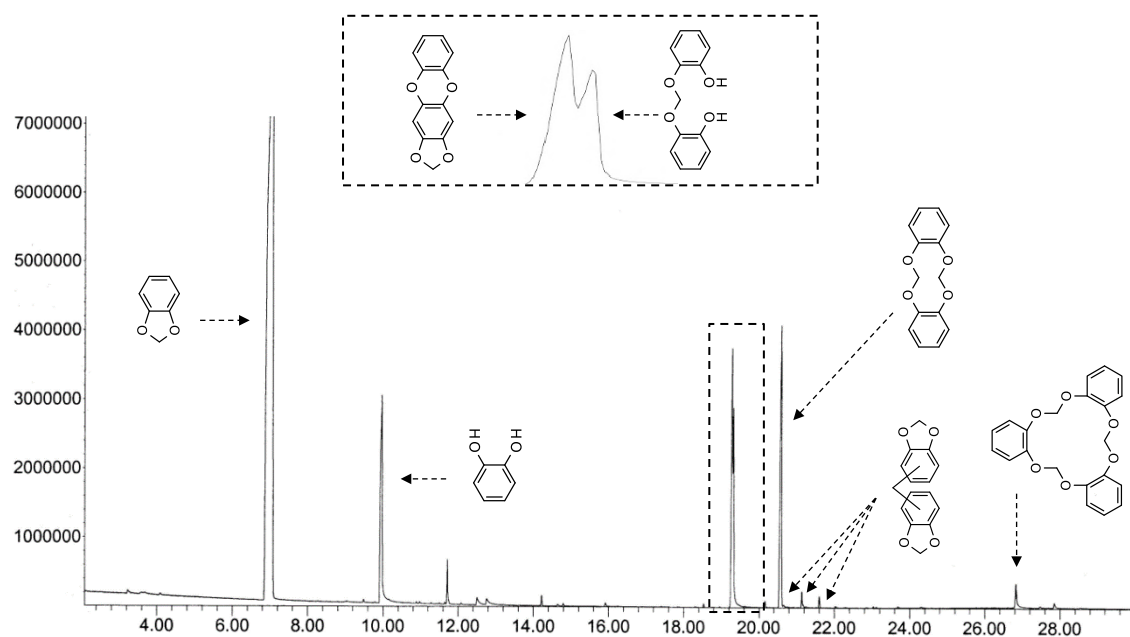


Figure A2-1: GC-MS total ion chromatogram of 1,3-benzodioxole synthesised from catechol via a two-hour reaction

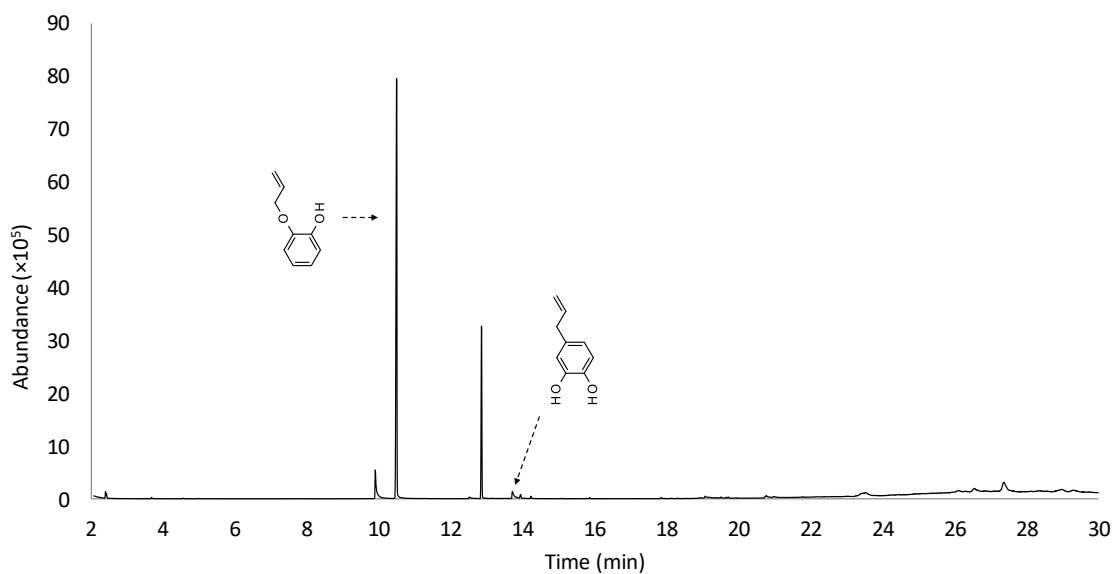


Figure A2-2: GC-MS total ion chromatogram of 3-hr reaction aliquot from the synthesis of 4-allylcatechol from 2-allyloxyphenol

Table A2-1: GC-MS total ion chromatogram area report of 3-hr reaction aliquot from the synthesis of 4-allylcatechol from 2-allyloxyphenol

Peak #	Ret Time	Type	Width	Area	Start Time	End Time
1	2.416	PV	0.019	1380679	2.385	2.43
2	2.442	VV	0.02	1165589	2.43	2.516
3	3.695	BB	0.026	441555	3.591	3.813
4	9.914	BV	0.039	14754514	9.846	10.179
5	10.503	BB	0.03	1.47E+08	10.409	10.937
6	12.524	PV	0.063	1249080	12.389	12.714
7	12.863	BB	0.024	48792074	12.782	13.107
8	13.722	BV	0.05	4699168	13.646	13.825
9	13.84	VV	0.045	797129	13.825	13.908
10	13.948	VB	0.037	1744877	13.908	14.055
11	14.234	BV	0.024	638222	14.154	14.278
12	15.87	VB	0.028	364390	15.83	15.955
13	17.86	VV	0.026	338573	17.831	17.91
14	18.934	PV	0.045	343917	18.829	18.966
15	19.077	VV	0.068	1811870	18.966	19.263
16	19.518	BV	0.027	340484	19.45	19.628
17	19.66	PV	0.028	306286	19.628	19.689
18	19.721	VV	0.029	393448	19.689	19.772
19	20.775	PV	0.074	2578969	20.687	20.935
20	20.985	VB	0.076	1282848	20.935	21.187
21	21.783	VV	0.033	299521	21.734	21.873
22	23.282	PV	0.041	488340	23.207	23.305
23	23.476	VV	0.094	4280278	23.305	23.494
24	23.54	VV	0.088	4387662	23.494	23.713
25	24.477	VV	0.099	944052	24.34	24.496
26	24.774	VV	0.05	419160	24.726	24.784
27	24.934	VV	0.124	2504048	24.803	25.016
28	25.089	VV	0.077	1300240	25.016	25.111
29	25.133	VV	0.081	1331677	25.111	25.201
30	25.245	VV	0.043	851154	25.201	25.259
31	25.277	VV	0.025	416737	25.259	25.286
32	25.992	VV	0.101	2716607	25.891	26.002
33	26.117	VV	0.13	7716244	26.002	26.225
34	26.286	VV	0.08	2657510	26.225	26.311
35	26.328	VV	0.108	3675841	26.311	26.438
36	26.561	VV	0.178	15533014	26.438	26.824
37	26.874	VV	0.065	2482214	26.824	26.9
38	27.376	VV	0.166	27374946	27.217	27.78
39	28.342	VV	0.162	5336528	28.227	28.481
40	28.957	VV	0.148	5255567	28.73	28.968
41	28.98	VV	0.089	4390732	28.968	29.176
42	29.314	VV	0.158	5142846	29.176	29.558

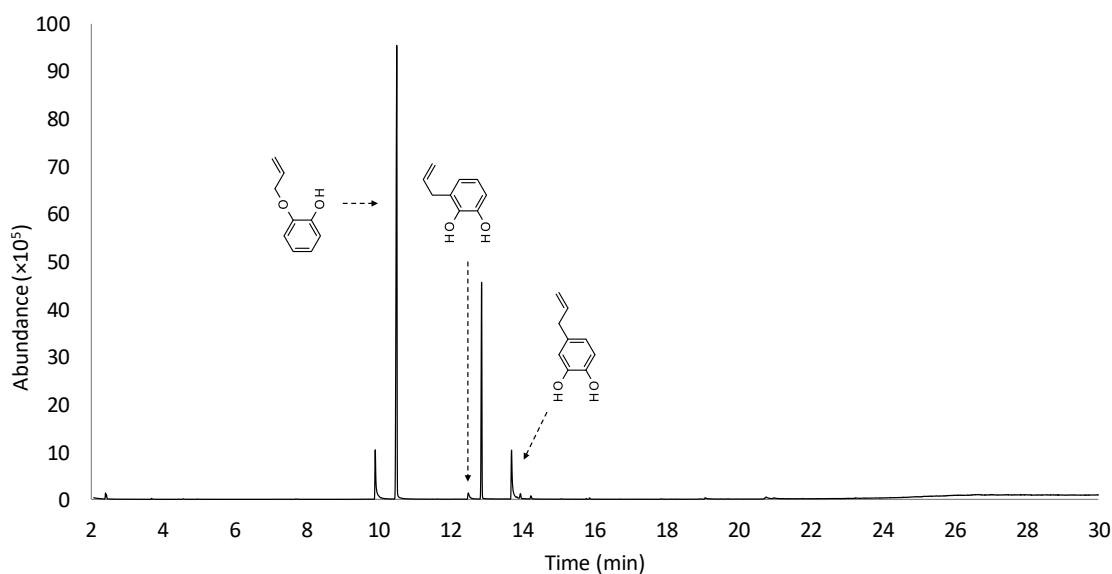


Figure A2-3: GC-MS total ion chromatogram of 8-hr reaction aliquot from the synthesis of 4-allylcatechol from 2-allyloxyphenol

Table A2-2: GC-MS total ion chromatogram area report of 8-hr reaction aliquot from the synthesis of 4-allylcatechol from 2-allyloxyphenol

Peak #	Ret Time	Type	Width	Area	Start Time	End Time
1	2.416	BV	0.032	2591869	2.377	2.518
2	3.696	BB	0.026	322517	3.555	3.785
3	9.911	BV	0.035	25319021	9.846	10.366
4	10.506	VV	0.032	1.82E+08	10.366	10.811
5	12.496	BV	0.053	4954876	12.409	12.805
6	12.864	VB	0.024	67802377	12.805	13.115
7	13.697	BV	0.034	24181174	13.583	13.822
8	13.84	VV	0.042	1373575	13.822	13.904
9	13.943	VV	0.037	2554350	13.904	14.059
10	14.234	BV	0.034	1283157	14.162	14.279
11	15.774	BV	0.034	267064	15.649	15.831
12	15.868	VB	0.027	523778	15.831	15.928
13	19.079	BV	0.059	1193533	19.021	19.283
14	20.774	VV	0.076	2431664	20.692	20.929
15	20.987	VV	0.072	1134279	20.929	21.163
16	24.793	PV	0.069	238356	24.633	24.804
17	24.917	VV	0.074	423975	24.804	24.932
18	24.954	VV	0.033	139231	24.932	24.972
19	25.166	VV	0.094	729240	24.972	25.212
20	25.225	VV	0.021	105222	25.212	25.237
21	25.317	VB	0.093	600664	25.237	25.405
22	25.915	PV	0.121	423631	25.741	25.95
23	26.084	VV	0.087	273349	25.989	26.106
24	26.656	VV	0.067	700180	26.608	26.784

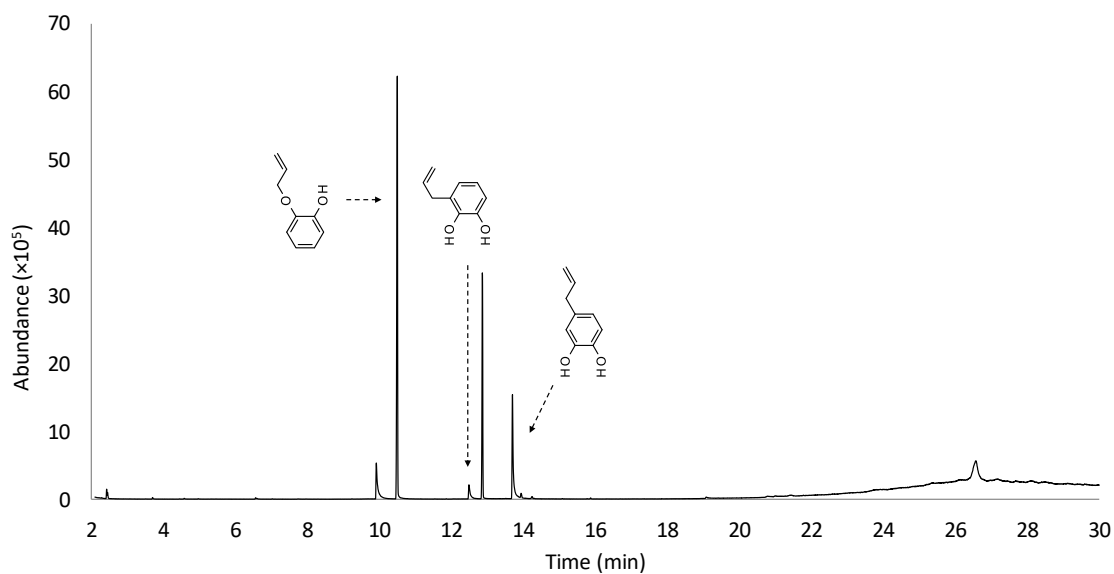


Figure A2-4: GC-MS total ion chromatogram of 24-hr reaction aliquot from the synthesis of 4-allylcatechol from 2-allyloxyphenol

Table A2-3: GC-MS total ion chromatogram area report of 24-hr reaction aliquot from the synthesis of 4-allylcatechol from 2-allyloxyphenol

Peak #	Ret Time	Type	Width	Area	Start Time	End Time
1	2.414	PV	0.017	1485354	2.388	2.429
2	2.44	VB	0.022	1208231	2.429	2.504
3	3.691	PB	0.03	480968	3.563	3.797
4	6.555	BV	0.011	70516	6.475	6.577
5	9.91	BV	0.046	17439207	9.818	10.302
6	10.49	BV	0.026	1.01E+08	10.405	10.751
7	12.484	BV	0.047	7110497	12.436	12.789
8	12.857	VV	0.024	48823205	12.789	13.063
9	13.692	BV	0.047	34248088	13.638	13.899
10	13.933	VV	0.038	1900855	13.899	14.05
11	14.237	BV	0.035	615356	14.13	14.272
12	15.864	BV	0.027	266160	15.808	15.939
13	19.082	BB	0.056	659982	19.009	19.176
14	20.78	PV	0.125	1645220	20.535	20.953
15	20.996	VV	0.042	496613	20.953	21.02
16	21.039	VV	0.045	393191	21.02	21.092
17	21.424	VV	0.115	1568304	21.286	21.56
18	21.78	VV	0.103	535185	21.56	21.873
19	21.95	VV	0.067	192499	21.873	21.996
20	22.218	VV	0.114	442806	21.996	22.23
21	22.324	VV	0.092	209481	22.23	22.376
22	22.39	PV	0.027	52397	22.376	22.422
23	22.471	VV	0.033	81151	22.445	22.524
24	22.604	PV	0.056	186420	22.524	22.637
25	23.02	VV	0.066	416635	22.934	23.061
26	23.092	VV	0.036	188451	23.061	23.109
27	23.715	PV	0.09	1408327	23.365	23.725
28	23.765	VV	0.046	605607	23.725	23.778

Peak #	Ret Time	Type	Width	Area	Start Time	End Time
29	23.807	VV	0.063	818509	23.778	23.857
30	23.92	VV	0.064	865338	23.857	23.956
31	24.018	VV	0.07	482558	23.956	24.03
32	24.041	VV	0.053	304646	24.03	24.127
33	24.156	PV	0.023	99101	24.127	24.177
34	24.24	VV	0.041	259215	24.177	24.256
35	24.299	VV	0.043	241088	24.256	24.325
36	24.341	VV	0.025	105319	24.325	24.361
37	24.405	VV	0.037	169476	24.361	24.416
38	24.522	VV	0.078	424050	24.416	24.536
39	24.543	VV	0.012	36608	24.536	24.551
40	24.567	VV	0.023	60437	24.551	24.594
41	24.81	BV	0.061	701712	24.674	24.832
42	24.85	VV	0.034	296927	24.832	24.872
43	24.885	VV	0.025	244608	24.872	24.908
44	24.922	VV	0.029	231221	24.908	24.94
45	24.964	VV	0.027	260179	24.94	24.975
46	25.043	VV	0.059	790213	24.975	25.062
47	25.11	VV	0.052	547545	25.062	25.122
48	25.281	VV	0.126	2677723	25.122	25.292
49	25.34	VV	0.045	1440024	25.292	25.351
50	25.387	VV	0.067	1952888	25.351	25.424
51	25.435	VV	0.023	585132	25.424	25.448
52	25.483	VV	0.039	1220089	25.448	25.499
53	25.536	VV	0.076	2808301	25.499	25.614
54	25.642	VV	0.048	1520247	25.614	25.677
55	25.687	VV	0.027	705274	25.677	25.705
56	25.745	VV	0.047	1265438	25.705	25.755
57	25.767	VV	0.026	713239	25.755	25.784
58	25.966	VV	0.134	5579865	25.784	25.992
59	26.133	VV	0.099	5709259	25.992	26.153
60	26.168	VV	0.03	1187183	26.153	26.183
61	26.201	VV	0.04	1610330	26.183	26.226
62	26.265	VV	0.055	2088896	26.226	26.284
63	26.313	VV	0.042	1923072	26.284	26.336
64	26.572	VV	0.16	43818021	26.336	26.911
65	26.971	VV	0.073	1942912	26.911	27.021
66	27.13	VV	0.074	2483087	27.021	27.143
67	27.167	VV	0.037	1130179	27.143	27.188
68	27.197	VB	0.098	2380089	27.188	27.411
69	27.68	PV	0.086	1145324	27.625	27.783
70	28.115	VV	0.107	2056055	27.95	28.145
71	28.153	VV	0.06	926366	28.145	28.223
72	28.4	PV	0.047	442724	28.315	28.413
73	28.473	VV	0.049	703673	28.413	28.499
74	28.509	VB	0.06	613679	28.499	28.646
75	29.117	PV	0.081	206594	29.005	29.129

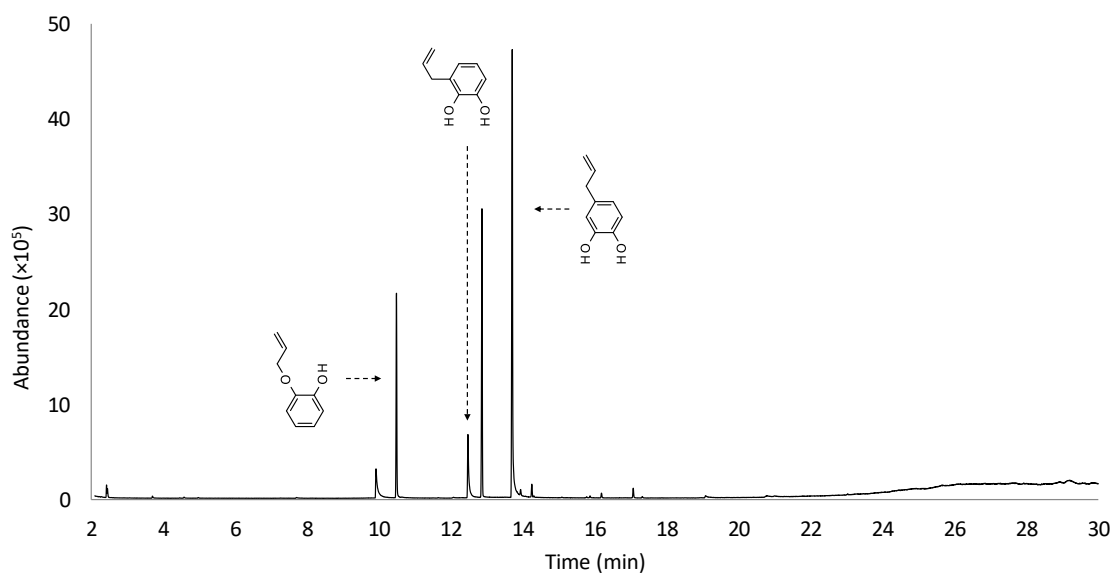


Figure A2-5: GC-MS total ion chromatogram of 48-hr reaction aliquot from the synthesis of 4-allylcatechol from 2-allyloxyphenol

Table A2-4: GC-MS total ion chromatogram area report of 48-hr reaction aliquot from the synthesis of 4-allylcatechol from 2-allyloxyphenol

Peak #	Ret Time	Type	Width	Area	Start Time	End Time
1	2.414	PV	0.017	1439418	2.377	2.429
2	2.44	VB	0.022	1191672	2.429	2.528
3	3.692	BV	0.026	365032	3.662	3.757
4	9.91	BV	0.052	11362504	9.834	10.279
5	10.477	BV	0.023	30559208	10.35	10.597
6	12.466	BV	0.036	16636859	12.262	12.797
7	12.856	PB	0.024	44921565	12.797	13.027
8	13.697	BV	0.028	85383046	13.622	13.903
9	13.931	VV	0.035	1841884	13.903	14.059
10	14.243	BV	0.024	2046901	14.158	14.277
11	15.863	VV	0.032	447093	15.82	15.971
12	16.181	VB	0.027	860725	16.145	16.288
13	17.064	BB	0.026	1699982	16.978	17.173
14	17.316	BB	0.029	277513	17.244	17.397
15	19.077	BB	0.059	959681	19.009	19.263
16	20.778	PV	0.082	1041185	20.545	20.909
17	20.987	VV	0.085	568407	20.909	21.111
18	23.027	PV	0.028	224191	22.972	23.082
19	23.818	PV	0.107	485548	23.587	23.834
20	24.292	VV	0.094	765246	24.147	24.304
21	24.313	VV	0.016	120648	24.304	24.322
22	24.468	VV	0.102	1365704	24.322	24.486
23	24.587	VV	0.102	1070189	24.486	24.606
24	24.633	VV	0.052	600569	24.606	24.67
25	24.892	VV	0.201	2695221	24.67	24.905
26	24.939	VV	0.042	621080	24.905	24.955
27	25.074	VV	0.149	1645384	24.955	25.127

Peak #	Ret Time	Type	Width	Area	Start Time	End Time
28	25.147	VV	0.062	763469	25.127	25.221
29	25.288	VV	0.037	433319	25.253	25.307
30	25.471	VV	0.132	1928417	25.307	25.481
31	25.523	VV	0.046	892259	25.481	25.542
32	25.661	VV	0.141	3678113	25.542	25.738
33	25.748	VV	0.022	418395	25.738	25.761
34	25.798	VV	0.062	1119851	25.761	25.824
35	25.88	VV	0.054	1306224	25.824	25.9
36	26.103	VV	0.148	4372378	25.9	26.121
37	26.131	VV	0.074	1610004	26.121	26.2
38	26.213	VV	0.024	470666	26.2	26.226
39	26.265	VV	0.048	1139401	26.226	26.291
40	26.344	VV	0.111	2725143	26.291	26.449
41	26.475	VV	0.055	1196963	26.449	26.523
42	27.631	VV	0.098	565515	27.478	27.684
43	28.926	PB	0.101	1164718	28.731	29.021
44	29.2	BV	0.166	3847562	29.025	29.434
45	29.85	PV	0.027	114167	29.695	29.862

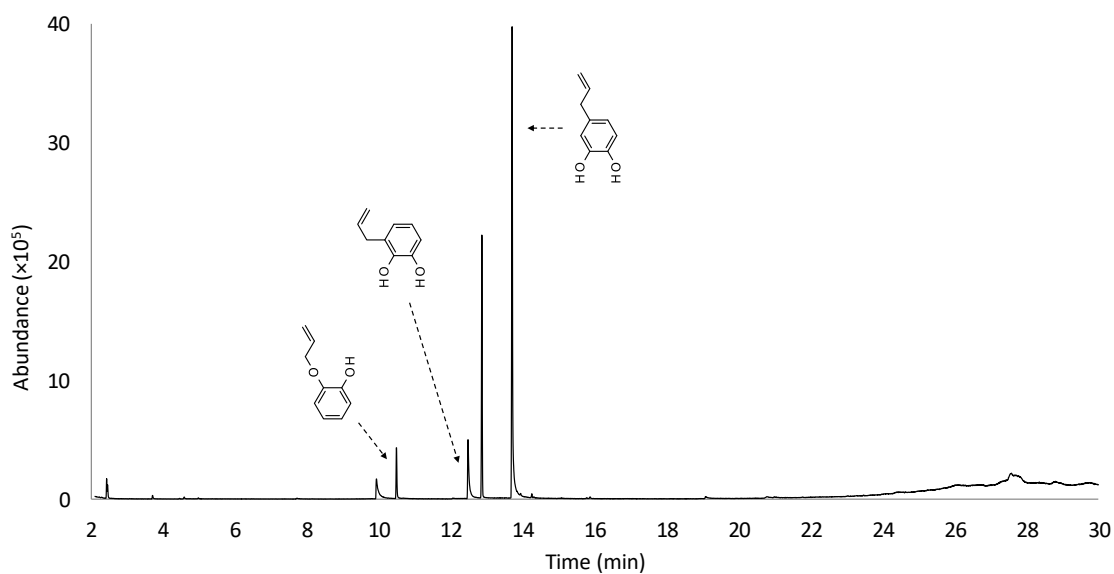


Figure A2-6: GC-MS total ion chromatogram of 72-hr reaction aliquot from the synthesis of 4-allylcatechol from 2-allyloxyphenol

Table A2-5: GC-MS total ion chromatogram area report of 72-hr reaction aliquot from the synthesis of 4-allylcatechol from 2-allyloxyphenol

Peak #	Ret Time	Type	Width	Area	Start Time	End Time
1	2.414	PV	0.021	1782008	2.389	2.429
2	2.44	VV	0.022	1519111	2.429	2.521
3	3.691	BB	0.026	491637	3.634	3.769
4	4.572	BV	0.032	335521	4.495	4.654
5	9.92	PB	0.063	7819351	9.788	10.346
6	10.476	BV	0.025	6787382	10.354	10.616
7	12.467	PV	0.04	13769655	12.436	12.738
8	12.852	BB	0.023	31678709	12.789	13.075
9	13.694	BV	0.028	72644336	13.638	13.907
10	13.931	VV	0.044	1047430	13.907	14.055
11	14.242	BV	0.022	471874	14.19	14.274
12	15.862	BV	0.034	248366	15.828	15.929
13	19.075	BV	0.07	877864	18.985	19.307
14	20.778	BB	0.058	314281	20.62	20.846
15	24.459	PV	0.218	1148865	24.221	24.61
16	26.113	PV	0.169	1713018	24.61	26.194
17	26.223	VB	0.093	505615	26.194	26.336
18	27.581	BV	0.166	12498060	26.863	27.641
19	27.698	VV	0.233	10310335	27.641	28.025
20	28.807	BV	0.179	3625735	28.644	29.219
21	29.767	VBA	0.23	3103040	29.486	29.977

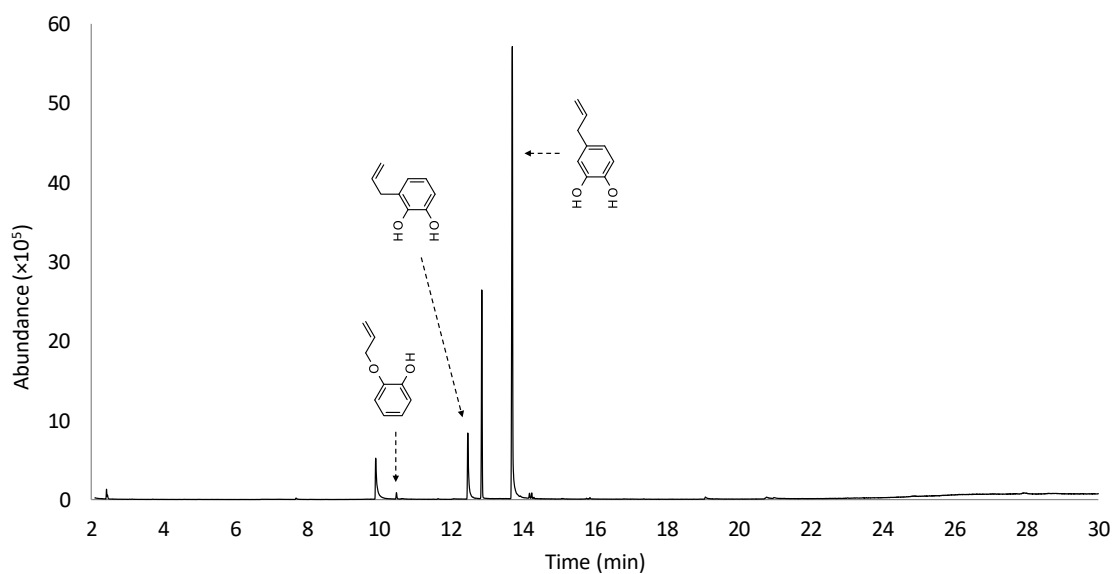


Figure A2-7: GC-MS total ion chromatogram of 96-hr reaction aliquot from the synthesis of 4-allylcatechol from 2-allyloxyphenol

Table A2-6: GC-MS total ion chromatogram area report of 96-hr reaction aliquot from the synthesis of 4-allylcatechol from 2-allyloxyphenol

Peak #	Ret Time	Type	Width	Area	Start Time	End Time
1	2.414	BV	0.024	2001993	2.349	2.54
2	7.686	BB	0.034	367542	7.553	7.779
3	9.901	BV	0.058	17700468	9.834	10.425
4	10.478	VV	0.027	1392497	10.425	10.576
5	12.463	BV	0.036	20845720	12.417	12.77
6	12.852	PV	0.024	38881457	12.77	12.948
7	13.699	BV	0.029	1.09E+08	13.4	13.915
8	13.928	VB	0.068	1112257	13.915	14.106
9	14.177	BV	0.023	897958	14.146	14.21
10	14.24	VV	0.023	1002620	14.21	14.277
11	14.3	VV	0.025	240916	14.277	14.349
12	15.861	VB	0.031	368727	15.819	15.935
13	19.072	PV	0.059	1078781	19.024	19.243
14	20.774	PV	0.084	1382531	20.691	20.929
15	20.977	VV	0.062	626815	20.929	21.1
16	24.829	PV	0.058	181712	24.576	24.872
17	27.922	PV	0.085	958132	27.819	28.053

Appendix 3: NMR Spectra

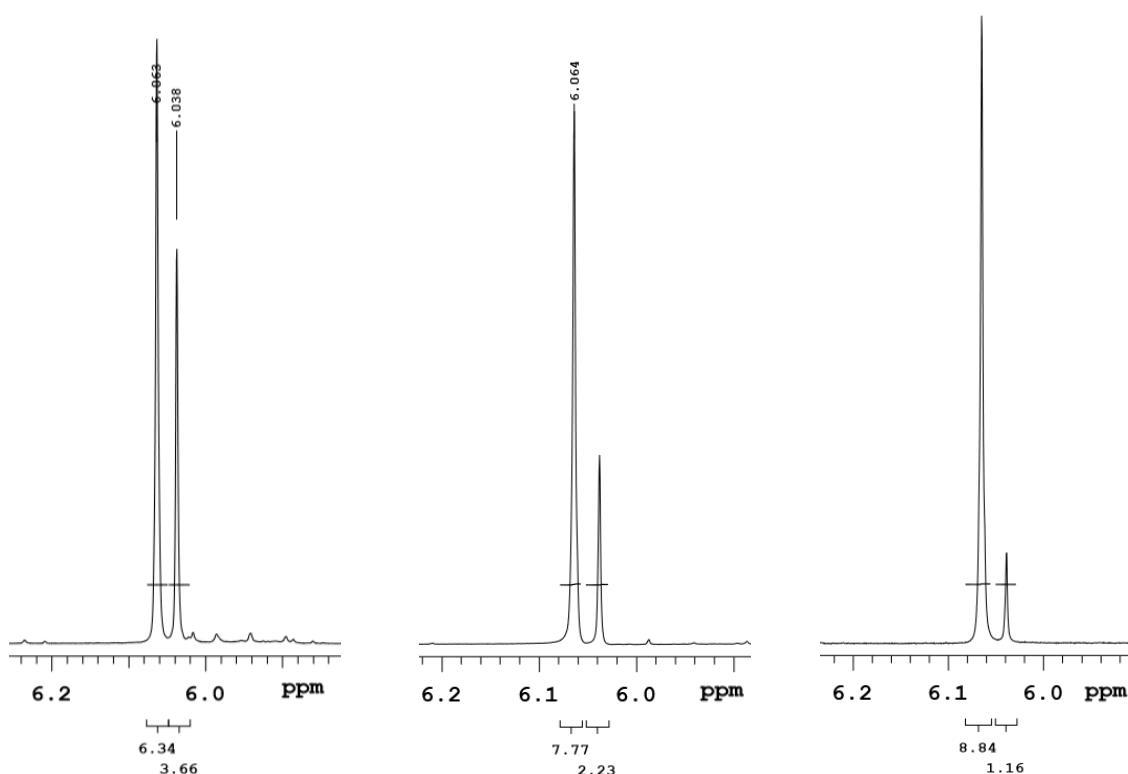


Figure A3- 1: Sections of the ^1H NMR spectra of the bromination of 3,4-methylenedioxypropiohenone reaction products showing starting material : product $\text{O}-\text{CH}_2-\text{O}$ ^1H integration ratio when the following reaction conditions were trialed: dichloromethane solvent and 18 hr reaction (left), dichloromethane solvent and 24 hr reaction (middle), and 1,2-dichloroethane solvent and 24 hr reaction (right).

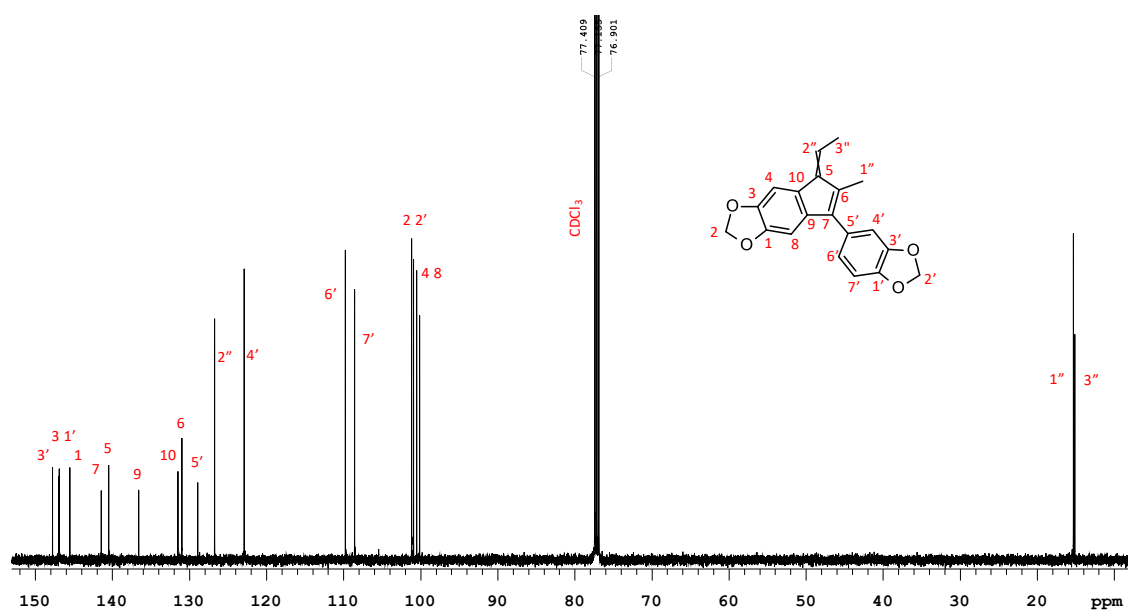


Figure A3-2: ^{13}C NMR spectrum of 7-(1,3-benzodioxol-5-yl)-5-ethylidene-6-methyl-cyclopenta[f][1,3]benzodioxole

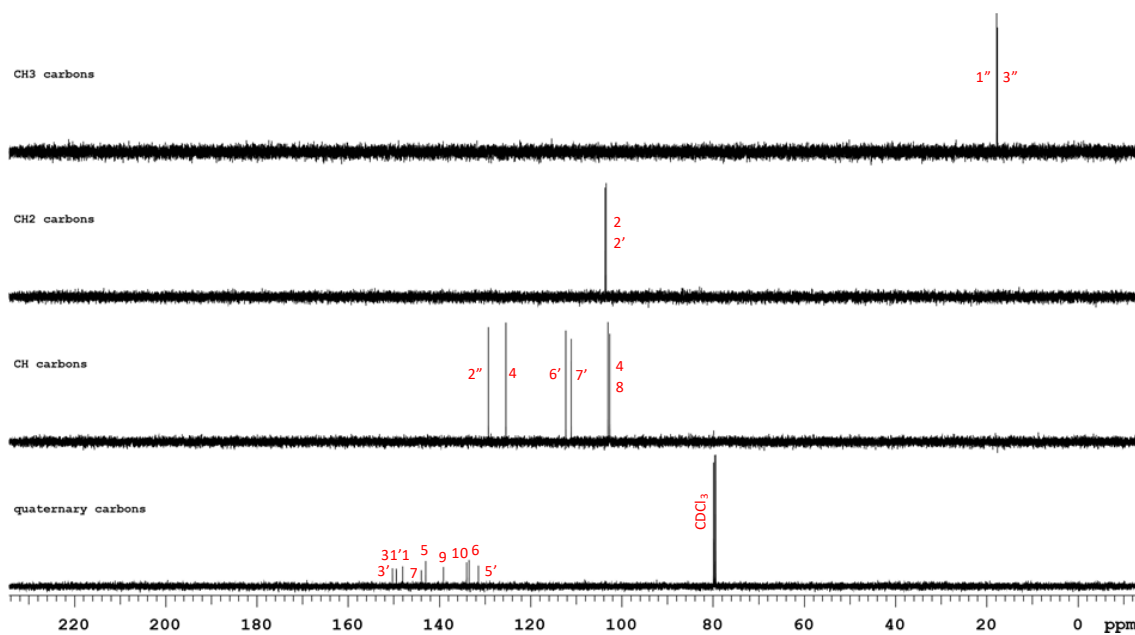


Figure A3-3: DEPT ^{13}C NMR spectrum of 7-(1,3-benzodioxol-5-yl)-5-ethylidene-6-methyl-cyclopenta[f][1,3]benzodioxole

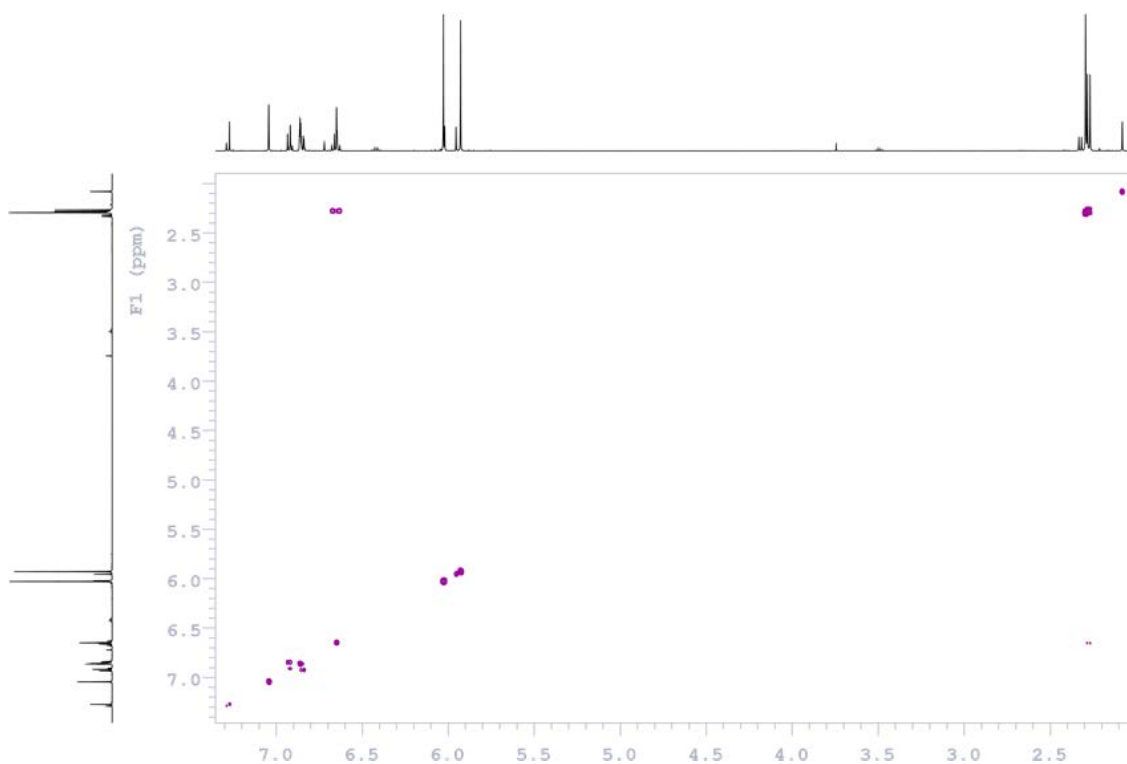


Figure A3-4: COSY NMR spectrum of 7-(1,3-benzodioxol-5-yl)-5-ethylidene-6-methyl-cyclopenta[f][1,3]benzodioxole

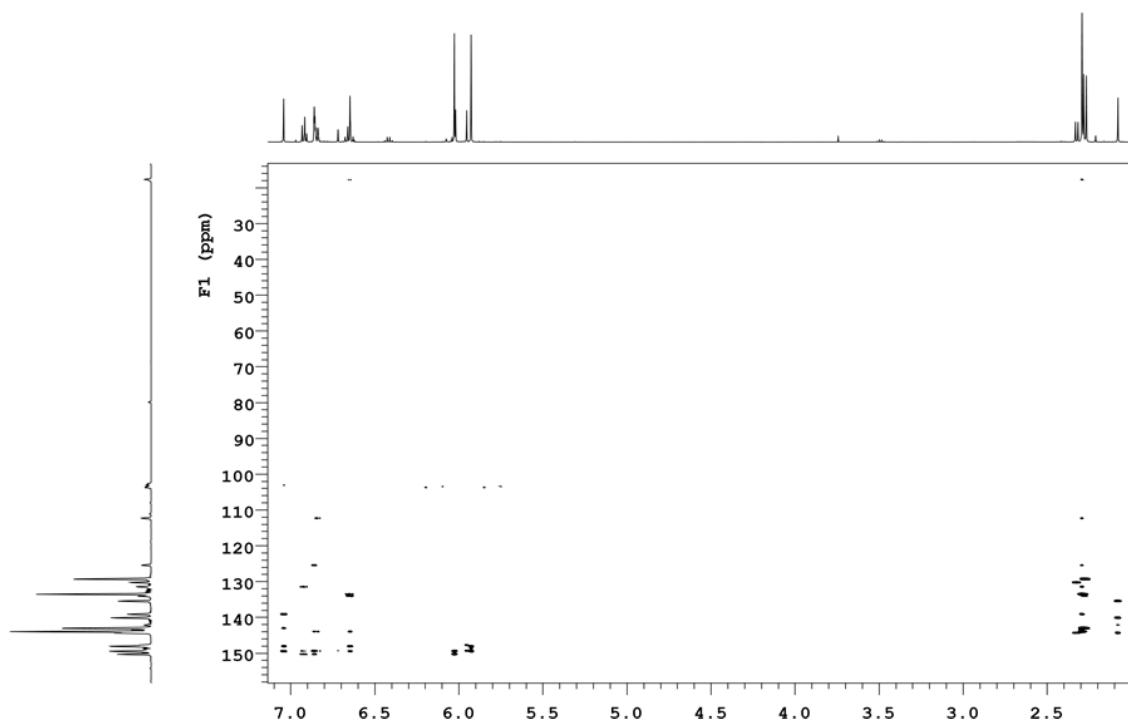


Figure A3-5: ^1H , ^{13}C - HMBC NMR spectrum of 7-(1,3-benzodioxol-5-yl)-5-ethylidene-6-methyl-cyclopenta[f][1,3]benzodioxole

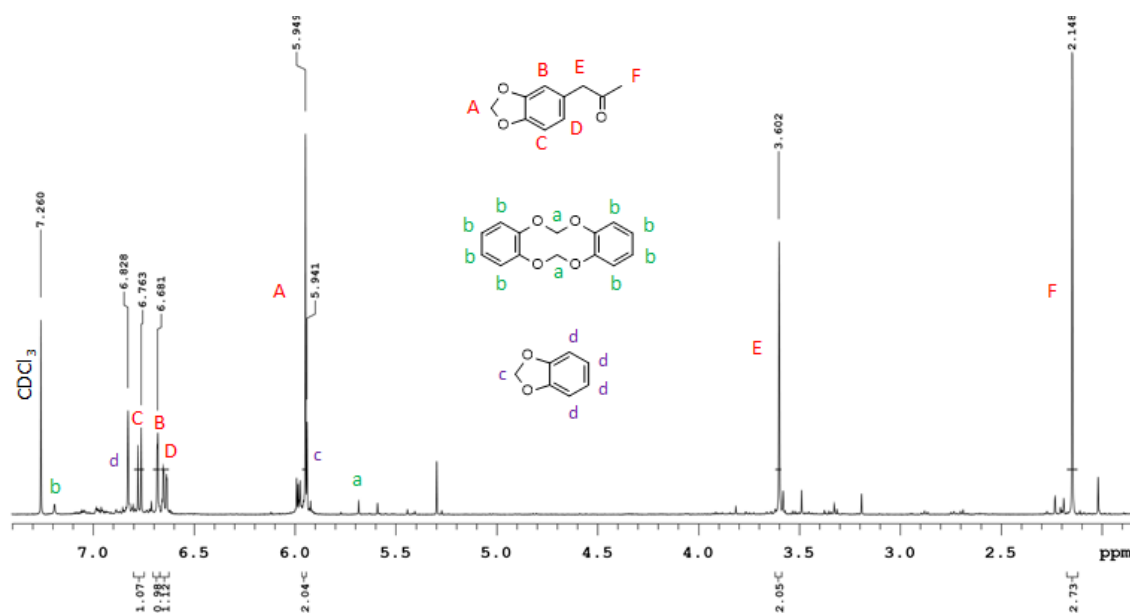
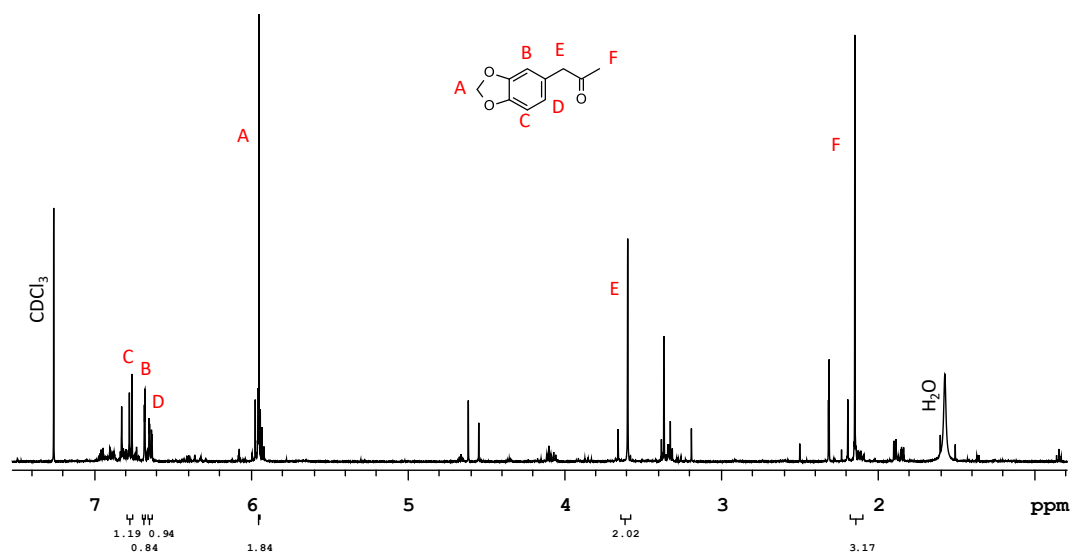
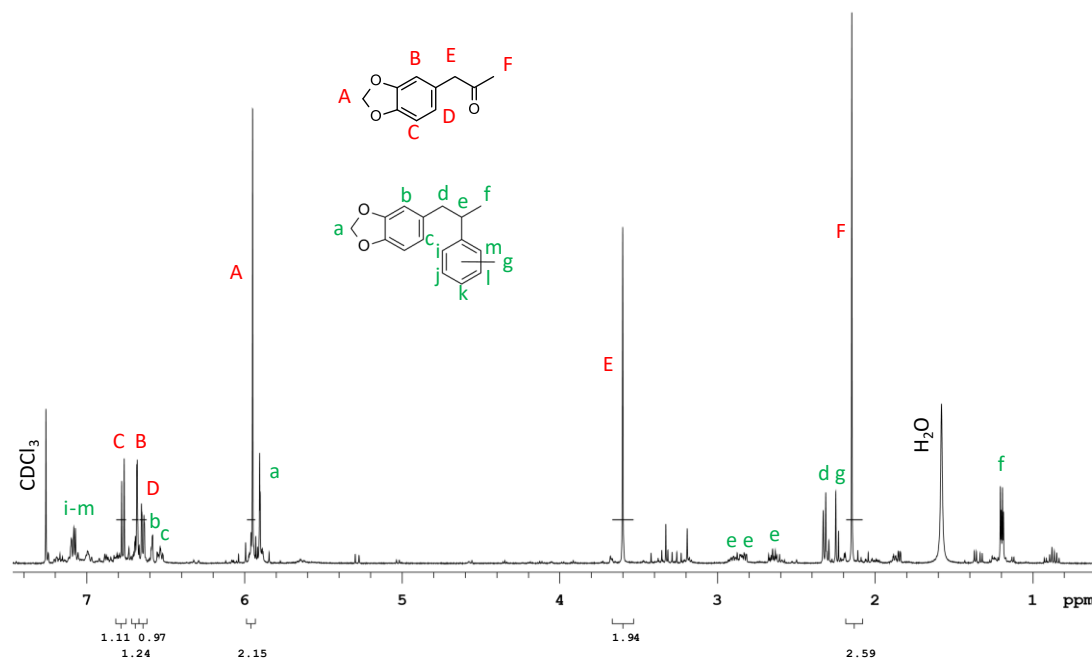


Figure A3-6: ^1H NMR spectrum of MDP2P synthesised via Route 1A

Figure A3-7: ^1H NMR spectrum of MDP2P synthesised via Route 2AFigure A3-8: ^1H NMR spectrum of MDP2P synthesised via Route 3A

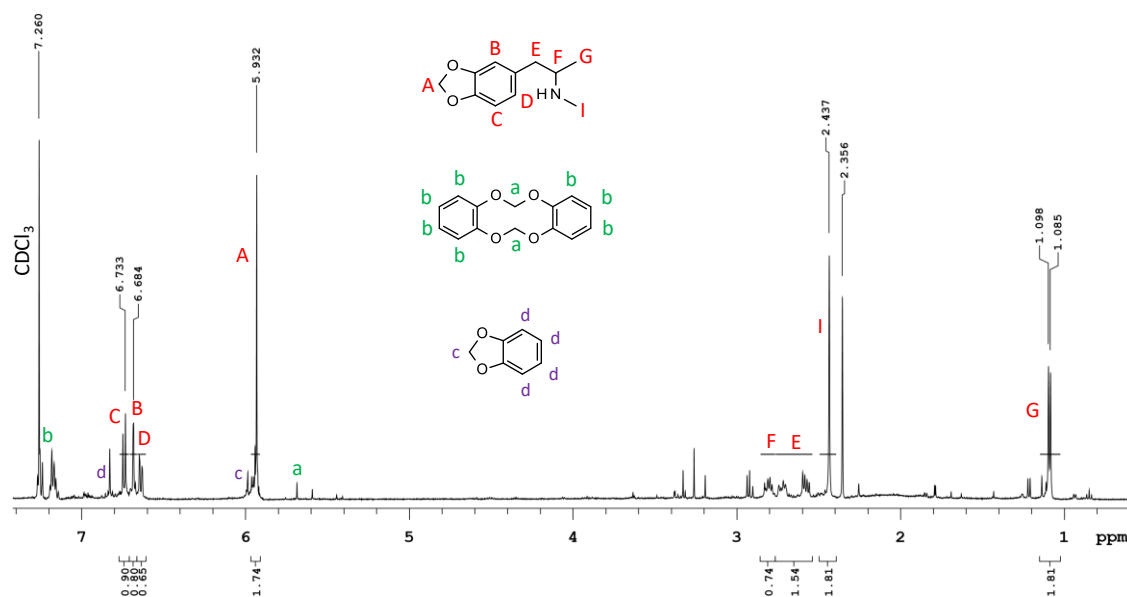


Figure A3-9: ¹H NMR spectrum of MDMA synthesised via Route 1A

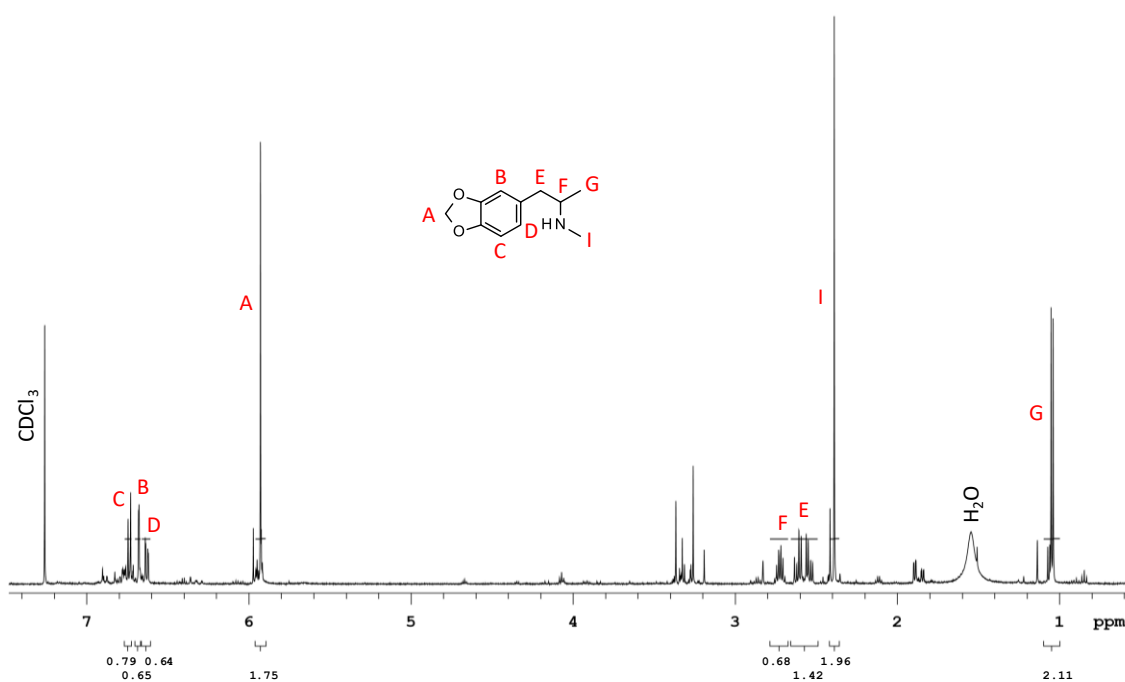
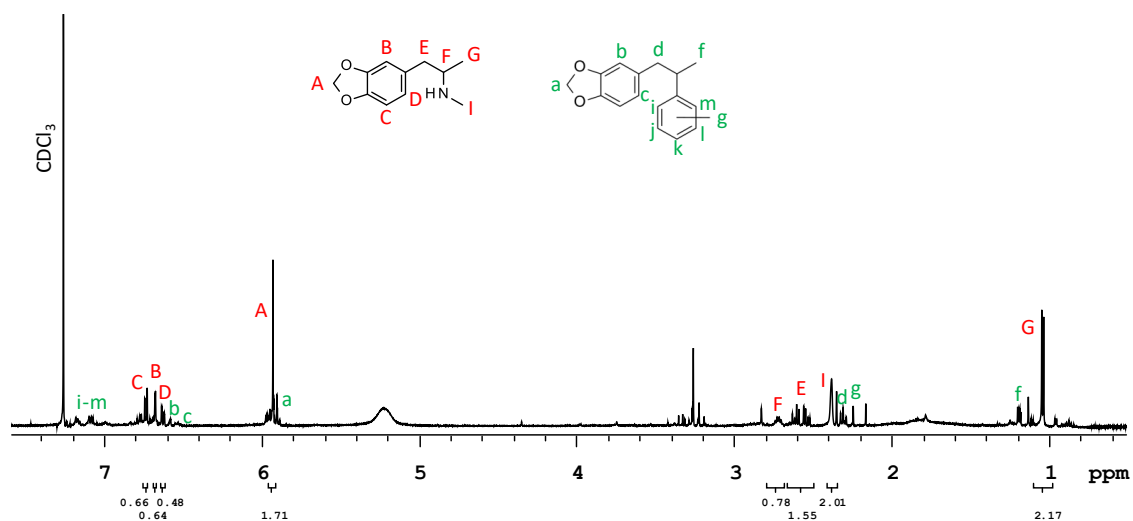
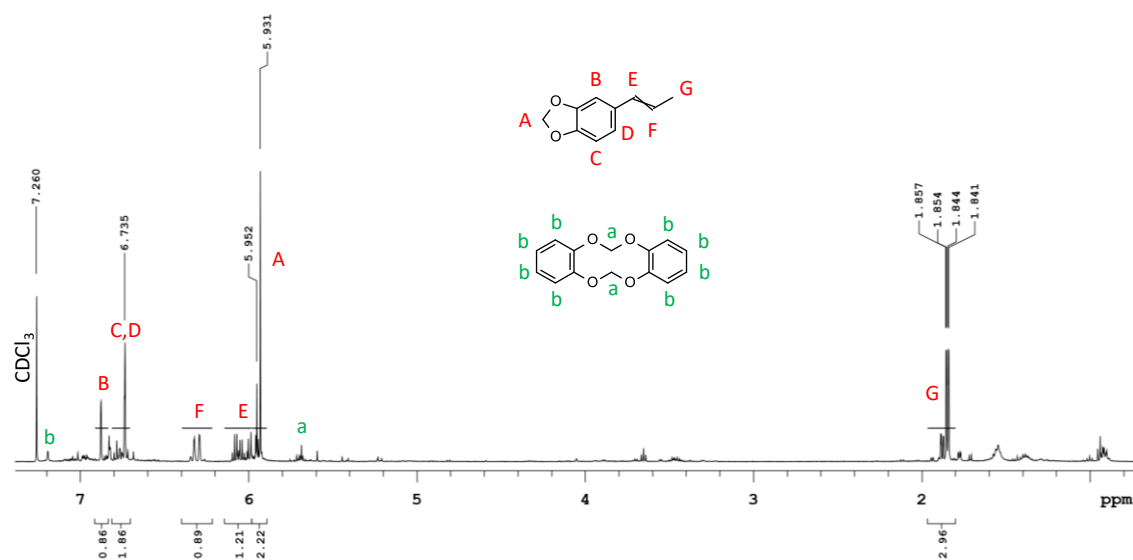
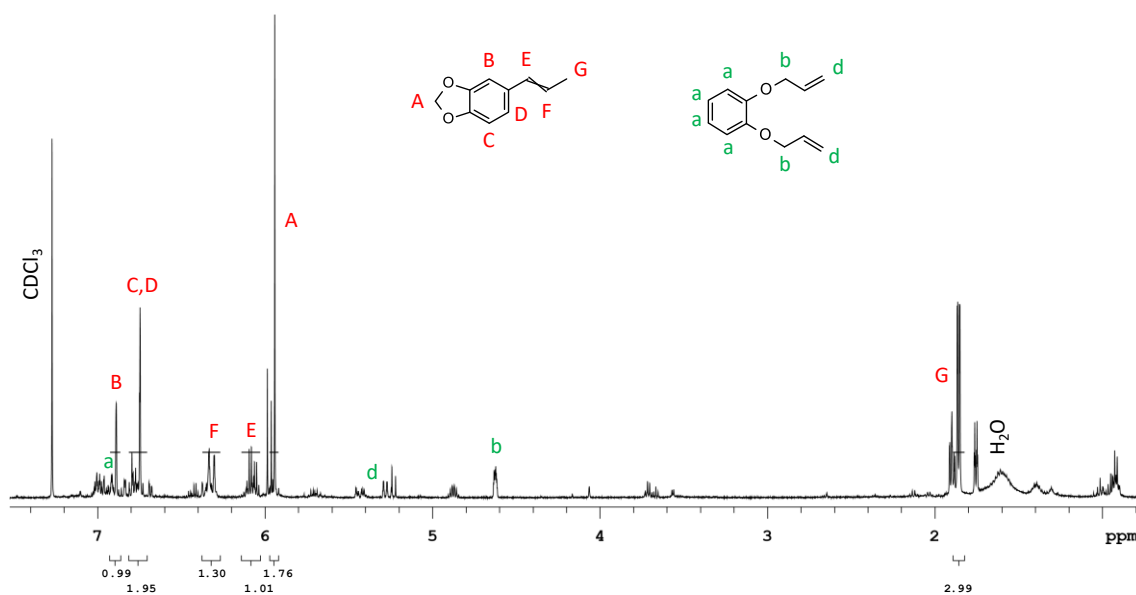
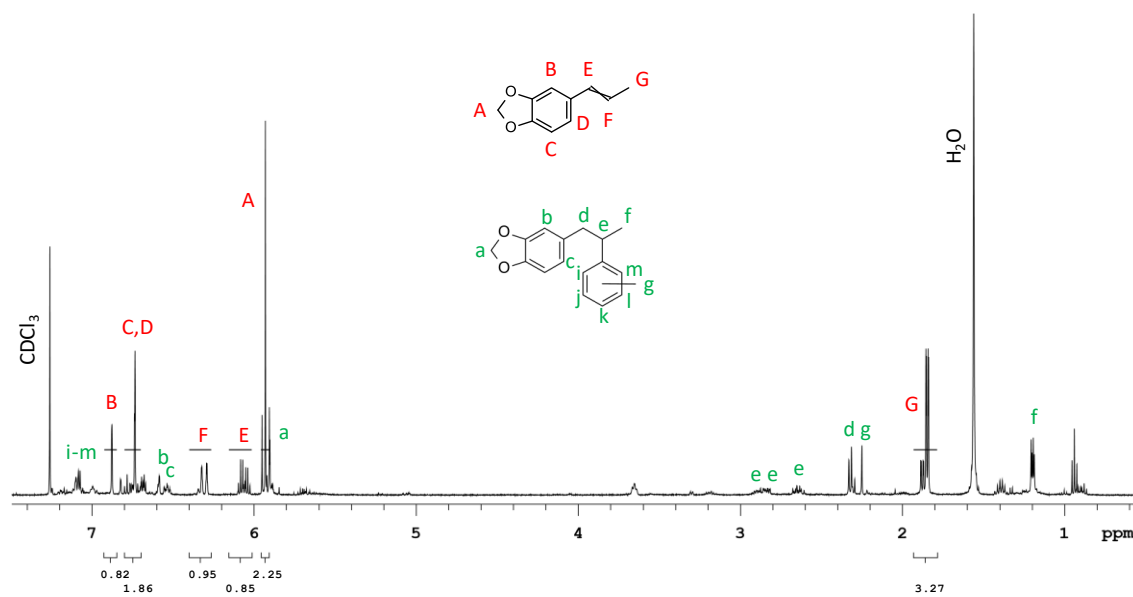
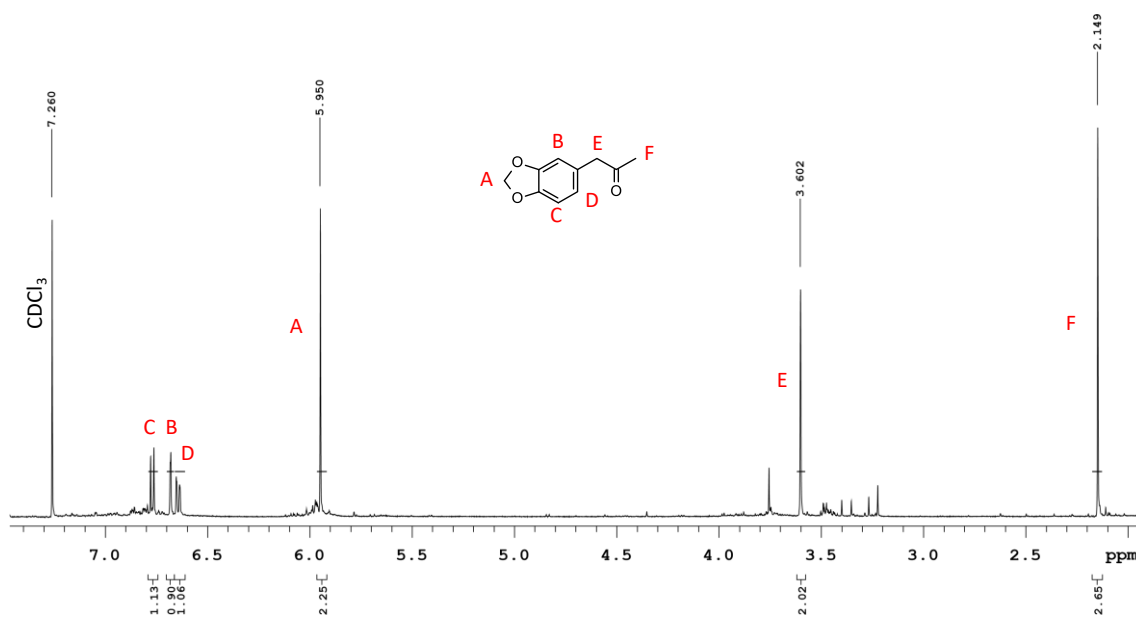
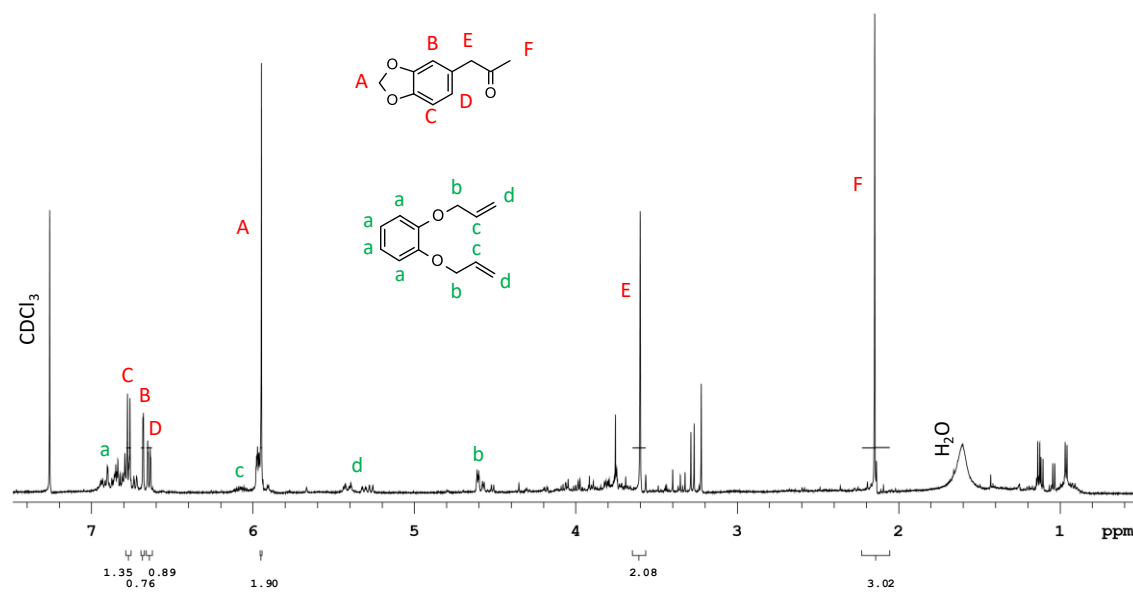
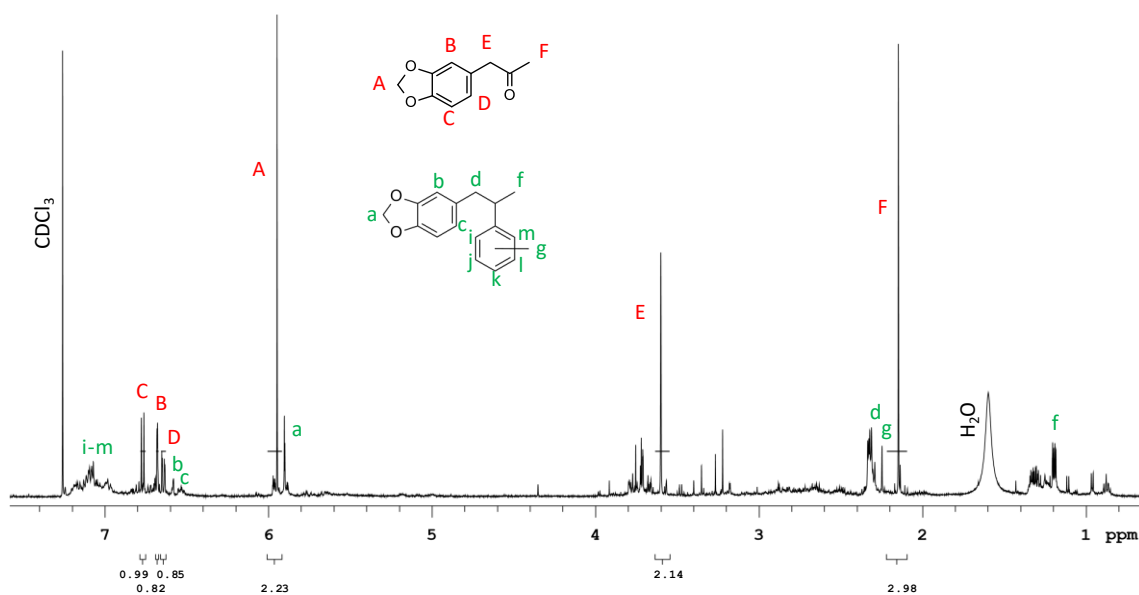
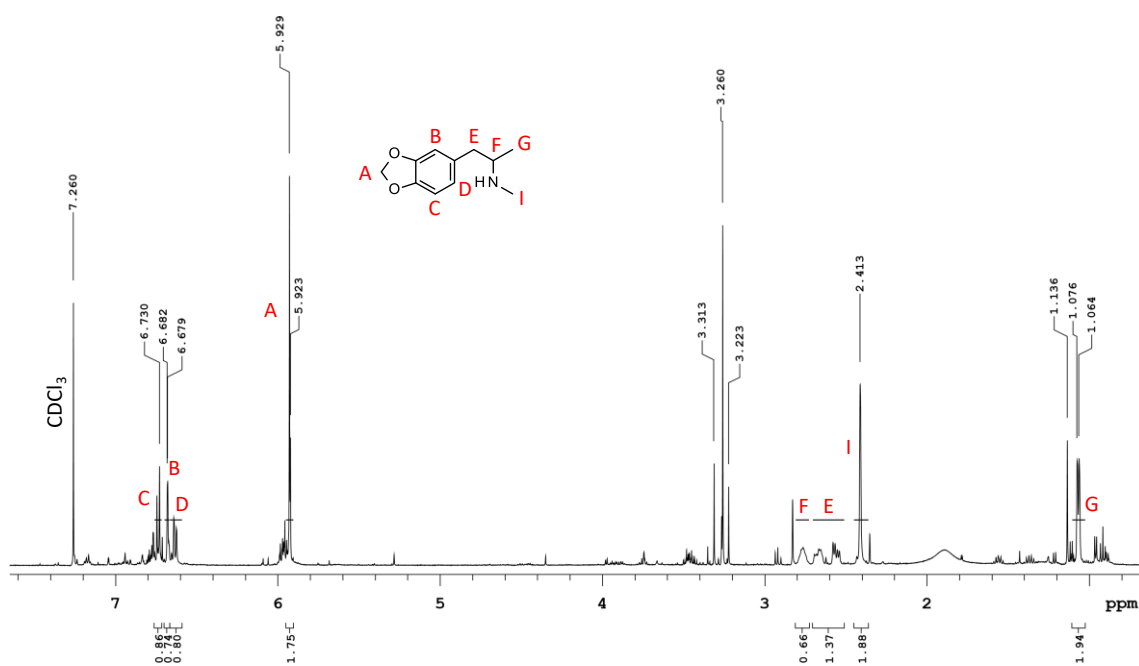


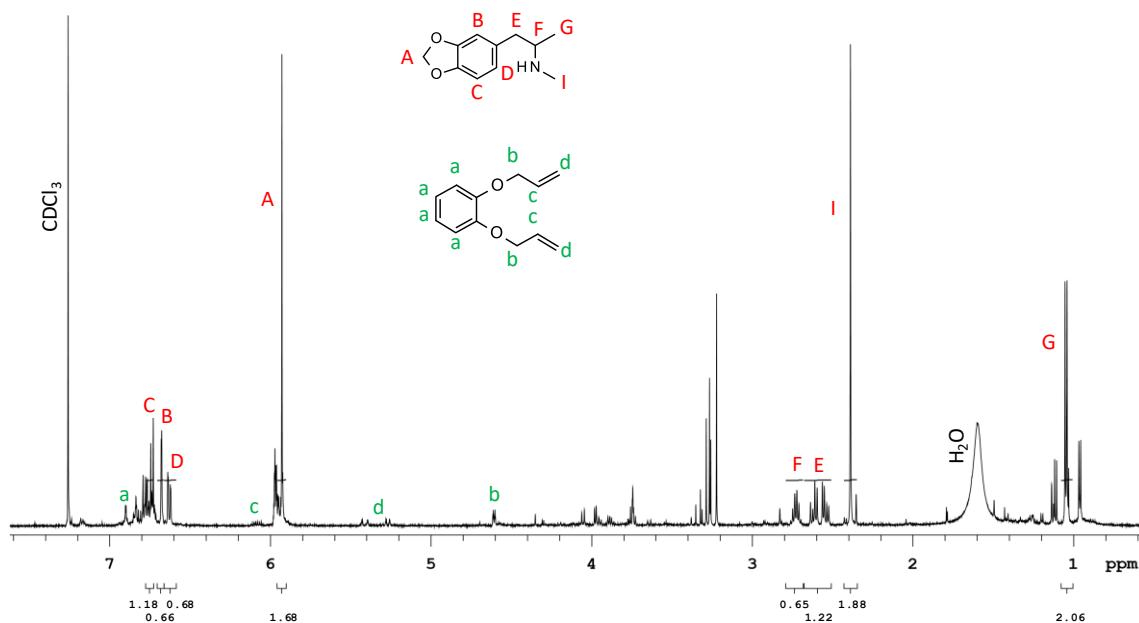
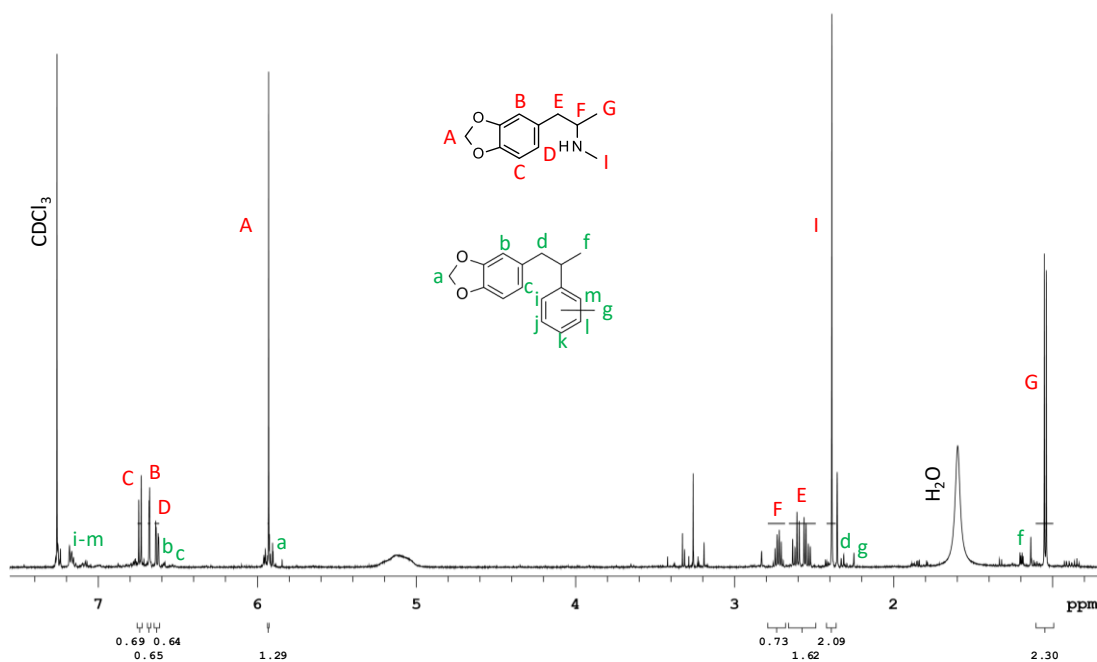
Figure A3-10: ^1H NMR spectrum of MDMA synthesised via Route 2A

Figure A3-11: ¹H NMR spectrum of MDMA synthesised via Route 3AFigure A3-12: ¹H NMR spectrum of isosafrole synthesised via Route 1B

Figure A3-13: ¹H NMR spectrum of isosafrole synthesised via Route 2BFigure A3-14: ¹H NMR spectrum of isosafrole synthesised via Route 3B

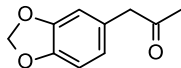
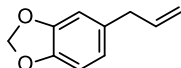
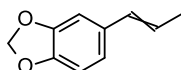
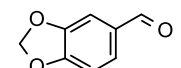
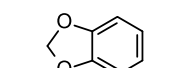
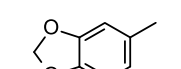
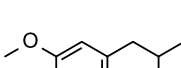
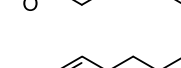
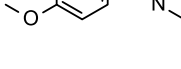
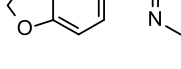
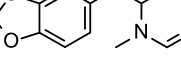
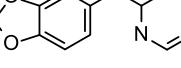
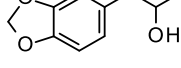
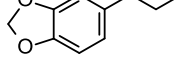
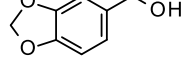
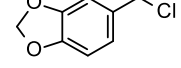
Figure A3-15: ¹H NMR spectrum of MDP2P synthesised via Route 1BFigure A3-16: ¹H NMR spectrum of MDP2P synthesised via Route 2B

Figure A3-17: ¹H NMR spectrum of MDP2P synthesised via Route 3BFigure A3-18: ¹H NMR spectrum of MDMA synthesised via Route 1B

Figure A3-19: ¹H NMR spectrum of MDMA synthesised via Route 2BFigure A3-20: ¹H NMR spectrum of MDMA synthesised via Route 3B

Appendix 4: Organic Impurities

Table A4-1: Organic impurities discussed in thesis chapters

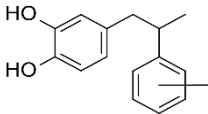
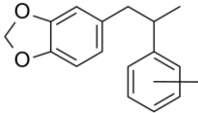
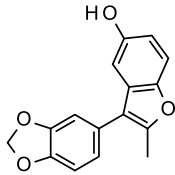
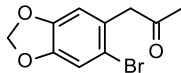
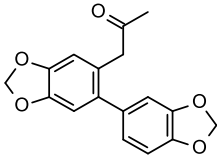
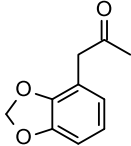
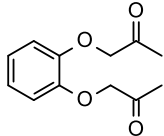
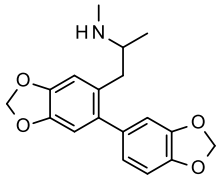
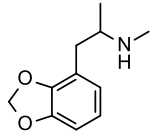
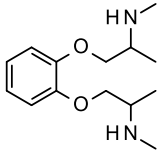
NO.	NAME	STRUCTURE	DISCUSSED IN CHAPTERS:			
			1	3	4	5
1	MDP2P		✓	X	X	✓
2	safole		✓	X	X	✓
3 (a-b)	isosafole		✓	X	✓	✓
4	piperonal		✓	X	X	X
5	1,3-benzodioxole		✓	X	✓	✓
6	3,4-methylenedioxy toluene		✓	X	X	X
7	N-methyl-1-[1,2-dimethoxy-4-(2-aminopropyl)]benzene		✓	X	X	X
8	PMA		✓	X	X	X
9	1,2-(methylenedioxy)-4-(2-N-methyl-aminopropyl) benzene		✓	X	X	X
10	N-formyl-3,4-methylene dioxymethamphetamine		✓	X	X	X
11	N-formyl-3,4-methylene dioxymphetamine		✓	X	X	X
12	1-(3,4-methylenedioxy) phenyl-propan-2-ol		✓	X	X	X
13	3,4-methylenedioxy yphenylpropane		✓	X	X	X
14	3,4-methylenedioxy phenylmethanol		✓	X	X	X
15	piperonyl chloride		✓	X	X	X
16	3,4-methylenedioxy-N-methylbenzylamine		✓	X	X	X

NO.	NAME	STRUCTURE	DISCUSSED IN CHAPTERS:			
			1	3	4	5
17	MDA		✓	X	X	X
18	N,N-dimethyl-3,4-methylenedioxy amphetamine		✓	X	X	X
19	N-ethyl-3,4-methylenedioxy amphetamine		✓	X	X	X
20	N-ethyl-N-methyl-3,4-methylenedioxy amphetamine		✓	X	X	X
21	N,N-di-(1-3,4-methylenedioxy)phenyl-2-propylmethylamine		✓	X	X	X
22 (a-c)	2,4-dimethyl-3,5-bis(3,4-methylenedioxyphenyl) tetrahydrofuran		✓	X	X	✓
23	3,4-methylenedioxy propiophenone		✓	✓	X	X
24 (a-b)	1-(1,3-benzodioxol-5-yl)-1-methoxy-propan-2-ol		✓	X	X	✓
25	1-(3,4-methylenedioxy phenyl)-1-methoxy propan-2-one		✓	X	X	✓
26	1-(3,4-methylenedioxyphenyl)-1-methoxypropane		✓	X	X	✓
27	methyl 3-(1,3-benzodioxol-5-yl)propanoate		✓	X	X	X
28	1-(3,4-methylenedioxyphenyl)-1,3-dimethoxypropane		✓	X	X	✓

NO.	NAME	STRUCTURE	DISCUSSED IN CHAPTERS:			
			1	3	4	5
29	3-(3,4-methylenedioxyphenyl)-1,1-dimethoxypropane		✓	X	X	✓
30	piperonylnitrile		✓	X	X	X
31	1-(3,4-methylenedioxyphenyl)-2-propanone oxime		✓	X	X	X
32	piperonal dimer		✓	X	X	X
33	vanillin dimer		✓	X	X	X
34	N-acetylpiperidine		✓	X	X	X
35	(5-(1,3-benzodioxol-5-yl)-1-(1-piperidyl)pent-4-en-1-one		✓	X	X	X
36	(5-(1,3-benzodioxol-5-yl)-1-(1-piperidyl)pent-2-en-1-one		✓	X	X	X
37	2-chloro-4,5-methylenedioxyphenyl-2-propanone		✓	X	X	X
38	2-chloro-4,5-methylenedioxy methamphetamine		✓	X	X	X
39	1,3-benzodioxole dimer		✓	✓	✓	✓
40 (a-c)	4,4'-, 4,5'-, and 5,5'-methylenebis-1,3-benzodioxole		✓	✓	✓	✓
41	5-bromo-1,3-benzodioxole		✓	X	✓	✓
42	5,5'-bi-1,3-benzodioxole		✓	X	✓	✓

NO.	NAME	STRUCTURE	DISCUSSED IN CHAPTERS:			
			1	3	4	5
43	1-(1,3-benzodioxol-5-yl)-2-methylimino-propan-1-one		✓	✓	X	X
44	dibutyl benzene-1,2-dicarboxylate		✓	X	X	X
45	N-methylpropanamide		✓	X	X	X
46	[1,3]dioxolo[4,5-b]oxanthrene		X	✓	X	X
47	1,3-benzodioxole trimer		X	✓	✓	✓
48	(2-hydroxyphenyl) propanoate		X	✓	X	X
49	[2-(chloromethoxy)phenyl] propanoate		X	✓	X	X
50	(2-propanoyloxyphenyl) propanoate		X	✓	X	X
51	5-[1-(1,3-benzodioxol-5-yl)prop-1-enyl]-1,3-benzodioxole		X	✓	X	X
52 (a-b)	(5E)- and (5Z)-7-(1,3-benzodioxol-5-yl)-5-ethylidene-6-methylcyclopenta[f][1,3]benzodioxole		X	✓	X	X
53	[2-(bromomethoxy)phenyl] propanoate		X	✓	X	X

NO.	NAME	STRUCTURE	DISCUSSED IN CHAPTERS:			
			1	3	4	5
54	1-(1,3-benzodioxol-5-yl)-N-methyl-propan-1-imine		X	✓	X	X
55	1-(1,3-benzodioxol-5-yl)-N1, N2-dimethyl-propane-1,2-diimine		X	✓	X	X
56	butylated hydroxytoluene		X	✓	X	X
57	5,6-dibromo-1,3-benzodioxole		X	X	✓	X
58	5-bromo-6-(2-propenyl)-1,3-benzodioxole		X	X	✓	X
59	5-allyl-6-(1,3-benzodioxol-5-yl)-1,3-benzodioxole		X	X	✓	X
60	catechol		X	X	✓	X
61	1,2-diallyloxybenzene		X	X	✓	✓
62	2-allyloxyphenol		X	X	✓	X
63	3-allylcatechol		X	X	✓	X
64	4-allyl-1,3-benzodioxole		X	X	✓	X
65 (a-b)	4-propen-1-enyl-1,3-benzodioxole		X	X	✓	✓
66	safrole dimer		X	X	✓	X

NO.	NAME	STRUCTURE	DISCUSSED IN CHAPTERS:			
			1	3	4	5
67 (a-c)	4-[2-(<i>o</i> , <i>p</i> and <i>m</i> -tolyl)propyl]benzene-1,2-diol		X	X	✓	X
68 (a-c)	4-[2-(<i>o</i> , <i>p</i> and <i>m</i> -tolyl)propyl]1,3-benzodioxole		X	X	✓	✓
69	3-(1,3-benzodioxol-5-yl)-2-methyl-benzofuran-5-ol		X	X	X	✓
70	1-(6-bromo-1,3-benzodioxol-5-yl)propan-2-one		X	X	X	✓
71	1-[6-(1,3-benzodioxol-5-yl)-1,3-benzodioxol-5-yl]propan-2-one		X	X	X	✓
72	1-(1,3-benzodioxol-4-yl)propan-2-one		X	X	X	✓
73	1-(2-acetonyloxyphenoxy)propan-2-one		X	X	X	✓
74	1-[6-(1,3-benzodioxol-5-yl)-1,3-benzodioxol-5-yl]-N-methyl-propan-2-amine		X	X	X	✓
75	1-(1,3-benzodioxol-4-yl)-N-methyl-propan-2-amine		X	X	X	✓
76	N-methyl-1-[2-[2-(methylamino)propoxy]phenoxy]propan-2-amine		X	X	X	✓

NO.	NAME	STRUCTURE	DISCUSSED IN CHAPTERS:			
			1	3	4	5
77	MDP2P dimethyl acetal		X	X	X	✓
78 (a-b)	5-bromo-6-prop-1-enyl-1,3-benzodioxole		X	X	X	✓
79 (a-b)	5-(1,3-benzodioxol-5-yl)-6-prop-1-enyl-1,3-benzodioxole		X	X	X	✓
80	1,2-dipropoxybenzene		X	X	X	✓
81	isosaftrole dimer		X	X	X	✓
82	1-(1,3-benzodioxol-4-yl)-1-methoxy-propan-2-ol		X	X	X	✓
83	MDP2P dimer		X	X	X	✓
84	1,3-benzodioxole-5-carboxylic acid		X	X	X	✓

Appendix 5: Synthesis and organic impurity profiling of 4-methoxymethamphetamine hydrochloride and its precursors

Rebecca Tam, **Erin Heather**, Ronald Shimon, Brandon Lam, Andrew McDonagh.

Forensic Science International 272 (2017) 184 – 189.

Abstract

4-Methoxymethamphetamine (PMMA) was synthesised from star anise and from 4-methoxytoluene and the organic impurity profiles examined. These two starting materials are unrestricted chemicals in many jurisdictions and contain the requisite functional groups and are thus well suited for clandestine manufacturers. *trans*-Anethole was extracted from star anise and oxidised to 4-methoxyphenyl-2-propanone (PMP2P). 4-Methoxytoluene was oxidised to anisaldehyde, converted to 4-methoxyphenyl-2-nitropropene, and then reduced to PMP2P. The PMP2P obtained by both methods was then converted to PMMA via the Leuckart reaction. 4-Methoxymethamphetamine hydrochloride (PMMA·HCl) was synthesised from PMMA using hydrogen chloride gas. Both of the examined synthetic methods were found to be feasible routes into PMMA·HCl. The products of each step were analysed by gas chromatography - mass spectrometry (GC-MS) and proton nuclear magnetic resonance spectroscopy (^1H NMR). Impurities were examined in an attempt to identify route specific compounds, which may provide valuable information about the synthetic pathway and precursors.

1. Introduction

4-Methoxymethamphetamine (or *p*-methoxymethamphetamine, PMMA) is a synthetic substance that is an analogue of methamphetamine and closely related in structure to 3,4-methylenedioxymethamphetamine (MDMA) (Figure 1) [107]. Drug analogues often appear in the illicit market as substitutes for other substances as well as being marketed in their own right. PMMA is a stimulant with similar [108, 109] but possibly more short-lived [4] effects compared to those of MDMA. It has been suggested that there is a small margin between a safe and lethal dose of PMMA [109].

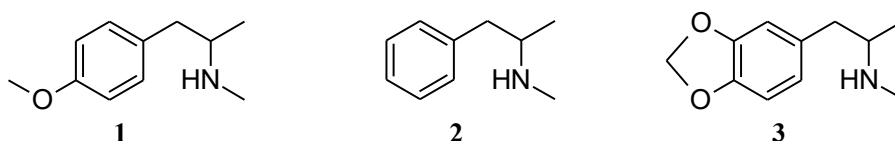
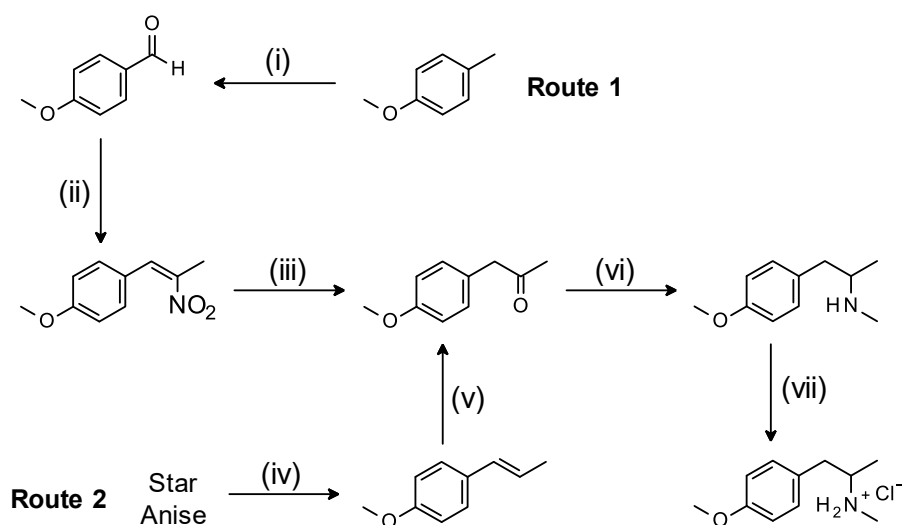


Figure 1: Structure of PMMA (1), methamphetamine (2) and MDMA (3)

PMMA manufacturers can use synthetic routes adopted from the synthesis of methamphetamine and MDMA. A starting material that is commonly described in the literature is *trans*-anethole (4-methoxyphenyl-2-propene), which is similar in structure to the MDMA precursor isosafrole. Another feasible starting material is anisaldehyde (4-methoxybenzaldehyde), which has a similar structure to the MDMA precursor piperonal and the methamphetamine precursor benzaldehyde. Interestingly, many of the PMMA precursor chemicals can be synthesised or obtained from natural sources and household products. For example, *trans*-anethole is found in star anise oil (>90%), aniseed oil (80 - 90%) and fennel oil (80%). Alternatively, anisaldehyde can be synthesised from 4-methoxytoluene. The use of uncontrolled precursors such as these by clandestine laboratory operators may significantly reduce the risk associated with detection, and thus be an attractive method of manufacture. In this context, organic impurity profiling is of significant interest to law enforcement agencies as it can provide valuable information about production methods. While there has been a significant amount of research into the organic impurity profiling of many illicit substances such as methamphetamine and MDMA [17, 110], there is quite limited information about the impurities that are associated with the synthesis of PMMA [111].



Scheme 1: Synthesis of PMMA from 4-methoxytoluene (Route 1) and *trans*-anethole extracted from star anise (Route 2). (i) K_2SO_8 , $CuSO_4$ (ii) $CH_3CH_2NO_2$, CH_3COONH_4 , CH_3COOH (iii) Fe , CH_3COOH (iv) H_2O extraction (v) 1. H_2O_2 , $HCOOH$ 2. H_2SO_4 (vi) CH_3NHCHO , $HCOOH$, HCl (vii) HCl

This paper presents the results of organic impurity profiling of 4-methoxymethamphetamine hydrochloride (PMMA·HCl) synthesised from 4-methoxytoluene (Scheme 1, Route 1) and from *trans*-anethole extracted from star anise (Scheme 1, Route 2). These routes are important because they utilise readily available materials and have been reported in freely available literature.

2. Materials and Methods

2.1 General

GC-MS analyses were performed using an Agilent 6890 series gas chromatography coupled with an Agilent 5973 network mass selective detector. The column used was a 30 m long Zebron ZB 5 ms 5% polysilarylene- 95% polydimethylsiloxane column, with an internal diameter of 0.25 μm . Helium was used as the carrier gas at 1.0 mL/min. The injection volume and temperature program for PMMA and its precursor was used as followed. The injection volume was 1.0 μL per injection, split mode with a ratio of 13.2:1. The temperature program used was; 50 $^{\circ}\text{C}$ with a 2 minute hold time, then ramped at 15 $^{\circ}\text{C}$ per minute until 290 $^{\circ}\text{C}$. The injection volume and temperature program for PMMA hydrochloride was used as followed. The injection volume was 2.0 μL per injection, splitless mode. The temperature program used was; 50 $^{\circ}\text{C}$ held for 1 minute, then ramped to 150 $^{\circ}\text{C}$ at 10 $^{\circ}\text{C}$ per minute, held for 4 minute, ramped at 14 $^{\circ}\text{C}$ per minute until 290 $^{\circ}\text{C}$. Mass spectrometry was performed in positive ionisation mode with a mass spectrum from 29-350 amu. The fragmentations listed are for the pure substance only. ^1H NMR spectroscopy was performed using an Agilent Direct Drive 500 MHz NMR Spectrometer. The machine operated at 499.86 MHz with 64 scans collected. Spectra are available in the supplementary information files.

2.2 Chemicals

Star anise was purchased from a local grocery store. All purchased chemicals were used as-received. The following chemicals were purchased from AJAX Chemicals: ammonium acetate, copper (II) sulfate, dichloromethane, ethyl acetate, glacial acetic acid, 36% hydrochloric acid, magnesium sulfate (anhydrous), sodium hydroxide and sodium sulfate (anhydrous). The following were purchased from Sigma Aldrich: anisaldehyde, 4-methoxytoluene, *N*-methylformamide, nitroethane and potassium persulfate. The following were purchased from various suppliers: concentrated sulfuric acid (BDH), 28% ammonia solution (Chem-Supply), 30% hydrogen peroxide (Chem-Supply), methanol (Chem-Supply), formic acid (Fluka), iron pin dust (M&B).

2.3 Synthesis

2.3.1 4-Methoxyphenyl-2-propanone (PMP2P) from 4-methoxytoluene

Synthesis of anisaldehyde: A solution of 4-methoxytoluene (2.250 g, 18.4 mmol) in 70 mL of acetonitrile was added to a mixture of potassium peroxydisulfate (10 g, 37 mmol), copper sulfate

(1.0 g, 6.3 mmol) in 70 mL water. The mixture was stirred at 65-70 °C for 3 h and allowed to cool. The product was extracted with 3 x 10 mL of dichloromethane and washed with 10 mL water. The organic extracts were dried over anhydrous sodium sulfate, decanted and concentrated using the rotary evaporator producing a dark orange liquid. Yield: 2.099 g. ¹H NMR: Supplementary Figure 1. GC-MS: Supplementary Figure 10.

Synthesis of 4-methoxyphenyl-2-nitropropene (PMP2NP): Anisaldehyde (1.004 g), nitroethane (2.0 mL, 28 mmol) and ammonium acetate (200 mg, 2.6 mmol) were dissolved in 2.0 mL glacial acetic acid. The mixture was stirred at reflux for 6 h and allowed to cool. Next, water was added and the product was extracted with 2 x 10 mL dichloromethane. The organic extracts were washed with a concentrated sodium hydrogen carbonate solution and water, then dried over anhydrous sodium sulfate. The solvent was removed using the rotary evaporator, producing a dark orange brown liquid. Yield: 1.23 g. ¹H NMR: Supplementary Figure 2. GC-MS: Supplementary Figure 11.

Synthesis of PMP2P: A solution of 4-methoxyphenyl-2-nitropropene (0.800 g) in 20 mL glacial acetic acid was added to a mixture of iron pin dust (2.00 g, 35.8 mmol) in 10 mL glacial acetic acid. The mixture was stirred for 10 minutes, refluxed for 2 hours and allowed to cool. Next, water was added and the mixture was filtered to remove unreacted iron dust pin. The filtrate was extracted with 2 x 10 mL dichloromethane and washed with concentrated sodium hydrogen carbonate solution and water. The organic extracts were dried with anhydrous magnesium sulfate and concentrated using the rotary evaporator, producing a dark brown solid. Yield: 490 mg. ¹H NMR: Supplementary Figure 3. GC-MS: Supplementary Figure 12.

2.3.2 PMP2P from Star anise

Extraction of trans-anethole: ground star anise (30 g) was added to 500 mL of water in a 1 L round bottom flask attached to a swan-neck splash head, condenser and receiving adapter. The mixture was gently heated and 250 mL distillate was collected into a conical flask containing 30 mL ethyl acetate. The distillate was extracted with 3 x 25 mL ethyl acetate. The organic extracts were dried over anhydrous sodium sulfate and concentrated using the rotary evaporator, producing a clear oil. Yield 3.01 g. ¹H NMR: Supplementary Figure 6. GC-MS: Supplementary Figure 15.

Synthesis of PMP2P: Performic acid was formed by stirring formic acid (2.5 mL, 23.6 M, 59 mmol) with hydrogen peroxide (2.0 mL, 9.9M, 20 mmol) at room temperature for 30 min. The performic acid was then added dropwise to *trans*-anethole (1.00 g) in 10 mL of dichloromethane, ensuring that the temperature did not exceed 40 °C. The mixture was refluxed for 21 h and allowed to

cool. The product was extracted with 3 x 10 mL of dichloromethane and washed with 10 mL of 1.25 M sodium hydroxide. The solvent was removed using a rotary evaporator to leave a red-orange oil. The oil was redissolved in methanol (5 mL) and then sulfuric acid (20 mL, 2.7 M, 54 mmol) was added. The resulting solution was heated under reflux for 2 h and allowed to cool. The product was extracted with dichloromethane (3 x 10 mL) and washed with 5 mL water and 10 mL of 1.25 M sodium hydroxide. The organic extracts were dried over anhydrous sodium sulfate and the solvent was removed with the rotatory evaporator, producing a dark brown oil. Yield: 0.74 g. ^1H NMR: Supplementary Figure 7. GC-MS: Supplementary Figure 16.

2.3.3 PMMA·HCl from PMP2P

Synthesis of PMMA: A mixture of *N*-methylformamide (2.4 g, 41 mmol), formic acid (1.14 g, 23.6 M, 22.1 mmol) and 4-methoxyphenyl-2-propanone (0.500 mg) was heated at 180 °C overnight and then allowed to cool. To the mixture, hydrochloric acid (10 mL, 4.8 M, 48 mmol) was added and the mixture was again heated under reflux overnight and allowed to cool. Ammonium hydroxide solution (30%) was added until the solution was basic, which was then extracted with dichloromethane (3 x 10 mL). The organic layers were combined and dried with magnesium sulfate and the solvent removed using a rotary evaporator to yield a brown oil. Yield: 0.40 g. ^1H NMR: Supplementary Figure 4 and 8. GC-MS: Supplementary Figure 13 and 17.

Synthesis of PMMA·HCl: A hydrogen chloride gas generator was constructed using a dropping funnel containing concentrated sulfuric acid connected to a side-arm flask containing sodium chloride and a magnetic stir bar. Silicone tubing was connected from the side-arm flask to a gas wash bottle filled with dry sulfuric acid. Two gas wash bottles were connected in sequence to a two-neck round bottom flask filled with anhydrous diethyl ether, PMMA free base (0.100 g), and a magnetic stir bar. The second neck of the round bottom flask was connected to a bubbling trap (beaker of water and inverted small funnel). Hydrogen chloride gas was generated by dropping sulfuric acid onto sodium chloride at a gentle rate. The gas was then bubbled through the ether solution. The resultant white solid was collected by filtration under reduced pressure, washed with diethyl ether (10 mL) and dried in air. Yield: 53 mg. ^1H NMR: Supplementary Figure 5 and 9. GC-MS: Supplementary Figure 14 and 18.

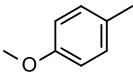
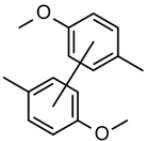
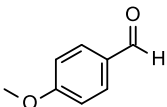
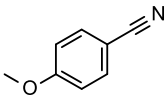
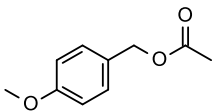
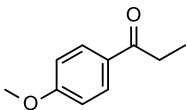
3. Results and Discussion

PMMA·HCl was synthesised from 4-methoxytoluene (Route 1) and from star anise (Route 2) with each synthetic step performed at least in duplicate. To mimic the procedures that might be expected in a moderately equipped clandestine laboratory, rigorous purification of precursors and products was not performed. Impurities were identified for each product through analysis of their mass fragmentation patterns using GC-MS. The identification of the impurities was also confirmed by ^1H NMR spectroscopy when distinct chemical shifts were produced.

3.1 *Para*-methoxyphenyl-2-propanone from 4-methoxytoluene

Para-methoxyphenyl-2-propanone (PMP2P) was synthesised from 4-methoxytoluene in three steps as shown in Scheme 1. The identified impurities are listed in Table 1. With the exception of compounds **6** and **9**, the identified impurities are route specific. The starting material, 4-methoxytoluene (**4**) and intermediate, anisaldehyde (**6**), were identified as impurities in PMP2P indicating that these reactions did not proceed to completion.

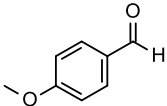
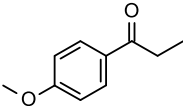
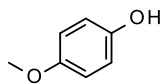
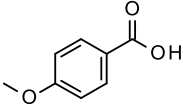
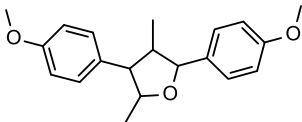
Table 1: Organic impurities identified in PMP2P synthesised from 4-methoxytoluene

No.	Impurity Structure	Impurity Name	m/z
4		4-Methoxytoluene	122, 121, 107, 91, 77
5 (a-b)		2,5'-Dimethoxy-2',5-dimethyl-1,1'-biphenyl / 5,5'-dimethoxy-2,2'-dimethyl-1,1'-biphenyl	242, 227, 211, 195, 134, 121, 91, 77
6		Anisaldehyde	136/135, 107, 92, 77
7		4-Methoxybenzonitrile	133, 118, 103, 90, 76, 63
8		4-Methoxybenzyl acetate	207, 180, 138, 121, 91, 77
9		4-Methoxyphenyl-1-propanone	164, 135, 121, 107, 92, 77

Compounds **5 (a-b)** are two structural isomers that are reaction by-products of the oxidation of 4-methoxytoluene when the reaction is performed in an acidic solution [112]. Compounds **7** and **8** are reaction by-products of the synthesis of PMP2NP from anisaldehyde. Compound **7** is formed via the reaction of hydroxylamine (formed *in situ*) with anisaldehyde (see Supplementary Figure 19) while compound **8** is formed by the reaction of ammonium acetate and anisaldehyde [113]. Compound **9** is an oxidation reaction by-product in the synthesis of PMP2P from PMP2NP.

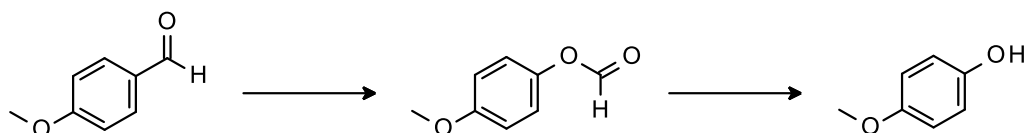
3.2 PMP2P from Star Anise

Table 2: Organic impurities identified in PMP2P synthesised from *trans*-anethole extracted from star anise

No.	Impurity Structure	Impurity Name	m/z
6		Anisaldehyde	136/135, 107, 92, 77
9		4-Methoxyphenyl-1-propanone	164, 135, 121, 107, 92, 77
10		4-Methoxyphenol	124, 109, 81, 65, 53
11		4-Methoxybenzoic acid	152/151, 135, 121, 108, 92, 77
12 (a-d)		2,4-Dimethyl-3,5-bis(4'-methoxyphenyl) tetrahydrofuran	268, 253, 255, 207, 165, 152, 134

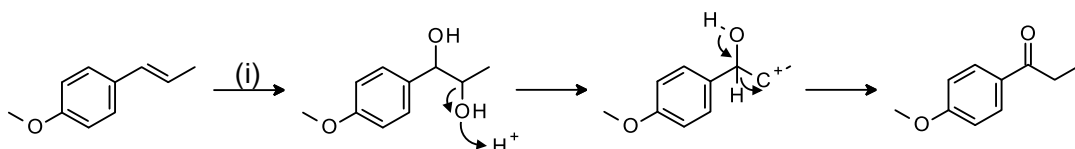
Star anise was steam distilled to extract the essential oils, of which *trans*-anethole was the principle component. Forty organic impurities were identified in the extract, all of which had previously been identified as components of the star anise essential oil [114]. Importantly, these impurities were not subsequently detected in PMP2P synthesised from this material, with the exception of anisaldehyde. PMP2P was synthesised from the obtained *trans*-anethole using a peracid oxidation and acid dehydration reaction (Scheme 1). The five identified impurities are listed in Table 2.

Compounds **10** and **12 (a-d)** are route specific impurities which were only identified in PMP2P synthesised via Route 2. 4-Methoxyphenol (**10**) is synthesised from anisaldehyde (an organic impurity identified in *trans*-anethole) via a Baeyer-Villiger oxidation reaction as shown in Scheme 2 [115]. Compounds **12 (a-d)** are four diastereoisomers that are formed when *trans*-anethole reacts with the relatively stable intermediate carbocation generated during the peracid oxidation and acid dehydration reaction [116].



Scheme 2: The formation of 4-methoxyphenol (compound 10) [115].

Anisaldehyde (**6**) was identified as an impurity in the synthesised PMP2P, which may be due its presence in the reaction precursor, *trans*-anethole, but we cannot discount that it may also be formed as a reaction by-product. Compound **9** may be formed from the rearrangement of the glycol intermediate (Scheme 3) during the synthesis of PMP2P. Compound **11** was formed by oxidation of anisaldehyde by hydrogen peroxide. These three compounds are not route specific impurities as **6** and **9** were also identified in PMP2P synthesised via Route 1 and **11** is a potential reaction by-product of the oxidation of 4-methoxytoluene.



Scheme 3: Formation of 4-methoxyphenyl-1-propanone (compound 9) in Route 2. (i) a. H_2O_2 , HCOOH , b. H_2SO_4

3.3 PMMA·HCl from PMP2P

PMMA·HCl was synthesised from PMP2P (obtained from both synthetic routes) via the Leuckart reaction to form PMMA and subsequent salt formation using gaseous HCl. The organic impurities identified in PMMA and PMMA·HCl are listed in Tables 3 and 4, respectively. Despite the variation in the organic impurities detected between the two synthetic routes, we are hesitant to label any of these impurities as route specific. The discrepancies between the identification of Leuckart reaction by-products in PMMA synthesised via Route 1 and Route 2 was likely a result of slight variations in reaction conditions of the Leuckart reaction itself.

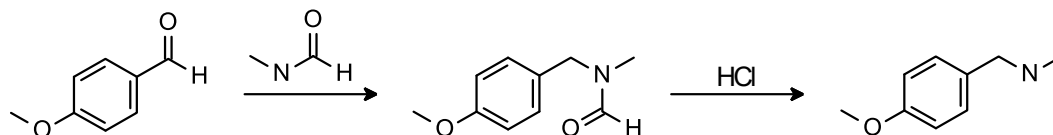
Table 3: Organic impurities identified in PMMA synthesised from 4-methoxytoluene (Route 1) and from star anise (Route 2)

No.	Impurity Structure	Impurity Name	m/z	Synthetic Route
13		4-Methoxyphenyl-2-propanone	164, 121, 91, 77	2
14		N-formyl-p-methoxyamphetamine	207, 192/191, 165, 121, 58	1*
15		1-(4-Methoxyphenyl)-N,N-dimethylmethanamine	165, 121, 91, 77, 58	1
16		1-(4-Methoxyphenyl)-N-methylmethanamine	151/150, 136, 121, 106, 91, 77	1 and 2
17		4-Methoxydimethylamphetamine	192, 121, 72	1 and 2
18		4-Methoxy-N-ethylmethamphetamine	150, 135, 121, 107, 72, 58	1
19		4-Methoxyamphetamine	164, 150, 121, 107, 58	1

* This impurity was detected in only one of the duplicate reactions.

The precursor (PMP2P, compound **13**) was identified as an impurity in PMMA synthesised via Route 2 and the Leuckart intermediate (compound **14**) was identified as an impurity in PMMA synthesised via Route 1. Compounds **15** and **16** arise from reactions with anisaldehyde present in PMP2P synthesised via Route 1 and Route 2. Anisaldehyde can react with *N*-methylformamide, a reagent used in the Leuckart reaction, to form **16** (Scheme 4). Compound **15** is formed by a reaction between anisaldehyde and dimethylformamide, an impurity identified in the *N*-methylformamide reagent. This dimethylformamide impurity also reacts with PMP2P to form **17**. Compound **18** can be formed from the reaction of PMMA with acetic acid carried over from the previous reaction. Importantly, acetic acid is used in the synthesis of PMP2P from PMP2NP (and also in the synthesis of PMP2NP from anisaldehyde) as shown in Route 1 but it is not used in Route 2. While this may indicate that **18** is a route specific impurity,

the common nature of acetic acid makes drawing any strong conclusion from its presence somewhat perilous. Compound **19** is a characteristic by-product of the Leukart reaction using PMP2P [111].



Scheme 4: Formation of 4-methoxyphenyl-N-methylmethanamine (compound 16).

PMMA (**1**) was identified as an organic impurity in PMMA·HCl synthesised via Route 2. Compounds **13** and **14** were carried over unchanged through the reaction and identified in PMMA·HCl. Compounds **20** and **21** are the hydrochloride salts of compounds **16** and **17**. The formation of these hydrochloride salts is demonstrated by the downfield shift of the corresponding signals in the ^1H NMR spectrum of PMMA·HCl (Supplementary Figure 4) compared to the NMR spectrum of PMMA (Supplementary Figure 5). This downfield shift is due to the positive charge on the dialkylammonium group, which has a deshielding effect.

Table 4: Organic impurities identified in PMMA·HCl synthesised from 4-methoxytoluene (Route 1) and star Anise (Route 2)

No.	Impurity Structure	Impurity Name	m/z	Synthetic Route
1		4-Methoxymethamphetamine	178, 121, 58	2
13		4-Methoxyphenyl-2-propanone	164, 121, 91, 77	2
14		N-formyl-p-methoxyamphetamine	207, 192/191, 165, 121, 58	1*
20		4-Methoxyphenyl-N-methylmethanamine	151/150, 136, 121, 106, 91, 77	1 and 2
21		4-Methoxyphenyl-N,N-dimethyl-2-propanamine	192, 121, 72	1 and 2

* This impurity was detected in only one of the duplicate reactions.

4. Conclusions

4-Methoxymethamphetamine may be synthesised using *trans*-anethole extracted from star anise or 4-methoxytoluene as aromatic precursors. *Trans*-anethole may be oxidised directly to 4-methoxyphenyl-2-propanone (PMP2P) while 4-methoxytoluene can be oxidised to anisaldehyde, converted to P2PNP and then reduced to give PMP2P. The PMP2P obtained from both synthetic routes was then converted to PMMA via the Leuckart reaction. The PMMA hydrochloride salt (PMMA·HCl) was obtained using hydrogen chloride gas. Both of the examined synthetic methods were found to be feasible routes into PMMA·HCl.

The products of each step, analysed by GC-MS and ¹H NMR, contained a number of impurities, but only some of which were route specific compounds. PMP2P synthesised from 4-methoxytoluene contained four impurities that were not observed in the material prepared from *trans*-anethole, while the PMP2P synthesised from *trans*-anethole contained two impurities that were not observed in the material prepared from 4-methoxytoluene. Analysis of the synthesised PMMA and PMMA·HCl suggests that the identified organic impurities do not unambiguously indicate which of the two synthetic routes was utilised. We conclude that while the organic impurities identified in PMP2P allow discrimination between the two synthetic pathways examined here, this is not the case for PMMA or its hydrochloride salt. Further organic impurity profiling of PMP2P and PMMA synthesised using alternate methods (ie. wacker oxidation of estragole and reductive amination of PMP2P respectively) could provide further discriminatory information.

References

References

- [1] United Nations Office on Drugs and Crime. 2017, *World Drug Report 2017*, ISBN: 978-92-1-148291-1, United Nations publication, Sales No. E.17.XI.6.
- [2] United Nations Office on Drugs and Crime. 2018, *World Drug Report 2018*, ISBN: 978-92-1-148304-8 United Nations Publication, Sales No. E.18.XI.9.
- [3] D. M. Zgonjanin, E. S. Loncar & M. M. Tasic. *Analysis of forensic samples of "Ecstasy" tablets seized in Novi Sad during the 2004 year*. Acta Period Technology, **2005**. 36, 247-59.
- [4] A. S. Alexander Shulgin 1991, *Phenethylamines I Have Known And Loved: A Chemical Love Story*, <https://erowid.org/library/books_online/pihkal/pihkal.shtml>.
- [5] United Nations Office on Drugs and Crime. 2016, *World Drug Report 2016*, ISBN: 978-92-1-148286-7 United Nations Publications, Sales No. E.16.XI.7.
- [6] United Nations Office on Drugs and Crime. 2014, *World Drug Report 2014*, ISBN: 978-92-1-148277-5, United Nations publication, Sales No. E.14.XI.7.
- [7] United Nations Office on Drugs and Crime. 2013, *World Drug Report 2013*, ISBN: 978-92-1-148273-7, United Nations Publication, Sales No. E.13.XI.6.
- [8] P. Jacob III & A. T. Shulgin 1996, *Novel n-substituted-2-amino-3',4'-methylenedioxypiofenones*, WO1996039133 A1, <<https://www.google.com.au/patents/WO1996039133A1?cl=en>>.
- [9] J. P. Kelly. *Cathinone derivatives: A review of their chemistry, pharmacology and toxicology*. Drug Testing and Analysis, **2011**. 3, 439.
- [10] T. A. Dal Cason, R. Young & R. A. Glennon. *Cathinone: an investigation of Several N-alkyl and methylenedioxy-substituted analogs*. Pharmacology Biochemistry and Behavior, **1997**. 58, 1109-16.
- [11] Green List. International Narcotics Control Board,. **2016**, *List of Psychotropic Substances under International Control. In accordance with the Convention on Psychotropic Substances of 1971*, Annex to the annual statistical report on psychotropic substances (form P). Available at [06 November 2016], <https://www.incb.org/documents/Psychotropics/greenlist/2016/V1604744_Eng.pdf>
- [12] Rhodium: Drug Chemistry Archive. **2004**, Available at [24/11/2018], <<http://www.erowid.org/archive/rhodium/chemistry/index.html> or alternatively <http://www.drugs-forum.com/chemistry/chemistry/index.html>>
- [13] H. A. S. Buchanan, N. N. Daeid, W. Meier-Augenstein, H. F. Kemp, W. J. Kerr & M. Middleditch. *Emerging use of isotope ratio mass spectrometry as a tool for discrimination of 3,4-methylenedioxymethamphetamine by synthetic route*. Analytical Chemistry, **2008**. 80, 3350-6.
- [14] J. Coppen. 1995, *Flavours and fragrances of plant origin*, Food and Agriculture Organization of the United Nations.

- [15] J. Panten & H. Surburg. 2015, '*Flavors and Fragrances, 4. Natural Raw Materials*', *Ullmann's Encyclopedia of Industrial Chemistry*.
- [16] J. Panten & H. Surburg. 2016, '*Flavors and Fragrances, 3. Aromatic and Heterocyclic Compounds*', *Ullmann's Encyclopedia of Industrial Chemistry*.
- [17] N. Stojanovska, S. Fu, M. Tahtouh, T. Kelly, A. Beavis & K. P. Kirkbride. *A review of impurity profiling and synthetic route of manufacture of methylamphetamine, 3,4-methylenedioxymethylamphetamine, amphetamine, dimethylamphetamine and p-methoxyamphetamine*. *Forensic Science International*, **2013**. 224, 8-26.
- [18] M. Collins, A. Heagney, F. Cordaro, D. Odgers, G. Tarrant & S. Stewart. *Methyl 3-[3',4'-(methylenedioxy)phenyl]-2-methyl glycidate: an ecstasy precursor seized in Sydney, Australia*. *J Forensic Sci*, **2007**. 52, 898-903.
- [19] M. Cox & G. Klass. *Synthesis by-products from the Wacker oxidation of safrole in methanol using p-benzoquinone and palladium chloride*. *Forensic Science International*, **2006**. 164, 138-47.
- [20] M. Cox, G. Klass, S. Morey & P. Pigou. *Chemical markers from the peracid oxidation of isosafrole*. *Forensic Science International*, **2008**. 179, 44-53.
- [21] P. Gimeno, F. Besacier, M. Bottex, L. Dujourdy & H. Chaudron-Thozet. *A study of impurities in intermediates and 3,4-methylenedioxymethylamphetamine (MDMA) samples produced via reductive amination routes*. *Forensic Science International*, **2005**. 155, 141-57.
- [22] C. Koper, C. van den Boom, W. Wiarda, M. Schrader, P. de Joode, G. van der Peijl & A. Bolck. *Elemental analysis of 3,4-methylenedioxymethylamphetamine (MDMA): A tool to determine the synthesis method and trace links*. *Forensic Science International*, **2007**. 171, 171-9.
- [23] R. J. Renton, J. S. Cowie & M. C. H. Oon. *A study of the precursors, intermediates and reaction by-products in the synthesis of 3,4-methylenedioxymethylamphetamine and its application to forensic drug analysis*. *Forensic Science International*, **1993**. 60, 189-202.
- [24] M. Świst, J. Wilamowski & A. Parczewski. *Basic and neutral route specific impurities in MDMA prepared by different synthesis methods: Comparison of impurity profiles*. *Forensic Science International*, **2005**. 155, 100-11.
- [25] M. Collins. *Some new psychoactive substances: Precursor chemicals and synthesis-driven end-products*. *Drug Testing and Analysis*, **2011**. 3, 404.
- [26] K. Zaitsu, M. Katagi, H. T. Kamata, T. Kamata, N. Shima, A. Miki, H. Tsuchihashi & Y. Mori. *Determination of the metabolites of the new designer drugs bk-MBDB and bk-MDEA in human urine*. *Forensic Science International*, **2009**. 188, 131.
- [27] H. T. Kamata, N. Shima, K. Zaitsu, T. Kamata, A. Miki, M. Nishikawa, M. Katagi & H. Tsuchihashi. *Metabolism of the recently encountered designer drug, methylone, in humans and rats*. *Xenobiotica*, **2006**. 36, 709.

- [28] Australian Crime Commission,. **2009**, *Code of Practice for Supply Diversion into Illicit Drug Manufacture*, Available at [06 November 2016], <<http://www.pacia.org.au/Content/drugs.aspx>>
- [29] A. Bortz 2011, 'Synthesis and Analysis of B-ketone Analogues of Amphetamine-type Stimulants', Dissertation, University of Technology Sydney.
- [30] M. Collins. *Illicit drug profiling: the Australian experience – revisited*. Australian Journal of Forensic Sciences, **2017**. 49, 591-604.
- [31] R. Gallagher, R. Shimmom & A. M. McDonagh. *Synthesis and impurity profiling of MDMA prepared from commonly available starting materials*. Forensic Science International, **2012**. 223, 306-13.
- [32] A. F. M. Cláudio, M. G. Freire, C. S. R. Freire, A. J. D. Silvestre & J. A. P. Coutinho. *Extraction of vanillin using ionic-liquid-based aqueous two-phase systems*. Separation and Purification Technology, **2010**. 75, 39-47.
- [33] Rhodium: Drug Chemistry Archive. **2004**, *The Complete Book of Ecstasy: The Chapter 5 - The Main Precursors*, Available at [25/11/2018], <<https://erowid.org/archive/rhodium/chemistry/tcboe/chapter5.html>>
- [34] Rhodium: Drug Chemistry Archives. **2004**, *Piperonal and Safrole from Vanillin and Eugenol*, Available at [03/01/2019], <<https://erowid.org/archive/rhodium/chemistry/methylenation.html>>
- [35] E. Heather 2012, 'Synthesis and Profiling of 3,4-Methylenedioxymethamphetamine from Readily Available Starting Materials', Dissertation, University of Technology Sydney.
- [36] P. N. Shingate, P. P. Dongre & D. M. Kannur. *New method development for extraction and isolation of piperine from black pepper*. International Journal of Pharmaceutical Sciences and Research, **2013**. 4, 3165+.
- [37] M. Rathnawathie & K. A. Buckle. *Determination of piperine in pepper (Piper nigrum) using high-performance liquid chromatography*. Journal of Chromatography A, **1983**. 264, 316-20.
- [38] L. Gorgani, M. Mohammadi, G. D. Najafpour & M. Nikzad. *Sequential Microwave-Ultrasound-Assisted Extraction for Isolation of Piperine from Black Pepper (Piper nigrum L.)*. Food and Bioprocess Technology, **2017**. 10, 2199-207.
- [39] Rhodium: Drug Chemistry Archives. **2004**, *Piperonal from pepper*, Available at [06/01/2019], <<https://www.erowid.org/archive/rhodium/chemistry/3base/piperonal.pepper/index.html>>
- [40] Rhodium: Drug Chemistry Archives. **2004**, *Cleavage of Alkenes to Aldehydes Using Potassium Permanganate*, Available at [06/01/2019], <<https://www.erowid.org/archive/rhodium/chemistry/alkene2aldehyde.kmno4-thf.html>>

- [41] C. M. Plummer, T. W. Breadon, J. R. Pearson & O. A. H. Jones. *The synthesis and characterisation of MDMA derived from a catalytic oxidation of material isolated from black pepper reveals potential route specific impurities*. *Science & Justice*, **2016**. 56, 223-30.
- [42] Rhodium: Drug Chemistry Archives. **2004**, *Notes on the synthesis of MDMA precursors from Eugenol*, Available at [06/01/2019], <<https://erowid.org/archive/rhodium/chemistry/eugenol.mdma.html>>
- [43] H. Fiege, H.-W. Voges, T. Hamamoto, S. Umemura, T. Iwata, H. Miki, Y. Fujita, H.-J. Buysch, D. Garbe & W. Paulus. 2000, 'Phenol Derivatives', *Ullmann's Encyclopedia of Industrial Chemistry*, Wiley-VCH Verlag GmbH & Co. KGaA.
- [44] B. Lin & X. Yang. *Research on the synthesis for safrole*. *Guangdong Huagong*, **2003**. 30, 6-7.
- [45] Rhodium: Drug Chemistry Archive. **2004**, *Synthesis of Safrole*, Available at, <<https://erowid.org/archive/rhodium/chemistry/safrole.html>>
- [46] Rhodium: Drug Chemistry Archive. **2004**, *Synthesis of 4-allyl-pyrocatechol (3,4-dihydroxyallylbenzene)*, Available at [24/11/2018], <<https://erowid.org/archive/rhodium/chemistry/allylpyrocatechol.html>>
- [47] Rhodium: Drug Chemistry Archive. **2004**, *Synthesis of 4-Allylcatechol & Mechanism of Claisen Rearrangement in Catechols*, Available at [03/01/2018], <<https://erowid.org/archive/rhodium/chemistry/allylcatechol.html>>
- [48] M. Collins, J. Huttunen, I. Evans & J. Robertson. *Illicit drug profiling: the Australian experience*. *Australian Journal of Forensic Sciences*, **2007**. 39, 25-32.
- [49] M. Morelato, A. Beavis, M. Tahtouh, O. Ribaux, P. Kirkbride & C. Roux. *The use of forensic case data in intelligence-led policing: The example of drug profiling*. *Forensic Science International*, **2013**. 226, 1-9.
- [50] H. Salouros. *Illicit drug chemical profiling: current and future state*. *Australian Journal of Forensic Sciences*, **2018**. 50, 689-96.
- [51] M. Morelato, A. Beavis, M. Tahtouh, O. Ribaux, P. Kirkbride & C. Roux. *The use of organic and inorganic impurities found in MDMA police seizures in a drug intelligence perspective*. *Science & Justice*, **2014**. 54, 32-41.
- [52] M. Collins, A. Doddridge & H. Salouros. *Cathinones: Isotopic profiling as an aid to linking seizures*. *Drug Testing and Analysis*, **2016**. 8, 903-9.
- [53] H. A. S. Buchanan, W. J. Kerr, W. Meier-Augenstein & N. N. Daéid. *Organic impurities, stable isotopes, or both: A comparison of instrumental and pattern recognition techniques for the profiling of 3,4-methylenedioxymethamphetamine*. *Analytical Methods*, **2011**. 3, 2279-88.
- [54] M. Świst, J. Wilamowski & A. Parczewski. *Determination of synthesis method of ecstasy based on the basic impurities*. *Forensic Science International*, **2005**. 152, 175-84.

- [55] R. J. H. Waddell-Smith. *A review of recent advances in impurity profiling of illicit MDMA samples*. Journal of Forensic Science, **2007**. 52, 1297-304.
- [56] J. Y. K. Cheng, M. F. Chan, T. W. Chan & M. Y. Hung. *Impurity profiling of ecstasy tablets seized in Hong Kong by gas chromatography–mass spectrometry*. Forensic Science International, **2006**. 162, 87-94.
- [57] S.-F. Teng, S.-C. Wu, C. Liu, J.-H. Li & C.-S. Chien. *Characteristics and trends of 3,4-methylenedioxymethamphetamine (MDMA) tablets found in Taiwan from 2002 to February 2005*. Forensic Science International, **2006**. 161, 202-8.
- [58] K. Andersson, K. Jalava, E. Lock, Y. Finnon, H. Huizer, E. Kaa, A. Lopes, A. Poortman-van der Meer, M. D. Cole, J. Dahlén & E. Sippola. *Development of a harmonised method for the profiling of amphetamines: III. Development of the gas chromatographic method*. Forensic Science International, **2007**. 169, 50-63.
- [59] K. Andersson, E. Lock, K. Jalava, H. Huizer, S. Jonson, E. Kaa, A. Lopes, A. Poortman-van der Meer, E. Sippola, L. Dujourdy & J. Dahlén. *Development of a harmonised method for the profiling of amphetamines VI: Evaluation of methods for comparison of amphetamine*. Forensic Science International, **2007**. 169, 86-99.
- [60] L. Aalberg, K. Andersson, C. Bertler, H. Borén, M. D. Cole, J. Dahlén, Y. Finnon, H. Huizer, K. Jalava, E. Kaa, E. Lock, A. Lopes, A. Poortman-van der Meer & E. Sippola. *Development of a harmonised method for the profiling of amphetamines: I. Synthesis of standards and compilation of analytical data*. Forensic Science International, **2005**. 149, 219-29.
- [61] M. Świst, J. Wilamowski, D. Zuba, J. Kochana & A. Parczewski. *Determination of synthesis route of 1-(3,4-methylenedioxyphenyl)-2-propanone (MDP-2-P) based on impurity profiles of MDMA*. Forensic Science International, **2005**. 149, 181-92.
- [62] P. Gimeno, F. Besacier, H. Chaudron-Thozet, J. Girard & A. Lamotte. *A contribution to the chemical profiling of 3,4-methylenedioxymethamphetamine (MDMA) tablets*. Forensic Science International, **2002**. 127, 1-44.
- [63] J. D. Power, P. Kavanagh, G. McLaughlin, J. O'Brien, B. Talbot, M. Barry, B. Twamley, G. Dowling & S. D. Brandt. *Identification and characterization of an imidazolium by-product formed during the synthesis of 4-methylmethcathinone (mephedrone)*. Drug Testing and Analysis, **2015**. 7, 894.
- [64] F. Westphal, T. Junge, U. Girreser, W. Greibl & C. Doering. *Mass, NMR and IR spectroscopic characterization of pentedrone and pentylone and identification of their isocathinone by-products*. Forensic Science International, **2012**. 217, 157.
- [65] S. D. McDermott, J. D. Power, P. Kavanagh & J. O'Brien. *The analysis of substituted cathinones. Part 2: An investigation into the phenylacetone based isomers of 4-methylmethcathinone and N-ethylcathinone*. Forensic Science International, **2011**. 212, 13-21.
- [66] S. D. Brandt, S. Freeman, H. R. Sumnall, F. Measham & J. Cole. *Analysis of NRG 'legal highs' in the UK: identification and formation of novel cathinones*. Drug Testing and Analysis, **2011**. 3, 569-75.

- [67] B. Miserez, O. Ayrton & J. Ramsey. *Analysis of purity and cutting agents in street mephedrone samples from South Wales*. Forensic Toxicology, **2014**. 32, 305-10.
- [68] C. R. Maheux, I. Q. Alarcon, C. R. Copeland, T. S. Cameron, A. Linden & J. S. Grossert. *Identification of polymorphism in ethylone hydrochloride: synthesis and characterization*. Drug Testing and Analysis, **2016**. 8, 847.
- [69] P. Kavanagh, J. O'Brien, J. Fox, C. O'Donnell, R. Christie, J. D. Power & S. D. McDermott. *The analysis of substituted cathinones. Part 3. Synthesis and characterisation of 2,3-methylenedioxy substituted cathinones*. Forensic Science International, **2012**. 216, 19.
- [70] C. R. Maheux, C. R. Copeland & M. M. Pollard. *Characterization of three methcathinone analogs: 4-methylmethcathinone, methylone, and bk-MBDB*. Microgram Journal, **2010**. 7, 42.
- [71] S. Armenta, S. Garrigues, M. de la Guardia, J. Brassier, M. Alcalà, M. Blanco, C. Perez-Alfonso & N. Galipienso. *Detection and characterization of emerging psychoactive substances by ion mobility spectrometry*. Drug Testing and Analysis, **2015**. 7, 280.
- [72] T. A. Dal Cason. *The characterization of some 3,4-methylenedioxycathinone (MDCATH) homologs*. Forensic Science International, **1997**. 87, 9.
- [73] L. D. Simmler, T. A. Buser, M. Donzelli, Y. Schramm, L. H. Dieu, J. Huwyler, S. Chaboz, M. C. Hoener & M. E. Liechti. *Pharmacological characterization of designer cathinones in vitro*. British Journal of Pharmacology, **2013**. 168, 458.
- [74] R. Nageswara Rao & M. V. N. Kumar Talluri. *An overview of recent applications of inductively coupled plasma-mass spectrometry (ICP-MS) in determination of inorganic impurities in drugs and pharmaceuticals*. Journal of Pharmaceutical and Biomedical Analysis, **2007**. 43, 1-13.
- [75] S. Comment, E. Lock, C. Zingg & A. Jakob. *The analysis of Ecstasy tablets by ICP/MS and ICP/AES*. Z Zagadnien Nauk Sadowych, **2001**. 46, 131-46.
- [76] N. Lewen. *The use of atomic spectroscopy in the pharmaceutical industry for the determination of trace elements in pharmaceuticals*. Journal of Pharmaceutical and Biomedical Analysis, **2011**. 55, 653-61.
- [77] F. A. Orellana, C. G. Gálvez, M. T. Roldán & C. García-Ruiz. *Applications of laser-ablation-inductively-coupled plasma-mass spectrometry in chemical analysis of forensic evidence*. TrAC Trends in Analytical Chemistry, **2013**. 42, 1-34.
- [78] R. J. H. Waddell, D. N. Nic & D. Littlejohn. *Classification of ecstasy tablets using trace metal analysis with the application of chemometric procedures and artificial neural network algorithms*. Analyst, **2004**. 129, 235-40.
- [79] S. Benson, C. Lennard, P. Maynard & C. Roux. *Forensic applications of isotope ratio mass spectrometry—A review*. Forensic Science International, **2006**. 157, 1-22.
- [80] F. Mas, B. Beemsterboer, A. C. Veltkamp & A. M. A. Verweij. *Determination of 'common-batch' members in a set of confiscated 3,4-(methylenedioxy)-methylamphetamine*

- samples by measuring the natural isotope abundances: a preliminary study.* Forensic Science International, **1995**. 71, 225-31.
- [81] A. de Korompay, J. C. Hill, J. F. Carter, N. NicDaeid & R. Sleeman. *Supported liquid-liquid extraction of the active ingredient (3,4-methylenedioxymethylamphetamine) from ecstasy tablets for isotopic analysis.* Journal of Chromatography A, **2008**. 1178, 1-8.
- [82] F. Palhol, C. Lamoureux, M. Chabrilat & N. Naulet. *15N/14N isotopic ratio and statistical analysis: an efficient way of linking seized Ecstasy tablets.* Analytica Chimica Acta, **2004**. 510, 1-8.
- [83] F. Palhol, C. Lamoureux & N. Naulet. *15N isotopic analyses: a powerful tool to establish links between seized 3,4-methylenedioxymethylamphetamine (MDMA) tablets.* Analytical and Bioanalytical Chemistry, **2003**. 376, 486-90.
- [84] I. Billault, F. Courant, L. Pasquereau, S. Derrien, R. J. Robins & N. Naulet. *Correlation between the synthetic origin of methamphetamine samples and their 15N and 13C stable isotope ratios.* Analytica Chimica Acta, **2007**. 593, 20-9.
- [85] H. A. S. Buchanan, N. N. Daéid, W. J. Kerr, J. F. Carter & J. C. Hill. *Role of five synthetic reaction conditions on the stable isotopic composition of 3,4-methylenedioxymethylamphetamine.* Analytical Chemistry, **2010**. 82, 5484-9.
- [86] W. Bonthron & J. W. Cornforth. *The methylenation of catechols.* Journal of the Chemical Society, **1969**. 1202-4.
- [87] L. C. King & G. K. Ostrum. *Selective bromination with copper(II) bromide.* The Journal of Organic Chemistry, **1964**. 29, 3459-61.
- [88] J. McMurry. 2008, *Organic Chemistry*, 7th ed edn, Thomson-Brooks/Cole, Belmont, CA.
- [89] R. W. Evans, J. R. Zbieg, S. Zhu, W. Li & D. W. C. MacMillan. *Simple Catalytic Mechanism for the Direct Coupling of α -Carbonyls with Functionalized Amines: A One-Step Synthesis of Plavix.* Journal of the American Chemical Society, **2013**. 135, 16074-7.
- [90] National Center for Biotechnology Information., *PubChem Compound Database; CID=6329*, Available at [26/01/2019], <<https://pubchem.ncbi.nlm.nih.gov/compound/6329>>
- [91] M. G. Cabiddu, E. Cadoni, S. De Montis, C. Fattuoni, S. Melis & M. Usai. *A re-examination of the methylenation reaction.* Tetrahedron, **2003**. 59, 4383-7.
- [92] J. Xu, J. Xia & Y. Lan. *Convenient and efficient synthesis of 1,1-bis-(4-alkylthiophenyl)-1-alkenes via tandem friedel–crafts acylation and alkylation of sulfides and acyl chlorides.* Synthetic Communications, **2005**. 35, 2347.
- [93] E. A. Voudrias & M. Reinhard. *Reactivities of hypochlorous and hypobromous acid, chlorine monoxide, hypobromous acidium ion, chlorine, bromine, and bromine chloride in electrophilic aromatic substitution reactions with p-xylene in water.* Environmental Science & Technology, **1988**. 22, 1049-56.

- [94] S. Mallik, K. M. Parida & S. S. Dash. *Studies on heteropoly acid supported zirconia: III: Oxidative bromination of phenol using phosphotungstic acid supported on zirconia*. Journal of Molecular Catalysis A: Chemical, **2007**. 261, 172-9.
- [95] F. A. Carey, R. J. Sundberg & R. J. Sundberg. 2001, *Advanced Organic Chemistry, Part B : Reactions and Synthesis (4th Edition)*, Kluwer Academic Publishers, Hingham, UNITED STATES.
- [96] U. Tilstam & H. Weinmann. *Activation of Mg Metal for Safe Formation of Grignard Reagents on Plant Scale*. Organic Process Research & Development, **2002**. 6, 906-10.
- [97] R. G. Lange. *Cleavage of Alkyl o-Hydroxyphenyl Ethers*. The Journal of Organic Chemistry, **1962**. 27, 2037-9.
- [98] D. Sang, X. Tu, J. Tian, Z. He & M. Yao. *Anchimerically Assisted Cleavage of Aryl Methyl Ethers by Aluminum Chloride-Sodium Iodide in Acetonitrile*. ChemistrySelect, **2018**. 3, 10103-7.
- [99] D. Sang, M. Yao, J. Tian, X. Chen, L. Li, H. Zhan & L. You. *Pyridine Improves Aluminum Triiodide Induced Selective Cleavage of Alkyl o -Hydroxyphenyl Ethers: A Practical and Efficient Procedure for the Preparation of Hydroxychavicol by Demethylation of Eugenol*. Synlett, **2017**. 28, 138-42.
- [100] M. Schäffer, T. Gröger, M. Pütz & R. Zimmermann. *Forensic profiling of sassafras oils based on comprehensive two-dimensional gas chromatography*. Forensic Science International, **2013**. 229, 108-15.
- [101] J. J. Li. 2009, 'Wacker oxidation', *Name Reactions*, Springer, Berlin, Heidelberg.
- [102] J. J. Li. 2006, 'Wacker oxidation', *Name Reactions*, Springer, Berlin, Heidelberg.
- [103] G. Zhang, X. Xie, Y. Wang, X. Wen, Y. Zhao & C. Ding. *Highly selective Wacker reaction of styrene derivatives: a green and efficient aerobic oxidative process promoted by benzoquinone/NaNO₂/HClO₄ under mild conditions*. Organic & Biomolecular Chemistry, **2013**. 11, 2947-50.
- [104] Rhodium: Drug Chemistry Archive. **2004**, *MDMA Synthesis by Reductive Amination of MDP2P Using Aluminum Amalgam and Nitromethane*, Available at [08/09/2019], <<https://chemistry.mdma.ch/hiveboard/rhodium/ritter-alhg.html>>
- [105] M. Hassam, A. Taher, G. E. Arnott, I. R. Green & W. A. L. van Otterlo. *Isomerization of Allylbenzenes*. Chemical Reviews, **2015**. 115, 5462-569.
- [106] C. W. M. Koo 2013, 'Investigations Into Selected Aspects of the Chemistry of Illicit Drugs', University of South Australia.
- [107] R. A. Glennon, A. E.-K. M. Ismaiel, B. Martin, D. Poff & M. Sutton. *A preliminary behavioral investigation of PMMA, the 4-methoxy analog of methamphetamine*. Pharmacology Biochemistry and Behavior, **1988**. 31, 9-13.
- [108] R. A. Glennon, R. Young, M. Dukat & Y. Cheng. *Initial Characterization of PMMA as a Discriminative Stimulus*. Pharmacology Biochemistry and Behavior, **1997**. 57, 151-8.

- [109] T. D. Steele, J. L. Katz & G. A. Ricaurte. *Evaluation of the neurotoxicity of N-methyl-1-(4-methoxyphenyl)-2-aminopropane (para-methoxymethamphetamine, PMMA)*. Brain Research, **1992**. 589, 349-52.
- [110] E. Heather, R. Shimmon & A. M. McDonagh. *Organic impurity profiling of 3,4-methylenedioxymethamphetamine (MDMA) synthesised from catechol*. Forensic Science International, **2015**. 248, 140-7.
- [111] J. Kochana, J. Wilamowski, A. Parczewski & M. Surma. *Synthesis of standards of the most important markers of Leuckart p-methoxymethamphetamine (PMMA)*. Forensic Science International, **2003**. 134, 207-13.
- [112] 1986, in W. J. Mijs & C. R. H. I de Jonge (eds), *Organic Syntheses by Oxidation with Metal Compounds*, Plenum Press, New York.
- [113] M. Guy, S. Freeman, J. F. Alder & S. D. Brandt. *The Henry reaction: spectroscopic studies of nitrile and hydroxylamine by-products formed during synthesis of psychoactive phenylalkylamines*. Central European Journal of Chemistry, **2008**. 6, 526-34.
- [114] Q. Wang, L. Jiang & Q. Wen. *Effect of three extraction methods on the volatile component of Illicium verum Hook. f. analyzed by GC-MS*. Wuhan University Journal of Natural Sciences, **2007**. 12, 529-34.
- [115] D. Waumans, Bruneel, N., Hermans, B., Tytgat, J. *A rapid and simple GC/MS screening method for 4-methoxyphenol in illicitly prepared 4-methoxyamphetamine (PMA)*. Microgram Journal, **2003**. 1, 184 - 9.
- [116] D. Waumans, B. Hermans, N. Bruneel & J. Tytgat. *A neolignan-type impurity arising from the peracid oxidation reaction of anethole in the surreptitious synthesis of 4-methoxyamphetamine (PMA)*. Forensic Science International, **2004**. 143, 133-9.